NISTIR 8056
http://dx.doi.org/10.6028/NIST.IR.8056

Applied and Computational Mathematics Division

Summary of Activities for Fiscal Year 2014

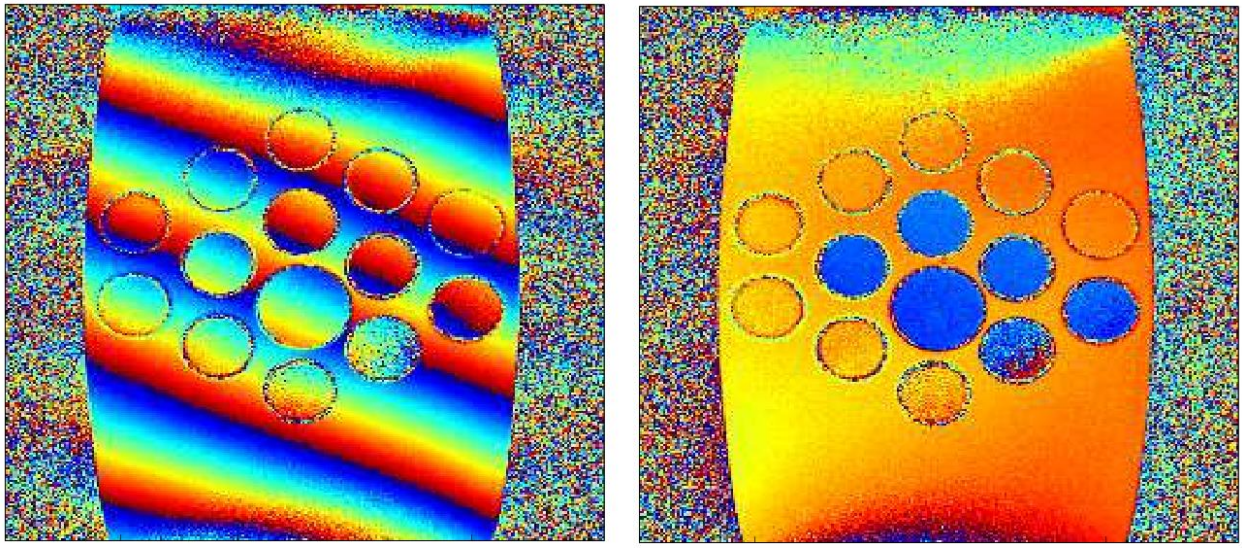

National Institute of Standards and Technology
U.S. Department of Commerce

NISTIR 8056

Applied and Computational Mathematics Division

Summary of Activities for Fiscal Year 2014

Ronald F. Boisvert, Editor
Applied and Computational Mathematics Division
Information Technology Laboratory

http://dx.doi.org/10.6028/NIST.IR.8056

April 2015

U.S. Department of Commerce
Penny Pritzker, Secretary

National Institute of Standards and Technology
Willie E. May, Acting Under Secretary of Commerce for Standards and Technology and Acting Director

Abstract

This report summarizes recent technical work of the Applied and Computational Sciences Division of the Information Technology Laboratory at the National Institute of Standards and Technology (NIST). Part I (Overview) provides a high-level overview of the Division's activities, including highlights of technical accomplishments during the previous year. Part II (Features) provides further details on eight projects of particular note this year. This is followed in Part III (Project Summaries) by brief synopses of all technical projects active during the past year. Part IV (Activity Data) provides listings of publications, technical talks, and other professional activities in which Division staff members have participated. The reporting period covered by this document is October 2013 through December 2014.

For further information, contact Ronald F. Boisvert, Mail Stop 8910, NIST, Gaithersburg, MD 20899-8910, phone 301-975-3812, email boisvert@nist.gov, or see the Division's web site at http://www.nist.gov/itl/math/index.cfm.

Cover Visualization: Staff in NIST's Applied and Computational Mathematics Division are exploring possibilities for quantitative measurement of the magnetic moment of local iron distribution in human tissue. This distribution is suspected to be an important bio-marker for brain function and irregularities have been associated with traumatic brain injury. It is proposed that magnetic moments can be mapped by phase measurement of MRI signals. This figure shows one such measurement. The image on the left reveals a heavily-wrapped phase image. The linear oscillation of phase across the image is the result of an offset of the k-space acquisition data. Division staff members have developed an analysis which estimates and corrects for this offset. The result is shown in the image on the right. Correcting for this large systematic background effect will allow for more fine-scale analysis of magnetic moment distribution in the future. See page 51.

Section Visualizations: The word cloud found at the start of each Part of this document was created using Wordle, http://www.wordle.net/, using the text of this document as input.

Acknowledgements: Thanks to Catherine Graham and Ginger White for assisting in the compilation of Parts III and IV of this document. The word art at the start of each major section was created using Wordle (http://wordle.net/) to process the text of this document.

Contents

Part I

Overview

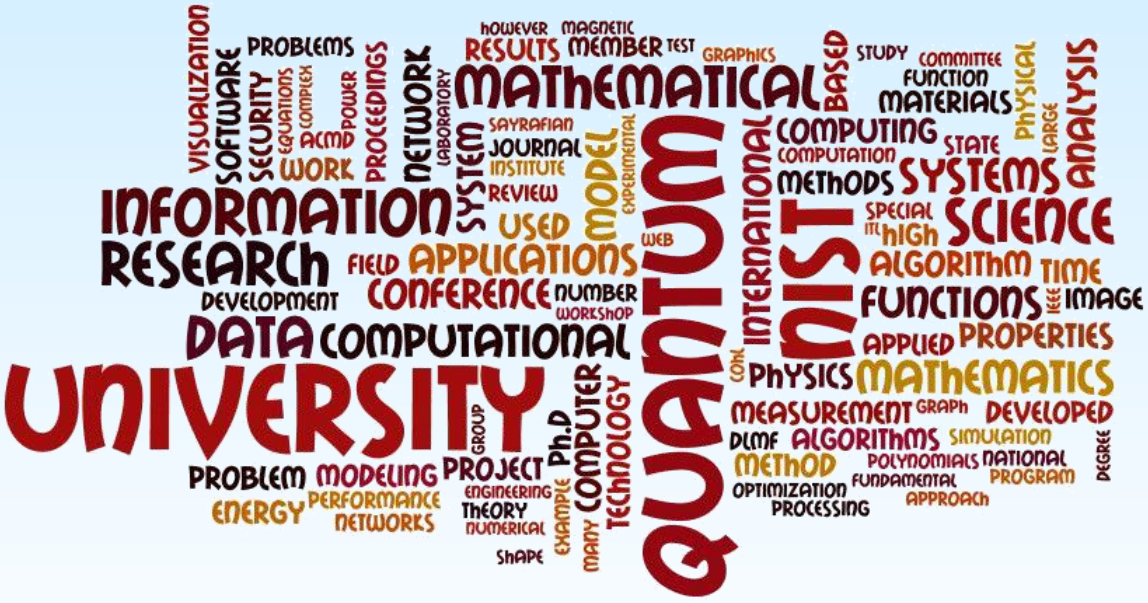

Introduction

Founded in 1901, the National Institute of Standards and Technology (NIST) is a non-regulatory federal agency within the U.S. Department of Commerce. NIST's mission is to promote U.S. innovation and industrial competitiveness by advancing measurement science, standards, and technology in ways that enhance economic security and improve our quality of life. The NIST Laboratory program is broad-ranging, with research efforts encompassing physics, electrical engineering, nanotechnology, materials science, chemistry, bioscience, engineering, fire research, and information technology.

The Information Technology Laboratory (ITL) is one of seven major laboratories and user facilities at NIST. ITL seeks to (a) accelerate the development and deployment of information and communication systems that are reliable, usable, interoperable, and secure; (b) advance measurement science through innovations in mathematics, statistics, and computer science; and (c) conduct research to develop the measurements and standards infrastructure for emerging information technologies and applications.

The Applied and Computational Mathematics Division (ACMD) is one of six technical Divisions in ITL. ACMD provides leadership within NIST in the use of applied and computational mathematics to solve science and engineering problems arising in measurement science and related applications. In that role ACMD staff members

- perform research and development in applied mathematics and computational science and engineering, including analytical methods, numerical and symbolic algorithms, advanced computing and communications architectures and applications, and high performance scientific visualization;
- engage in peer-to-peer collaborations in the application of mathematical and computational technologies to NIST problems;
- develop and disseminate mathematical reference data, software, and related tools; and
- work with internal groups and external organizations to develop standards, test procedures, reference implementations, and other measurement technologies for advanced scientific computation on current and future architectures.

Division staff is organized into four groups:

Mathematical Analysis and Modeling Group (*Timothy Burns, Leader*)

Performs research and maintains expertise in applied mathematics, mathematical modeling, and numerical analysis for application to measurement science.

Mathematical Software Group (*Michael Donahue, Leader*)

Performs research and maintains expertise in the methodology and application of mathematical algorithms and software in support of computational science within NIST as well as in industry and academia.

Computing and Communications Theory Group (*Ronald Boisvert, Acting Leader; Isabel Beichl and Xiao Tang, Project Leaders*)

Performs research and maintains expertise in fundamental mathematics, physics, and measurement science necessary to enable the development and analysis of current and future computing and communications systems.

High Performance Computing and Visualization Group (*Judith Terrill, Leader*)

Performs research and maintains expertise in the methodologies and tools of high performance scientific computing and visualization for use in measurement science.

The technical work of the Division is organized into six thematic areas; these are described in the sidebar. Project descriptions in Section III of this document are organized according to these broad themes.

Division Thematic Areas

Mathematics of Metrology. Mathematics plays an important role in the science of metrology. Mathematical models are needed to understand how to design effective measurement systems, and to analyze the results they produce. Mathematical techniques are used to develop and analyze idealized models of physical phenomena to be measured, and mathematical algorithms are necessary to find optimal system parameters. Finally, mathematical and statistical techniques are needed to transform measured data into useful information. The goal of this work is to develop fundamental mathematical methods and analytical tools necessary for NIST to continue as a world-class metrology institute, and to apply them to critical measurement science applications.

Advanced Materials. Delivering technical support to the nation's manufacturing industries as they strive to out-innovate and out-perform the international competition has always been a top priority at NIST. This has also emerged as a major White House priority in recent years, in which NIST is playing an increasingly central role. Mathematical modeling, computational simulation, and data analytics are key enablers of emerging manufacturing technologies. This is most clearly evident in the Materials Genome Initiative, an interagency program with the goal of significantly reducing the time from discovery to commercial deployment of new materials through the use of modeling, simulation, and informatics. ACMD's role in advanced manufacturing centers on the development and assessment of modeling and simulation tools, with emphasis on uncertainty quantification, as well as support of NIST Laboratory efforts in such areas as materials modeling and smart manufacturing.

High Performance Computing and Visualization. Computational capability is advancing rapidly, with the result that modeling and simulation can be done with greatly increased fidelity (e.g., higher resolution, more complex physics). However, developing the requsite large-scale parallel applications remains highly challenging, requiring expertise that scientists rarely have. In addition, the hardware landscape is changing rapidly, so new algorithmic techniques must constantly be developed. We are developing and applying such expertise for application to NIST problems. In addition, computations and laboratory experiments often produce large volumes of scientific data, which cannot be readily comprehended without some form of visual analysis. We are developing the infrastructure necessary for advanced visualization of scientific data, including the use of 3D immersive environments and applying this to NIST problems. One of our goals is to develop the 3D immersive environment into a true interactive measurement laboratory.

Quantum Information. An emerging discipline at the intersection of physics and computer science, quantum information science is likely to revolutionize science and technology in the same way that lasers, electronics, and computers did in the 20th century. By encoding information into quantum states of matter, one can, in theory, exploit the seemingly strange behavior of quantum systems to enable phenomenal increases in information storage and processing capability, as well as communication channels with high levels of security. Although many of the necessary physical manipulations of quantum states have been demonstrated experimentally, scaling these up to enable fully capable quantum computers remains a grand challenge. We engage in (a) theoretical studies to understand the power of quantum computing, (b) collaborative efforts with the multi-laboratory experimental quantum science program at NIST to characterize and benchmark specific physical implementations of quantum information processing, and (c) the demonstration and assessment of technologies for quantum communication.

Foundations of Measurement Science for Information Systems. Modern information systems are astounding in their complexity. Software applications are built from thousands of interacting components. Computer networks interconnect millions of independently operating nodes. Large-scale networked applications provide the basis for services of national scope, such as financial transactions and power distribution. In spite of our increasing reliance on such systems, our ability to build far outpaces our ability to secure. Protocols controlling the behavior of individual nodes lead to unexpected macroscopic behavior. Local power anomalies propagate in unexpected ways leading to large-scale outages. Computer system vulnerabilities are exploited in viral attacks resulting in widespread loss of data and system availability. The actual resilience of our critical infrastructure is simply unknown. Measurement science has long provided a basis for the understanding and control of physical systems. Such deep understanding and insight is lacking for complex information systems. We seek to develop the mathematical foundations needed for a true measurement science for complex networked information systems.

Mathematical Knowledge Management. We work with researchers in academia and industry to develop technologies, tools, and standards for representation, exchange, and use of mathematical data. Of particular concern are semantic-based representations which can provide the basis for interoperability of mathematical information processing systems. We apply this to the development and dissemination of reference data for applied mathematics. The centerpiece of this effort is the Digital Library of Mathematical Functions, a freely available interactive and richly linked online resource, providing essential information on the properties of the special functions of applied mathematics, the foundation of mathematical modeling in all of science and engineering.

Highlights

In this section we identify some of the major accomplishments of the Division during the past year. We also provide news related to ACMD staff.

Technical Accomplishments

ACMD has made significant technical progress on many fronts during the past year. Here we highlight a few notable technical accomplishments. Further details are provided in Part II (Features) and Part III (Project Summaries).

Mathematics of Metrology. Cryopreservation, whose goal is to preserve biological cells, tissue and organs by storing them at very low temperature, broadly impacts the medical and agriculture industries and has a growing role in forensic science. Cooling, warming and preservation strategies must be carefully designed to avoid ice nucleation and chemical toxicity, which impact survival rates, while optimizing time and cost. Nevertheless, very little is actually known about the physical processes surrounding cryopreservation. In order to be able to develop improved protocols and measurements for such processes, Division scientists have begun an effort to develop the foundations of mathematical modeling in cryobiology. In particular, they are developing a thermodynamic framework suitable for cryobiological applications, including mathematical models for thermal transport, chemical transport, mass transport and solidification processes of an externally-cooled ternary mixture that surrounds a biological cell. See page 21.

Successful nanoelectronics manufacturing requires high quality imaging and accurate measurements at the subnanometer scale. The helium ion microscope (HIM) is an important new imaging and metrology tool that can provide the needed accuracy. However, HIM images are often noisy, and important background structures may not be easily discernible due to the weak signal. Techniques that can overcome such degradations are of paramount interest. We have discovered an unexpectedly effective two-stage recovery and enhancement method. This involves a preliminary image-specific adaptive histogram equalization of the image. Such equalization enhances background information while significantly magnifying noise, and is not generally advisable with noisy data. However, at the second stage, an effective and easy-to-use denoising technique, based on progressive low exponent Lévy fractional diffusion smoothing, can be successfully applied to this histogram equalized image with magnified noise. See page 26.

The development of new algorithms and computer codes for the solution of partial differential equations (PDEs) usually involves the use of proof-of-concept test problems. Such test problems have a variety of uses such as demonstrating that a new algorithm is effective, verifying that a new code is correct in the sense of achieving the theoretical order of convergence, and comparing the performance of different algorithms and codes. Self-adaptive methods to determine a quasi-optimal grid are a critical component of the improvements that have been made in PDE algorithms in recent years. Although such adaptive mesh refinement techniques are now in widespread use in applications, they remain an active field of research. We have developed a web-based resource to provide a standard set of problems suitable for benchmarking and testing adaptive mesh refinement algorithms and error estimators. The development of computational benchmarks like this is an important component of the metrology infrastructure for scientific computing. See page 53.

Advanced Materials. The first 3D version of NIST's Object-Oriented Finite Element (OOF) software, called OOF3D[1], was released on-line in September 2014. An advanced software tool for studying the relationship between the microstructure of a material and its overall mechanical, dielectric, or thermal properties, the original OOF2 performed two-dimensional finite element calculations on grids derived from two dimensional micrographs. OOF3D performs the same task but does three dimensional calculations on three dimensional images, making it more directly applicable to real materials. See page 18.

[1] The first release of OOF3D, which is numbered 3.0.0 (because the first version of OOF2 was 2.0.0), is available at http://www.ctcms.nist.gov/oof/oof3d.

High Performance Computing and Visualization. In a virtual measurement tour-de-force, ACMD scientists have calculated the nonrelativistic base energy levels for the four electrons in the element beryllium as well as the entire isoelectronic series up through atomic number 113, i.e., positive ions of all the other elements having the same number of electrons as beryllium[2]. With eight digits of accuracy, these results represent the most accurate computations ever done of these quantities. Years of effort have been put in to developing the foundational analytical and numerical machinery to solve the few-electron Schrödinger system with no approximations other than the truncation of infinite series. The four-electron case is particularly exciting as, due to the ACMD formalism, higher electron systems will present no new analytical difficulties. Such a method could enable computation of other atomic properties—electron affinity and ionization potential, for example—that are important for astrophysics and other fields of atomic research. See page 31.

Recently, ACMD scientists, working with EL, the University of Strasbourg, and SIKA Corporation, have gained fundamental insights into mechanisms that control the rheological properties of complex fluids like suspensions. Using their expertise in the application of high performance computers and visualization, along with access to DOE supercomputers, they discovered a universal law that allows one to predict the flow behavior of hard sphere suspensions from the properties of the matrix fluid. These ideas are being applied to create a standard reference material (SRM 2493) for mortars, the first time a SRM was developed based on supercomputer simulations. Such SRMs are useful for calibration of rheometers used in research and development to create a new generation of products such as high performance and eco-friendly cement-based materials. See page 34.

Mathematical Knowledge Management. Special functions are fundamental tools needed for mathematical and computational modeling in the sciences and engineering. Developers of algorithms and software for the evaluation of special functions need a reliable source of function values in order to test their implementations. While many libraries or systems efficiently produce function values, few offer any information about the accuracy of their computations. To fill this need, we are working with colleagues at the University of Antwerp to provide users of the NIST Digital Library of Mathematical Functions (DLMF) the ability to generate tables of special functions on demand whose accuracy is carefully controlled, and whose results come with a reliable statement of uncertainty. A prototype of the DLMF "Live Tables" has been completed and is currently accessible online. See page 38.

We have taken a major step in improving the accessibility of the 3D interactive graphics in the Digital Library of Mathematical Functions (DLMF) with the release of DLMF Version 1.07 in March 2014. Previously these graphics were rendered using two common technologies, VRML and X3D, which require users to download a plugin based on their operating system. Not only is this inconvenient for users, it poses difficulties for those maintaining the site, since updates of the plugin, web browser, and even the operating system can affect the quality of the visualization. To remedy this problem we converted the DLMF 3D graphics to a recently available standard format, WebGL. WebGL visualizations are visible on Windows, Mac, and Linux platforms in most HTML5 compatible browsers. See page 104.

Quantum Information. One-time memories are a basic primitive for constructing more general cryptographic tools, such as one-time programs. One-time programs could enable construction of electronic tokens or electronic cash, or enable certain forms of software protection. ACMD has developed a new theoretical construction for one-time memories based on isolated qubits. (Isolated qubits are a special class of quantum devices, which have long coherence times, but do not allow entangling operations. These may be realizable in well-studied quantum systems such as solid-state nuclear spins.) These results demonstrate, for the first time, that quantum-based one-time memories can achieve several of the basic requirements for use in cryptographic applications. See page 15.

Many applications of quantum mechanics to communication and cryptography rely on experimental tests of Bell inequalities. These tests also provide the strongest evidence against local realism (LR) as a possible explanation of quantum non-determinism. While there have been many experiments demonstrating the required violation of Bell inequalities, so-far they have suffered from loopholes and problems with

[2] Electron energy levels also depend on relativistic and quantum electrodynamic effects caused by the atom's nucleus, but they're negligible until you get to higher atomic number atoms.

quantifying the evidence against LR. ACMD mathematicians have developed a powerful strategy for analyzing Bell-test data that can quantify the evidence against LR in a configuration-independent way. They have applied this method to Bell-test data from the University of Illinois to show that it violates LR without being subject to the so-called detection loophole. A conventional analysis did not show this violation. Such analyses will be critical to the success of the NIST Innovations in Measurement Science Project *Quantum Randomness as a Secure Resource*, which aims to provide random bits to the NIST Randomness Beacon guaranteed by the laws of physics to not have been known before measurement. See pages 81 and 84.

Finally, this year we helped establish the Joint Center for Quantum Information and Computer Science (QuICS), which was formally inaugurated on October 31, 2015. A collaborative venture of NIST, the University of Maryland and Research Directorate of the National Security Agency/Central Security Service, QuICS will conduct basic research to understand how quantum systems can be effectively used to store, transport and process information. The work of QuICS will be carried out jointly by staff of the participating institutions, as well as by graduate students, postdocs, and visiting scientists. See page 91.

Foundations of Measurement Science for Information Systems. RF-enabled wearable sensors offer an attractive set of e-health applications, among which are monitoring of temperature, respiration, heart rate, and blood pressure. As these sensors are small and mainly rely on very small batteries to carry out their functions, prolonging their operational lifetime could significantly help their commercial applications. We are investigating the feasibility of capturing and storing kinetic energy from human body motion to power such devices. To do this we have developed a statistical model of acceleration generated as a result of typical human motion, modeled a micro-harvester device suitable for wearable/implantable applications, and modeled and characterized the instantaneous power that can be generated by the device. See page 24.

Technology Transfer and Community Engagement

The volume of technical output of ACMD remains high. During the last 18 months, Division staff members were (co-)authors of 42 articles appearing in peer-reviewed journals and 35 papers in conference proceedings. Fifteen additional papers have been accepted for publication, while 43 others are undergoing review. Division staff gave 50 invited technical talks and presented 50 others in conferences and workshops.

ACMD continues to maintain an active Web site with a variety of information and services, most notably the Digital Library of Mathematical Functions, though legacy services no longer actively maintained, like the Guide to Available Mathematical Software, the Matrix Market, and the SciMark Java benchmark still see significant use. During calendar year (CY) 2014, the division web server satisfied more nearly 5 million requests for pages during more than 1.1 million user visits. In total, there have been more than 371 million "hits" on ACMD Web servers since they went online as NIST's first web servers in 1994. Another indication of the successful transfer of our technology is references to our software in refereed journal articles. For example, our OOMMF software for nano-magnetic modeling was cited in 167 such papers published in CY 2014 alone.

Members of the Division are also active in professional circles. Staff members hold a total of 19 editorial positions in peer-reviewed journals. For example, ACMD faculty appointee Dianne O'Leary serves at Editor-in-Chief of the *SIAM Journal on Matrix Analysis and Applications.* Staff members are also active in conference organization, serving on 31 organizing/steering/program committees. Of note, ACMD played an important role as sponsor or (co-)organizer of several significant events this year, including the following:

- *Bell Labs-NIST Workshop on Large-Scale Networks*[3]. Murray Hill, NJ. October 25, 2013. Murray Hill, NJ. (Vladimir Marbukh, Co-Organizer)
- *Workshop on Uncertainty Quantification in Materials Modeling*[4], Institute for Mathematics and Its Applications, University of Minnesota. December 16-17, 2013. (Andrew Dienstfrey, Co-Organizer)

[3] http://ect.bell-labs.com/who/iis/research/workshops/NIST-BellLabsWorkshopOct25-2013x.pdf

[4] http://www.ima.umn.edu/2013-2014/SW12.16-17.13/?event_id=SW12.16-17.13

- *UMD-NIST Symposium on Network Science*. University of Maryland. January 24, 2014. (Assane Gueye, Co-Organizer)
- *NIST-UMD Workshop on Quantum Information and Computer Science*[5]. University of Maryland. March 31 – April 1, 2014. (Stephen Jordan and Yi-Kai Liu, Co-Organizers)
- *Third International Workshop on Combinatorial Testing*[6]. Cleveland, OH. March 31, 2014. (Raghu Kacker and Yu Lei, Co-Organizers)
- *IEEE 25th Annual Conference on Personal, Indoor and Mobile Radio Communications* (PIMRC)[7]. Washington, DC. September 2-5, 2014. (Kamran Sayrafian, Principal Organizer and Chair of the Technical Program Committee)
- *Workshop on Dynamics of and on Networks*[8]. Santa Fe Institute, NM. December 1-5, 2014. (NIST grant provided partial funding for this event.)

Plans are underway for several major events in the coming year:

- *13th International Symposium on Orthogonal Polynomials, Special Functions and Applications* (OPSFA)[9]. NIST, Gaithersburg, MD. June 1-5, 2015. (Daniel Lozier, Co-Organizer and Howard Cohl, Member of the Program Committee).
- *Conference on Intelligent Computer Mathematics* (CICM)[10]. Washington, DC. July 13-17, 2015. (Bruce Miller and Abdou Youssef, Co-Organizers)
- *Workshop on Uncertainty Quantification in Materials Modeling*[11], Purdue University, West Lafayette, IN. July 28-31, 2015. (Andrew Dienstfrey, Co-Organizer)

Service within professional societies is also prevalent among our staff. For example, Barry Schneider is serving as Vice-Chair and Chair-Elect of the Division of Computational Physics of the American Physical Society (APS). Geoffrey McFadden was elected to the position of Member-at-Large of the Council of the Society for Industrial and Applied Mathematics (SIAM). Faculty appointee Michael Mascagni is a Member of the Board of Directors of the International Association for Mathematics and Computers in Simulation (IMACS). Ronald Boisvert continues to serve as a member of the Publications Board of the Association for Computing Machinery (ACM). Staff members are also active in a variety of working groups. For example, Ronald Boisvert and Andrew Dienstfrey serve as members of the International Federation for Information Processing (IFIP) Working Group 2.5 on Numerical Software, Donald Porter is a member of the Tcl Core Team, Bruce Miller is a member of W3C's Math Working Group, and Sandy Ressler is a member of the Web3D Consortium. Barry Schneider represents NIST on the High End Computing (HEC) Interagency Working Group of the Federal Networking and Information Technology Research and Development (NITRD) Program.

For further details, see Section IV, Activity Data.

Staff News

The past year saw many staffing changes. Among these are the following.

Arrivals

Yvonne Kemper began a stay in ACMD as a NIST National Research Council (NRC) Postdoctoral Associate in December 2013. She received a Ph.D. in mathematics from the University of California at Davis in 2013, where she wrote a thesis on structural measurements of simplicial complexes and convex polytopes.

[5] http://www.nist.gov/itl/math/quics-workshop.cfm
[6] http://www.research.ibm.com/haifa/Workshops/iwct2014/program.shtml
[7] http://www.ieee-pimrc.org/2014/
[8] http://www.santafe.edu/gevent/detail/science/1739/
[9] http://www.siam.org/meetings/opsfa13/
[10] http://cicm-conference.org/2015/cicm.php?event=&menu=general
[11] http://www.ima.umn.edu/2014-2015/SW7.28-31.15/

At NIST she has been working with Isabel Beichl on approximating the chromatic polynomials of large-scale networks.

Barry Schneider, a long-time Program Manager in the Division of Physics at the National Science Foundation, as well as a NIST Guest Researcher, began a full-time appointment in ACMD in January 2015 as one of the principals in the NIST Digital Library of Mathematical Functions project. An expert in computational physics and high performance computing, Schneider will also contribute to ACMD work in these areas.

Michael Mascagni, a Professor of Computer Science at Florida State University, began a faculty appointment in ACMD in late FY 2013. He is spending the 2014-15 academic year on sabbatical at NIST. An expert in high performance computing and Monte Carlo methods, Mascagni is focusing on applications in materials modeling at NIST.

Departures

Sean Colbert-Kelly completed his term as a NIST/NRC Postdoctoral Associate in ACMD September 2014. He went on to a position at Noblis, a non-profit science and engineering think-tank in the Washington, DC area. At NIST Colbert-Kelly developed and analyzed models of surfactants and ferro-electric liquid crystals. He continues as a NIST guest researcher.

In July 2014 **Michael Cromer** completed his term as an NIST/NRC Postdoctoral Associate, assuming the position of Assistant Professor in the Mathematical Sciences Department at the Rochester Institute of Technology. At NIST Cromer worked with Geoffrey McFadden on models of shear banding in polymer solutions.

Daniel Kaslovsky, recipient of an NSF Postdoctoral Fellowship for Transformative Computational Science using CyberInfrastructure, who was carrying out his research in ACMD in Boulder, accepted a permanent position at Seagate Technology in Longmont, Colorado.

Students

During FY 2014 ACMD was able to support the work of 39 student interns, including 11 graduate students, 13 undergraduates, and 15 high school students. See Table 1 for a complete listing.

Figure 1. *Some of ACMD's summer interns. From left to right: Jimmy Li (Richard Montgomery High School), Alex Danoff (Wootton High School), Jessie Hirtenstein (American University), Wenqing Xu (Montgomery Blair High School), David Gunby (Georgetown Day School), Justin Oh (Brown University), Brandon Alexander (UMBC).*

Table 1. *Student Interns in ACMD*

Name	Institution	Type		Mentor	Project
Brandon Alexander	UMBC	U	SURF	H. Cohl	MediaWiki Extension Development for Digital Repository of Mathematical Formulae.
Sharan Arkalgud	Thomas Jefferson H.S. for Science andTechnology	HS	Vol	S. Langer	Image Processing Algorithms Implementation
Kathleen Arnett	Richard Montgomery High School	HS	Vol	H. Cohl	Digital Repository of Mathematical Formulae
Hazma Attak		G	FGR	J. Terrill	Visualization with D3
Martina Barbi	University of Bologna	G	FGR	K. Sayrafian	Dynamic channel modeling in body area networks
Michael Baume	University of Maryland	G	DGR	S. Jordan	Mathematical analysis of quantum algorithms
Earl Bellinger	SUNY Oswego	G	NPSC	J. Terrill	Data mining
Styvens Belloge	ISIMA	G	FGR	J. Terrill	Visualization and analysis of the National Vulnerability Database
Luis Catacora	University of Maryland	U	SURF	J. Terrill	Visualization with D3
Faical Congo	ISIMA	G	FGR	S. Langer	Software development for the OOF materials modeling system
Theodore Corrales	Montgomery Blair H.S.	HS	SVP	H. Cohl	Digital Repository of Mathematical Formulae
Alex Danoff	Thomas S. Wooton H.S.	HS	SVP	H. Cohl	Digital Repository of Mathematical Formulae
Romain Desaymons	ISIMA	G	FGR	J. Terrill	Parallelization of Hydratica
Bryan Gard	Louisiana State University	G	NPSC	E. Knill	Quantum measurement analysis
Behnaz Ghouchani	City College of NY	U	SURF	B. Schneider	Exponential time differencing methods.
Mohamed Gueye	City College of NY	U	SURF	S. Ressler	Web based information visualization.
David Gunby	Georgetown Day H.S.	HS	SVP	F. Hunt	Communication in engineering
Jessica Hirtenstein	American University	U	SURF	H. Cohl	Orthgonal polynomials and special functions.
Kim Jablonski	Jacobs Univeristy Bremen	U	FGR	B. Miller	Mathematical Knowledge Management
Adam Keith	University of Colorado	U	PREP	E. Knill	Quantum information theory
Lucianna Kiffer	Tulane University	U	SURF	S. Langer	Software development for the OOF materials modeling system
Lukas Kohlhase	Jacobs Univeristy Bremen	U	FGR	B. Miller	Mathematical knowledge management
Nadav Kravitz	University of Maryland	U	SURF	S. Glancy	Quantum state estimation
Jimmy Li	Richard Montgomery H.S.	HS	SHIP	H. Cohl	Media Wiki Extensions
Amber Liu	Poolesville H.S.	HS	SVP	H. Cohl	Digital Repository of Mathematical Formulae
Shraeya Madhu	Poolesville H.S.	HS	SVP	H. Cohl	Digital Repository of Mathematical Formulae
Jacob Migdall	Poolesville H.S.	HS	SVP	H. Cohl	Digital Repository of Mathematical Formulae
Azeem Mohammed	Poolesville H.S.	HS	SVP	H. Cohl	Digital Repository of Mathematical Formulae
Sung-Ho Oh	Brown University	U	SURF	F. Hunt	Spreading information, consensus in a network
Ayotunde Olutade	Jackson State University	U	SURF	J. Terrill	Visualization with D3
Alicia Ouyang	River Hill H.S.	HS	SHIP	J. Terrill	D3 visualization of HydratiCA Data
Jane Pan	University of Maryland	U	SURF	S. Langer	Detecting geometry and structure in images
Moritz Schubotz	Technische Universitaet Berlin	G	FGRRS	H. Cohl	MediaWiki Extension development for the Digital Repository of Mathematical Formula
Diamond Smith	Charles H. Flowers H.S.	HS	SVP	H. Cohl	Digital Repository of Mathematical Formulae
James van Meter	University of Colorado	G	PREP	E. Knill	Relativistic quantum information
Michael Vetter	Poolesville H.S.	HS	SVP	H. Cohl	Digital Repository of Mathematical Formulae
Peter Wills	University of Colorado	G	PREP	E. Knill	Statistical analyses for quantum information
William Xu	Montgomery Blair H.S.	HS	SVP	H. Cohl	*q*-hypergeometric orthogonal polynomials
Cherry Zou	Poolesville H.S.	HS	SVP	H. Cohl	Digital Repository of Mathematical Formulae

Legend

G	*Graduate student*	*PREP*	*Professional Research Experience Program (Boulder)*
U	*Undergraduate*	*FGR*	*Foreign Guest Researcher*
HS	*High school*	*NPSC*	*National Physical Sciences Consortium Fellow*
		NSF	*National Science Foundation Fellow*
		DGR	*Domestic Guest Researcher*
		SURF	*Summer Undergraduate Research Fellowship*
		SHIP	*Summer High school Internship Program*
		SVP	*Student Volunteer Program*

ACMD staff members are quite active in the education of graduate students, serving both as Ph.D. advisers and as members of thesis committees. For a complete list, see page 127.

Recognition

Division staff garnered a number of professional recognitions during the past year. These are described below.

Manny Knill was selected to receive one of twelve 2013 Arthur Flemming Awards. Administered by the Trachtenberg School of Public Policy and Public Administration of George Washington University, the Flemming Award honors outstanding men and women in the Federal service. At the June 2014 ceremony in Washington, DC, Knill was recognized as "one of the world's leading theorists in the field of quantum information science and engineering."

Figure 2. *Charles Romine, Director of the NIST Information Technology Laboratory, presents the Washington Academy of Sciences Award in Mathematics and Computer Science to Ronald Boisvert.*

Ronald Boisvert was selected to receive the 2014 Award in Mathematics and Computer Science from the Washington Academy of Sciences (WAS). The award was conferred during ceremonies held at the Sphinx Club in Washington, DC on May 8, 2014. Awardees are also recognized as Fellows of the WAS.

Jeffrey Fong has received the 2014 Lifetime Achievement Award from the International Conference on Computational Engineering and Science (ICCES). Fong was cited for his "seminal contributions to reliability engineering and probabilistic mechanics." The ICCES Lifetime Achievement Award recognizes sustained and significant contributions in the form of research, teaching, and service to the community, in the technical areas of the ICCES series of conferences. The award ceremony took place on June 16, 2014 during the ICCES conference in Changwon, Korea.

Raghu Kacker received a Department of Commerce Silver Medal "for enabling unprecedented levels of software reliability through development of innovative software testing methodologies and tools." The medal recognizes the accomplishments of the combinatorial testing project whose current activities are described on page 101. D. Richard Kuhn of the ITL Computer Security Division was a joint honoree.

A portrait of **Jack Edmonds** was enshrined in the NIST Gallery of Distinguished Scientists, Engineers and Administrators in ceremonies held at the NIST Gaithersburg Laboratories on October 10, 2014. Administered by the Standards Alumni Association, the gallery honors former NIST staff members who made outstanding contributions during their tenure here. Edmonds was recognized for "prolific and fundamental contributions in combinatorial optimization and discrete mathematics." He was one of the creators of the fields of combinatorial optimization and polyhedral combinatorics, which emerged during the period of his tenure at NIST from 1959-69. In addition, Edmonds produced many deep and important theoretical results in matroid theory. His contributions also helped pave the way for modern computational complexity theory. He was the first to describe the complexity class NP, to describe a tractable computation as one that is solvable in polynomial time, and to state the now widely held conjecture that the complexity classes P and NP are

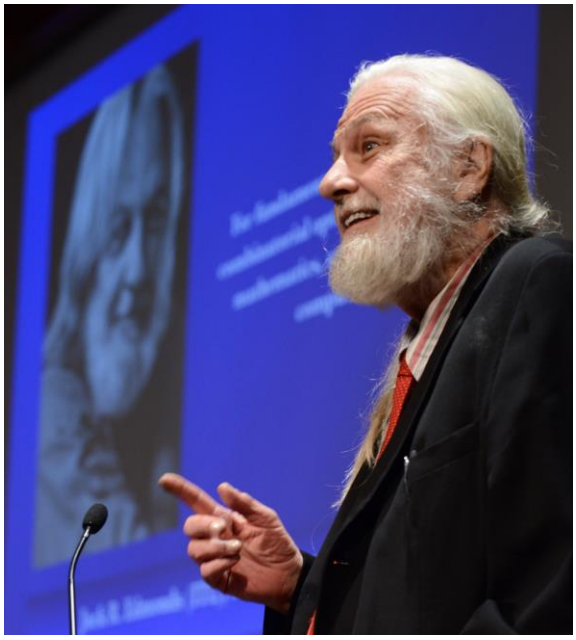

Figure 3. *Jack Edmonds delivers remarks at the 2014 Alumni Portrait Gallery Ceremony.*

not equivalent. For futher details, see the account of Sipser published in the 1992 *Proceedings of the ACM Symposium on the Theory of Computing*[12].

Chris Schanzle received the Outstanding Service Award from the NIST Chapter of Sigma Xi, the Scientific Research Society. Schanzle was cited for his "exceptional service in support of the ITL Applied and Computational Mathematics Division (ACMD), the Statistical Engineering Division (SED), and their collaborators … which enables state-of-the-art computational science in support of the NIST Laboratory programs."

ACMD staff members and associates garnered three of the six annual ITL awards presented in 2014:

- Outstanding Contribution to ITL: **Bruce Miller**. For technical excellence in development of the computational infrastructure underlying the NIST Digital Library of Mathematical Functions.
- Outstanding Journal Paper: **Yanbao Zhang, Scott Glancy and Manny Knill**, Efficient Quantification of Experimental Evidence against Local Realism, *Physical Review* A **88**, 052119.
- Outstanding Technical Support: **Chris Schanzle**. (Joint Award) For extraordinary leadership and dedication to users in securing the ITL computing environment through the upgrading of systems for secure BIOS and Windows 7.

Finally, ACMD Administrative Assistant **Ginger White** completed her studies at the University of Maryland in December 2013 and was awarded a Master's in Business Administration.

[12] http://dx.doi.org/10.1145/129712.129771

Part II

Features

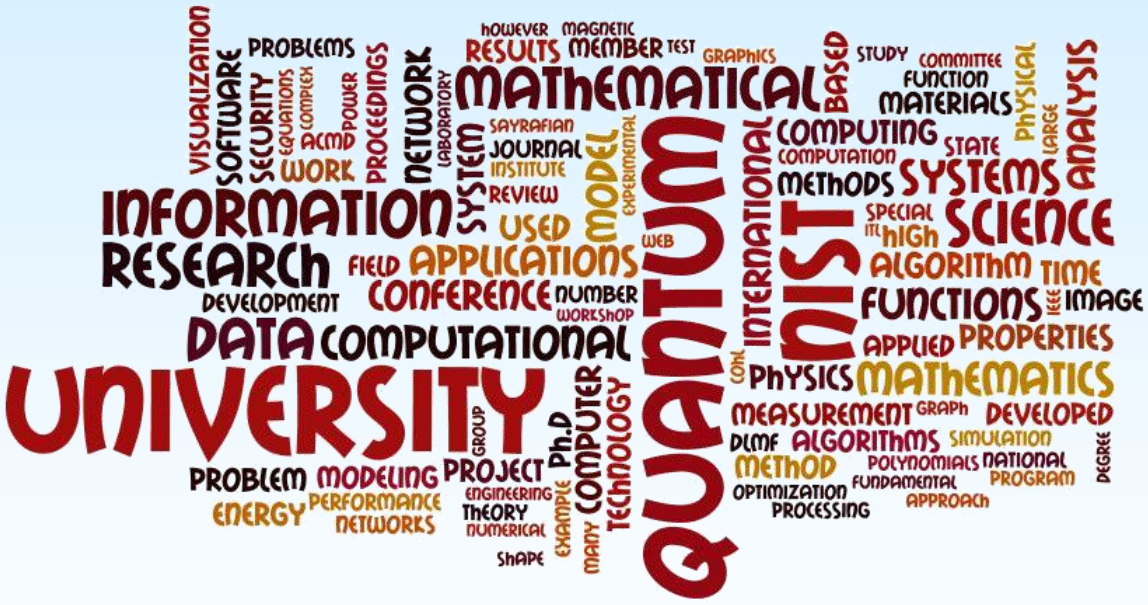

Tamper-Resistant Cryptographic Hardware using Isolated Qubits

Tamper-resistant cryptographic hardware is used to protect information that is stored in devices that are under the physical control of an adversary. For instance, tamper-resistant hardware can prevent a thief from reading private data from a stolen smartphone, or making unauthorized copies of movies from a streaming video player. In these situations, while the data may be protected by encryption, an adversary can circumvent this protection by finding the secret keys that are used to decrypt the data; these keys must be present somewhere in the device while it is running. Tamper-resistant hardware can prevent an adversary from reading these secret keys, and can disable the device if it is accessed improperly.

Designing tamper-resistant hardware is a difficult task. One would like to design devices whose security follows directly from the laws of physics. Alas, neither classical nor quantum physics seems capable of providing such guarantees. Nevertheless, we have discovered a conceptually elegant approach to solving this problem, using a special class of quantum mechanical devices called isolated qubits*. Using this approach, we provide theoretical constructions of cryptographic primitives called* one-time memories*, as well as tamper-resistant "black boxes" called* one-time programs*.*

Yi-Kai Liu

Figure 4. *An adversary who has physical access to a device can read all of the data stored on it, including secret keys used for encryption and decryption. Tamper-resistant hardware provides a solution to this problem.*

Originally proposed by Shafi Goldwasser, Yael Tauman Kalai and Guy Rothblum in 2008 [1], a one-time program is a program that can be run exactly once. After the program has run, it stops working, and "self-destructs." In addition, the program reveals nothing about its internal operation; thus it behaves like an oracle, or "black box." One-time programs are a simple but powerful form of software protection and access control. They are convenient objects for theoretical investigation, which are applicable (at least in principle) to a wide range of security problems. For example, a one-time program can provide access to encrypted data, without revealing the decryption keys, and while limiting the amount of data that can be decrypted.

Goldwasser, Kalai and Rothblum showed that one-time programs can be constructed from simpler devices called *one-time memories*. A one-time memory stores two (pre-programmed) messages, and allows a user to read either of the messages, but not both of them. Thus, a one-time memory is equivalent to a one-time program that only takes a single bit of input. One-time memories are simpler to construct than one-time programs, because they only perform table lookups, rather than arbitrary computations.

We would like to construct one-time memories whose security is guaranteed by basic principles of physics. In particular, we desire information-theoretic security, which holds against adversaries with unlimited computational power. However, this turns out to be impossible using classical physics. In classical physics, information can always be copied, at least in principle, and so at a fundamental level, there is no way to prevent the adversary from duplicating the entire one-time memory, and then reading one message from the original memory and the other message from the duplicate memory – thus breaking the security guarantee.

In quantum physics, things seem more promising, because of surprising phenomena that occur when information is encoded in superpositions of quantum states. In particular, the *no-cloning theorem* guarantees that an unknown quantum state cannot be copied. But in fact, this is not sufficient for our purposes. There are general "no go" theorems in quantum cryptography, discovered around 1996 by Dominic Mayers, Hoi-Kwong Lo and H. F. Chau [5-7], which show that any construction for quantum bit-commitment or oblivious transfer can be broken by performing measurements that use *entanglement*. (We will say more about entanglement later.) These results imply the impossibility of one-time memories using quantum physics.

Something different is needed, then, in order to construct one-time memories. We show that this can be done using a special class of quantum devices, called *isolated qubits*. These are qubits that can only be accessed using a special subset of quantum operations, known as *local operations and classical communication*, or LOCC. Intuitively, these are quantum operations

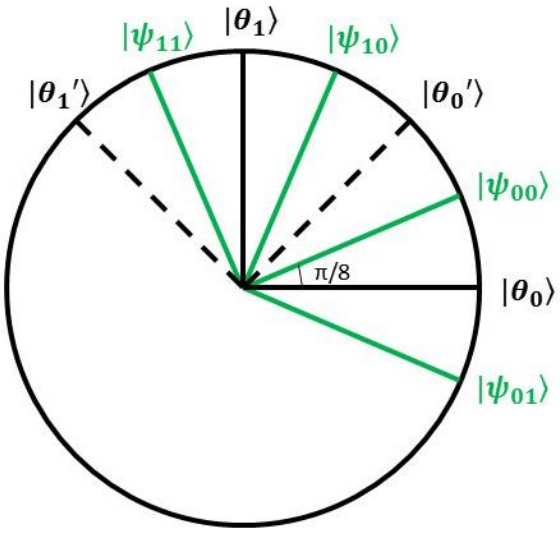

Figure 5. *One possible implementation of conjugate coding. A single qubit is prepared in one of four possible states* $|\psi_{ab}\rangle$*, which encode two classical bits a and b; these states are represented by two-dimensional vectors, drawn in green. To gather information about the bit a, one performs a measurement in the horizontal/vertical basis, represented by the vectors* $|\theta_0\rangle$ *and* $|\theta_1\rangle$*, drawn in black. This measurement returns an outcome m, which may be either 0 or 1, with probability* $|\langle\theta_m|\psi_{ab}\rangle|^2$*, that is, the square of the inner product of* $|\psi_{ab}\rangle$ *and* $|\theta_m\rangle$*. One can check that m = a with probability* $\cos^2(\pi/8) \approx 0.85$*. To gather information about the bit b, one performs a measurement in the diagonal basis, represented by the vectors* $|\theta_0'\rangle$ *and* $|\theta_1'\rangle$*, drawn with dashed lines. This measurement returns an outcome m, such that m = b with probability* $\cos^2(\pi/8) \approx 0.85$*.*

on single qubits, combined with classical control signals between the qubits.

To understand the properties of isolated qubits, it is helpful to think in terms of *entanglement*. Roughly speaking, quantum entanglement is a special kind of correlation between particles, which is stronger than that allowed in classical physics. Quantum entanglement is a powerful resource for communication and computation. It plays an essential role in quantum teleportation, and quantum algorithms for factoring large numbers in polynomial time. Yet entangled quantum states are also fragile, and easily damaged by interactions with their surrounding environment. To work with these entangled states, quantum computers have to perform elaborate error correction procedures.

Isolated qubits can only be accessed using LOCC operations, which cannot generate entanglement. Indeed, isolated qubits are designed so that it is *impossible* to prepare entangled states, or perform entangling operations. This is much easier than building a quantum computer; indeed, there are natural physical systems, such as solid-state nuclear spins, that have these properties. Moreover, it turns out that the *absence* of entanglement can be useful for cryptography. One can design protocols where an *honest* user does not need entanglement in order to participate, but a *dishonest* user needs entanglement in order to cheat (reminiscent of the "no go" theorems mentioned previously). This, roughly speaking, is how our one-time memories work.

More precisely, our one-time memories use an idea called *conjugate coding*, which was first proposed by Stephen Wiesner in the 1970s [8]. The basic idea is to encode two classical bits, *a* and *b*, into a single qubit, such that by performing different kinds of measurements on the qubit, one can gather information about either *a* or *b* (see Figure 5). One cannot reconstruct *a* or *b* perfectly; one can only guess the correct value with probability ≈ 0.85. However, by extending this idea to use a classical error-correcting code and multiple qubits, one can get a scheme that allows either *a* or *b* to be reconstructed reliably. This will be our candidate for a one-time memory.

The above scheme uses multiple qubits, and so the question naturally arises: what happens if one performs entangling operations on them? Wiesner pointed out that one can actually learn *both* of the messages *a* and *b* in this way. Using entangling operations, one can run the decoding procedure in superposition, and thereby learn *a* without damaging the quantum state; one can then repeat this procedure to learn *b*. This attack would break the security of our scheme.

Fortunately, we are able to avoid this problem, by building our one-time memories out of isolated qubits, where entangling operations are simply impossible. (One can check that our scheme still works correctly using isolated qubits, as the honest parties only need to perform LOCC operations.)

We then prove that these one-time memories are secure: we show that any adversary who performs only LOCC operations *cannot* learn both *a* and *b*, i.e., entanglement is *necessary* in order to break the security of this scheme. This is the main technical contribution of our work [2-4].

The proof requires several ingredients. The choice of a suitable error-correcting code is crucial for security and efficiency; we get good results by using a particular class of codes that are linear over *GF*(2), approach the capacity of the *q*-ary symmetric channel, and are efficiently decodable. We prove security using a high-order entropic uncertainty relation, which was originally devised for quantum cryptography in the bounded storage model. To complete the proof, we use a novel form of privacy amplification, with a fixed (deterministic) hash function that may be known to the adversary beforehand; this is needed because one-time memories are non-interactive, in contrast to interactive protocols such as quantum key distribution.

This result is an important step in a broader research project, whose goal is to build one-time programs (and other kinds of tamper-resistant hardware) whose security is based on physical principles. This project can be organized around different levels of abstraction:

1. Physical devices, e.g., solid-state nuclear spins.

2. Isolated qubits: a mathematical model of the physical devices.
3. One-time memories: cryptographic primitives built from isolated qubits.
4. One-time programs: general functionalities built from one-time memories.

Thus far, we have mainly studied constructions for one-time memories using isolated qubits. The next step will be to develop experimental implementations of isolated qubits, keeping in mind that real physical devices are never a perfect match for their idealized mathematical descriptions. Another step will be to understand the security issues that arise when many one-time memories are linked together to form one-time programs ("composable security"). Ultimately, by putting together all of these pieces, we hope to obtain a more rigorous methodology for building tamper-resistant cryptographic hardware.

References

[1] S. Goldwasser, Y. T. Kalai and G. N. Rothblum, One-Time Programs, in *Proceedings of CRYPTO 2008*, 39-56.

[2] Y.-K. Liu, Privacy amplification in the isolated qubits model, in *Proceedings of EUROCRYPT 2015*, to appear.

[3] Y.-K. Liu, Single-shot Security for One-time Memories in the Isolated Qubits Model, in *Proceedings of CRYPTO 2014*, Part II, 19-36.

[4] Y.-K. Liu, Building One-Time Memories from Isolated Qubits, in Proceedings of *Innovations in Theoretical Computer Science (ITCS) 2014*, 269-286.

[5] H.-K. Lo and H. F. Chau, Is Quantum Bit Commitment Really Possible? *Physical Review Letters* **78** (1997), 3410.

[6] H.-K. Lo, Insecurity of Quantum Secure Computations, *Physical Review A* **56**:2 (1997), 1154-1162.

[7] D. Mayers, Unconditionally Secure Quantum Bit Commitment is Impossible, *Physical Review Letters* **78** (1997), 3414-3417.

[8] S. Wiesner, Conjugate Coding, *ACM SIGACT News*, **15**:1 (1983), 78-88. (Original manuscript written circa 1970.)

Participants

Yi-Kai Liu (ACMD)

Computing Properties of Materials with Complex 3D Microstructures

Many macroscopic properties of materials, such as strength, hardness and corrosion resistance are dependent upon microstructure, the complex arrangement of material components visible only under a microscope. Material scientists wish to understand the mechanisms by which microstructure influences macroscopic properties, with the ultimate goal of designing new materials with particular microstructures in order to obtain desired properties. We have been developing software to enable matrial scientists to model such systems starting with an image of the microstructure. Previous versions of the software, OOF1 and OOF2, did two dimensional calculations on two dimensional images. By moving into three dimensions, OOF3D makes the calculations more directly relevant to real materials.

Stephen Langer

The OOF Project is a long running collaboration between the Applied and Computational Mathematics Division and the NIST Material Measurement Laboratory to model the properties of materials with complex microstructures. Such materials have complicated structure on scales larger than the atomic scale, but smaller than the macroscopic, everyday, scale. Metals are common examples. They are often composed of assemblies of grains, each of which is a single crystal, but which is oriented differently from its neighbors. The exact arrangement of the microscopic orientations can affect the macroscopic properties of the material. Ceramics are another example, often being composed of microscopic crystalline grains embedded in an amorphous matrix. Biological materials also often have complex microstructures. Bone appears to be a solid at large length scales, but is microscopically revealed to have an intricate porous structure. Artificial materials can also be constructed with complex microstructures by weaving, laminating, or etching.

Modeling a material mathematically or computationally gives researchers insights into why the material behaves the way that it does, and allows them to predict ways in which the material properties might be improved. There are two general schemes for modeling microstructures. The first is to assume that the randomness and complexities in the microstructure can be averaged out in a homogenization procedure. The second is to perform a brute force computation of the properties of a particular configuration of the microstructure and to examine in detail how that particular instance behaves. The first method has the advantage that it can be applied to large systems and can in some cases lead to analytical results. On the other hand, homogenization discards information and cannot compute effects that depend upon the less probable (but still extant) features of a microstructure. For a simple example, consider a material made of two components with very different thermal conductivities. The thermal conductivity of the bulk material will depend on whether or not the high conductivity regions can be joined together to form a continuous path from one side of the sample to another. A homogenization method that assumes a regular repeating structure is unlikely to compute the correct bulk conductivity. A brute force computation won't compute the correct average behavior (even if the word "average" can be well defined) but repeated brute force calculations will compute the correct result for particular samples, and give insight into their statistical distribution.

OOF is a tool for brute force computations of the properties of microstructures. Using it, a researcher starts with a real or simulated image of a microstructure, assigns material properties to the features of the image, constructs a finite element mesh, and solves the relevant physics equations for the properties of interest. The solution can be viewed at the microscopic level, or averaged over the whole system to compute its effective macroscopic properties. OOF solves a wide variety of linear and nonlinear problems in elasticity, polarization, and thermal conductivity, including couplings such as piezoelectricity and thermal expansion.

The OOF project began in the late 1990's with OOF1, which was written in C++ and could only solve two dimensional static elasticity and thermal conductivity systems. OOF2, which was a complete rewrite of OOF1 in a combination of C++ and Python, improved OOF's modularity enormously and added the ability to solve time-dependent systems, but was still restricted to two dimensions. OOF3D, which was released this past year, does almost everything that OOF2 can do, but does it in three dimensions. There were two reasons for limiting OOF1 and OOF2 to two dimensions: at the time there were few experimental methods for obtaining detailed 3D microstructures, and 2D calculations are substantially easier than 3D ones. The situation has changed, and now there are many techniques being used to get 3D microstructural data [1], so there is a need for a 3D version of OOF.

Migrating from two to three dimensions has been a multi-year effort. The basic control structures and graphical user interface used in OOF2 survives unchanged in OOF2, with the exception of the code for displaying microstructures and meshes, which had to be completely replaced. Both programs use PyGTK [2] for

user interface components (menus, buttons, and other widgets), but OOF2 uses the Gnome canvas [3] for displaying two dimensional images and other graphical objects, while OOF3D uses the VTK [4] visualization toolkit. Using VTK efficiently required modifying some of OOF2's methods for storing and manipulating images and meshes, but most of the code for setting up and solving equations could be transferred virtually unchanged from OOF2 to OOF3D. (The exceptions were the boundary condition code, which had to be extended to handle two dimensional boundaries, and the OOF2 code for handling plane-stress, plane-strain, and their generalizations, which had to be eliminated.)

Using either OOF2 or OOF3D involves the following steps.

1. Load an image and assign material properties to its features. For example, each pixel (or voxel, in 3D) could be given a particular elasticity modulus and crystal orientation. Figure 6 is a small sample from a micrograph of bone, showing that it is constructed from two different materials on the microscale.
2. Superimpose a uniform mesh on the image. In 2D, this can be either a triangular or quadrilateral mesh. In 3D, it must be tetrahedral (for now).
3. Modify the mesh so that it is a good representation of the image, by moving nodes and subdividing (refining) elements. (Figure 7 shows an OOF3D mesh adapted to the image in Figure 6. Elements from only one material are filled in.) OOF provides a number of mesh modification tools. Ideally, after the mesh is modified all of the pixels within every mesh element will have the same material properties as the other pixels within that element; that is, the ideal element will be homogeneous. The OOF2 and OOF3D mesh modification tools use the homogeneity as part of an element fitness function, and it is important that the function be a continuous function of the mesh node positions. To make the homogeneity continuous, the program needs to compute the fractional area or volume of pixels through which an element edge passes. This calculation is the most CPU intensive part of the 3D mesh construction process and is one of the biggest under-the-hood differences between OOF2 and OOF3D.
4. Define which fields (temperature, displacement, etc.) will be defined on the mesh, and which equations (force balance, heat flow, etc.) will be solved. These must be consistent with the material properties assigned to the image.
5. Set boundary conditions and initial values.
6. Choose a solver and solve the equations. OOF2 offers a number of different solution methods, but

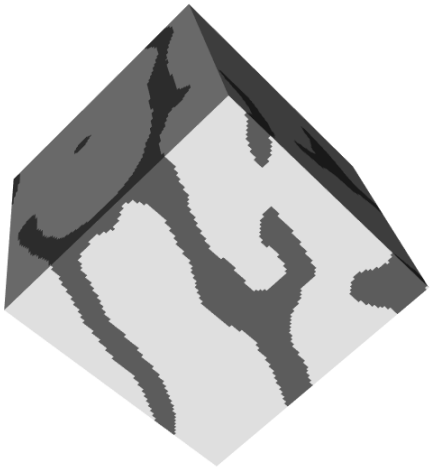

Figure 6. *Small sample from a micrograph of bone, showing that it is constructed from two different materials on the microscale.*

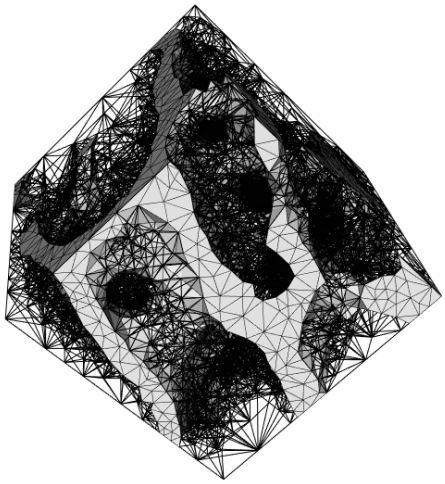

Figure 7. *An OOF3D mesh adapted to the image above.*

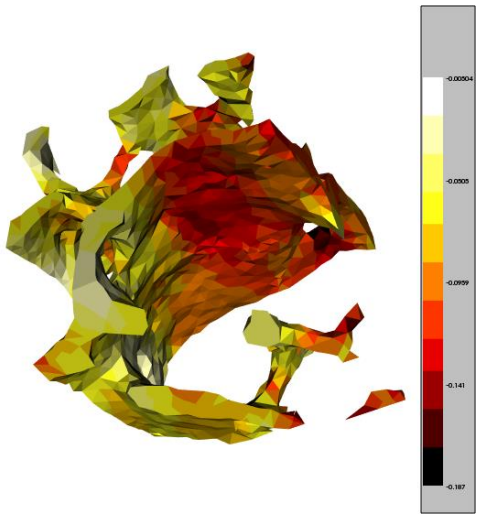

Figure 8. *Example result from a computational simulation run using the mesh above.*

also has a "Basic" mode which makes reasonable default choices for non-expert users.

7. Visualize the results and compute output quantities. Figure 8 demonstrates a possible solution on the bone sample from Figure 6. The two materials have been given different thermal conductivities and a temperature gradient has been imposed on the sample. The colors indicate the local value of the heat flux. (Because the input conductivities and the boundary conditions were arbitrarily chosen for this example, the actual values of the outputs aren't meaningful.)

Development continues on both OOF2 and OOF3D. Future work will allow the programs to compute more physical properties, particularly plasticity and surface effects. Both programs can benefit from parallel processing, and OOF3D will get more flexible methods for user interaction.

OOF3D can be downloaded from NIST (see below). It runs only on Linux and Macintosh OS X systems, although it can be used inside a Linux virtual machine on Windows.

References

[1] A. P. Cocco, et al. Three-dimensional Microstructural Imaging Methods for Energy Materials, *Physical Chemistry Chemical Physics* **15** (2013), 16377.

[2] http://www.pygtk.org/

[3] https://developer.gnome.org/libgnomecanvas/stable/GnomeCanvas.html

[4] http://www.vtk.org/

Participants

Stephen Langer (ACMD), Gunay Doğan (Theiss Research), Yannick Congo (ISIMA) and Andrew Reid (NIST MML).

http://www.ctcms.nist.gov/oof/
http://www.ctcms.nist.gov/oof/oof3d

Modeling and Optimization in Cryobiology

Cryopreservation, whose goal is to preserve biological cells, tissue and organs by storing them at very low temperature, broadly impacts the medical and agriculture industries and has a growing role in forensic science. In the field of cryobiology, which sits at the intersection of biology, chemistry and physics, mathematical and computational science plays an increasing and crucial role in establishing, investigating and interpreting approximate models that can be used to predict and control complex processes. Optimization techniques applied to these computational models allow cryobiologists to develop effective and efficient cooling and warming protocols that can be applied to biological specimens in practice. Our work has been directed towards this problem on numerous fronts. First, we have developed first principle models of thermal, chemical and mass transport in cryobiological systems. These mathematical models take the form of coupled partial differential equations with multiple moving boundaries representing (solid-liquid) phase boundaries and semi-permeable cellular membranes. Second, we have begun the process of establishing computational strategies for solving these mathematical models to enable predictions for the thermal and chemical environment inside a biological cell. Third, we have started to develop optimization and control techniques for investigations of cooling strategies that can be used to help improve existing cryoprotocols and to establish new ones.

Anthony Kearsley

Cryopreservation is the maintenance of the viability of biological cells, tissues, and organs at very low, *cryogenic*, temperatures (< −150° C). Cryopreservation, and more generally cryobiology—the study of biological organisms at cryogenic temperatures—broadly impacts the field of medicine, plays a crucial role in agriculture and is important in the fight to maintain earth's biodiversity.

Since the first successful cryopreservation of human spermatozoa (1954) and later embryos and oocytes (mid 1980s) cryopreservation has played an increasing role in the medical industry for assisted reproduction and in vitro fertilization (IVF) [2]. The cryopreservation of larger-scale biospecimens (e.g., articular cartilage, the cornea, ovarian tissue), which is complicated by their larger size, complex shapes and presence of vascular and layered structures, is an important capability enabling organ transplantation and other medical applications, including "biobanking" and "personalized medicine."

Figure 9. *Oocyte or immature ovum.*

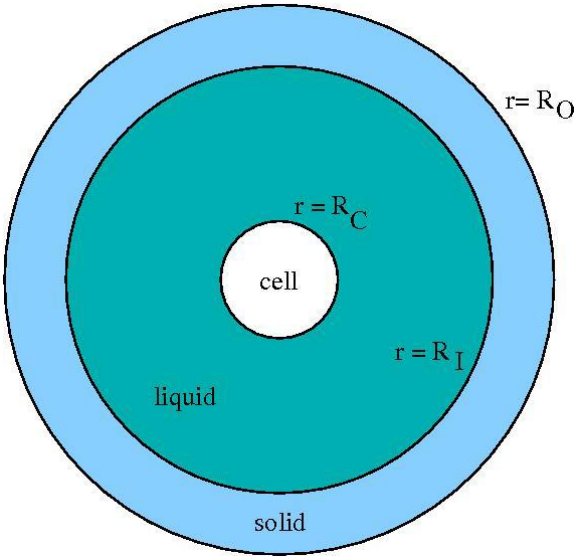

Figure 10. *Discretization of oocyte, a spherical cell at center: R_C, an aqueous ternary solution between R_C and R_I and cooling at R_O.*

The agriculture industry relies on cryopreservation of embryos and spermatozoa for assisted reproduction, and to address concerns about preserving farm animal genetic diversity. In addition to livestock, biobanking has been important for other species as well. A cryobanking initiative based at the Smithsonian Institution[13] containing over 1 million samples from over 18,000 species aims to preserve a wide range of biological specimens including ones for rare and endangered species. There are also efforts towards preservation of genetic materials for agriculture (e.g., seed banks), worldwide efforts for cryopreservation of threatened or

[13] The Pan-Smithsonian Cryo-Initiative

endangered plant species, as well as other efforts driven by the food industry.

There is also considerable interest in the understanding, preservation and processing of frozen biological samples in forensic science. For instance, processing at cryogenic temperatures has found a range of uses ranging from the detection of volatile substances in arson investigations to the recovery of DNA. Other cold-temperature forensic applications, which are in some cases more relevant at non-cryogenic temperatures, include the measurement of volatile organic compounds in bodily fluids, the postmortem analysis of frozen tissue, and the need to understand the stability and degradation of evidence contained in frozen samples of bodily fluids, tissues and bones.

The role of mathematical sciences in cryobiology is on the rise. The development of more effective and efficient cooling and warming cryoprotocols for a broad range of biospecimens require improved mathematical models of thermal, chemical and mass transport processes and sophisticated control and optimization schemes (see for example [4]). This project is directed towards addressing these needs.

Fundamental scientific questions in the field of cryobiology, as well as practical issues in cryopreservation protocols, are incredibly complex and span the breadth of plant and animal genetic diversity. This diversity creates an immense challenge for the development of cryoprotocols. Even though information gained from one species may be helpful in the understanding and development of cryoprotocols for a related species or sample type, this is not always the case, and in general a cryoprotocol developed for one species may not be effective for another species. Indeed, successful cryopreservation varies among individuals within a given species and varies with age, for example, for a given individual.

The biological details (plant versus animal, seed versus shoot/sprout, cell versus tissue) are coupled in critical ways to physical processes such as thermal, mass and chemical transport. These transport processes are in turn coupled to motion of both phase transforming boundaries (e.g., freezing or melting solid–liquid interfaces) and flexible, semipermeable biological membranes. The physical processes that are shared among these diverse systems, and the associated mathematical descriptions, provide a basis for which understanding of cryopreservation can be advanced. Also shared among these diverse systems is the goal of identifiying optimal cooling, warming and preservation strategies measured with respect to various objectives such as ice nucleation, chemical toxicity (and ultimately survival rates) not to mention time and cost. The predictive capabilities of mathematical and computational models to aid in the development of effective cryoprotocols for these systems are thus of considerable importance.

Over the last half century there has been a considerable amount of work in bio-heat and mass-transport, and these models and theories have been readily and repeatedly applied to cryobiology with much success. However, there are significant gaps between experimental and theoretical results that suggest missing links in models. One source for these potential gaps is that cryobiology is at the intersection of several very challenging aspects of transport theory: it couples multicomponent, moving boundary, multiphase solutions that interact through a semipermeable elastic membrane with multicomponent solutions in a second time-varying domain, during a two-hundred Kelvin temperature change with multi-molar concentration gradients and multi-atmosphere pressure changes.

In order to address these challenges we have been developing, from first principles, a theory of coupled heat and mass transport in cryobiological systems accounting for these effects. In our work, we fix ideas to the geometrically simple case of the cooling and dehydration of a single cell, such as an oocyte (see Figure 9), whose primary characterization is that its membrane is semi-permeable.

A major component in the current understanding of cryobiology that provides the basis for many prevailing cryopreservation strategies is the classical "two factor hypothesis" [3]. This hypothesis suggests that an optimal cooling rate lies somewhere between two extremes: (1) cool too quickly and the cell cannot remove water (dehydrate) fast enough to avoid intracellular ice formation that damages or kills the cell, and (2) cool too slowly and chemical toxicity due to overexposure of the cell to high solute concentrations causes cell injury or death. Successful cryopreservation also in general relies on the introduction of additional solutes known as cryoprotective agents (CPAs) into the surrounding fluid. Of interest here are membrane-permeable CPAs (e.g., glycerol, ethylene glycol and other small-molecule polyols) that enter the cell (and water exits the cell) and have the effect of (1) achieving more safely (ideally, at least) a desired level of dehydration with a lower intracellular salt concentration, and (2) promoting intracellular glass formation (vitrification) via an increase in intracellular viscosity and decrease in melting temperature while reducing the tendency towards ice formation. Extracellular (non-permeating) CPAs (e.g., glucose, sucrose and other sugars) are also used to help dehydrate the cell prior to cooling and to promote vitrification.

Our first step in the development of a mathematical model for thermal transport, chemical transport, mass transport and solidification processes of an externally-cooled ternary mixture that surrounds a biological cell, was to establish a thermodynamic framework suitable for cryobiological applications [1]. This work involved the identification of various forms for the Gibbs free energy for non-dilute chemical systems and forms for chemical potential gradients used in the definition of

chemical fluxes. These forms for chemical fluxes involve transport models for both naturally occurring solutes and the CPAs in these biological systems. Literature on models, experiments and measurements in cryobioloigical systems involve a variety of measures of chemical composition (e.g., mole fraction, molarity, molality, etc.) and our contributions include formulations with respect to these different choices.

Ongoing and future efforts in this direction include

- the development of bulk transport models as well as their coupling to both phase-change (solidification) boundaries and the semi-permeable cell membrane,
- the formulation and computations of partial differential equations and coupled boundary conditions specific for a spherical cell geometry surrounded by a ternary solution, and
- addressing the cryobiology-driven question of control of the thermal and chemical state of the cell by manipulation of the external container temperature.

References

[1] D. M. Anderson, J. D. Benson and A. J. Kearsley. Foundations of Modeling in Cryobiology—I: Concentration, Gibbs Energy, and Chemical Potential Relationships, *Cryobiology* **69** (2014), 349-360.

[2] L. Herrero, M. Martínez and J. A. Garcia-Velasco. Current Status of Human Oocyte and Embryo Cryopreservation, *Current Opinion in Obstetrics and Gynecology* **23**:4 (2011), 245-250.

[3] P. Mazur, S. Leibo and E. Chu, A Two-factor Hypothesis of Freezing Injury: Evidence from Chinese Hamster Tissue-Culture Cells, *Experimental Cell Research* **71**:2 (1972), 345–55.

[4] J. D. Benson, A. J. Kearsley and A. Z. Higgins, Mathematical Optimization of Procedures for Cryoprotectant Equilibration using a Toxicity Cost Function, *Cryobiology* **64** (2012), 144-151.

Participants

Anthony Kearsley, Daniel Anderson, Andrew Dienstfrey and Geoffrey McFadden (ACMD), James Benson (Northern Illinois University), Adam Higgins (Oregon State University)

Modeling of Kinetic-based Micro Energy-Harvesters for Wearable and Implantable Sensors

The promise of wearable and implantable wireless sensors have generated a great deal of interest in the field of health information technology. However, there are still numerous challenging issues, including reliability, cost, sensing and actuator technology, privacy and security, and power efficiency. RF-enabled wearable sensors offer an attractive set of e-health applications, among which are monitoring of temperature, respiration, heart rate, and blood pressure. As these sensors are small and mainly rely on very small batteries to carry out their functions, prolonging their operational lifetime could significantly help their commercial applications. We are investigating the feasibility of capturing and storing kinetic energy from human body motion to power such devices. To do this we have developed a statistical model of acceleration generated as a result of typical human motion, modeled a micro-harvester device suitable for wearable/implantable applications, and modeled and characterized the instantaneous power that can be generated by the device.

Kamran Sayrafian

Energy Harvesting (EH) refers to the process of capturing and storing energy from external sources or ambient environment. There are few sources from which we can harvest energy for wearable and implantable medical sensors, amongst them are body heat and body movement. For example, a thermopile device can be attached to the body to convert its thermal energy into electrical energy. This is called thermoelectric EH. On the other hand, random motion of our arms and legs can generate kinetic energy that piezoelectric materials can convert to electrical energy. Kinetic energy harvested from human body motion seems to be one of the most convenient and attractive solutions for wearable or implantable wireless sensors in healthcare applications. Due to their small size, such sensors have a very limited battery power supply which necessitates frequent recharge or even sensor replacement. Energy harvesting can prolong the battery lifetime of these sensors. This could directly impact their everyday use and significantly help commercial applications such as monitoring of physiological signs (i.e., telemedicine).

Kinetic-based energy harvesting devices operate similarly to a spring and damper system. The direction of the force that acts on the mass distinguishes two categories of kinetic-based EH, namely direct versus inertial force. With direct force the direction of the force opposes the motion; while in the inertial method (i.e., acceleration) force is applied along with the motion. The most common examples of direct force EH are the heel strike, shoe sole (bending the ball of the foot), and knee joints (i.e., movement of adjacent body parts). A good example of inertial EH that is already in widespread use is the kinetic watch. An advantage of inertial EH devices is that they employ a single attachment point to its internal moving structure; therefore, its overall physical size can be minimized as compared to direct force energy harvesters. This makes them an appropriate candidate for wearable or implantable body sensors that are desired to be very small in size.

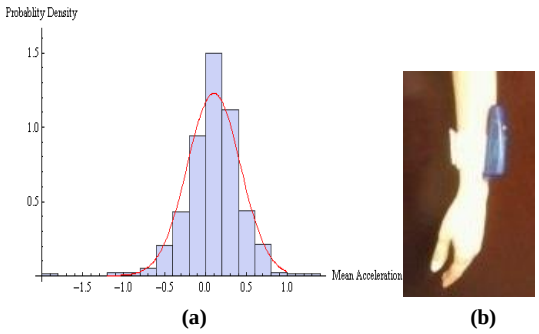

Figure 11. *(a) Histogram of average acceleration of the human arm, (b) Placement of the accelerometer.*

Current research on energy harvesting mostly focuses on device technology. However, a fundamental question that needs to be addressed is the amount of harvestable energy which can be made available to wearable and implantable sensors. Our research objective is to investigate this question by statistical modeling of acceleration generated as a result of typical human motion, modeling of a micro-harvester device suitable for wearable/implantable applications, and then modeling and characterizing the instantaneous power that can be generated by the device.

To characterize the input acceleration, we have chosen human arm and leg motion, though we plan to extend this to other parts of the body as well. At this point, the placement of the micro-harvester on the body is not the main focus of our research. Instead, we would like to have a better understanding of the amount of harvestable energy. To measure acceleration, we use a triaxial accelerometer that can be attached to the forearm or leg, and secured with a strap to prevent unnecessary movement (see Figure 11b).

The measurement samples are time-stamped and stored in the on-board memory so that they can be retrieved at a later time. The amplitude and frequency of human body acceleration during normal daily activities can range from -12 g to 12 g and up to 20 Hz respectively. However, there are rare occurrences of higher

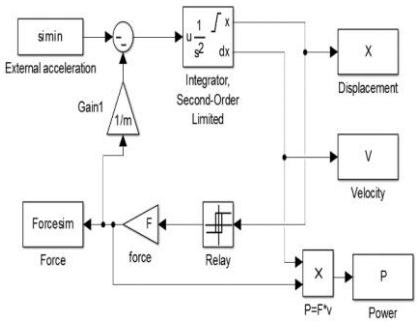

Figure 12. *Simulink model of the CFPG main component.*

frequencies, for example at the foot and during heel strike when walking. We chose a sampling rate of 64 Hz for acceleration measurements with an amplitude range of ±6 g. The accelerometer was worn for up to 8 h by 30 individuals[14]; a total of 240 h of data were obtained. Participants in this study were staff in NIST's ITL. Figure 11a shows the histogram of average acceleration due to typical human forearm movement during the day.

Using a mathematical model of an appropriate micro-harvester architecture, namely a Coulomb-force parametric generator (CFPG), we developed a methodology [1, 2] to estimate the average generated mechanical power from typical human motion. Our preliminary results show that for a small inertial-based micro-harvester with dimension 1 cm × 1 cm × 1 mm, the average harvested power is around 1 µW to 2 µW for the forearm and around 4 µW to 10 µW for leg motion. Since wearable/implantable medical sensors are envisioned to operate at microwatt levels, such EH mechanism seems to be a promising technique for prolonging operational lifetime or equivalently reducing the required frequency of recharge.

Next, we have started to model the internal architecture of the CFPG in order to study the temporal behavior of the generated power. Having such a dynamic model not only helps to have a more accurate estimation of the amount of power generated from various human movements, but also allows us to optimize the design or operational parameters of the micro-harvester (e.g., size/dimension, electrostatic holding force, etc.) with the characteristics of the input acceleration. To achieve this, we used Simulink to create an implementation of the main mechanical component in a CFPG device, ensuring that it satisfies all physical constraints that impact the generated power. In doing so, we modified the mathematical model (i.e., a nonlinear differential equation) that represents the operation of the device. The Simulink implementation of this model is depicted in Figure 12. Several test scenarios were generated to verify its validity. This model can be used to measure the amount of mechanical power generated. The conversion to electrical power is done through a transducer module inside a micro-harvester. We plan to develop a Simulink model for the transducer, and study the power generated by various input excitations.

Another objective in our study is to characterize the impact of the internal micro-harvester physical parameters (e.g., electrostatic force) on the amount of generated power. Once set, such parameters are typically kept constant irrespective of the input acceleration. In our research, we would like to show that by judiciously choosing parameters one can maximize the average generated power. We have formulated and solved an optimization problem that captures the above statement. Preliminary results show that about a 5-fold gain in the amount of harvested power can be expected.

Integration of micro-energy harvesting technology with wearable sensors seems to be a promising approach in prolonging the operational lifetime of wearable and implantable medical sensors. Optimizing the architectural and design parameters of the harvester device based on the characteristics of the input acceleration will further increase the amount of the generated power. This is a prime example of a cyber-physical system (CPS) that highlights how joint design of the cyber and physical components can improve the system efficiency. By adaptively tuning the internal parameters of the EH device for various human body motions, one can expect an improved efficiency in harvesting kinetic energy. We plan to continue this research and study the impact of adaptive optimization on the harvestable power using a CFPG architecture.

[14] Approval for use of human subjects in the course of this study has been documented in NIST IRB Case 358.

References

[1] N. Yarkony, K. Sayrafian and A. Possolo, Statistical Modeling of Harvestable Kinetic Energy for Wearable Medical Sensors, in *Proc. of the IEEE International Symposium on a World of Wireless Mobile and Multimedia Networks*, Montreal, Canada, June 14-17, 2010

[2] N. Yarkony, K. Sayrafian and A. Possolo, Energy Harvesting from the Human Leg Motion, in *Proc. of the 8th Int. Conference on Pervasive Computing Technologies for Healthcare*, Oldenburg, Germany, May 2014

[3] M. Dadfarnia, K. Sayrafian, P. Mitcheson and J. Baras, Maximizing Output Power of a CFPG Micro Energy-Harvester for Wearable Medical Sensors, in *Proc. of the 4th Int. Conference on Wireless Mobile Communication and Healthcare*, Athens, Greece, Nov. 2014

Participants

Kamran Sayrafian (ACMD), Mehdi Dadfarnia (NIST EL), Antonio Possolo (NIST ITL), Paul Mitcheson (Imperial College, UK)

Recovery of Background Structures in Nanoscale Helium Ion Microscope Imaging

Successful nanoelectronics manufacturing requires high quality imaging and accurate measurements at the sub-nanometer scale. The Helium Ion Microscope (HIM) is an important new imaging and metrology tool that can provide the needed accuracy. At a given energy level, the wavelength of He ions is much smaller than that of electrons at the same energy. As a result, HIM imaging can produce up to four times higher resolution than is possible with current large sample scanning electron microscopes (SEM), along with higher contrast and greater depth of field. Moreover, the secondary electrons that carry the sample's surface detail information are generated in higher quantities by He irradiation than with electron beams, leading to much greater surface detail in HIM images. Indeed, because the secondary electron yield is so large, low probe currents on the order of one pico ampere, can be used effectively to acquire useful HIM images while minimizing damage to the sample. These and other advantages of HIM imaging are more fully explored in [10] and [11]. However, such low probe currents can induce degradations: HIM images are often noisy, and important background structures may not be easily discernible due to the weak signal. Techniques that can overcome such degradations are of paramount interest. We have discovered an unexpectedly effective recovery and enhancement method, which is discussed below.

Alfred S. Carasso

The first commercial HIM instrument, a Zeiss Orion Plus was installed at NIST in 2008, under a cooperative research and development agreement. Considerable HIM imaging experience has since been accumulated at NIST, and that experience is being shared with the manufacturer. One particularly important imaging technique developed by the NIST Semiconductor and Dimensional Metrology Division, is the *fast scan* method which produces much sharper images, [4-6]. This methodology is based on super-fast acquisition of a large number of image frames. Due to the small beam currents generally used in scanning particle beam microscopy, these individual frames are inherently very noisy, but exhibit significantly less drift-related distortions. The drift correction takes place after finding the center of each frame, properly aligning these frames, and adding them together into a single image. Such composed images contain much less noise and exhibit significantly less blur and deformation than do images obtained by traditional slow scan methods, or images obtained by simply adding together fast image frames without compensating for drift. To improve repeatability, this technique must be used with the minimum number of fast images, which limits the achievable signal to noise ratio. In many cases, the resulting composed image is still somewhat noisy and some type of noise processing may be beneficial.

Separately and independently, and over several years, considerable expertise has been acquired in ACMD on the use of *Lévy fractional diffusion* in image restoration, with application to medical and astronomical images [1, 2]. Most recently, [3], a significant new application was made to forensic latent fingerprint enhancement. The experience gained in the above fingerprint work led to the development of a useful *Interactive Data Language* (IDL) software routine [8] for enhancing noisy HIM images, as well as other images in which background structures are not easily discernible due to a weak signal.

This two stage enhancement approach involves a preliminary image-specific *adaptive histogram equalization* of the given HIM image [12]. Such equalization enhances background information while significantly magnifying noise, and is not generally advisable with noisy data. However, at the second stage, an effective and easy to use denoising technique, based on *progressive* low exponent Lévy fractional diffusion smoothing, can be successfully applied to this histogram equalized image with magnified noise. As may be inferred from Figure 14, such *slow motion* Lévy smoothing can be fine-tuned interactively so as to preserve the detailed surface morphology of the sample. Comparable fidelity to surface detail was not found feasible with some other better-known denoising techniques, such as methods based on minimizing the image "total variation" (TV) norm [7, 9], or methods based on thresholding curvelet transforms [13, 14]. This is illustrated in Figure 15, which should be viewed at high magnification on a high resolution monitor. The superior enhancement in Figure 14 may partially be explained on the basis of Eq. 5.

Progressive Low Exponent Lévy Fractional Diffusion Smoothing. Given a noisy image $f(x,y)$, the smoothing procedure results from solving an initial value problem for a special type of diffusion equation, with the image $f(x,y)$ as initial data. Such smoothing is applied to the whole image, and not just to a selected portion of the image. With fixed p with $0 < p \leq 1$, consider the linear fractional diffusion initial value problem in $L^2(R^2)$,

$$w_t = -(-\Delta)^p w, \quad t > 0, \quad w(x,y,0) = f(x,y) \qquad (1)$$

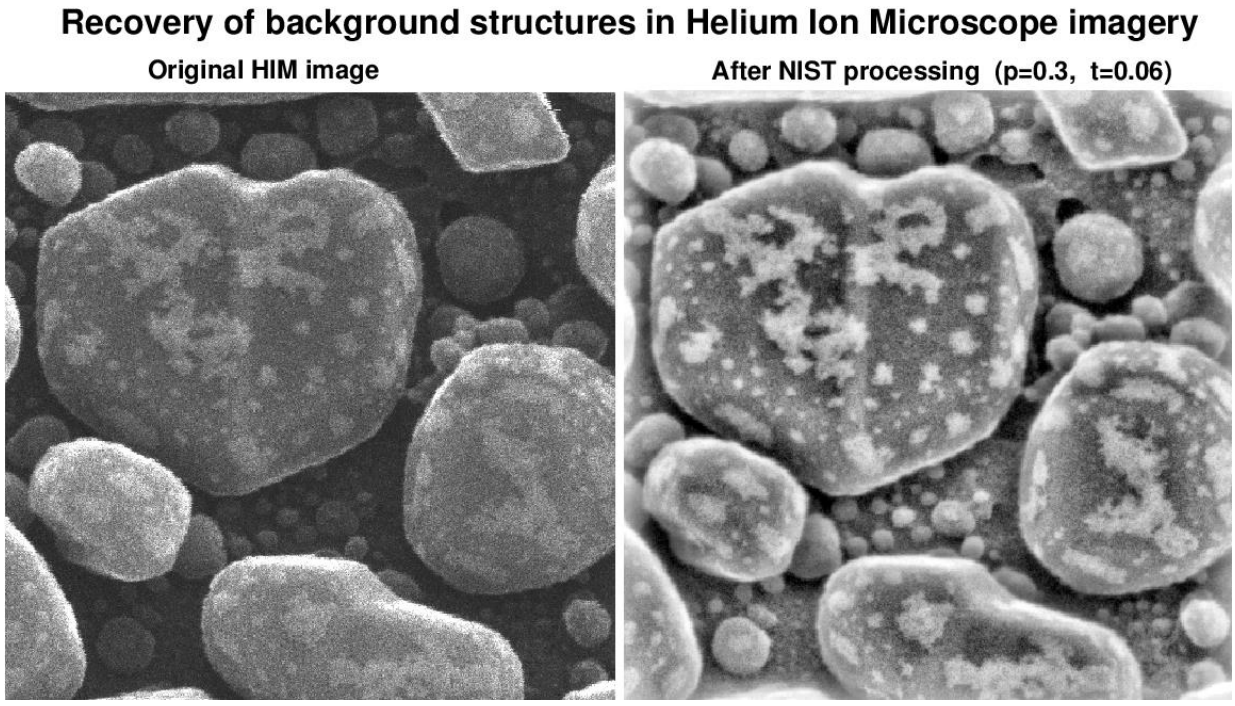

Figure 13. *NIST processing of original 600 nm field of view HIM image of Au-decorated gold on carbon sample. Two step process results in a companion image displaying significant background structural detail that is not readily apparent in the original image.*

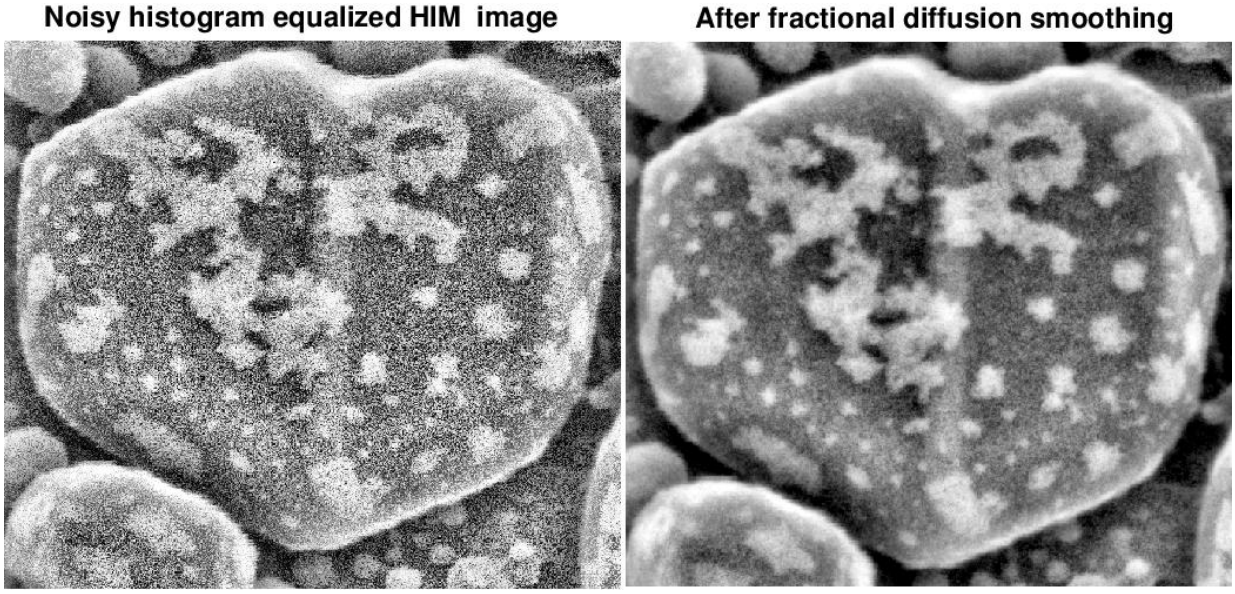

Figure 14. *Two stage NIST process involves preliminary adaptive histogram equalization in original HIM image (left). This enhances background information but significantly amplifies noise. Second stage (right) applies versatile fractional diffusion smoothing that can filter out noise while preserving delicate morphological details.*

where Δ denotes the 2D Laplacian. This reduces to the classical heat conduction equation when $p = 1$. However, our smoothing procedure uses values of $p \ll 1$, such as $p = 0.1$, for example. Define the 2D Fourier transform of the image $f(x,y)$ by

$$\mathcal{F}\{f\} = \hat{f}(\xi,\eta) \equiv \int_{R^2} f(x,y)\exp\{-2\pi i(\xi x + \eta y)\}\,dx\,dy \quad (2)$$

Eq. 1 has the unique Fourier domain solution

$$\widehat{w}(\xi,\eta,t) = \exp\{-t[(2\pi\xi)^2 + (2\pi\eta)^2]^p\}\hat{f}(\xi,\eta), \quad t > 0 \quad (3)$$

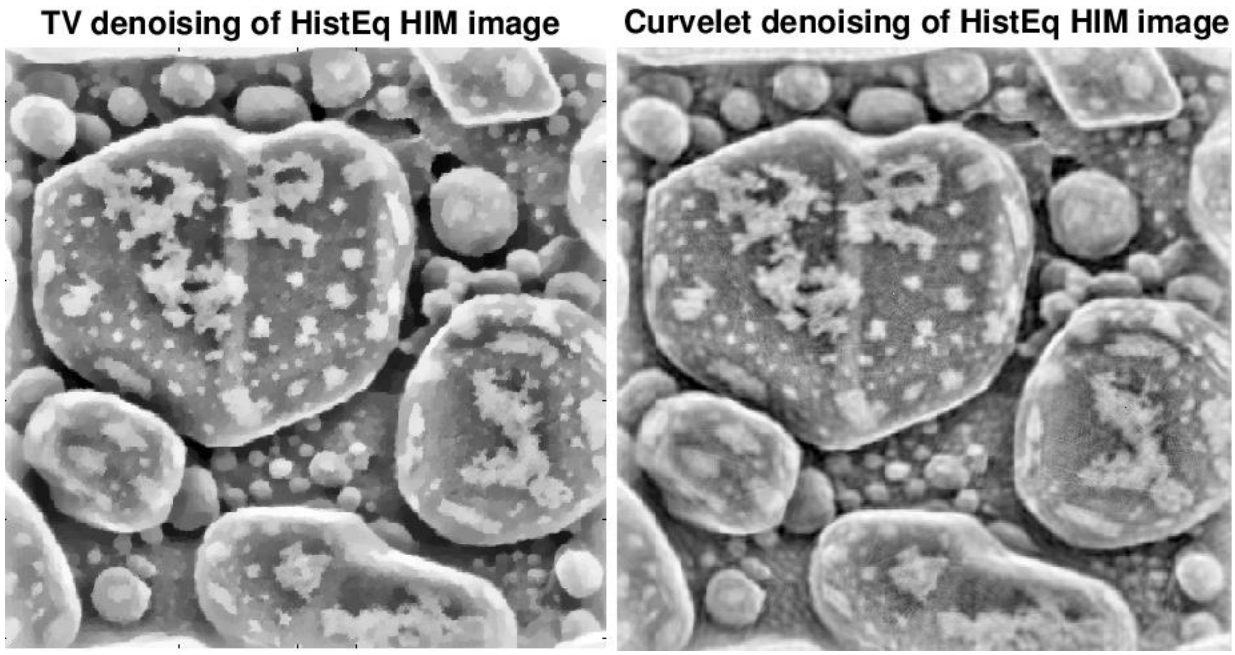

Figure 15. *Split Bregman Total Variation (TV) denoising (left) generally does not preserve small-scale surface detail with sufficient fidelity. Denoising using Curvelet Thresholding (right) is time-consuming, and can generate misleading artifacts. Here, spurious criss-crossing lines in Curvelet image become clearly visible under magnification, when viewed on high resolution monitors.*

from which $w(x,y,t)$ can be found by inverse Fourier transformation

$$w(x,y,t) = \int_{R^2} \exp\{2\pi i(\xi x + \eta y)\} \times \exp\{-t[(2\pi\xi)^2 + (2\pi\eta)^2]^p\}\hat{f}(\xi,\eta)\, d\xi\, d\eta \quad (4)$$

As is evident from Eq. 3, $w(x,y,t)$ becomes increasingly smoother as t increases. However, for small p, and over a short time interval, the smoothed image may be expected to retain many of the essential features present in the initial data $f(x,y)$. This expectation is reflected in the following sharp inequality which expresses the rate at which $\|\nabla w(.,t)\|_2$ becomes infinite as $t \downarrow 0$. With e = 2.71828...,

$$\|\nabla w(.,t)\|_2 \le \{2pte\}^{-\frac{1}{2p}}\|f\|_2, \quad t > 0. \quad (5)$$

In the case of Gaussian smoothing, corresponding to p = 1, this inequality implies $\|\nabla w(.,t)\|_2 = O(t^{-\frac{1}{2}})$ as $t \downarrow 0$. In contrast, $\|\nabla w(.,t)\|_2 = O(t^{-5})$, ~as $t \downarrow 0$, when p = 0.1. This suggests that for small $t > 0$ and $p \ll 1$, the solution $w(x,y,t)$ retains considerably more of the small scale features in the initial data $f(x,y)$, than is the case with Gaussian smoothing. The above inequality may also possibly explain why Lévy fractional diffusion smoothing in Figure 14 leads to higher fidelity than is the case with the methods used in Figure 15.

IDL Code for FFT Implementation of Slow Motion Lévy Smoothing. Adaptive histogram equalization is a useful enhancement technique for images where significant information is suspected of being hidden in dark regions. However, in practice, usefully recovered background information is often obscured by the amplification of the accompanying noise, and the resulting improvements may not be particularly helpful without additional intervention. Here, the adaptively equalized HIM image is used as the initial data $f(x,y)$ in Eq. (1). Forward and inverse FFT are used to implement the operations in Eq. 3 and Eq. 4 respectively, at any $t >$ 0. After pre-selecting the Lévy exponent p, and a tentative maximum smoothing time T_{max} at which to terminate the smoothing process, Eq. 4 can be evaluated at finitely many intermediate times $0 = t_0 < t_1 < t_2 < t_3 < \ldots = T_{max}$, to create a suite of *progressively smoother* images. Such a suite can be acquired and displayed in a few seconds, even with 1024 × 1024 pixel images. Several different pairs (p, T_{max}) can be explored in a matter of minutes.

The success of this method in practice derives in large measure from the ability to explore efficiently in parameter space and visually select the best result. There is no single set of parameters that will be useful in all cases, nor is there an automatic way of selecting the best set of parameters. However, a trained and experienced human analyst can generally locate useful parameter values and determine the proper amount of fine tuning that best displays the information sought.

The example in Figure 16 demonstrates significant background recovery and sharpening in a HIM image. Useful application of the method to a *fast scan* composed SEM image, is shown in Figure 17. Note the low values of p and t in these images and in Figure 13.

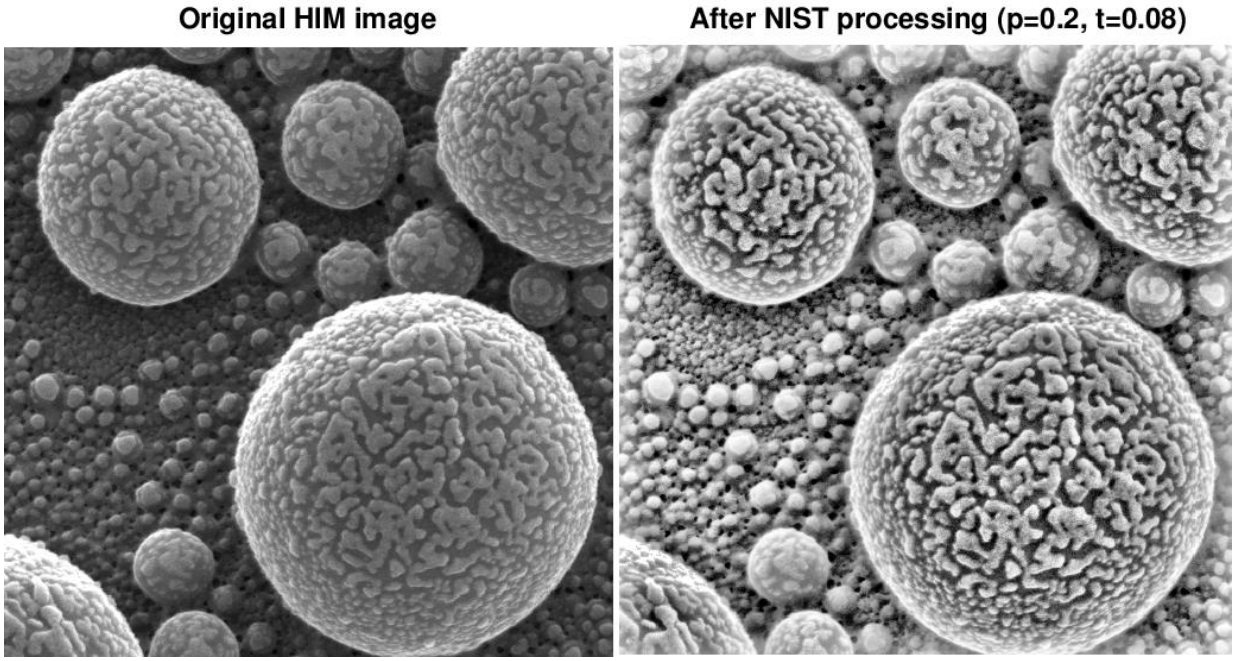

Figure 16. *NIST processing of original 1.5 μm field of view HIM image of Au decorated tin ball sample.*

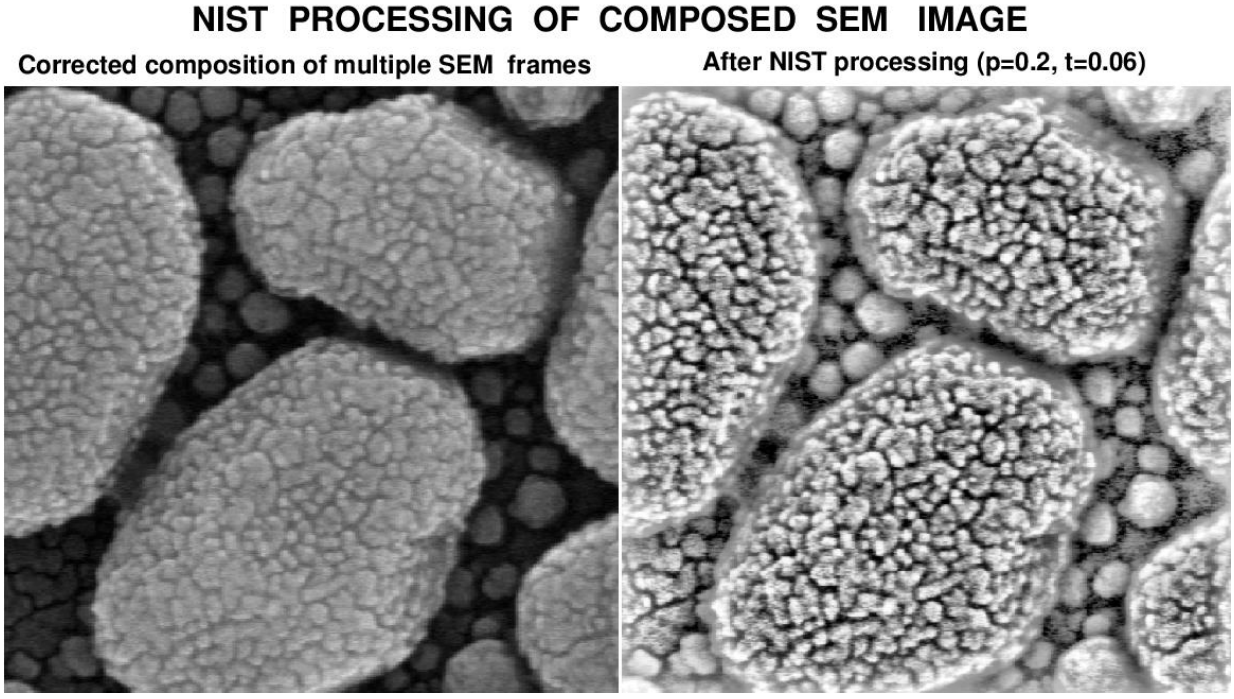

Figure 17. *NIST processing of composed SEM image of platinum decorated gold on carbon sample, with a field of view of 441 nm.*

References

[1] A. S. Carasso, The APEX Method in Image Sharpening and the Use of Low Exponent Lévy stable laws, *SIAM Journal on Applied Mathematics* **63** (2002), 593–618.

[2] A. S. Carasso, APEX Blind Deconvolution of Color Hubble Space Telescope Imagery and Other Astronomical Data, *Optical Engineering* **45** (2006), 107004.

[3] A. S. Carasso, A Framework for Reproducible Latent Fingerprint Enhancements, *Journal of Research of the NIST* **119** (2014).

[4] P. Cizmar, A. E. Vladár and M. T. Postek, Real-time Scanning Charged-particle Microscope Image Composition with Correction of Drift, *Microscopy and Microanalysis* **17** (2010), 302-308.

[5] P. Cizmar, A. E. Vladár and M. T. Postek, Advances in Modeling of Scanning Charged Particle Microscopy Images, *Proceedings of the SPIE* **7729** (2010), 7729OZ.

[6] P. Cizmar, A. E. Vladár and M. T. Postek, Advanced Image Composition with Intra-frame Drift Correction, *Proceedings of the SPIE* **8036** (2011), 80360D.

[7] T. Goldstein and S. Osher, The Split Bregman Method for L_1 regularized problems, *SIAM Journal on Imaging Science* **2** (2009), 323–343.[15]

[8] *ITTVIS Interactive Data Language (IDL)*, http://www.exelisvis.com/IDL.aspx.

[9] A. Marquina and S. Osher, Explicit Algorithms for a New Time Dependent Model Based on Level Set Motion for Nonlinear Deblurring and Noise Removal, *SIAM Journal on Scientific Computing* **22** (2000), 387–405.

[10] M. T. Postek and A. E. Vladár, Helium Ion Microscopy and its Application to Nanotechnology and Nanometrology, *Scanning* **30** (2008), 457-462.

[11] M. T. Postek, A. Vladár, C. Archie and B. Ming, Review of Current Progress in Nanometrology with the Helium Ion Microscope, *Measurement Science and Technology* **22** (2011), 1–14.

[12] W. K. Pratt, *Digital Image Processing*, (2012), Wiley-Interscience, New York.

[13] R. Sivakumar, Denoising of Computer Tomography Images using Curvelet Transform, *ARPN Journal of Engineering and Applied Sciences* **2** (2007), 21–26.

[14] J. L. Starck, E. J. Candès and D. L. Donoho, The Curvelet Transform for Image Denoising, *IEEE Transactions on Image Processing* **11** (2002), 670-684.

Participants

Alfred S. Carasso (ACMD) and Andras Vladár (NIST PML)

[15] See also http://www.math.ucla.edu/ tagoldst/code.html.

High Precision Calculations of Fundamental Properties of Few-Electron Atomic Systems

Atomic structure calculations have always had a large impact in spectroscopy. They not only are invaluable in the analysis of complex spectra by providing reliable term positions and level designations, but they also contribute to an understanding of the underlying physical processes. Our work is devoted to the development of a rigorous method that delivers energy levels for small atomic and molecular systems of such a high precision as to enable the prediction, theoretically, of fundamental atomic properties more accurately than even the most accurate experiments.

James Sims

NIST has long been involved in supplying critically evaluated data on atomic and molecular properties such as the atomic properties of the elements contained in the Periodic Table and the vibrational and electronic energy level data for neutral and ionic molecules contained in the NIST Chemistry WebBook[16]. Fundamental to this endeavor is the ability to predict, theoretically, a property more accurately than even the most accurate experiments. It is our goal to be able to accomplish this for few-electron atomic systems.

The revolutions in physics in the early decades of the past century provided essentially exact, predictive theories for all chemical properties and processes. However, the mathematical intractability of the Schrödinger equation prevented the computation of accurate numerical solutions for either atomic or molecular systems until recently. In the past two decades, there have been breathtaking improvements in computer hardware and innovations in mathematical formulations and algorithms, leading to "virtual experiments" becoming a more and more cost-effective and reliable way to investigate chemical and physical phenomena.

Virtually all *ab initio* methods of quantum chemistry in some way involve the orbital approximation, in which the many-electron wave function (Ψ) is represented as superpositions of antisymmetrized products of one-electron functions. Such configuration interaction (CI) methods have been quite successful in approaching or reaching experimental accuracy for relative energies of modestly-sized atoms and molecules. However, orders of magnitude improvements are needed to expand the world's spectroscopic database into currently inaccessible realms, establish its building blocks beyond dispute, and supersede more expensive experimental approaches.

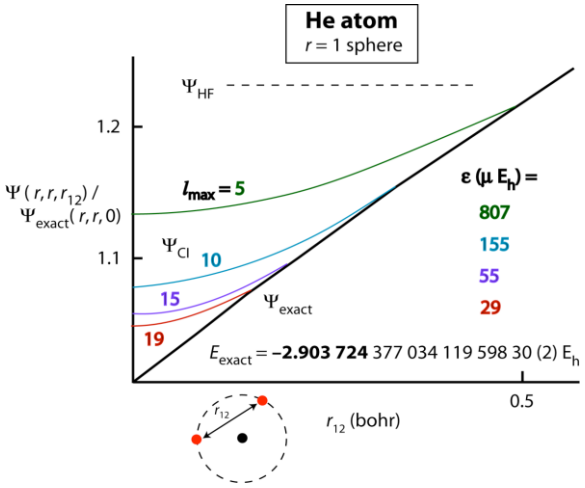

Figure 18. *Failure of conventional CI wave functions to describe the electron cusp in the helium atom. The cusp region of the full Cartesian coordinate space can be envisioned by reflecting the plots about the vertical axis.*

The essential flaw in theoretical methods built on the orbital approximation is their inability to correctly describe the mathematical cusp behavior of many-body wave functions in regions of close electron proximity, the so-called electron cusp region of the exact electronic wave function [1-3]. This flaw leads to incomplete accounting of instantaneous, short-range correlation among electrons. We are undertaking the theoretical development of our hybrid Hylleraas-CI wave function method to solve the electron cusp problem and bring subchemical accuracy to atomic systems with more than two electrons. A depiction of the electron-electron cusp in an essentially exact Hy-CI wave function of the helium (He) atom ground state is shown in Figure 18. In the region of the electron coalescence point, the exact wave function is linear in the interelectronic distance (r_{12}). However, conventional quantum chemical CI wave functions, which effectively incorporate only even powers of r_{12}, do not have sufficient flexibility to fully relax into the conical region of the cusp, and thus poorly account for the short-range electron correlation. In Figure 18, these deficiencies are clearly exhibited by CI wave functions using special analytical and numerical techniques for extremely high angular momentum (l) cutoffs. With an orbital (one-electron) basis saturated through $l = 5$, CI is too large by 14 % at the coalescence point, and the corresponding error in the electronic energy is 807 microhartree (μh). Even after extending the basis set to an unprecedented $l = 30$, the result of some

[16] http://webbook.nist.gov/chemistry/

70 years of trying [4], the best CI treatment for He is accurate to only 5 decimal places, demonstrating that converging absolute energies even to the μh level is essentially impossible in practical computations with orbital treatments. In contrast, the early work of Hylleraas [5] showed the astounding superiority of explicitly-correlated methods, which directly incorporate the r_{12} variable into the wave function. Our hybrid Hylleraas-CI result shown in Figure 18 achieved better than 20 digits of accuracy in the absolute energy [4], at least 14 orders of magnitude better than the best conventional CI treatments, a result that is "essentially exact for all practical purposes." The challenge for computational scientists is to extend the phenomenal accomplishments on atomic helium to three, four, and more electron states and to molecular systems.

Hylleraas's original method (Hy) has been extended to three electrons [6, 7] resulting in some of the most accurate calculations on lithium (Li) and Li-like systems to date, way beyond spectroscopic accuracy. Like helium, virtual experiments can be done that are more accurate than current experimental capabilities, but not without huge computational costs. (The lithium calculations require an estimated 6,000 times more computational power than helium). However, already at the four electron level there are significant unresolved integration problems with the original Hy approach.

The central problem, from a computational point of view, is how to represent the electron-electron correlations without the mathematical and computational problems becoming prohibitive. To get around this problem and make calculations of spectroscopic accuracy or better for systems with more than three electrons, we have developed a hybrid Hy-CI method that merges the ease of calculation of the CI method with the more rapid convergence of the Hy method in such a way that it offers the hope of breaking the four electron integral barrier. (With only a single r_{ij} in any term, the most difficult integrals are the four electron integrals which are present in beryllium.) This would enable extension to systems with more than four electrons.

We are exploring the utility of our hybrid Hy-CI method for both three electron lithium systems and the four electron beryllium atom and its iso-electronic sequence. In the case of lithium, we have computed four excited states of the lithium atom to two orders of magnitude greater than has been done before [8]. In the case of beryllium, not only has the ground state non-relativistic energy of the atom been calculated, but also the same property has been calculated for the entire beryllium iso-electronic sequence, i.e., all four-electron ions of all the elements in beryllium's column in the periodic table, to historic levels of accuracy, in some cases reducing the error by a factor of a thousand or more. Figure 19 shows the result, where the smooth nature of the curve that results from the data points is evident.

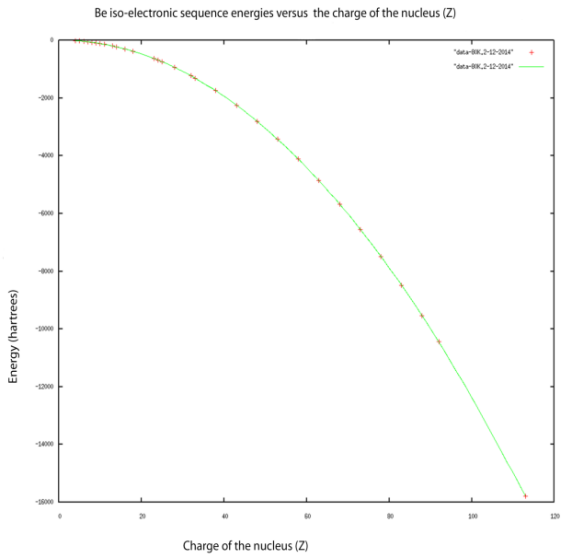

Figure 19. *Plot of non-relativistic energies in hartrees versus nuclear charge Z for Z = 4 through 113.*

The importance of the current results is that accurate and dependable compilations of non-relativistic atomic energies are useful calibration points for the development of more sophisticated models used in electronic structure calculations. In addition, the calculation of physical energies of interest, e.g., a transition energy or familiar chemical ionization potentials or electron affinities, involve these non-relativistic energies. So the non-relativistic energies need to be calculated accurately to guarantee the accuracy of the result, and hence can be regarded as fundamental atomic data. Once they have been computed "essentially exactly for all practical purposes," as in the current case, they can be used to obtain more and more accurate ionization potentials, electron affinities, etc., as the other (correction) terms become known to increasing accuracy.

The results of the beryllium iso-electronic sequence study were published recently in the *Journal of Chemical Physics* [9]. All results reported in the paper were obtained using quadruple precision (30+ digits) floating point subroutines written in Fortran 90 and utilize parallel computing. For a 79,137-term wave function we achieved a factor of 120 speedup on 128 processors for the $O(n^3)$ step running on NIST's cluster of 7892 Intel/AMD 64-bit processors running CentOS Linux. The availability of the Z expansion given in our article opens up access to interesting applications such as the critical charge below which the four electron atom is not bound.

In the coming year we plan to continue to develop the four electron integral mathematics and codes, including the publication of a paper on fast, efficient, and accurate calculations of four electron integrals. The improved codes will be used in a benchmark calculation on the Be atom as well as eventually in a calculation on an $N > 4$ electron system.

References

[1] T. Kato, On the Eigenfunctions of Many-particle Systems in Quantum Mechanics, *Communications in Pure and Applied Mathematics* **10** (1957), 151-177.

[2] R. T. Pack and W. B. Brown, Cusp Conditions for Molecular Wavefunctions, *Journal of Chemical Physics* **45** (1966), 556-559.

[3] W. Kutzelnigg and J. D. Morgan III, Rates of Convergence of the Partial-wave Expansions of Atomic Correlation Energies, *Journal of Chemical Physics* **96** (1992), 4484-4508.

[4] J. S. Sims and S.A. Hagstrom, High precision Hy-CI Variational Calculations for the Ground State of Neutral Helium and Heliumlike Ions, *International Journal of Quantum Chemistry* **90** , 1600-1609 (2002).

[5] E. A. Hylleraas, Neue Berechnung der Energie des Heliums im Grundzustande, sowie des tiefsten Terms von Ortho-Helium, *Zeitschrift für Physik* **54** (1929), 347-366.

[6] Z.-C. Yan, W. Nörtershäuser, and G. W. F. Drake, High Precision Atomic Theory for Li and Be+: QED Shifts and Isotope Shifts, *Physical Review Letters* **100** (2008), 243002.

[7] M. Puchalski, D. Kedziera and K. Pachucki, Ground state of Li and Be+ using Explicitly Correlated Functions, *Physical Review A* **80** (2009), 020101.

[8] J. S. Sims and S. A. Hagstrom, Hy-CI Study of the 2 Doublet S Ground State of Neutral Lithium and the First Five Excited Doublet S States, *Physical Review A*, **80**, 2009.

[9] J. S. Sims and S. A. Hagstrom, High Precision Calculation of the Nonrelativistic Energies for the Ground States of the Beryllium Isoelectronic Sequence Up Through Z = 113, *Journal of Chemical Physics* **140** (2014), 224312.

Participants

James Sims (ACMD) and Stanley Hagstrom (Indiana University)

Rheology of Dense Suspensions

Understanding the mechanisms of dispersion or agglomeration of particulate matter in complex fluids, such as suspensions, is of importance in many industries such as pharmaceuticals, coatings, and concrete. These fluids are disordered systems consisting of a variety of components with disparate properties that interact in many different ways. Modeling and predicting the flow of such systems represents a scientific challenge requiring large scale computer simulations. In collaboration with scientists in NIST's Engineering Laboratory, we are developing a software system capable of performing large scale simulations of dense suspensions. It is highly parallel and has been shown to efficiently scale up to at least 128,000 processors on a DOE supercomputer. Our main goal is to advance understanding of the flow properties of a specific material, fresh concrete, a dense suspension composed of cement, water, sand, and rocks.

Our current focus is on enabling the use of vane rheometers for measuring the flow properties of fresh concrete, something not currently possible. While existing "concrete rheometer" measurements can be found to correlate, they usually do not agree well. A vane geometry combined with a strongly random suspension will result in complex local stress and strain/strain rate fields. Our simulations will enable us to map out these fields, in 3D, and bring insight into the vane design process, leading to optimized vanes for both measurement and mixing applications.

We are also using this simulator to help design new standard reference materials (SRMs) which will be used for calibrating mortar and concrete rheometers. Results from the simulation of a recently released cement SRM (SRM 2492) [1] are being used in in the development of SRMs for both mortar and concrete, which are expected to be released within the next few years. These SRMs will use uniform size hard spheres as the suspended particles. An early test simulation is shown in Figure 20.

William George

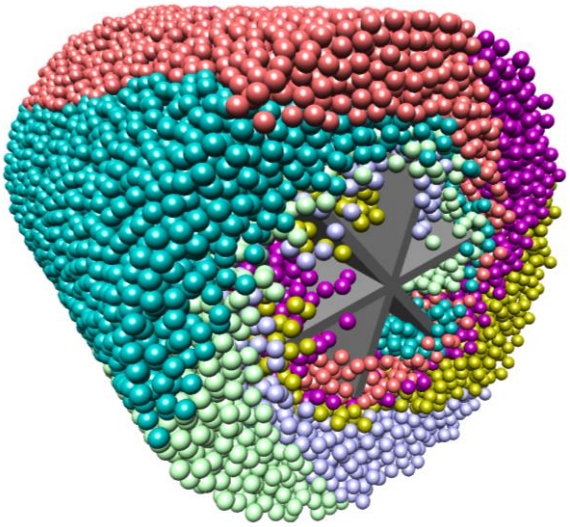

Figure 20. *Snapshot of a 6-blade vane rheometer simulation. The suspended spheres are color coded by the section in which they started. Only 6 of the 12 sections are shown here in order to see details around the vane blades.*

Concrete is the most widely used building material in the world, representing a 100 billion dollar industry in the US upon which our nation's physical infrastructure relies. There is now a strong interest in making concrete a more sustainable material by finding new ways to recycle it, and by changing its ingredients in order to reduce the amount of green-house gas from its production. (According to the World Business Council for Sustainable Development, the manufacture of concrete's key ingredient, cement, is responsible for at least 5 % of global carbon dioxide production.) As new mixture designs for concrete are developed to meet these needs, it is important to measure and control rheological properties, i.e., flow properties, to satisfy performance specifications. Failure to control the flow of concrete on a job site can lead to significant cost overruns and delay.

Fluids are characterized by *yield stress* and *viscosity*, properties which can vary as a function of shear rate. Yield stress is the force applied per unit area to initiate a flow. Viscosity is the applied force per unit area needed to maintain a shear rate. Shear rate is the velocity gradient perpendicular to the flow direction. The local stress in a vane rheometer is illustrated in Figure 21.

Many factors control viscosity and yield stress. For example, in building materials such as concrete, viscosity and yield stress depend on the ratio of water to cement, the volume of sand or rocks used, as well as their shape and size distribution. There can be great variations in materials depending on their history and where they were obtained. For example, rocks from quarries are usually angular because they are crushed when processed, whereas rocks obtained from river beds are typically rounded due to erosion. Additionally, it turns out that the more similar in size the rocks in a concrete suspension, the harder it is to get that concrete to flow. In this case, the concrete may actually jam when poured through a narrow opening, causing construction delays. Clearly, to optimize the flow properties of concrete and other suspensions, one needs to understand the relationship between flow and properties of the fluid's constituents.

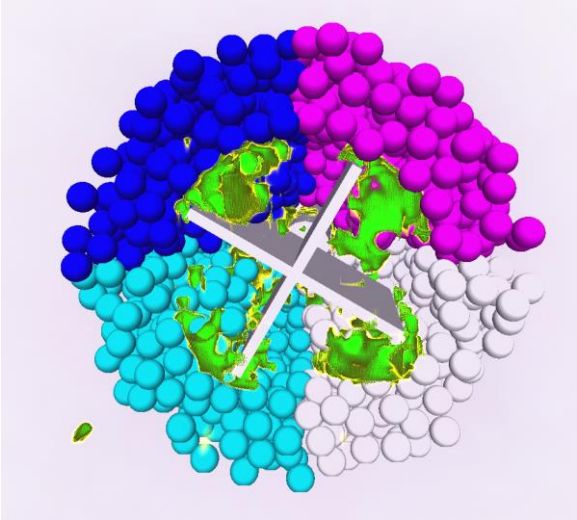

Figure 21. *A snapshot of a 4-blade vane rheometer simulation displayed with a volume visualization of the magnitude of the local stress within the system. As in Figure 20, the suspended spheres are color coded by the section in which they started. Only 4 of the 8 sections are shown here in order to see details around the vane blades. For the added volume visualization, stress is color-coded from yellow (low stress), to green (high stress), with stresses below a set threshold show in light purple.*

QDPD. Our application, QDPD (Quaternion based Dissipative Particle Dynamics) [2], uses two computational methods for simulating fluid flow: Dissipative Particle Dynamics (DPD) [3] and Smoothed Particle Hydrodynamics (SPH) [4]. These are both mesh-free Lagrangian methods in which the fluid is represented as a set of mesoscopic particles that move in a continuous space, with each particle accounting for the microscopic particles in a small volume of fluid. Forces between these particles are limited in range allowing for a highly parallel implementation of these methods. This is similar to traditional molecular dynamics (MD) in that particles move according to Newton's laws, however the interparticle interactions are designed such that much larger time-steps can be used in the algorithm when compared to MD simulations. This allows for the study of physical behavior that occurs on time scales many orders of magnitude larger than what would be possible using MD techniques. Each solid object (e.g., a rock, or grain of sand) in a simulation is represented by a group of these DPD/SPH particles that are further constrained to always move such that their positions relative to the other particles that comprise the solid object remain unchanged.

In addition to the forces computed using the DPD and SPH techniques, other forces are computed to better account for the interaction between the suspended particles, that is, the sand and gravel. These additional forces include lubrication forces that help keep the particles separated, and, to model colloidal systems, van der Waals forces that introduce an attractive interparticle interaction and Brownian forces are utilized.

The original DPD algorithm used an Euler method for updating the positions of the free particles, that is, the particles that represent the fluid, and a leap-frog algorithm for updating the positions of the solid objects. The NIST algorithm, called QDPD, is a modification that uses a velocity Verlet method to update the positions of both the free particles and the solid objects. In addition, the solid object motion is determined from the quaternion-based scheme of Omelyan [5] (hence the Q in QDPD).

A typical simulation may entail keeping track of up to 100,000 solids of varying shape and size. Further, many of the forces between particles depend on the local surface curvature of the aggregate at points close to neighboring aggregates, which requires keeping track of the location, orientation and shortest distance between neighboring solids. Clearly, modeling such systems necessitates large scale simulations to accurately predict their properties. We have adopted and developed some novel approaches, originally based on cellular automata methods that can successfully take into account many of the features of a suspension. QDPD has been validated by both theory and experiments on idealized systems and has been extended to account for random shaped objects with different interparticle interactions.

Starting with the original serial version of this simulator we enhanced QDPD to utilize the power of large parallel machines regularly using 8000+ processors, and, for large production runs, using up to 128,000 processors when running on the IBM Blue Gene/Q, *Mira*, at the Leadership Computing Facility of Argonne National Laboratory. QDPD remains under constant development to improve its capabilities as well as to improve its parallel performance.

Supercomputer Access. During the 2014 calendar year we have had access to the IBM Blue Gene/Q supercomputer *Mira*, having been awarded 40 million CPU-hours of compute time on this machine from the DOE INCITE program (Innovative and Novel Computational Impact on Theory and Experiment). This access has enabled us to perform several very large simulations of 4-blade and 6-blade vane rheometers.

Visualization. A major part of this project involves the development and use of specialized visualization software to investigate the results of our simulations. This includes both the display of the systems under study as well as techniques to probe and measure aspects of the system we are viewing. For performance reasons we rely heavily on the programmable capabilities of GPUs (Graphics Processing Units). For example, within the images in each of the figures, each suspended sphere is rendered within the GPU as a *point sprite*, i.e., a 2D textured image at a single 3D point, which requires only

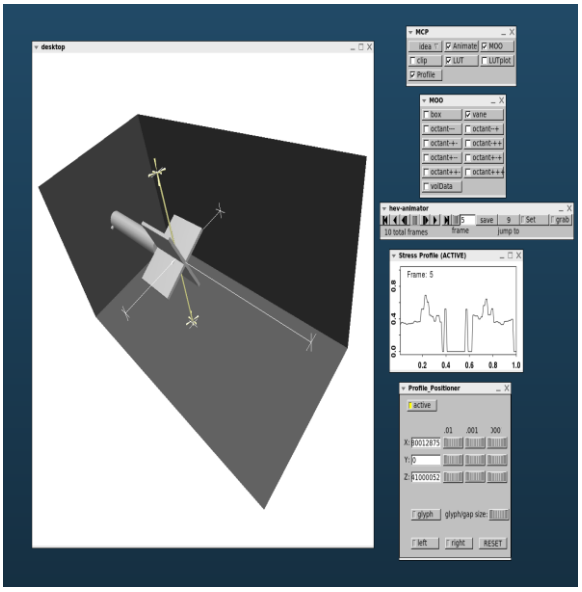

Figure 22. *Interactively positioning a line probe in a system. Each endpoint is indicated with a 3D cursor consisting of 3 orthogonal pairs of small cones surrounding the chosen point. The endpoints of this line probe can be positioned anywhere within the simulation box shown in this image. The hard spheres and volume visualization of the stress have been turned off for this image in order to highlight the probe.*

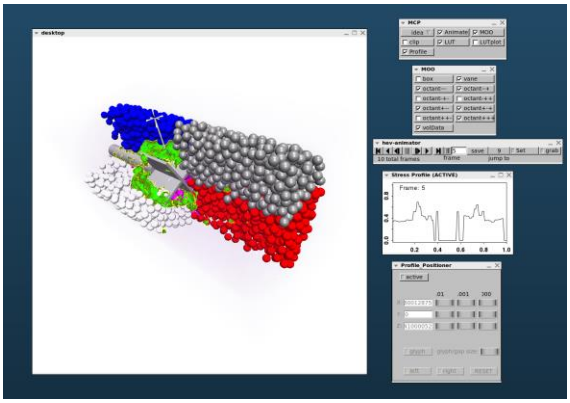

Figure 23. *This is the identical display as in Figure 4 except that now we have turned on the volume visualization of the stress data as well as some of the hard spheres. The stress along the probe line is shown in the sub-window labeled "Stress Profile." This plot is dynamically generated and updates each frame as the simulation is animated.*

location and size information for display, rather than using a polygonal representation of these spheres. We also use volume visualization techniques to display various properties within the system, such as in Figure 21 which shows the local stress value throughout the system. As shown in Figure 22 and Figure 23, we can interactively probe a system to compute and show values of properties at specific locations or areas in the system. All of our visualizations can also be used within our 3D immersive visualization system for full immersion into the simulated systems. This display system consists of three large displays (each approximately 2.5 m by 2.5 m), arranged as two walls and a floor forming the corner of a cube.

Results. Over the last few years our simulations have provided fundamental insights into mechanisms that control the onset of flow in suspensions that can be linked to macroscopic properties such as yield stress and viscosity. We have developed a novel way of describing the interparticle stress fields and their spatial correlations and through this technique it was discovered that under shearing, although the suspended particles remain in a liquid order, the interparticle stress is strongly anisotropic [6, 7]. In addition, a transition under flow was observed: during a transient regime at low deformation, the stress propagates along the compression direction of the shear, whereas at larger deformations the stress is organized into layers parallel to the flow direction. Further, we found that yield stress is shear rate dependent [8]. The higher the shear rate the greater the yield stress. However, in the limit of zero shear rate, yield stress was found to go to zero as a consequence of temperature effects. Further, by examining the very long time scale behavior of the rocks, we can link their motion to viscoelastic properties of the suspension.

We have recently modeled cementitious materials composed of cement and fly ash [9]. Here we studied the effect on flow properties of substituting 10 % of cement with fly ash. To do this we modeled a system of angular shaped particles (cement) combined with smaller spheres (representing ultra fine fly ash), and found that there is a decrease in yield stress and viscosity of the suspension in comparison with the same system without fly ash.

From our studies, we have discovered that, given the rheological properties of a non-Newtonian fluid matrix we can predict the rheological properties of suspensions composed of hard spheres in the fluid [10]. We are applying these ideas to predict the flow of dense suspensions consisting of 1 mm diameter glass beads suspended in a matrix fluid of known properties, NIST SRM 2492 [1]. Such suspensions are currently being evaluated as a new candidate SRM for mortars. As a consequence of this discovery, one only needs to measure the fluid properties of the matrix fluid, which is generally far easier to do than measuring the suspension itself. Hence, fewer experiments are needed to obtain the rheological properties, thus saving cost and time. Currently these results apply only to hard sphere suspensions, however. In the coming year we plan to test this scaling approach on suspensions composed of more complex shaped inclusions.

Potential Impact. Our results can be used to accelerate the design of new high-performance cement-based materials by reducing the time and costs associated with research and development. For example, the ability to use computational models to study suspensions would

accelerate research into *waste stream processing*, in which industrial waste materials are incorporated into cement with the goal of maintaining or enhancing concrete performance, while at the same time reducing the environmental impact of this industrial waste. One such candidate waste material is fly ash, which has been shown to be useful as a substitute for some portion of the cement used in concrete. Reducing the need for cement would lead to a reduction in the production of carbon dioxide related to cement production.

Finally, while the main thrust of our research focuses on predicting the rheological properties of cement based materials such as concrete, an improved general understanding of rheological properties derived from this research should have a broad impact. Suspensions are utilized in a wide variety of technological processes and, as our study is largely parametric in nature, results will be transferable to other suspensions of interest such as nanoparticle systems. Understanding mechanisms for the dispersion or agglomeration of such systems remains a challenge in many industries ranging from pharmaceuticals to coatings.

References

[1] C. F. Ferraris, P. Stutzman, J. Winpigler, and W. F. Guthrie, Certification of SRM 2492: Bingham Paste Mixture for Rheological Measurements, NIST Special Publication SP 260-174 Rev. 2012.

[2] N. Martys, Study of a Dissipative Particle Dynamics Based Approach for Modeling Suspensions, *Journal of Rheology* **49**:2 (2005), 401-424.

[3] P. J. Hoogerbrugge and J. M. V. A. Koelman, Simulating Microscopic Hydrodynamic Phenomena with Dissipative Particle Dynamics, *Europhysics Letters* **19** (1992), 155-160.

[4] J. J. Monaghan, Smoothed Particle Hydrodynamics, *Reports on Progress in Physics* **68** (2005), 1703–1759.

[5] I. P. Omelyan, On the Numerical Integration of Motion for Rigid Polyatomics: the Modified Quaternion Approach, *Computer Physics* **12** (1998), 97.

[6] N. S. Martys, D. Lootens, W. George and P. Hebraud, Contact and Stress Anisotrophies in Start-up Flow of Colloidal Suspensions, *Physical Review E* **80** (2009), 031401.

[7] P. Hebraud, D. Lootens, and N. Martys. "Stress Organization in an Attractive Concentrated Colloidal Suspension under Flow," XVIth International Conference on Rheology, Lisbon, Portugal, August 5, 2012.

[8] N. S. Martys, M. Khalil, W. George, D. Lootens and P. Hebraud, Stress Propagation in a Concentrated Colloidal Suspension under Shear, *European Physics Journal E* **35** (2012), 20.

[9] N. S. Martys, Multiscale Modeling of the Flow of Cement Based Materials, in *Rilem State of the Art Report on Numerical Simulations of Fresh Concrete Flow*, August 2010.

[10] M. Liard, N. S. Martys, W. L. George, D. Lootens and P. Hebraud, Scaling Laws for the Flow of Generalized Newtonian Suspensions. *Journal of Rheology* **58** (2014), 1993.

Participants

William George, Steven Satterfield, Marc Olano, and Judith Terrill (ACMD), Nicos Martys and Clarissa Ferraris (NIST EL), Edward Garboczi (NIST MML), Pascal Hébraud (CNRD/ESPCI, France)

DLMF Standard Reference Tables on Demand

Mathematical software designers, numerical analysts and other researchers often need high quality tables of function values, but most current libraries and systems that produce such tables offer limited information about accuracy. To address this void, NIST ACMD and the University of Antwerp Computational Mathematics (CMA) Research Group are collaborating to build the DLMF Standard Reference Tables (DLMF Tables) web service. DLMF Tables will provide a standard of comparison for testing numerical software by computing, on demand, special functions to user-defined accuracy with guaranteed error bounds. ACMD is building and integrating the site's front end user interface with CMA's back end computational engine based on their MpIeee library, an IEEE compliant C++ library for base 2^n or 10^m mixed precision floating point arithmetic. We recently released a beta version, marking the completion of the first phase of the web service development project. More functions are in the pipeline, and additional site enhancements and comprehensive testing are currently in provess.

Bonita Saunders

Numerical software designers and application programmers typically use tables of elementary and special functions in order to test software or validate numerical computations. Although searching through published tables was once the norm, this has been superseded by the use of specialized software libraries, computer algebra systems, or online computing facilities. Unfortunately, most results obtained with these tools come with little information about the accuracy of the results. One notable exception is MpIeee [2-5], a C++ multiple-precision floating-point library developed and maintained by the University of Antwerp Computational Mathematics (CMA) Research Group. MpIeee, which covers a substantial subset of special functions, uses algorithms based on series and continued fraction representations, in conjunction with a detailed analysis of the rounding errors that allows results to be computed to lie within an arbitrarily prescribed relative error. Currently, MpIeee covers real variables only, but CMA is actively working to expand its coverage to more functions and eventually to complex variables.

The high quality of the CMA Research Group's work in the field of software for special functions over many years has driven ACMD's decision to collaborate with CMA to build the DLMF Standard Reference Tables (DLMF Tables) web service[17], an online service that allows users to create their own tables of special function values with an error certification. ACMD is building the front end user interface to work with the back end computational engine based on the MpIeee library.

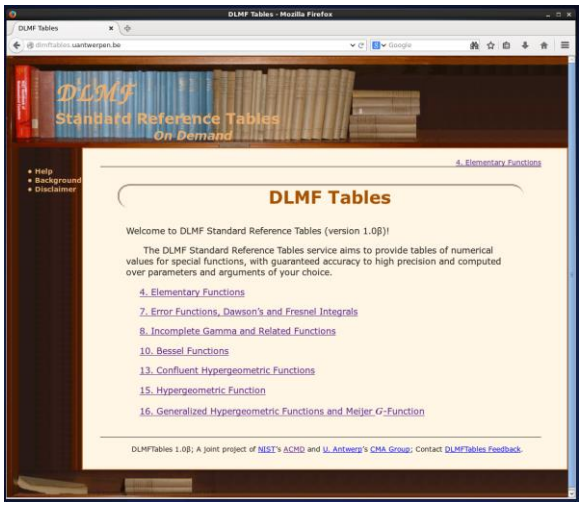

Figure 24. *Table of contents for DLMF Tables website.*

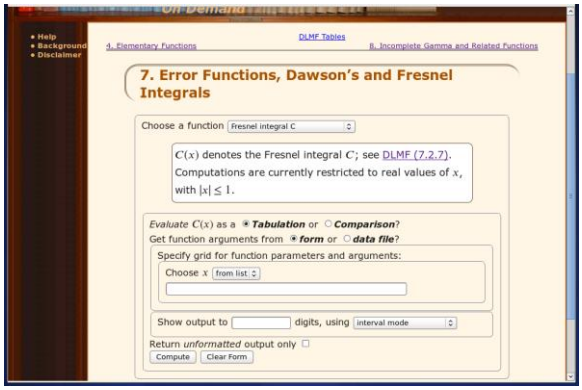

Figure 25. *Input screen for Fresnel integral* $C(\boldsymbol{x})$.

The top level structure of DLMF Tables is organized according to the NIST Digital Library of Mathematical Functions (DLMF). As Figure 24 shows, the table of contents lists the chapters available, with all entries currently corresponding to chapters in the DLMF. After a chapter is selected, the input screen (Figure 25) for that chapter appears; the user chooses a function and requests either a tabulation or comparison. This determines what additional user input will be required. Users will note that each function description contains a link to the definition in the DLMF.

[17] http://dlmftables.uantwerpen.be/

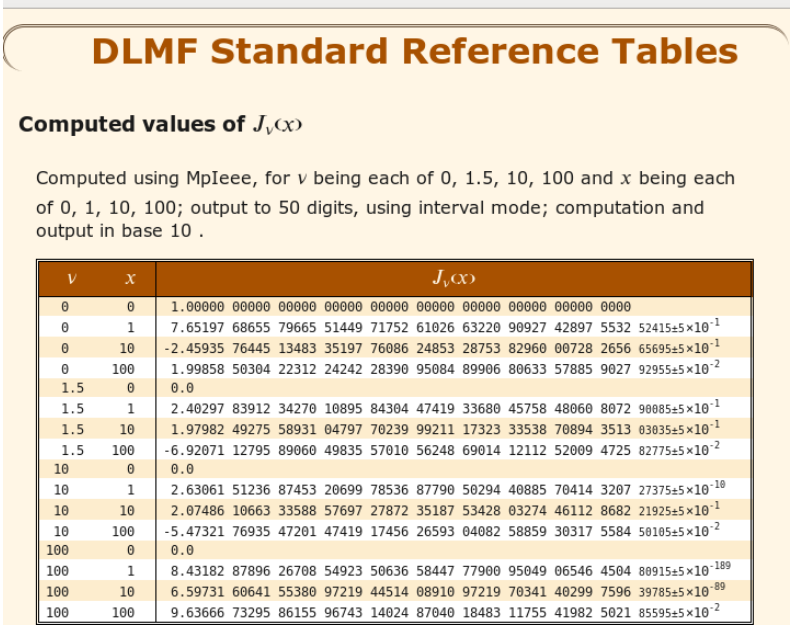

DLMF Standard Reference Tables

Computed values of $J_\nu(x)$

Computed using MpIeee, for ν being each of 0, 1.5, 10, 100 and x being each of 0, 1, 10, 100; output to 50 digits, using interval mode; computation and output in base 10 .

ν	x	$J_\nu(x)$
0	0	1.00000 00000 00000 00000 00000 00000 00000 00000 00000 0000
0	1	7.65197 68655 79665 51449 71752 61026 63220 90927 42897 5532 52415±5×10^{-1}
0	10	-2.45935 76445 13483 35197 76086 24853 28753 82960 00728 2656 65695±5×10^{-1}
0	100	1.99858 50304 22312 24242 28390 95084 89906 80633 57885 9027 92955±5×10^{-2}
1.5	0	0.0
1.5	1	2.40297 83912 34270 10895 84304 47419 33680 45758 48060 8072 90085±5×10^{-1}
1.5	10	1.97982 49275 58931 04797 70239 99211 17323 33538 70894 3513 03035±5×10^{-1}
1.5	100	-6.92071 12795 89060 49835 57010 56248 69014 12112 52009 4725 82775±5×10^{-2}
10	0	0.0
10	1	2.63061 51236 87453 20699 78536 87790 50294 40885 70414 3207 27375±5×10^{-10}
10	10	2.07486 10663 33588 57697 27872 35187 53428 03274 46112 8682 21925±5×10^{-1}
10	100	-5.47321 76935 47201 47419 17456 26593 04082 58859 30317 5584 50105±5×10^{-2}
100	0	0.0
100	1	8.43182 87896 26708 54923 50636 58447 77900 95049 06546 4504 80915±5×10^{-189}
100	10	6.59731 60641 55380 97219 44514 08910 97219 70341 40299 7596 39785±5×10^{-89}
100	100	9.63666 73295 86155 96743 14024 87040 18483 11755 41982 5021 85595±5×10^{-2}

Figure 26. *Output table for Bessel function* $J_\nu(x)$.

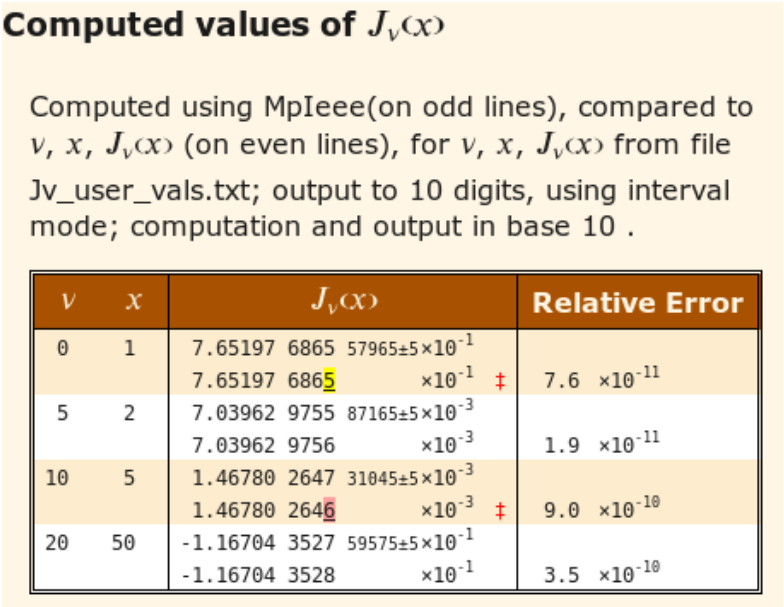

Computed values of $J_\nu(x)$

Computed using MpIeee(on odd lines), compared to ν, x, $J_\nu(x)$ (on even lines), for ν, x, $J_\nu(x)$ from file Jv_user_vals.txt; output to 10 digits, using interval mode; computation and output in base 10 .

ν	x	$J_\nu(x)$	Relative Error
0	1	7.65197 6865 57965±5×10^{-1}	
		7.65197 6865 ×10^{-1} ‡	7.6 ×10^{-11}
5	2	7.03962 9755 87165±5×10^{-3}	
		7.03962 9756 ×10^{-3}	1.9 ×10^{-11}
10	5	1.46780 2647 31045±5×10^{-3}	
		1.46780 2646 ×10^{-3} ‡	9.0 ×10^{-10}
20	50	-1.16704 3527 59575±5×10^{-1}	
		-1.16704 3528 ×10^{-1}	3.5 ×10^{-10}

Figure 27. *Output for comparison of DLMF Tables computations with table of function values submitted by user.*

Tabulation. Once a user selects *Tabulation* he may either enter function parameters and argument data directly into the form or upload a data file meeting the site's format specifications. The user may request up to 500 output digits and choose a mode for computation. The default output mode is interval mode, where a strict enclosure (lower and upper bound) is displayed for each requested function value. For example, if the user requests *n* digits, the computed function values are displayed in scientific notation with *n* digits, plus five extra digits (displayed smaller), along with exclusive error bounds (digits after ±) as shown in Figure 26. In most cases, this allows the user to determine the value to the desired number of digits using whatever rounding or truncation scheme preferred. No extra digits are shown when the computed value is exact.

Alternatively, instead of an interval enclosure the user may explicitly choose that output values be displayed exactly in one of the following rounding modes:

- round to nearest (even)
- round up (toward +∞)
- round down (toward -∞)
- round toward 0
- round away from 0.

When a rounding mode is chosen, output is shown with the number of digits requested without extra digits.

Comparison. When the user selects *Comparison*, a user-supplied data file is uploaded. The output table displays the reference values, computed in one of the user selected modes described above, alternated with the values provided by the user. The approximate relative error is also shown. Differences between reference values and uploaded values are highlighted in either yellow (warning) or red (error) as shown in Figure 27.

In particular, if the user uploads a file containing n-digit function values for a comparison based on interval mode, the upper and lower error bounds associated with each reference value form a sharp interval enclosure for the reference function evaluation. To accommodate possible rounding or truncation used to produce the uploaded values, we take the floor of the left endpoint (round toward -∞) and the ceiling of the right endpoint (round toward +∞) to n digits.

If the user's value falls outside this expanded interval, incorrect digits are highlighted in red and the user will see the message *Value not in interval enclosure at requested precision* when the cursor is placed near the dagger adjacent to the uploaded number.

If the user's value falls within the expanded interval (endpoints included), but does not match the round to nearest (even) value computed from the reference value,

digits in question are highlighted in yellow and the message will state *Value not equal to round to nearest*.

If the comparison is based on one of the rounding modes, the rounded reference values are exact and differences with the user's values are highlighted in red with the error message *Value is not correct*.

Launch. To allow a quick launch of the system, the first phase, or beta version, is being hosted at the Antwerp site. A public announcement of the site was published in the SIAM OP-SF newsletter [6] and NA-Digest [7]. Other activities included the publication of a proceedings paper based on talks given by Annie Cuyt and Daniel Lozier at the Workshop on Numerical Software: Design, Analysis, and Verification, Santander, Spain, July 4-6, 2012 [1], and a talk and poster on the project presented by Daniel Lozier at the Institute for Computational & Experimental Research in Mathematics (ICERM) Workshop at Brown University [8].

Future Work. Code verification and the trapping of bogus input data are of current concern. Bruce Miller and Chris Schanzle have worked on the input data problem, but algorithm and code verification is still needed. To help with this task, Andrew Dienstfrey is developing a formal testing structure where test results are carefully documented and stored in a repository. The repository will contain all test data files so that results can be duplicated when necessary.

In addition to testing, our immediate focus includes increasing the number of functions offered, inserting more user documentation, and possibly adding more extensive documentation for programmers. Once the DLMF Tables site is stabilized, we will have to tackle deferred decisions about its integration with the DLMF and its permanent location.

References

[1] F. Backeljauw, S. Becuwe, A. Cuyt, J. Van Deun, and D. Lozier, Validated Evaluation of Special Mathematical Functions, *Science of Computer Programming* **10** (2013), 1016.

[2] M. Colman, A. Cuyt and J. Van Deun, Validated Computation of Certain Hypergeometric Functions. *ACM Transactions on Mathematical Software* **38**:2 (2012), Article 11.

[3] F. Backeljauw, A Library for Radix-independent Multiprecision IEEE-compliant Floating-point Arithmetic Technical Report 2009-01, Department of Mathematics and Computer Science, Universiteit Antwerpen, 2009.

[4] A. Cuyt, V. B. Petersen, B. Verdonk, H. Waadeland and W. B. Jones, *Handbook of Continued Fractions for Special Functions*. Springer, New York, 2008.

[5] A. Cuyt, B. Verdonk, H. Waadeland, Efficient and Reliable Multiprecision Implementation of Elementary and Special Functions, *SIAM Journal on Scientific Computing* **28** (2006) 1437-1462.

[6] M. Muldoon and D. Dominici (eds.), *OP-SF NET* **22**:1 (January 2015), SIAM Activity Group on Orthogonal Polynomials and Special Functions.

[7] D. Dunlavy (ed.), *NA-Digest* **15**:2 (January 15, 2015).

[8] H. Cohl, D. Lozier, Outgrowths of the Digital Library of Mathematical Functions Project, Institute for Computational & Experimental Research in Mathematics (ICERM) Workshop on Challenges in 21st Century Experimental Mathematical Computation at Brown University, July, 2014.

Participants

Bonita Saunders, Bruce Miller, Marjorie McClain, Daniel Lozier, Andrew Dienstfrey and Chris Schanzle (ACMD), Annie Cuyt, Stefan Becuwe, and Franky Backeljauw (U. Antwerp)

http://dlmftables.uantwerpen.be/

Part III

Project Summaries

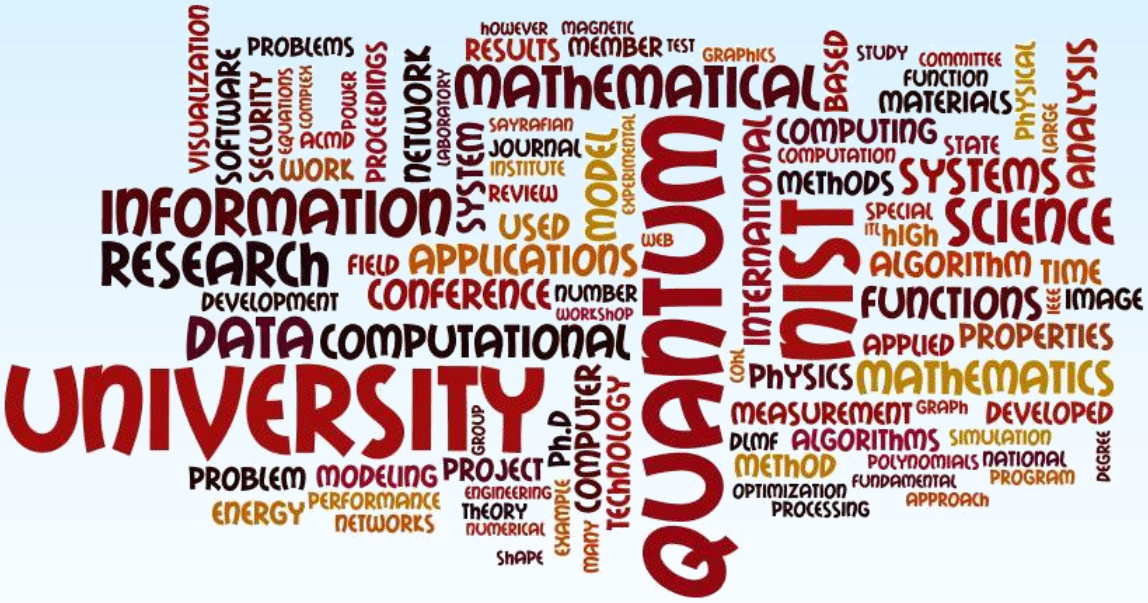

Mathematics of Metrology

Mathematics plays an important role in the science of metrology. Mathematical models are needed to understand how to design effective measurement systems, and to analyze the results they produce. Mathematical techniques are used to develop and analyze idealized models of physical phenomena to be measured, and mathematical algorithms are necessary to find optimal system parameters. Finally, mathematical and statistical techniques are needed to transform measured data into useful information. The goal of this work is to develop fundamental mathematical methods and analytical tools necessary for NIST to continue as a world-class metrology institute, and to apply them to critical measurement science applications.

Modeling and Optimization in Cryobiology

Anthony Kearsley
Daniel Anderson
Andrew Dienstfrey
Geoffrey McFadden
James Benson (Northern Illinois University)
Adam Higgins (Oregon State University)

See page 21.

Recovery of Background Structure in Nanoscale Helium Ion Microscope Imaging

Alfred S. Carasso
Andras Vladár (NIST PML)

See page 26.

Molecular Movies: Imaging Femtosecond Motion during Electrochemical Transitions

Bradley Alpert
Joel Ullom (NIST PML)
Chris Cromer (NIST PML)
Ralph Jimenez (NIST PML)

Vital to the development of next-generation nanomaterials, including photovoltaics and industrial catalysts, is an understanding gained through measurement of electron release, transport, and transfer in engineered nanostructures. This project, supported for the past four years by an Innovations in Measurement Science (IMS) grant, proposes a revolutionary, table-top x-ray imaging system to capture the motion of electrons, atoms, and molecules on femtosecond time scales and with picometer spatial resolution.

The combination of table-top x-ray lasers, a dramatic recent breakthrough developed at JILA, with transition-edge sensor (TES) microcalorimeter spectroscopy, intensively developed and refined in the Quantum Electronics and Photonics Division, promises to enable these new measurement capabilities. The integration of these components, accompanied by significant increase in detector array sizes, to achieve large increases in temporal and spatial resolution while maintaining extraordinary TES energy resolution, requires new data modeling and processing techniques. These techniques will overcome current limitations by

- Resolving temporal overlap in photon detection while achieving energy resolution of temporally isolated arrivals,
- Improving efficiency in elimination of low-frequency background noise, and
- Extending multiplexing and reducing cross talk in extracting the signals from 0.1 K to room temperatures.

Wiener filtering, long used among astronomers for estimating amplitudes of pulses of known shape contaminated with noise of known frequency content, is suitable for measuring isolated pulses. Novel processing approaches are being developed and characterized that rely on this knowledge but are suitable for overlapping pulses.

Analysis efforts this year focused on (1) demonstrating a new pulse processing technique, dubbed multi-pulse fitting, applicable when pulses are poorly separated in time but small enough to neglect detector response nonlinearity, (2) so-called arrival time corrections, which attempt to adjust for pulse shape dependence on photon sub-sample arrival time, due to readout nonideality, and (3) work to model nonlinearity of detector response, based on a model of detector dynamics governed by a two-dimensional phase space.

Multi-pulse fitting relies on a linear detector response model in which the signal is a superposition of pulses of a single shape and various amplitudes, noise coloring (i.e., its frequency dependence) is corrected, and by a pulse-height to photon energy calibration curve that corrects for deficiencies of this model. This method performs quite well, with low pulse rejection and low deterioration in energy resolution with increasing pulse

rate, up to about 100 counts per second per detector, provided photon energies are a modest fraction of the level that saturates the detector. A paper presenting these results is in preparation.

Arrival time corrections, made necessary by limitations in the detector readout circuitry that constrain its ability to precisely track a fast pulse rise, have challenged, teased, and frustrated analysis attempts of at least four members of our project, working separately and cooperatively, for more than two years. While repeatable, these nonideal behaviors depend strongly on sample rates, pulse magnitudes, and individual detector characteristics. Currently they comprise a significant fraction of the energy uncertainty. Perhaps improbably, one promising approach characterizes and quantifies a two-dimensional manifold in fifteen dimensions, for each of a few hundred detectors. The character of this problem is expected to change significantly with the new microwave multiplexers being developed for the project on massive detector arrays.

Detector nonlinear response, significant at higher photon rates and at energies approaching those that saturate the detectors, remain a challenge. We recently have retreated to the better characterized, ODE-governed dynamic response of detectors being developed for HOLMES, a large-scale experiment to determine the electron (anti-)neutrino mass (below).

[1] B. K. Alpert, R. D. Horansky, D. A. Bennett, W. B. Doriese, J. W. Fowler, A. S. Hoover, M. W. Rabin, and J. N. Ullom, Operation of Gamma-ray Microcalorimeters at Elevated Count Rates using Filters with Constraints, *Review of Scientific Instruments* **84**:5 (2013), 056107.

A Thousand-Fold Performance Leap in Ultrasensitive Cryogenic Detectors

Bradley Alpert
Joel Ullom (NIST PML)
Lawrence Hudson (NIST PML)
Terrence Jach (NIST MML)

Small arrays of ultrasensitive cryogenic detectors invented and developed at NIST have driven breakthroughs in x-ray materials analysis, nuclear forensics, and astrophysics. In addition to earning NIST a place on lists of the most important results in physics each of the past three years, they have been used by a team that announced in March, 2014, the detection of gravity waves. Despite these successes, NIST's existing cryogenic sensor technology is inadequate for new applications such as in-line industrial materials analysis, energy resolved x-ray imaging, and next-generation astrophysics experiments, which all require faster sensors, much larger arrays, or both. This year new support for Innovations in Measurement Science (IMS) was awarded to develop both of these capabilities in pursuit of 1000-fold increase in sensor throughput, via completely new sensor readout (microwave multiplexer) enabling much larger detector arrays and through major new, higher throughput, processing capabilities.

A major project connected to the NIST IMS effort is HOLMES, now underway in Italy to measure the mass of the electron (anti-)neutrino. This experiment, which will use NIST-developed microcalorimeters, SQUID amplifiers, and microwave multiplexer readout, relies on extreme statistics for the spectrum produced by the decay of ^{163}Ho. A principal source of error for microcalorimeter characterization of this spectrum is expected to be due to undetected near-simultaneous ^{163}Ho decay events (pile-ups). Improvements in processing that would allow better detection of nearly coincident pulse pairs could radically alter the design space for the detectors of the experiment.

Alpert conducted initial simulations, with a novel pile-up detection algorithm using NIST detector response models, that convinced the Italian team, led by Angelo Nucciotti, to consider a portion of the detector design space (for slower pulse rise) previously believed unusable for HOLMES. If feasibility is established, the resulting detectors would have reduced pulse rise (or arrival time) distortion and the readout electronics specifications would be less extreme. Further assessment of this part of the detector design space will rely on better elucidation of the detector nonlinear response, closely connected with the corresponding characterization for photon high count rate energy resolution.

[1] B. Alpert, M. Balata, D. Bennett, M. Biasotti, C. Boragno, C. Brofferio, V. Ceriale, M. De Gerone, R. Dressler, M. Faverzani, E. Ferri, J. Fowler, F. Gatti, A. Giachero, S. Heinitz, G. Hilton, U. Köster, M. Lusignoli, M. Maino, J. Mates, S. Nisi, R. Nizzolo, A. Nucciotti, G. Pessina, G. Pizzigoni, A. Puiu, S. Ragazzi, C. Reintsema, M. Ribeiro-Gomes, D. Schmidt, D. Schumann, M. Sisti, D. Swetz, F. Terranova, and J. Ullom, HOLMES: The Electron Capture Decay of ^{163}Ho to Measure the Neutrino Mass with sub-eV sensitivity, in review.

Stochastic Simulation in Chemical Spectroscopy

Anthony Kearsley
William Wallace (NIST MML)
Yutheeka Gadhyan (Pricewaterhouse Coopers)

Analytical chemistry, which has long been a foundation of industrial processes, is undergoing a transformation as new applications, new instrumentation, and new analytic methods are rapidly being developed and deployed.

Modern applications require information from myriads of different analytical instruments in varying

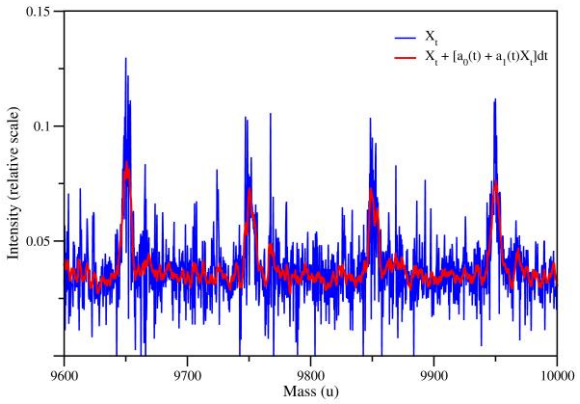

Figure 28. *Regression analysis of a data spectrum from a matrix-assisted laser desorption ionization reflectron time-of-flight (MALDI-RTOF) mass spectrometry study of narrow-polydispersity synthetic polymer.*

formats be synthesized with data from other sources for rapid processing. Here, information models must deal with the extremely complex problems of fitting, matching, filtering and analysis of structured, semi-structured and unstructured data. Very often linear regression or "binning" of data is used in conjunction with a derivative checker to find peaks and troughs. Unfortunately, this process is fraught with difficulties, making it difficult to reliably automate, and is thus often performed by a technician, by eye. This is, of course, simply impossible in many applications (e.g., medicine, forensics) where automation is necessary for the instrument to be practical.

Recently we have begun examining the use of stochastic differential equations (SDE) to model and build regression simulations of chemical spectra. Very loosely, one can construct an SDE that has two components: a drift component that captures a signal and a diffusion term that captures the noise. In so doing, the SDE naturally (and automatically) can split the instrument output into noise and true signal. Once this has been accomplished one can find peaks, examine structures, measure the area under structures, etc. SDE-based techniques are quite often used in financial modeling, albeit in a different way. This year we developed such a scheme and have analyzed the convergence and statistical properties of this method. Using a first order *Euler-Maruyama* discretization one can build an inexpensive numerical scheme to regress on chemical spectra accurately. Statistical information about the noise can be calculated inexpensively. To validate these ideas we derived and analyzed the SDE, and implemented a simple numerical integration together with associated convergence analysis that suggested a time-stepping scheme. We applied the regression to a data spectrum from a matrix-assisted laser desorption ionization reflectron time-of-flight (MALDI-RTOF) mass spectrometry study of narrow-polydispersity synthetic polymer [1]. Results appear promising (see Figure 28) as the regression technique outlined in [2] certainly follows the instrument output well and succeeds in automatically separating noise from signal.

Because this regression provides a statistical estimate of the noise, one has the ability to interrogate peaks in the spectrum, that is, to examine the estimated noise in a neighborhood of a peak that was identified by, for example, the software from the instrument. In the future more specialized problem-dependent selections for kernel type, statistical window-size, and other computational details are certain to emerge.

[1] C. M. Guttman, K. M. Flynn, W. E. Wallace and A. J. Kearsley, Quantitative Mass Spectrometry and Polydisperse Materials: Creation of An Absolute Molecular Mass Distribution Polymer Standard, *Macromolecules* **42** (2009), 1695–1702.

[2] A. Kearsley, Y. Gadhyan and W. E. Wallace, Stochastic Regression Modelling of Chemical Spectra, *Chemometrics and Intelligent Lab. Systems* **139** (2014), 26-32.

Clutter Measurements Pilot Project: Toward Evaluating Communications Spectrum Sharing Proposals

Bradley Alpert
Chriss Hammerschmidt (NTIA)
Robert Johnk (NTIA)
Jack Wang (NIST ITL)

Formation of the joint NIST and National Telecommunications and Information Administration (NTIA) Center for Advanced Communications (CAC) and the NIST Communications Technology Laboratory (CTL) aims to develop the scientific and engineering capacity and experience for technical assessment of spectrum sharing and commercialization proposals. Components of this expertise are already present, in the Electromagnetics Division of the NIST PML, the Public Safety Communications Research (PSCR) of the NTIA, and their collaborative research relationships in measurement and modeling within NIST and NTIA.

Kent Rochford, who leads CAC and CTL, suggested in April, 2014, that the researchers (listed above) begin a collaboration to form an initial research bridge between NIST and NTIA. Following a successful effort by Alpert and Wang for preliminary assessment of the uncertainty of in-building LTE cell phone path-loss surveys by Johnk, presented by Johnk at the PSCR Public Safety Broadband Stakeholder Conference, June, 2014, NTIA Institue for Telecommunications Sciences (ITS) lead Hammerschmidt proposed a one-year pilot project

to assess communications disruption due to environmental clutter (buildings, vegetation, power lines, etc.). Its objectives are to (1) collect representative clutter measurement data in support of ongoing rulemakings such as the 3.5 GHz Joint Working Group, (2) perform statistical analysis on these data and determine uncertainties, (3) refine the measurement methods in preparation for a comprehensive data collection program, and (4) provide measurement data to support refinement of existing propagation models.

Lack of experience of the researchers in evaluating uncertainties of communications channel losses, including those due to clutter, has prompted a flurry of initial activity to establish the project's direction. In particular, early surveys have suffered from (1) lack of repeatability due to position uncertainty and limited comparability between nominally identical surveys, (2) large discrepancy, even in uncluttered areas, between path loss surveys and those expected from the ITS Irregular Terrain Model of path loss, and (3) lack of a survey of environmental clutter, to serve as a potential independent, predictive variable.

Alpert has proposed denoising of GPS location data, based on combining with map data (to reflect travel on roads) and a model of vehicle inertia, to significantly reduce position uncertainty and improve comparability across surveys. The researchers agreed that GPS receivers intended for navigation already incorporate these features and ITS will acquire such a receiver and repeat some of the surveys. Alpert has proposed using LiDAR data, which is openly available for Boulder from a 2010 survey, as an independent clutter survey. He acquired these data and Hammerschmidt is processing them as an alternative input (to USGS data) to ITS, in an attempt to reconcile with path loss surveys away from cluttered areas. Alpert will also assess whether standard LiDAR processing give shape descriptions that might suffice as clutter inputs.

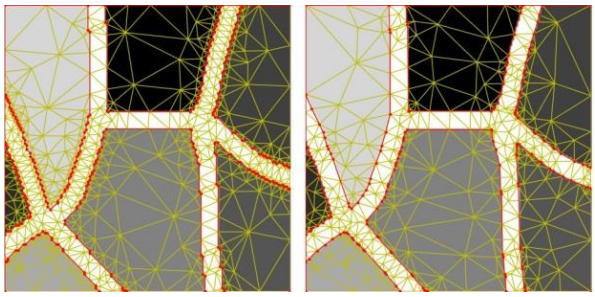

Figure 29. *Meshing a synthetic microstructure image. Compare previous result (left) with current result (right).*

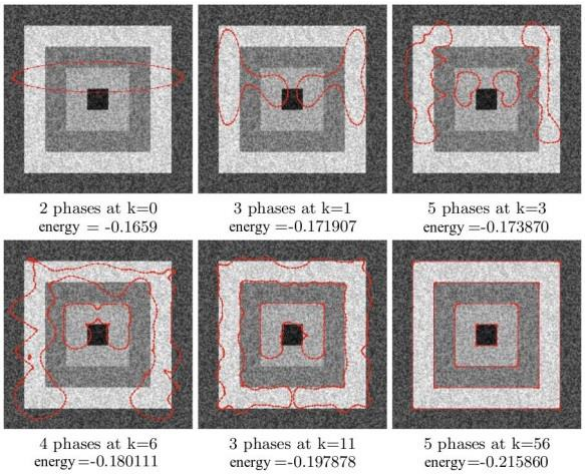

Figure 30. *Illustration of iterative curve evolution for multiphase image segmentation.*

Computational Tools for Shape Measurement and Analysis

Günay Doğan (Theiss Research)
Javier Bernal
Charles Hagwood (NIST ITL)
Ajay Kannan (Dartmouth College)
Jane Pan (UMBC)
Sharan Arkalgud (Thomas Jefferson High School)
Prashant Athavale (University of Toronto)

The main goal of this project is to develop efficient and reliable computational tools to detect geometric structures, such as curves, regions and boundaries, from given direct and indirect measurements, e.g., microscope images or tomographic measurements, as well as to evaluate and compare these geometric structures or shapes in a quantitative manner. This is important in many areas of science and engineering, where the practitioners obtain their data as images, and would like detect and analyze the objects in the data. Examples are microscopy images for cell biology or micro-CT (computed tomography) images of microstructures in material science. In 2014, we made advances in the following specific components of this project.

Shape dissimilarity metrics. We worked with Javier Bernal (ACMD) and Charles Hagwood (ITL/SED) to develop a fast method to compute the shape dissimilarity between closed curves. This is essential for large-scale shape analysis and statistics. The basis of our formulation is the elastic shape model of Srivastava et al. [1] used to compute geodesic distances between closed curves in 2D. This model is invariant with respect to translation, rotation, reparameterization, and can handle local stretching of curve features easily. The corresponding shape distance matches human intuition of shapes well and gives good results in practical applications. The downside of this model is that its computational cost is cubic with respect to the number of nodes on the given curves; it can be very expensive even for moderately

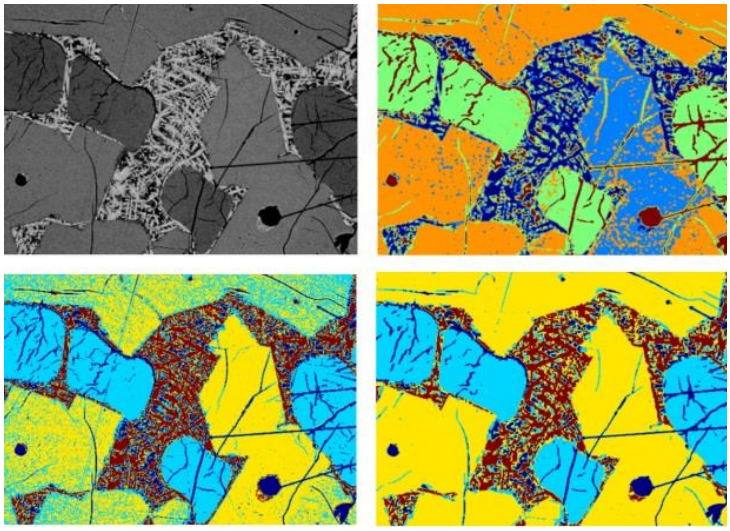

Figure 32. *Segmentation of micrograph (top-left) using a combination of total-variation denoising and k-means clustering (bottom-right). Without a good choice of k or denoising, the results are not as good (top-right, bottom-left).*

sized curves. We reformulated the underlying optimization and obtained an algorithm that is subquadratic in computational cost and behaves linearly in practice. Details are provided in a separate section on computation of shape geodesics.

Meshing segmented images. We worked with ACMD volunteer Ajay Kannan (Dartmouth College) to develop algorithms to characterize geometric structures in given 2D segmented images and to create meshes that exactly match the geometry in the images. The algorithm we developed extracts all grains, interfaces and junctions from the image and delineates the spatial relationships between them. Moreover it creates a triangulation that matches these structures exactly. Our algorithm is completely parameter-free and does not require any tuning or input from the user other than the segmented image. See Figure 29 for an illustration on a synthetic microstructure image.

Image segmentation. We pursued multiple approaches to address various image segmentation challenges. We implemented a multiphase version of a previous two-phase image segmentation algorithm, namely, the Chan-Vese approach, which uses level set evolution to detect region boundaries. Our new model uses a set of 1D curves to model boundaries of regions with approximately constant image intensity. Previous work in the literature requires multiple level set functions for the same problem, and requires the number of phases (regions) to be specified in advance, whereas, in our new model, this number of phases can change during the execution of the algorithm (see Figure 30 illustrating the adaptive segmentation process). Moreover, in order to realize robust termination of the iterative algorithm without user intervention, we developed a new dynamic stopping criterion that is effective under various difficult imaging scenarios, i.e. high noise, low contrast.

We developed the following additional image processing approaches and applications:

Clustering for image segmentation. We worked with SURF student Jane Pan to use the k-means clustering algorithm as a pre-segmentation algorithm. We used cluster stability analysis to automatically determine best clustering results out of several candidates. The combination of total-variation denoising and k-means clustering proved to be effective for many of the microstructure images we considered. See Figure 32 for an example of micrograph segmentation with this approach. It shows the original microstructure (top-left), clustering with wrong $k = 5$ (top-right), clustering without denoising (bottom-right), and good clustering after denoising (bottom-right).

Curve initialization for segmentation with junctions. We worked on extending the multiphase segmentation algorithm to handle junctions in region boundaries. To be able to initialize the extended version of the multiphase algorithm, one needs to extract two sets of boundary

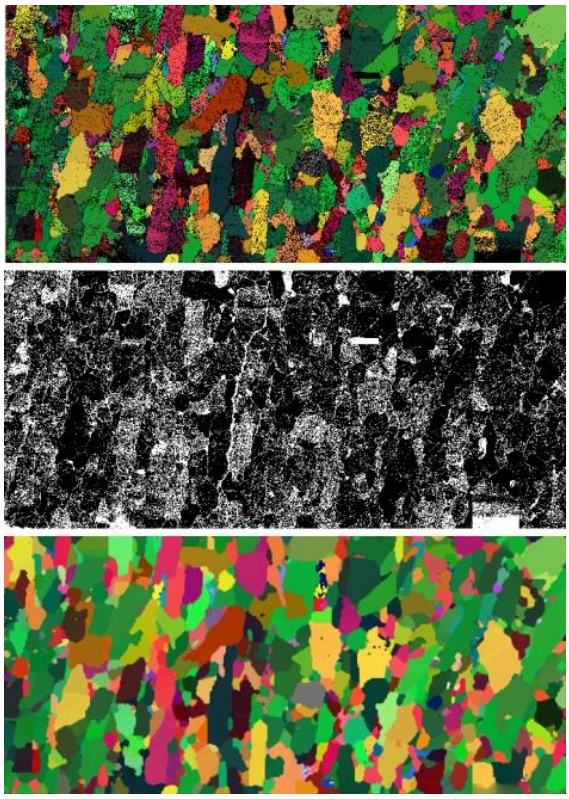

Figure 31. *An example of enhancement (bottom) of electron backscatter data imaging modality (top) with missing pixels (middle).*

curves from a given labeled image. We pursued this problem with SHIP student Sharan Arkalgud. The critical part of this problem was four-coloring of planar graphs (or maps). We developed a heuristic algorithm that gave promising preliminary results.

EBSD image enhancement. Electron backscatter data (EBSD) is an imaging modality that provides the orientation information for a crystal microstructure. It usually does not have the full information on a regular grid; some measurements might be missing, and some might be corrupted with noise. We worked with Prashant Athavale (University of Toronto) to develop a regularization algorithm that does both inpainting (completion of missing information) and piecewise constant smoothing. The result is very pleasing visually; the grains have constant orientation and grain boundaries are smooth (as expected from the physics). An example of the enhanced EBSD image is shown in Figure 31.

[1] Srivastava, E. Klassen, S. Joshi and I. Jermyn, Shape Analysis of Elastic Curves in Euclidean Spaces, *IEEE Transactions on Pattern Analysis and Machine Intelligence* **33:7** (2011), 1415–1428.

Computation of Shape Geodesics

Günay Doğan (Theiss Research)
Javier Bernal
Charles Hagwood (NIST ITL)

A major challenge of modern data sets is not only their sheer size, but also their elements may represent complex geometric structures and objects, e.g., proteins, cells, mechanical parts, facial surfaces, and other morphologies. Typically, one wants to cluster, classify or compare elements of such data sets, but performing such analyses requires defining a proper topological space where these entities reside. For data sets of such complex elements, the proper space may not be linear, thus making it impossible to use algorithmic tools designed for Euclidean spaces. This is the case for so-called shape spaces, which have been proposed for situations where elements of the data sets represent shapes of objects. A powerful shape space definition has been proposed by Srivastava et al. [1], enabling one to compute the elastic shape geodesic distance between closed planar curves. In [1], curves are considered as points in the appropriate Riemannian manifold, in which we can define and compute the geodesic distance between them. This geodesic distance measure is defined in a way that is invariant to scaling, translation, rotation and reparametrization of curves.

We have concentrated on the shape space framework of [1] and have developed a fast algorithm for computing the geodesic distance between the shapes of two closed curves. Such a fast algorithm is essential for large-scale shape analyses. The original algorithm proposed in [1] using dynamic programming has cubic time complexity with respect to the number of nodes per curve. This is computationally expensive. We propose a new fast algorithm whose asymptotic time complexity is roughly quadratic but which in our experiments demonstrated subquadratic, almost linear growth in running times depending on the type of curve data [2].

Mathematically, the shape distance computation is formulated as a global optimization over triplets of starting points, rotations and reparametrizations. With the starting point and rotation fixed, our algorithm computes a globally optimal reparametrization. For this, we developed a very fast iterative nonlinear constrained optimization algorithm initialized by the solution of a fast dynamic programming algorithm. The resulting reparametrization algorithm is plugged into another procedure of outer iterations that computes the optimal starting point and rotation separately. This separate optimization if done in the common naive way has quadratic time complexity as it takes place by looping through each node in one of the two curves. Recently,

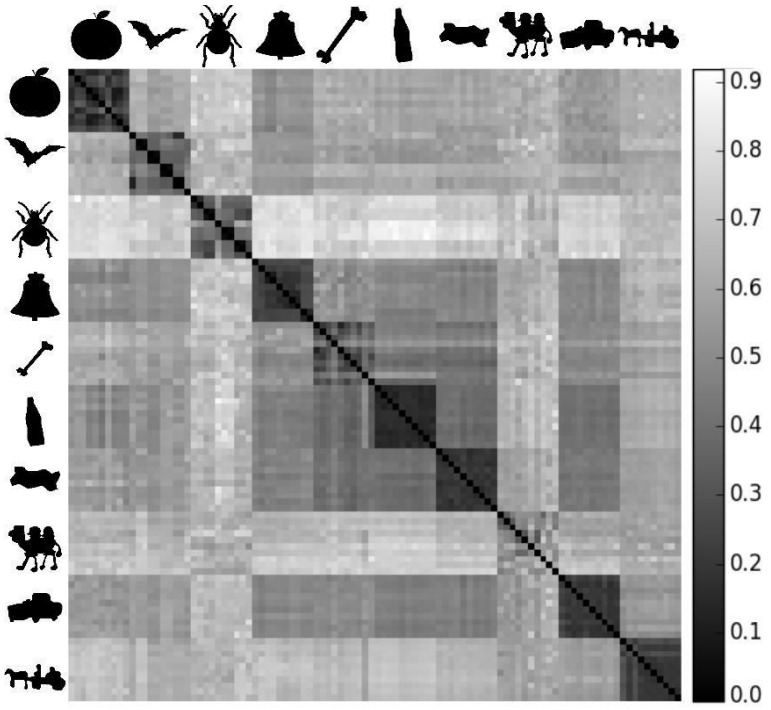

Figure 33. *Distance matrix of MPEG7 shape set.*

we developed a new algorithm for this based on the Fast Fourier Transform (FFT) that has O(N log N) complexity, where N is the number of nodes per curve. This resulted in an order of magnitude speed-up for the computation of the optimal starting point and rotation in our experiments. Accordingly, we found that our method for calculating accurate shape distance values, based on our new algorithms for computing optimal starting points, rotations and reparametrizations, does this at a fraction of the computational cost of previous approaches.

An illustration of our results with the MPEG7 shape data set is given in Figure 33, which provides a graphical illustration of the pairwise distances between 100 shape examples from the MPEG7 shape data set. For this example, we chose ten shape categories (apple, bat, beetle, bell, bone, bottle, brick, camel, car, carriage) and ten curve examples per category, resampled the curves at N=256 nodes, and computed the geodesic shape distances between the 100×100 pairs. As expected, the shape distances between curves in the same category, shown in the diagonal blocks, were smaller (appear darker in the figure), and the shape distances between curves from different categories, shown in off-diagonal blocks, were larger (appear brighter in the figure). We compared the original geodesic shape distance algorithm from [1] with our new algorithm. The original algorithm computed 100×100 distances in 129 hours, whereas our new algorithm computed the same distance matrix in 12.5 hours, a speed-up factor of 10. When the curves have more nodes, the speed-up is even more dramatic. For example, for curves with N=1024, our algorithm can be 50-1000 times faster than the original algorithm.

[1] A, Srivastava, E. Klassen, S. Joshi and I. Jermyn, Shape Analysis of Elastic Curves in Euclidean Space, *IEEE Transactions on Pattern Analysis and Machine Intelligence* **33:7** (2011) 1415-1428.

[2] G. Doğan, J. Bernal and C. Hagwood, A Fast Algorithm for Elastic Shape Distances between Closed Planar Curves, in review.

Neural Networks for Cell Feature Identification

Javier Bernal
Jose Torres-Jimenez (CINVESTAV, Mexico)

A backpropagation algorithm has been implemented for training neural networks to be used for the identification of subcellular features in cell images relevant to cell biologists. Approaches exist for recognizing objects or pattern classes associated with an image based on the use of sample patterns (training patterns) to estimate statistical parameters of each pattern class. However the statistical properties of the pattern classes might not be known or might be difficult to estimate. Therefore, the neural network approach that produces the required decision functions based solely on training without assumptions about probability density functions associated with the pattern classes may be more successful.

A neural network is a computational model that consists of computing elements called "neurons" organized as a network, reminiscent of the way in which neurons are believed to be interconnected in the brain. It is an adaptive system that changes its structure based on information that flows through the network during a training phase. It is mostly used for modeling relationships between input and output data and for partitioning data into classes.

During training with the backpropagation algorithm the average squared error between the networks' output and a target value is minimized for each point or pattern (in d-dimensional space) in the training set. Via training, coefficients of decision functions are obtained and associated with neurons in the network. Once the training is done other data points or patterns are put through the network and assigned to a class according to the output obtained. For our purposes the resulting implementation will be used for identifying pattern classes in d-dimensional space as each pixel in an image is associated with a d-dimensional pattern, the coordinates of the pattern corresponding to d distinct attributes associated with the pixel.

Since training a neural network as described is equivalent to minimizing an error function of several variables (weights in the network), a scaled conjugate gradient method (SCGM) has been implemented for this purpose as part of our backpropagation algorithm.

However, as the convergence of the weights with the SCGM can be slow at times during training, it is apparent that a hybridization of the SCGM and a metaheuristic algorithm such as the simulated annealing may be the way to alleviate this problem. Accordingly, an implementation of the simulated annealing algorithm to be used in tandem with the SCGM is underway.

Stable Explicit Time Marching in Well-posed or Ill-posed Nonlinear Parabolic Equations

Alfred S. Carasso

Significant progress has been made on stabilizing pure explicit time differencing in the numerical computation of multidimensional nonlinear parabolic equations on rectangular regions [4]. Explicit schemes are highly desirable because of their simplicity, but such schemes are seldom used as they entail prohibitive Courant stability restrictions on the time step Δt. Rather, unconditionally stable implicit schemes are commonly used, requiring

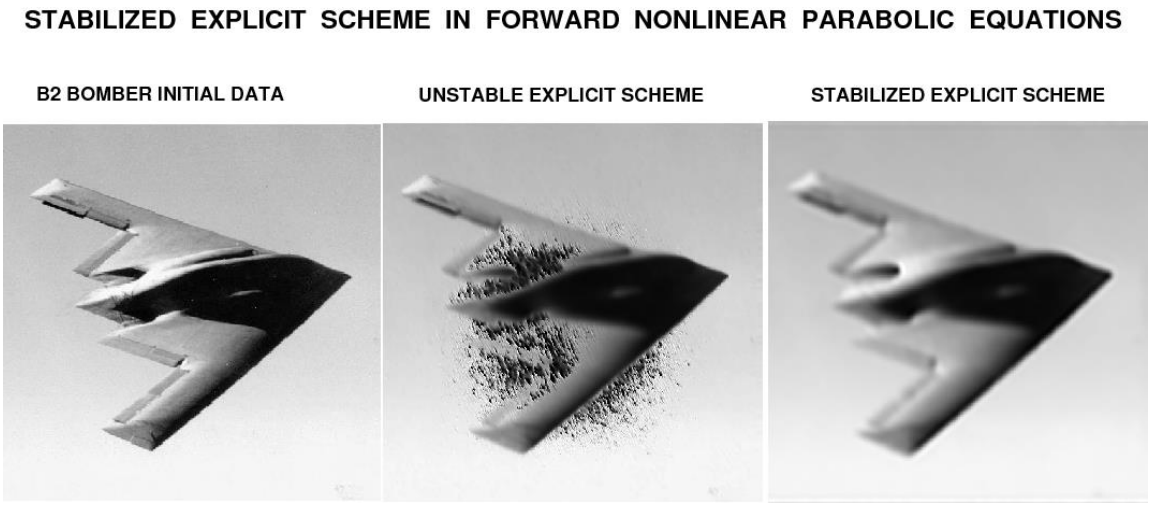

Figure 35. *Useful computation of well-posed forward nonlinear parabolic problems on 512×512 mesh, using stabilized explicit scheme with a value of Δt that is unstable in the uncompensated pure explicit scheme.*

computationally intensive solutions of the resulting algebraic systems of difference equations at each time step. The present stabilized explicit scheme uses easily synthesized linear smoothing operators at each time step to quench the instability. Smoothing operators $S = \exp\{-\varepsilon\, \Delta t\, (-\Delta)^p\}$, based on positive real powers of the negative Laplacian $(-\Delta)$, can be realized efficiently on rectangular domains using FFT algorithms. The stabilized explicit scheme requires no Courant restriction on the time step Δt, and is of great value in computing well-posed forward parabolic equations on fine meshes, by simply lagging the nonlinearity at the previous time step. Such stabilization leads to a *distortion* away from the true solution. However, that error is often small enough to allow useful results in many problems of interest

For ill-posed backward parabolic equations, all stepwise time marching algorithms, whether explicit or implicit, are necessarily *unconditionally unstable*. However, the stabilized explicit scheme is stable even when run *backward in time*. This opens the door to relatively easy and useful computation of multidimensional nonlinear backward parabolic equations, a category of problems that is widely believed to be intractable. The method complements the Quasi-Reversibility Method [5, 8], whose formulation is primarily oriented toward linear problems. There is considerable interest in such backward reconstructions, notably in the developing field of *environmental forensics* [3, 8], where contaminant transport is often modeled by parabolic advection dispersion equations [6, 7]. However, the class of nonlinear problems that can be handled by the present method is limited, although it is significant.

Let L be a linear autonomous second order elliptic differential operator with smooth variable coefficients in a rectangular region Ω in R^n, with homogeneous Dirichlet or Neumann boundary conditions on $\partial\Omega$. Let $\| \|_2$ denote the norm on $L^2(\Omega)$. The stabilized scheme involves the following *assumption* regarding the semigroups generated by $-(-\Delta)^p$ and $(L^*L)^{q/2}$: Given any $\omega > 0$, and q with $1 < q \leq 3$, there exist constants Γ, $\varepsilon > 0$, and $p \geq q$, such that for all $g \in L^2(\Omega)$ and sufficiently small time step Δt,

Figure 34. *Backward recovery from nonlinearly blurred data in 512×512 Liz Taylor image, using stabilized explicit scheme with $\Gamma = 1.0$, $\varepsilon = 7.5\times10^{-8}$, $p = 2.735$. Van Cittert procedure develops instabilities after 8 iterations.*

$$\| \exp\{-\varepsilon\, \Delta t\, (-\Delta)^p\}\, g \|_2 \le \Gamma \left\| \exp\left\{-\omega\, \Delta t\, (L^* L)^{\frac{q}{2}}\right\} g \right\|_2 \quad (1)$$

Results similar in nature to Eq. 1 are known in the deep theory of Gaussian estimates for heat kernels [1, 2]. In applications to nonlinear parabolic equations $u_t = Pu$, the operator L in Eq. 1 is assumed to be a useful linear approximation to the nonlinear elliptic operator P. Stabilization of the explicit scheme requires the selection of constants $\varepsilon > 0$, $p > 1$, and $\Gamma > 0$, together with subsequent interactive adjustment of these parameters based on prior knowledge about the solution. Having located a useful triple (ε, p, Γ), it is shown in [4] that a useful error bound can be obtained in terms of the parameters ω and q in the inequality in Eq. 1.

Fictitious nonlinear parabolic blurring and deblurring of 512×512 pixel images provide instructive mathematical examples. Underlying these images are highly irregular and jagged intensity surfaces, and these data can severely test potentially unstable computational algorithms. In Figure 35, useful results are obtained in a well-posed forward nonlinear parabolic equation using the stabilized explicit scheme with a time step Δt 10 times larger than required by the Courant condition. In Figure 34, useful backward in time reconstruction from severe nonlinear blurring is achieved. Moreover, in that problem, the computationally intensive Van Cittert iteration [9] becomes unstable after 8 iterations.

[1] W. Arendt and A. F. M. ter Elst, Gaussian Estimates for Second Order Elliptic Operators with Boundary Conditions, *Journal of Operator Theory* **38** (1997), 87-130.

[2] D. G. Aronson, Bounds for the Fundamental Solution of a Parabolic Equation, *Bulletin of the American Mathematical Society* **73** (1967), 890-896.

[3] J. Atmadja and A. C. Bagtzoglou, State of the Art Report on Mathematical Methods for Groundwater Pollution Source Identification, *Environmental Forensics* **2** (2001), 205-214.

[4] A. S. Carasso, Stable Explicit Time Marching in Well-Posed or Ill-Posed Nonlinear Parabolic Equations, NISTIR 8027, October 2014.

[5] R. Lattès and J. L. Lions, *The Method of Quasi-Reversibility*, American Elsevier, New York, 1969.

[6] J. D. Logan, *Transport Modeling in Hydrogeochemical Systems*, Springer, New York, 2001.

[7] R. N. Singh, Advection Diffusion Equation Models in Near-surface Geophysical and Environmental Sciences, *Journal of the Indian Geophysical Union* **17** (2013), 117-127.

[8] T. H. Skaggs and Z. J. Kabala, Recovering the History of a Groundwater Contaminant Plume: Method of Quasi-Reversibility, *Water Resources Research* **31** (1995), 2669-2673.

[9] P. H. Van Cittert, Zum Einfluss der Spaltbreite auf die Intensitätsverteilung in Spektrallinien II, *Zeitshrift für Physik* **69** (1931), 298-308.

Traceable Simulation of Magnetic Resonance Imaging

Zydrunas Gimbutas
Andrew Dienstfrey
Steve Russek (NIST PML)
Katy Keenan (NIST PML)
Karl Stupic (NIST PML)
Michael Boss (NIST PML)

Magnetic resonance imaging (MRI) is maturing as a quantitative biomedical imaging technology. For example, imaging facilities routinely report tumor volumes in units of mm^3, blood perfusion in units of ml g^{-1} min^{-1}, apparent diffusion coefficient in mm^2 s^{-1}, and temperature in K. However, as of a few years ago the use of SI units for these technologies was potentially unwarranted as SI traceability chains supporting these MRI measurement modalities were unclear if not non-existent. More recently NIST and partners have made substantial investments to develop such traceability chains. In the medical community, standard reference artifacts are referred to as *phantoms* and, in particular, NIST now supports several phantoms providing SI-traceable calibration artifacts for MRI scanners.

MRI is governed by solutions to

$$\frac{\mathrm{d}\mathbf{M}}{\mathrm{d}t} = \gamma \mathbf{M} \times \mathbf{B} - \frac{M_x \hat{\mathbf{x}} + M_y \hat{\mathbf{y}}}{T_2} + \frac{(M_0 - M_z)\hat{\mathbf{z}}}{T_1} + D\nabla^2 \mathbf{M}$$

known as the Bloch equations. Here $\mathbf{M}$ the magnetic moment arising from collections of nuclear spins, the gyromagnetic ratio γ is a physical constant, and $\mathbf{B}$ is the forcing magnetization. The quantities of medical interest are T_1, T_2 and D. The first two are tissue-dependent relaxation times. Experimental estimation of these times provides a two-parameter characterization of the material exhibiting the signal. This is the source of MRI's unparalleled capabilities for *in vivo* soft-tissue imaging. Moreover, D is an effective diffusion constant that reflects a combination of tissue porosity and anatomical structure. Refined control of the forcing function $\mathbf{B}$ using combinations of linear gradients and RF fields allows one to map distributions of T_1, T_2 and D. The details are numerous. The point of this brief discussion is to demonstrate that, while extremely challenging, predictive quantitative simulation of this imaging modality is nevertheless possible!

Virtual prototyping is highly desirable to improve the fundamental understanding of MRI capabilities resulting in significant reductions in time and costs to develop new scan technologies. A growing number of computer codes are available which claim to do just this. While there is uniform agreement on the potential for quantitative MRI simulation, neither NIST nor any other national metrology institution is currently positioned to certify the accuracy of such claims.

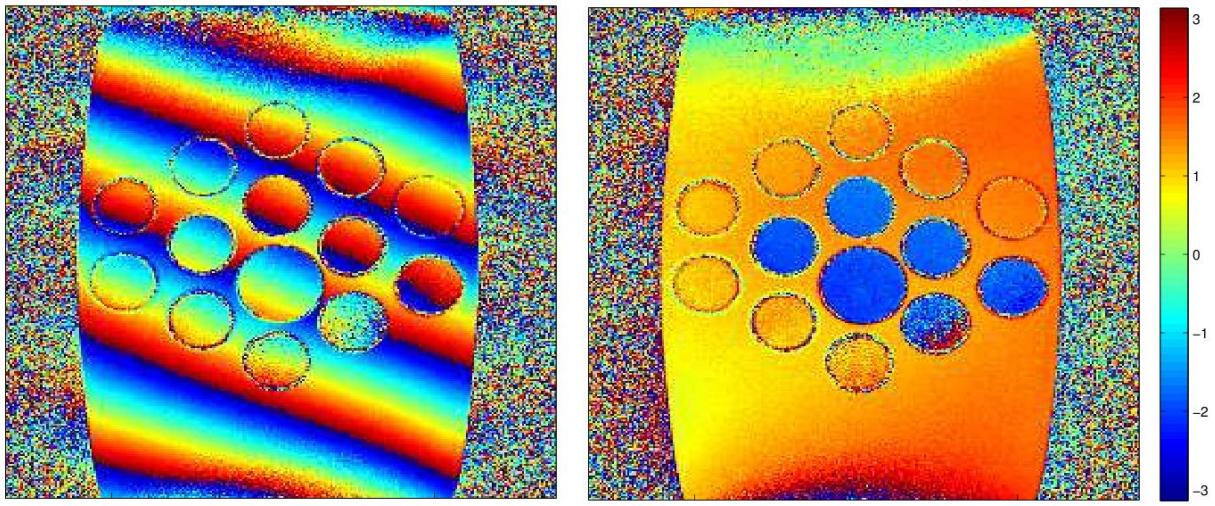

Figure 36. *The phase of the MRI signal as measured by the scanner contains a k-space offset. This results in the linear plane wave oscillation of phase shown in the image on the left. The right image shows this same phase measurement after applying the new correction analysis performed by NIST. This correction will allow for more detailed mapping of the distribution of magnetic moments in the future.*

In 2014 we developed an elementary MRI simulator to serve as the foundation for what we ultimately expect to become the computational reference for this community [1]. The NIST Bloch solver is parallelizable via OpenMP and includes several commonly used MRI sequences such as the gradient echo and spin echo sequence families, in both one and two dimensions, optionally combined with the inversion recovery step. We have also developed a new numerical scheme for acceleration of decaying exponential sums due to T_2 effects which allows much faster simulations of the received MRI signals. The method is based on the observation that the rates of T_2 are uniformly bounded within biomedical tissues of interest, therefore, over a finite measurement time the system of all possible signals can be compressed. For implementation efficiency, the proposed method is based on the interpolative decomposition of real decaying exponentials combined with the discrete Fourier transform. The interpolation basis of received MRI signals, interpolation nodes for time sampling, and signal scaling factors can all be precomputed, yielding a fast scheme involving a small number of the discrete (in general, non-uniform) Fourier transforms. A technical report is in preparation.

We have completed preliminary validations of the simulation results by comparison against measurements of T_1 and T_2 array phantoms provided by the MRI group at NIST. We are currently testing accuracy, performance, and comparing the simulation capabilities of several widely available MRI simulators and tools, such as SIMRI, JEMRIS, and ODIN [5-7]. In particular, quantitative error analysis of SIMRI simulator is under investigation. Such comparisons may serve as templates for the future computational benchmark problems.

In addition to virtual prototyping, there exist many research opportunities directly arising from experimental MRI signals analysis. In medical practice, quantitative measurement of T_1 and T_2 is useful for a wide range of assessments including: iron distribution in the brain which may serve as a biomarker for traumatic brain injury (see below), treatment monitoring for heart attacks, and multiple sclerosis [8]. These are just a few examples. In fact, the prospects for patho-physiological assessment enabled by quantitative-MRI are nearly limitless. The tradeoffs associated with this are time, cost, and accuracy. Together with the MRI measurement group at NIST, we are investigating T_1 and T_2 curve mapping techniques that use complex MRI signal data [2-4]. The new schemes compare favorably to the existing techniques that use only the magnitude of reconstructed MRI signal. For given accuracy, we expect a reduction in the number of MRI scans to be collected due to reduced numerical ranks of the fitting curves and possible use of model linearization. We have also discussed possibilities of developing non-linear gradient and phase error correction for the current NIST MRI measurement system.

A future line of investigation is exploring possibilities for quantitative measurement of the magnetic moment of local iron distribution. This distribution is suspected to be an important bio-marker for brain function, and irregularities that have been associated with traumatic brain injury. It is proposed that magnetic moments can be mapped by phase measurement of MRI signals. Figure 36 shows one such measurement. The image on the left reveals a heavily-wrapped phase image. The linear oscillation of phase across the image is the result of an offset of the k-space acquisition data. We have developed an analysis which estimates and corrects for this offset. The result is shown in the image on the

right. Correcting for this large systematic background effect will allow for more fine-scale analysis of magnetic moment distribution in the future.

[1] Z. Gimbutas and A. Dienstfrey, "MRI Simulators and their Performance", NIST Workshop on Standards for Quantitative MRI, July 14-17, 2014, NIST, Boulder, Colorado.

[2] N. Stikov, M. Boudreau, I. R. Levesque, C. L. Tardif, J. K. Barral, G. B. Pike, N. Stikov, et al., On the Accuracy of T_1 Mapping: Searching for Common Ground, *Magnetic Resonance in Medicine*, Feb 27, 2014.

[3] P. B. Kingsley, Signal Intensities and T_1 Calculations in Multiple-Echo Sequences with Imperfect Pulses, *Concepts in Magnetic Resonance* **11**:1 (1999), 29-49.

[4] P. B. Kingsley, Methods of Measuring Spin-Lattice (T_1) Relaxation Times: An Annotated Bibliography, *Concepts in Magnetic Resonance* **11**:4 (1999), 243-276.

[5] H. Benoit-Cattin, G. Collewet, H. Saint-Jaimes and C. Odet, The SIMRI Project: a Versatile and Interactive MRI Simulator, *Journal of Magnetic Resonance* **173**:1 (March 2005), 97-115.

[6] T. H. Jochimsen and M. von Mengershausen, ODIN - Object-oriented Development Interface for NMR, *Journal of Magnetic Resonance* **170**:1 (September 2004), 67-78.

[7] T. Stöcker, K. Vahedipour and D. Pugfelder, High-Performance Computing MRI simulations, *Magnetic Resonance in Medicine* **64**:1 (July 2010), 186-193.

[8] H.-L. Cheng, et al, Practical Medical Applications of Quantitative MR Relaxometry, *Journal of Magnetic Resonance Imaging* **36** (2012), 805-824.

Parallel Adaptive Refinement and Multigrid Finite Element Methods

William F. Mitchell
Marjorie A. McClain
Eite Tiesinga (NIST PML)
Paul Julienne (NIST PML)
John Villarrubia (NIST PML)
Garnett Bryant (NIST PML)

http://math.nist.gov/phaml

Finite element methods using adaptive refinement and multigrid techniques have been shown to be very efficient for solving partial differential equations (PDEs). Adaptive refinement reduces the number of grid points by concentrating the grid in the areas where the action is, and multigrid methods solve the resulting linear systems in an optimal number of operations. Recent research has focused on *hp*-adaptive methods where adaptivity is in both the grid size and the polynomial order of approximation, resulting in exponential rates of convergence. W. Mitchell has been developing a code, PHAML, to apply these methods on parallel computers. The expertise and software developed in this project are useful for many NIST laboratory programs, including material design, semiconductor device simulation, the quantum physics of matter, and simulation of scanning electron microscopes.

Recently we completed a study of the performance of 13 proposed *hp*-adaptive strategies in terms of accuracy vs. degrees of freedom and computation time vs. degrees of freedom. A paper presenting the results of this experiment appeared in *ACM Transactions on Mathematical Software* this year. For this experiment we gathered a collection of 12 test problems, most of which came from the numerical results section of papers on *hp*-adaptive refinement. These problems contain a variety of difficulties including singularities, sharp peaks, wave fronts, oscillations and boundary layers. Most of them are parametrized to adjust the strength of the difficulty. We found that the strategy which is most effective depends on the type of difficulty and the accuracy requirements. The so-called reference solution methods performed well in terms of accuracy vs. degrees of freedom, but are very expensive computationally. In terms of accuracy vs. computation time, the use of *a priori* knowledge is best for problems with known singularities and no other significant feature, while the method based on the decay rate of the coefficients of the *p*-hierarchical basis seems to be the best general purpose strategy.

The 12 test problems used in the study are all 2D linear elliptic PDEs. We believe it would be useful to create a collection of standard benchmark PDEs, appropriate for adaptive mesh refinement, of other types, including 3D, parabolic, hyperbolic, nonlinear, etc. We have created a web site [1] to make such a collection available to the research community. This year we made improvements to the design of the web site and added 15 more benchmark problems. The new problems include 1D, 3D, nonlinear, and parabolic problems.

There are three major collaborative efforts with PML to apply PHAML to their physical models.

- In a collaboration with Eite Tiesinga and Paul Julienne, we are using PHAML to study the interaction of atoms and molecules held in an optical trap. Previously we calculated the bound states, scattering properties and dynamics of two dipolar molecules held in a cylindrically symmetric trap, a 2D problem. We have extended these simulations to a 3D model without the assumption of cylindrical symmetry. This year we demonstrated that PHAML can be used to perform experiments to see how varying the parameters of a simulation affects the energy levels and wave functions. We performed computations with the 3D model of the interaction of two trapped RbCs dipoles in which we varied (1) the strength of the dipolement, and (2) the angle between the dipoles. Figure 37 shows how the first ten

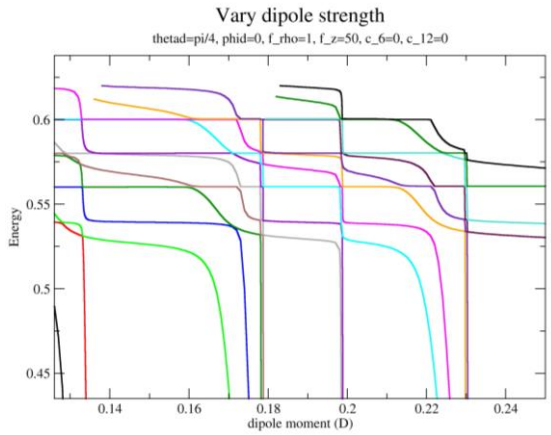

Figure 37. *Effect of the strength of the dipole moment on the first ten eigenenergies of a model of two trapped RbCs molecules.*

eigenvalues (energy levels) change as the strength of the dipole moment varies from 0.125 to 0.25 D.

- We are also collaborating with John Villarrubia to apply PHAML to the modeling of scanning electron microscope images of samples that contain a mixture of conducting and insulating regions. Villarrubia has a code that models electron scattering in materials, secondary electron production, and detection. We have coupled this code with PHAML which performs the finite element analysis to determine the electric fields that affect the image. This year we validated the use of PHAML for this application by comparing results with GetDP, the finite element program that was previously used. We performed several performance enhancements for this application and obtained a 5-fold speedup over GetDP. We also extended PHAML to handle floating constraints, which occur when the sample contains a stray piece of metal.
- We have begun a new collaboration with Garnett Bryant to apply PHAML to the simulation of quantum dot structures. Nanoscale semiconductor quantum dot structures can be modified, controlled, and manipulated by applied electric fields that arise from the local strain in the quantum dots. In this collaboration we will use PHAML to determine these applied fields and potentials down to the scale of the quantum dots. PHAML will be interfaced as needed with existing codes that are being used to describe these quantum dot structures.

Future work will continue to enhance PHAML with additional capabilities, robustness and efficiency, implement and study some recently proposed *hp*-adaptive strategies, complete the extension of PHAML to 3D problems, continue the development of the adaptive mesh refinement benchmark suite, and continue collaborations that use PHAML on NIST applications.

[1] NIST Adaptive Mesh Refinement Benchmark Problems, http://math.nist.gov/amr-benchmark.

[2] W. F. Mitchell and M. A. McClain, A Comparison of *hp*-Adaptive Strategies for Elliptic Partial Differential Equations, *ACM Transactions on Mathematical Software* **41**:1 (2014).

[3] W. F. Mitchell, A Collection of 2D Elliptic Problems for Testing Adaptive Algorithms, *Applied Mathematics and Computation* **220** (2013), 350-364.

[4] W. F. Mitchell, "Recent Advances in PHAML," SIAM Conference on Parallel Processing for Scientific Computing, Portland, OR, February 2014.

[5] W. F. Mitchell and M. A. McClain, "Performance of *hp*-Adaptive Strategies for Elliptic Partial Differential Equations," International Conference on Spectral and High Order Methods, Salt Lake City, UT, June 2014.

[6] W. F. Mitchell and M. A. McClain, "Performance of *hp*-Adaptive Strategies for Elliptic Partial Differential Equations," International Conference on Numerical Analysis and Applied Mathematics, Rhodes, Greece, September 2014.

Numerical Solutions of the Time-Dependent Schrödinger Equation

Barry I. Schneider
Klaus Bartschat (Drake University)
Xiaoxu Guan (Drake University)
Johannes Feist (Universidad Autónoma de Madrid)
Stefan Nagele (Vienna University of Technology)
Joachim Burgdörfer (Vienna University of Technology)
Renate Pazourek (Louisiana State University)

We have been collaborating for a number of years to develop numerically robust methods for solving the time-dependent Schrödinger equation. Although the methods that have been developed are quite general, the applications to date have concentrated on describing the single and double ionization of electrons exposed to intense, ultrafast, laser radiation.

These attosecond (10^{-18} s) pulses provide a new window to study the electronic motion in atoms and molecules on their natural timescale. To put this in context, the motion of electrons, responsible for chemical binding and electron transfer processes in nature, have a characteristic timescale of about 100 attoseconds. (It takes an electron 152 attoseconds to go around the hydrogen atom.) These processes can only be described using time dependent quantum mechanics and, where appropriate, need to be coupled to Maxwell's equations. At the end of the day, we wish to image quantum phenomena with subfemtosecond temporal and sub-Angstrom spatial resolution. Eventually, one can contemplate producing "molecular movies" of this motion in much the same way as it is done in molecular dynamics simulations of heavy particle processes.

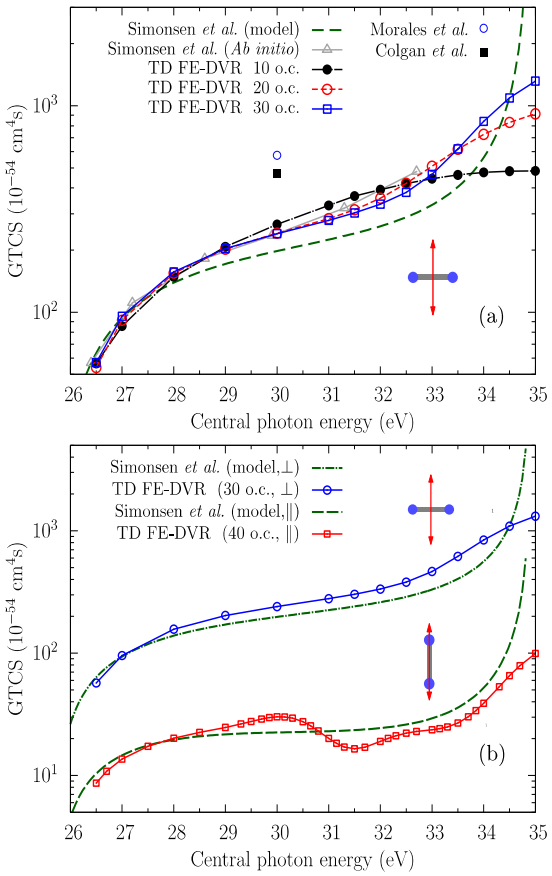

Figure 38. *Generalized total cross section for two-photon double ionization of the H_2 molecule. In the upper panel, the molecular axis is oriented perpendicular to the linear polarization vector (represented by a double-headed arrow) of the laser pulse. Our present results were obtained for pulse lengths of 10, 20, and 30 optical cycles. Also shown are the ab initio and the model results of Simonsen et al., as well as the cross sections of Colgan et al. and Morales et al. at 30 eV. The lower panel shows a comparison between our ab initio results obtained in the perpendicular and parallel geometries, with the corresponding predictions from a simple model suggested by Simonsen.*

The basic methodology as applied to atoms and simple diatomic molecules, has been described in [1-3] and [4] provides a detailed review of the work. The essential aspects have been

- development of the finite element discrete variable method (FEDVR) to spatially discretize the coordinates of the electrons, and
- use of the short iterative Lanczos method to propagate the wavefunction in time.

The method has been efficiently parallelized using MPI and scales linearly with the size of the FEDVR basis. Large scale calculations have been performed on a number of atoms and molecules using resources provided by the NSF Extreme Science and Engineering Discovery Environment (XSEDE). The group has received a competitively awarded allocation of more than 8 million service units for the current fiscal year.

During the past year, the group has concentrated its efforts on describing the H_2 molecule when exposed to radiation parallel and perpendicular to the internuclear axis. These studies provide benchmark calculations which may be used by others to test their numerical approaches. The calculations, described in [5-6], show quite different behavior from one another. This is a consequence of the difference in the intermediate excited states populated by the orientation of the radiation field with respect to the internuclear axis. In the parallel geometry, the very long-lived double excited states of H_2 require quite long pules to resolve the dynamics as the quantum state evolves in time while the perpendicular geometry is essentially insensitive to the length of the pulses. In Figure 38 we compare the current calculations in the perpendicular and parallel geometry with some others. The calculations show excellent agreement with other time-dependent approaches but disagree with calculations using time-independent methods. Resolving the detailed dynamics of these double excited states remains a computational challenge and the role of the pulses, particularly their length, is critical to understanding the physics.

Future developments will extend the methodology to polyatomic molecules and examine more efficient methods of propagating the wavefunction in time. In addition, there will be some effort to examine other partial differential equations to determine the generality of the approach beyond the current application to intense, short radiation.

[1] J. Feist, S. Nagele, R. Pazourek, E. Persson, B. I. Schneider, L. A. Collins and J. Burgdörfer, Nonsequential Two-Photon Double Ionization of Helium, *Physical Review A* **77**, 043420 (2008).

[2] X. Guan, K. Bartschat and B. I. Schneider, Dynamics of Two-photon Ionization of Helium in Short Intense XUV Laser Pulses, *Physical Review A* **77** (2008), 043421.

[3] X. Guan, K. Bartschat, and B. I. Schneider, Two-photon Double Ionization of H_2 in Intense Femtosecond Laser Pulses, *Physical Review A* **82** (2010), 041407.

[4] B. I. Schneider, J. Feist, S. Nagele, R. Pazourek, S. Hu, L. Collins and J. Burgdörfer, Recent Advances in Computational Methods for the Solution of the Time-Dependent Schrödinger Equation for the Interaction of Short, Intense Radiation with One and Two Electron Systems, in *Dynamic Imaging*, Theoretical and Numerical Methods Series: CRM Series in Mathematical Physics XV (A**.** Bandrauk and M. Ivanov eds.), 2011.

[5] X. Guan, K. Bartschat, B. I. Schneider, L. Koesterke, Resonance Effects in Two-Photon Ionization of H_2 by Femtosecond XUV Laser Pulses, *Physical Review A* **88** (2013), 043402.

[6] X. Guan, K. Bartschat, B. I. Schneider and L. Koesterke, Alignment and Pulse-duration Effects in Two-photon Double Ionization of H_2 by Femtosecond XUV Laser Pulses, *Physical Review A* **90** (2014), 043416.

Equilibrium and Stability of Liquid Drops on a Conical Substrate under Gravity

Asha K. Nurse
Sean Colbert-Kelly
Geoffrey B. McFadden
Sam R. Coriell (NIST MML)

Capillary forces lead to a rich collection of problems in physics, chemistry, and materials science that have both beauty and technological importance [1]. Shapes such as soap films, drops, and bubbles display interesting dynamical and equilibrium behavior, and have been studied in a variety of settings (see, e.g., the review articles [2, 3] and references therein).

Here we study the equilibrium and stability of an axisymmetric liquid drop that is resting on the side of a conical solid substrate under the combined effects of capillarity and gravity. This study is motivated by recent experimental observations of the behavior of clusters of biological cells that self-assemble at the bottom of patterned containers [4, 5]. Each compartment of the partitioned container includes a conical obstruction in its base that interrupts the tissue assembly, leading to toroidal clusters of cells at the base of each cone. After assembly, a cell cluster is often observed to climb up the side of the cone.

A possible mechanism for this dynamical behavior is based on the interplay of capillarity and gravitational forces: a toroidal tissue cluster would like to reduce its surface area, which it can do by reducing its major radius (the long way around the torus) by moving to higher positions on the cone. In climbing the cone the gravitational potential energy of the sample is increased, so the dynamical process must balance both forms of energy. A model of the dynamical process based on toroidally-shaped clusters evolving by surface diffusion has been used [4] to interpret the experimental observations, which occasionally included both tilting of the cell cluster relative to the cone axis (see Figure 39), and the development of fluted distortions in the azimuthal direction.

In the light of these interesting experiments it seems desirable to consider the simpler problem of determining the equilibrium and stability of liquid drops on a conical substrate. We formulate a variational statement of the problem in terms of an energy functional containing both surface energy and gravitational potential energy contributions subject to a volume constraint. Axisymmetric stationary shapes that extremize the energy then satisfy the Laplace-Young equation that represents the local balance of capillary, gravitational, and pressure forces at each point of the interface. Appropriate natural boundary conditions at the contact line where the drop, substrate, and surrounding fluid meet also follow from

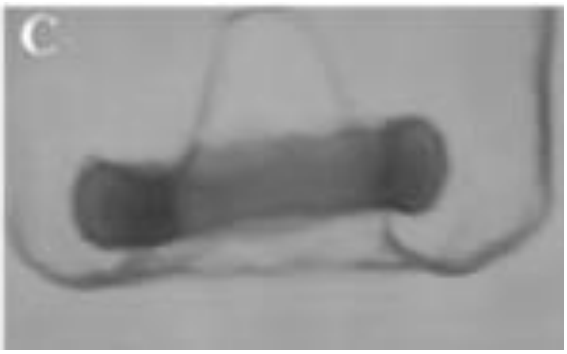

Figure 39. *Side view of a toroidal cluster of biological cells climbing the side of a conical obstacle in a patterned substrate [5]. The right hand side of the cluster is slightly higher than the left hand side, suggesting a possible asymmetric instability of an axisymmetric configuration.*

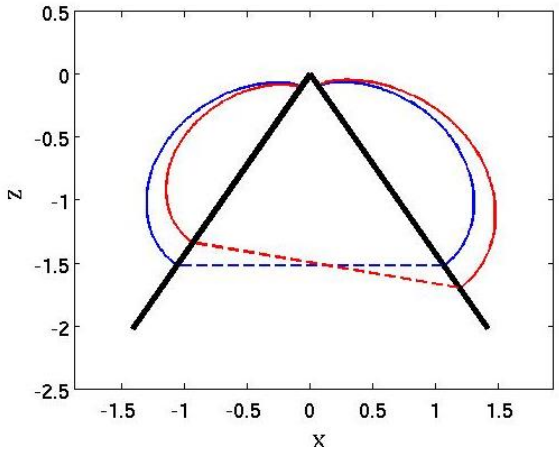

Figure 40. *Numerical calculation of the axisymmetric equilibrium shape (blue curve) and the asymmetric perturbed shape (red curve) producing a tilted drop [6]. Here gravity is in the downward direction, the half-angle of the cone is 35 degrees and the contact angle of the drop is 90 degrees.*

the variational principle, yielding the familiar Young boundary condition that determines the drop's contact angle at the trijunction. The second variation of the energy functional is examined numerically to determine the linear stability of the equilibrium shapes. Among the results, we find that the equilibrium shapes are often unstable to non-axisymmetric perturbations that produce tilting of the toroid relative to the cone axis; an example is shown in Figure 40. We also find a broad class of instabilities that resemble the Rayleigh instability that is responsible for the break-up of a cylindrical liquid jet into droplets whose radius is roughly that of the jet's circumference. This work has been submitted for publication [6] and is currently undergoing revision to address referee comments. A related paper is undergoing review [7].

[1] Pierre-Gilles de Gennes, Francoise Brochard-Wyart, and David Quere, *Capillarity and Wetting Phenomena:*

Drops, Bubbles, Pearls, Waves (Springer, Berlin, 2004).

[2] H. M. Princen, The Equilibrium Shape of Interfaces, Drops, and Bubbles: Rigid and Deformable Particles at Interfaces, in *Surface and Colloid Science* **2**, (Egon Matijevic, ed.), Wiley-Interscience, New York, 1969, 1-84.

[3] D. H. Michael, Meniscus Stability, *Annual Review of Fluid Mechanics* **81** (1981), 189-215.

[4] A. Nurse, L. B. Freund and J. Youssef, A Model of Force Generation in a Three-dimensional Toroidal Cluster of Cells, *Journal of Applied Mechanics* **79** (2012), 051013.

[5] J. Youssef, A. K. Nurse, L. B. Freund and J. R. Morgan, Quantification of the Forces Driving Self-assembly of Three-dimensional Microtissues, *Proceedings of the National Academy of Sciences* **108** (2011), 6993-6998.

[6] A. K. Nurse, S. Colbert-Kelly, S. R. Coriell and G. B. McFadden, Equilibrium and Stability of Axisymmetric Drops on a Conical Substrate under Gravity, in review.

[7] A.K. Nurse, S.R. Coriell and G. B. McFadden, On the Stability of Rotating Drops, in review.

Modeling Magnetic Fusion

Geoffrey McFadden
Antoine Cerfon (New York University)

A future source of commercial energy may be based on the controlled fusion of a hot plasma of hydrogen isotopes that is confined by a strong magnetic field. Quite often a toroidal geometry is envisioned in which the ions fuse to form helium and release energetic neutrons. A number of computational methods to model such magnetic fusion devices have been developed by researchers at New York University (NYU) and elsewhere to allow effective numerical simulations of the most essential features of modern tokomak and stellarator experiments.

G. McFadden and colleagues at NYU are currently participating in a benchmarking exercise to compare the simulation results produced by a number of codes that are in use by the fusion community [1, 2]. The benchmark is based on the DIII-D tokomak experiment at General Atomics in San Diego, California. We are evaluating the NSTAB equilibrium and stability code developed by Paul Garabedian and Mark Taylor at NYU [3], which uses a variational formulation of the equations of magneto-hydrodynamics to compute plasma equilibria that exhibit a family of nested flux surfaces that enable plasma containment [4]. The benchmarking exercise is being organized by researchers at the Princeton Plasma Physics Lab and Oak Ridge National Laboratory.

[1] A. Reiman, A. Cerfon, G. McFadden, et al., Tokamak Plasma High Field Side Response to a *n*=3 Magnetic Perturbation: A Comparison of 3D Equilibrium Solutions from Seven Different Codes, in review.

[2] A. Reiman, A. Cerfon, G. McFadden, et al., A Cross-Benchmarking and Validation Initiative for Tokamak 3D Equilibrium Calculations, in *Proceedings of the 25th IAEA Fusion Energy Conference* (AEA CN-221), St. Petersburg, Russia, 13-18 October 13-18, 2014.

[3] M. Taylor, A High Performance Spectral Code for Nonlinear MHD Stability, *Journal of Computational Physics* **110** (1994), 407-418.

[4] P. R. Garabedian and G. B. McFadden, Design of the DEMO Fusion Reactor Following ITER, *Journal of Research of the NIST* **114** (2009), 229-236.

Design-Basis Hurricane Winds and Missiles for Nuclear Power Plants

Florian A. Potra
Emil Simiu (NIST EL)
Brad Harvey (Nuclear Regulatory Commission)
Kevin Quinlan (Nuclear Regulatory Commission)

To ensure the safety of nuclear power plants in the event of a hurricane strike, U.S. Nuclear Regulatory Commission (NRC) regulations require that nuclear power plant designs consider the impact of hurricane-generated missiles in addition to the direct action of the hurricane wind. Hurricanes are capable of generating missiles from objects lying within the path of the hurricane wind and from the debris of nearby damaged structures. Protection from a spectrum of missiles (ranging from a massive missile that deforms on impact to a rigid penetrating missile) provides assurance that the structures, systems, and components important to safety will be available to mitigate the potential effects of a hurricane on plant safety.

The implementation of the Enhanced Fujita Scale in 2007 by the U.S. National Weather Service resulted in decreasing the design-basis tornado wind speeds suggested by the NRC. With the reduction of the design-basis tornado wind speeds, it was no longer clear that the revised design-basis tornado wind and missiles would bound the design-basis hurricane wind and missiles in all areas of the United States. This prompted studies into extreme wind gusts during hurricanes and their relationship to hurricane missile speeds. The study of missile speeds during hurricanes concluded that, because of assumed differences between the tornado and hurricane wind fields, airborne missiles can fly faster in a hurricane wind field having the same 3 second gust wind speed at 10 meters (33 feet) above terrain with open exposure as a tornado wind field.

Figure 41 presents the resulting map for hurricane wind speeds with annual exceedance probabilities of 10^{-7}. These wind speeds are representative of a 3 second peak gust wind speed at a height of 10 m (33 feet) above ground in flat open terrain, which is consistent with the definition of Exposure C in ASCE/SEI 7-05.

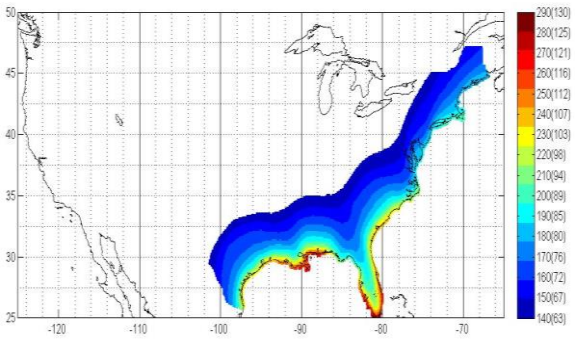

Figure 41. *Design-basis hurricane peak-gust wind speeds in mph (m/s) at 10-m height in flat open terrain, annual exceedance probability of 10^{-7} (from Figure 3-4 of NUREG/CR-7005).*

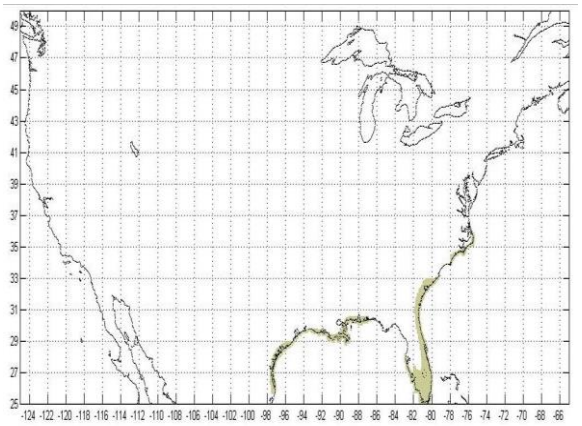

Figure 42. *Locations where design-basis hurricane wind speeds exceed those for tornadoes, annual exceedance probability of 10^{-7} (from Figure 3-6 of NUREG/CR-7005).*

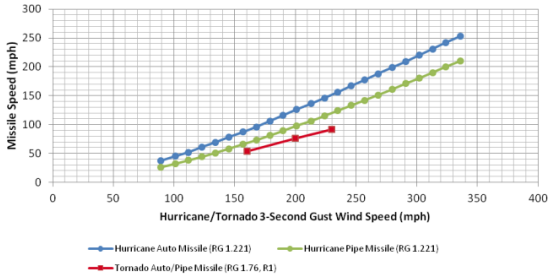

Figure 43. *Maximum horizontal speeds for the design-basis hurricane and tornado automobile and schedule 40 pipe missiles.*

Figure 42 shows locations that have design-basis hurricane wind speeds higher than the recommended design-basis tornado wind speeds. Along the Gulf and southern Atlantic coastlines, the hurricane-induced wind gusts can be higher than the regionalized gusts produced by tornadoes.

The resulting automobile and schedule 40 pipe horizontal missile speeds as derived from the analysis presented in NUREG/CR-7004 [1] and as incorporated into RG 1.221 are plotted in Figure 43. The NRC considers the design-basis hurricane missiles to be capable of striking in all directions with the horizontal speeds shown in Figure 43 and with a vertical speed of 26 m/s (58 mph). The horizontal hurricane missile speeds shown in Figure 43 represent maximum horizontal missile speeds in open terrain.

New numerical simulations show that airborne missiles can fly faster in a hurricane wind field than previously assumed. The results have been submitted recently for publication [2]. Further simulations with improved models are planned in the future.

[1] E. Simiu and F. A. Potra, *Technical Basis for Regulatory Guidance on Design-Basis Hurricane Borne Missile Speeds for Nuclear Power Plants*, NUREG/CR-7004, U.S. Nuclear Regulatory Commission, Washington, D.C., 2011.

[2] B. Harvey, E. Simiu, F. A. Potra, K. Quinlan and N. Chokshi, Design-basis Hurricane Winds and Missiles for Nuclear Power Plants, in review.

Algorithm Development and Uncertainty Quantification in Tomographic Radiation Transport Applications

Anthony Kearsley
Walid Keyrouz (NIST ITL)
Zachary Levine (NIST PL)
Adam Pintar (NIST ITL)

Radiation transport underlies many measurement techniques used at NIST and around the world. Examples include x-ray tomography, electron tomography, neutron tomography, and optical scattering for radiometry and medicine. The measurements of interest in radiation transport problems are the solutions to inverse problems. A source emits radiation, the radiation travels through a sample, and detectors observe the radiation afterward. Based on noisy observations, the properties of the sample, which are the quantities of interest, are inferred. Since the reconstructions are based on noisy data, the reconstructions are only estimates of the true sample properties. If another dataset was observed under the same conditions, the result would be different, and so too would the reconstruction.

An example of this problem is Greenhouse Gas Sequestration Monitoring (GGSM) (see Figure 44). Any carbon sequestration effort must be massive in scale to produce a noticeable effect in the amount of carbon dioxide released. It will be important to employ wide-scale automated systems to monitor for leaks; otherwise, the entire effort is in vain. Establishing the feasibility of such monitoring by analyzing Dual Optical Absorption Spectroscopy (DOAS) measurements with a pseudo-tomographic approach is a goal of researchers in this area. Uncertainty quantification is especially important

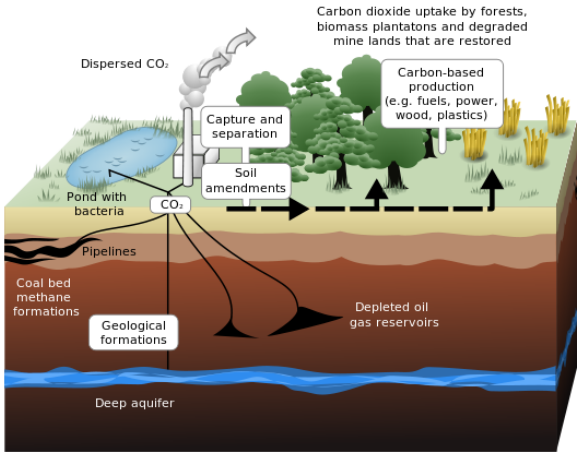

Figure 44. *Cartoon illustrating the GGSM problem: the desire is to capture $C0_2$ from, for example, power plant smoke stacks and store it (or transport it).*

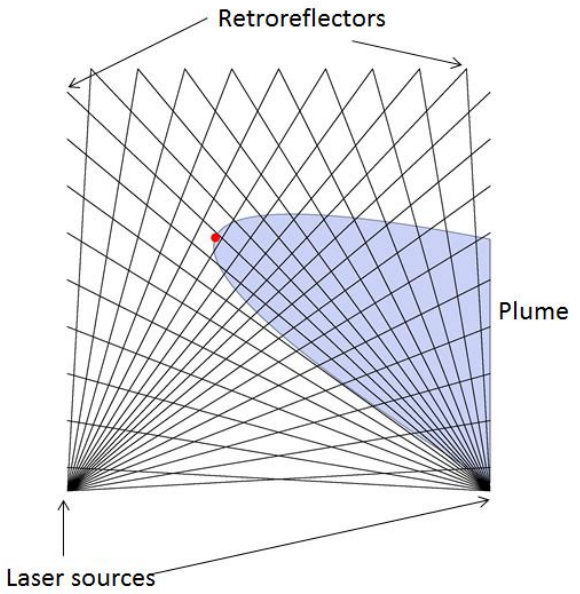

Figure 45. *Laser sources and reflectors are used to model the size, shape and location of a plume.*

when the data are information-poor because the estimated location of the leak may be quite far from the actual location. These situations can arise when relatively few measurements are made, or the leak is slow and the plume concentration is difficult to detect (see Figure 45).

Radiation transport models predict what detectors will observe under an assumed set of underlying conditions, i.e., a sample property or measurement of interest. To estimate the underlying conditions, they may be adjusted until there is good agreement between the predictions and the observations. The observations follow statistically independent Poisson distributions, where the Poisson mean is provided by the combination of the radiation transport model and the plume model. There is ample prior information about the underlying conditions since some parameters of the plume model such as the wind velocity may be measured separately.

Our work has examined formulating objective functions using point estimation and uncertainty quantification. These two things are linked by a posterior distribution. The point estimate will be the mode of the posterior distribution, i.e., the underlying condition with the highest probability given the observed data. There are other reasonable point estimates such as the posterior mean or median, but in cases where the information content of the data is high all three should be similar. Standard uncertainties are taken from the covariance matrix of the posterior distribution, and posterior intervals (regions in more than 1D) cover a specified amount of posterior probability (say 95 %).

We have also begun working on specialized optimization algorithms tailored to radiation transport problems. In situations where one wishes to optimize a "bumpy" function, the extent of the "bumpiness" is often caused by noise. Here it appears that there are two sources of noise. The data are noisy realizations of the predictions, and thus contain incomplete information about the nature of the true underlying conditions. Also, to realize a set of predictions from radiation transport models, Monte Carlo calculations are required, so the predictions themselves are noisy.

Robust and Efficient Optimization for Simulating Building Energy Usage

Anthony Kearsley
Amanda Pertzborn (NIST EL)
Jin Wen (Drexel University)
Shokouh Pourarian (Drexel University)
Dan Veronica (NIST EL)

About 82 % of electrical usage in the United States primarily arises from building consumption [1], and approximately 84 % of the life cycle energy use of a building is associated with its operation rather than material and construction costs [2]. Clearly, optimal operational decisions are crucial to energy efficiency and will become more and more important as buildings interact more with a smart electric grid. This adds new opportunities to move optimal decision making for each building into the realm of automated so-called cyber-physical systems (CPS) which are, in turn, governed by artificial intelligence. For example, information provided to the building control system by the smart grid, such as real-time electricity pricing, can be used to make decisions about whether to use the power generated by

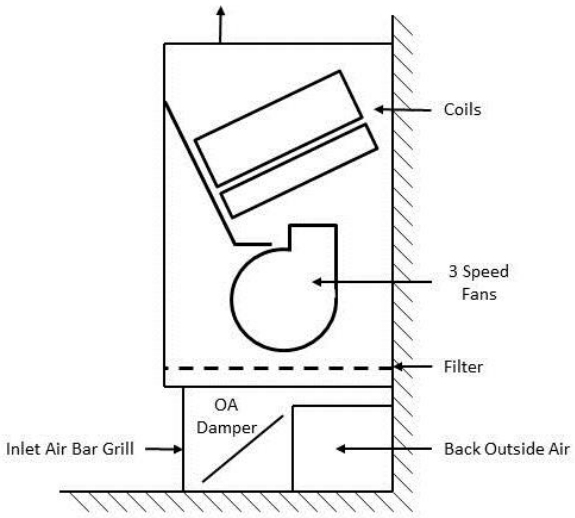

Figure 46. *Fan Coil Unit (FCU) geometry.*

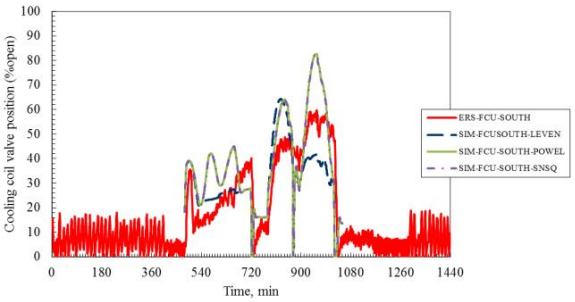

Figure 47. *Obvious inconsistency in numerical behavior of nonlinear solvers and failure to converge of the currently employed method.*

solar panels in the building itself or sell to a utility. Engineering development of the algorithms needed to provide this intelligence requires a robust simulation test bed that currently does not exist.

HVACSIM+, the current simulation test bed, was developed at NIST in the 1980s for the simulation of heating, ventilating, and air conditioning (HVAC) systems [3]. A specialized solver was originally developed for HVACSIM+ but recently the character of the nonlinear systems encountered has changed dramatically. Simulating energy usage in buildings today requires nonlinear models containing far more zones (or computational blocks) than previously, and the types of simulation scenarios have become more complicated.

An example of this can be illustrated in a "fan-coil" unit (FCU), a simple but economically important structure appearing in commercial, institutional and multifamily residential buildings. In Figure 46, a vertical floor-mounted four-pipe hydronic system including three parallel fans run by two electric motors with three speeds would be used to modulate the amount of ventilation supplied by way of a motorized damper in the outside air connection at the back of the unit. If one were to simulate this scenario, variables would be typically grouped into blocks, control logic, actuators, air flow, thermal flow and a sensor block variable. These blocks are combined into a resulting nonlinear system which is solved at every time step and then matched with two exterior building zones. For this example, east and south facing zones are selected on a summer day. The interior zones can be thought of as rooms in a building, while the exterior zones as the region adjacent to a building.

In summer the outdoor air damper is fully closed and the fan speed is normally adjusted at high. When the FCU is operating properly, the controller compares room temperature to the cooling set-point (74F or 23.33C) and heating set-point (70F or 21.11 C). If the actual room temperature is greater than (cooling set-point −1F (0.56 C)), the FCU is in cooling mode and if it is less than (heating set-point +1F (0.56 C)), the FCU is in heating mode. A dedicated proportional integral derivative (PID) loop is enabled for each mode to control the cooling or heating valve position. A PID loop is a means of regulating a process quantity (room temperature) by compensating it with closed-loop feedback of its error (difference between the room temperature and set-point), with the compensation amount computed using three gain coefficients.

It is interesting to note that even for this simple example there is no agreement between optimization methods (see Figure 47) and, perhaps more importantly, the currently employed method fails to converge at approximately $t = 900$.

Current research includes investigating the reformulation of the optimization problems and sophisticated, specialized nonlinear solution techniques. If CPS are to succeed at building a strong connection between the physical and computational worlds then a robust and dependable way to simulate, for example, scenarios like FCUs must be developed.

[1] DOE Buildings Energy Data Book[18], 12/6/2013.

[2] *World Business Council Energy Efficient Buildings (EEB) Report*[19], p. 22.

[3] D. Clark, HVACSIM+ Building Systems and Equipment Simulation Program Reference Manual, NBSIR 84-2996, National Bureau of Standards, 1984.

[18] http://buildingsdatabook.eren.doe.gov/TableView.aspx?table=6.1.1

[19] http://www.c2es.org/docUploads/EEBSummaryReportFINAL.pdf

Advanced Materials

Delivering technical support to the nation's manufacturing industries as they strive to out-innovate and outperform the international competition has always been a top priority at NIST. This has also emerged as a major White House priority in recent years, in which NIST is playing an increasingly central role. Mathematical modeling, computational simulation, and data analytics are key enablers of emerging manufacturing technologies. This is most clearly evident in the Materials Genome Initiative, an interagency program with the goal of significantly reducing the time from discovery to commercial deployment of new materials through the use of modeling, simulation, and informatics. ACMD's role in advanced manufacturing centers on the development and assessment of modeling and simulation tools, with emphasis on uncertainty quantification, as well as support of NIST Laboratory efforts in such areas as materials modeling and smart manufacturing.

Computing Properties of Materials with Complex 3D Microstructures

Stephen Langer
Gunay Dogan (Theiss Research)
Yannick Congo (ISIMA)
Andrew Reid (NIST MML)

See page 18.

Rheology of Dense Suspensions

William George
Steven Satterfield
Marc Olano
Judith Terrill
Nicos Martys (NIST EL)
Clarissa Ferraris (NIST EL)
Edward Garboczi (NIST MML)
Pascal Hébraud (CNRD/ESPCI, France)

See page 34.

Micromagnetic Modeling

Michael Donahue
Donald Porter
Robert McMichael (NIST CNST)
June Lau (NIST MML)

http://math.nist.gov/oommf/

Advances in magnetic devices such as recording heads, field sensors, spin torque oscillators, and magnetic nonvolatile memory (MRAM) are dependent on an understanding of magnetization processes in magnetic materials at the nanometer level. Micromagnetics, a mathematical model used to simulate magnetic behavior, is needed to interpret measurements at this scale. ACMD is working with industrial and academic partners, as well as with colleagues in NIST's CNST, MML, and PML, to improve the state-of-the-art in micromagnetic modeling.

Michael Donahue and Donald Porter in ACMD have developed a widely used public domain computer code for doing computational micromagnetics, the Object-Oriented Micromagnetic Modeling Framework (OOMMF). OOMMF serves as an open, well-documented environment in which algorithms can be evaluated on benchmark problems. OOMMF has a modular structure that allows independent developers to contribute extensions that add to the basic functionality of OOMMF. OOMMF also provides a fully functional micromagnetic modeling system, handling both two and three-dimensional problems, with sophisticated extensible input and output mechanisms. In FY 2014 alone, OOMMF software was downloaded more than 17,000 times, and use of OOMMF was acknowledged in more than 160 peer-reviewed journal articles. OOMMF has become an invaluable tool in the magnetics research community.

Key developments over the last year include:

- A new implementation for computing the cell-to-cell demagnetization tensor values that produces fourth order accuracy with respect to cell edge length. [1-2]
- Significant improvements to the convergence speed in the conjugate-gradient energy minimization code.
- An updated and improved set of online instructions for producing high-resolution visualizations of evolving magnetization patterns computed with OOMMF, with an extended example [3].

OOMMF is part of a larger activity, the Micromagnetic Modeling Activity Group (muMAG), formed to address fundamental issues in micromagnetic modeling through two activities: the development of public domain reference software, and the definition and dissemination of standard problems for testing modeling software. ACMD staff members are involved in development of the standard problem suite as well. A new standard problem 5, adapted from [4], addressing the proper calculation of the spin torque transfer effect was published [5] in September,

2014. New solutions to standard problem 4 were also published [6]. Ongoing work includes the production of standard problem 5 solutions for submission, and development of new standard problems.

In addition to the continuing development of OOMMF, the project also does collaborative research using OOMMF. Continued collaboration with the University of California, San Diego on porting OOMMF calculations to massively parallel graphical processing units (GPUs) has produced an article for publication [7]. Collaboration with the University of Maryland has demonstrated nanoscale control over magnetic anisotropy in a trans-critical Permalloy thin film via strain-mediated coupling to ferroelectric domains in $BaTiO_3$, a degree of control helpful in the aim to make compact and efficient memory devices. A new contributed OOMMF extension from Laboratoire de Physique des Solides (Universite Paris Sud) [9] adds calculation of the Dzyaloshinskii-Moriya interaction (DMI) to OOMMF simulations, enabling the study of skyrmions, a subject of widespread current interest. The availability of the OOMMF source played a key role in a new understanding of the effect of boundary conditions on the DMI.

The ACMD micromagnetic project produced two conference presentations [1, 2], and two manuscripts submitted for publication [7, 8] this past year.

[1] M. J. Donahue, "A fourth order Demagnetization Tensor for Rectangular Prisms," 58th Annual Magnetism and Magnetic Materials, Denver, CO, November 6, 2013.

[2] M. J. Donahue, "Implementation of a Localized Fourth Order Demagnetization Tensor," 59th Annual Magnetism and Magnetic Materials, Honolulu, HI, November 5, 2014.

[3] http://math.nist.gov/oommf/movies/oommfmovies.html

[4] M. Najafi, et al., Proposal for a Standard Problem for Micromagnetic Simulations including Spin-transfer Torque, *Journal of Applied Physics* **105** (2009) 113914-113921.

[5] http://www.ctcms.nist.gov/~rdm/std5/spec5.xhtml

[6] http://www.ctcms.nist.gov/~rdm/std4/spec4.html

[7] S. Fu, W. Cui, M. Hu, R. Chang, M. J. Donahue and V. Lomakin, Finite Difference Micromagnetic Solvers with Object Oriented Micromagnetic Framework on Graphics Processing Units, in review.

[8] S. W. Fackler, M. J. Donahue, T. Gao, P. N. A. Nero, S.-W. Cheong, J. Cumings and I. Takeuchi, Locally Controlled Magnetic Anisotropy in Trans-critical Permalloy Thin Films using Ferroelectric $BaTiO_3$ Domains, *Applied Physics Letters* **105** (2014) 212905.

[9] https://www.lps.u-psud.fr/spip.php?article2252

Shear Band Formation in Bulk Metallic Glasses

Timothy J. Burns
Vis Madhavan (Wichita State University)
Jue Chen (University of California)
Ryan Goh (University of Minnesota Twin Cities)
Emily McHenry (Louisiana State University)
Diego Torrejon (George Mason University)
Xin Yang (Simon Fraser University)

About thirty years ago, the problem of the localization of rapid plastic deformation of a number of polycrystalline metals into shear bands began to receive considerable attention, mainly due to its connection with military applications, such as armor penetration. However, the phenomenon had been observed much earlier in metal machining operations. At faster cutting speeds and larger depths of cut, the strips of work material removed by machining, called chips, were often observed to exhibit considerable structure, as a bifurcation took place in the material flow, from continuous, or fairly smooth chips, to serrated, or shear localized chips. The generally accepted explanation for the onset of this shear localization in polycrystalline metals is that the tendency of the material to work-harden with increasing plastic deformation is overcome by a competing tendency of the material to soften, due to "adiabatic" heat production caused by the rapid shearing of the material. Sometimes shear localized chips are advantageous, because they tend to break easily, thus simplifying chip removal. In other cases, localized chips degrade the quality of the finished surface, and they can cause tool damage. For all of these reasons, the localization of shear during high-speed machining of polycrystalline metallic alloys continues to be a subject of active research.

Recently, there has been a growing interest in the manufacture by machining of components made from amorphous metallic alloys, which are also called bulk

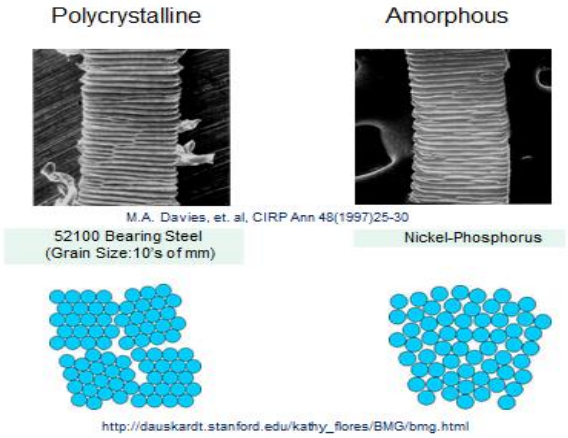

Figure 48. *Shear localized chips.*

metallic glasses (BMGs). These materials differ from common polycrystalline metallic alloys, because their atoms do not assemble on a crystalline lattice, and as a result, they have unique physical and chemical properties. See Figure 48. These materials have great technological potential, due to their superior mechanical behavior. These include a large elastic limit, very high strength and hardness, and resistance to corrosion and wear. To realize this potential, it is essential to overcome the severe ductility limitations of BMGs, which are caused by the formation of shear bands.

A number of theoretical studies have argued that this strain localization is controlled not by rapid heating, but rather by a change in the concentration of free volume in the material. This year, analysis of a model of the stability of a geometrically simple shearing deformation in a BMG was extended to include an inelastic dilatational strain resulting from changes in the free volume. The work supports the free volume concentration hypothesis.

This project was initiated at the request of Vis Madhavan, formerly of the NIST Engineering Laboratory, and currently at Wichita State University, and it has been assisted by numerical and analytical work of Jue Chen, Ryan Goh, Emily McHenry, Diego Torrejon, and Xin Yang, who were graduate student participants at an Institute for Mathematics and Its Applications workshop on Mathematical Modeling in Industry in August, 2013. A paper on this work is in preparation.

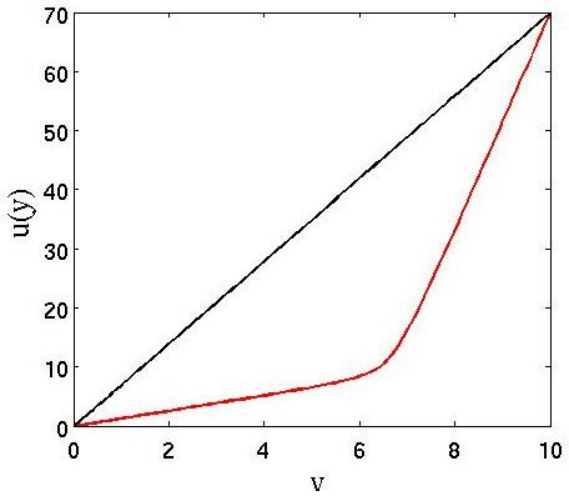

Figure 49. *Example of shear banding in a non-Newtonian fluid. The black curve shows the horizontal velocity u(y) versus height y for a Newtonian fluid flowing between parallel plates, which a characteristic linear profile. The red curve shows the flow profile for a non-Newtonian fluid that exhibits shear banding, with a thin transition layer near y = 6.5 that separates high shear and low shear regions of flow. Here h = 10 and V = 70.*

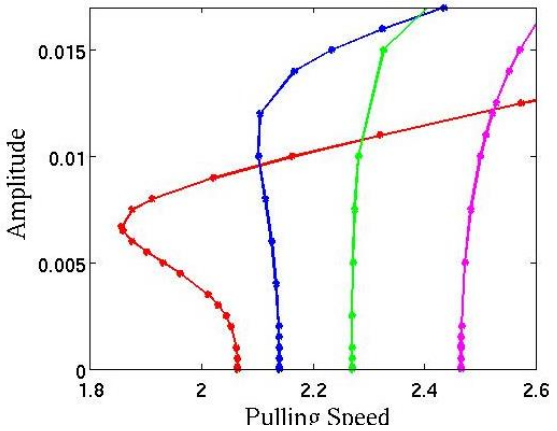

Figure 50. *Bifurcation diagram showing existence of solutions with multiple bands. Here the amplitude of the solution shown on the ordinate is a measure of the deviation of the flow magnitude from the simple linear profile, and the abscissa is the pulling speed V of the upper of two parallel plates. The red curve shows a hysteretic solution with a single interface, which is the first banded solution to bifurcate with increasing pulling speed. The blue, green, and magenta curves show solutions with two, three, and four interfaces.*

Modeling of Shear Banding in Polymer Solutions

Geoffrey McFadden
Michael Cromer

Complex fluids such as polymers and multicomponent solutions often display a complicated relationship between the local stress field and the state of strain in the liquid. These fluids typically involve a microstructure requiring detailed modeling combined with careful and precise analytic and numerical techniques. The fluids of interest include polymer solutions, surfactants (wormlike micelles), and colloids, each of which have a plethora of industrial applications, such as inks, in homecare products, enhanced oil recovery, and other materials science applications.

Simple Newtonian fluids usually exhibit a linear relation between the stress field and the strain rate in a flowing liquid. A simple example is the shear flow that is established between two parallel plates separated by a gap h. One plate is stationary, say in the plane $y = 0$, and the other, in the plane $y = h$, translates steadily in the x direction with a velocity V. The resulting flow field has a linear shear profile with the local velocity $u(y) = V\,y/h$ in the x direction. On the other hand, the response of a complex fluid in a similar geometry can be more complex, with significant deviations from the linear shear profile exhibited by a Newtonian fluid. For example, under some circumstances the flow may exhibit shear bands, where the flow has a piecewise linear profile with one or more narrow transition layers separating regions of uniform shear. An example is shown in Figure 49, where the flow is based on a non-Newtonian fluid model of a polymer solution [1].

An interesting feature of this model is that it supports shear banding for non-Newtonian fluids that possess a monotonic constitutive curve that relates shear and strain rate. The critical feature of the model is the coupling of the polymer stress to the concentration profile, with shear banding associated with inhomogeneous concentration profiles of the polymer in solution. Numerical simulations of the nonlinear governing equations using spectral techniques that allow accurate resolution of the interfacial regions have demonstrated flows with multiply banded flows, with additional bands occurring with increasing pulling velocities V [1]. In the past year complementary steady-state computations based on quasi-Newton methods with continuation techniques are able to track these transitions in bifurcation diagrams such as Figure 50. This approach allows the computation of both stable and unstable solutions, providing a detailed description of the hysteresis between the unbanded and banded flow states that is observed under some conditions. Additional research is addressing the detailed flow in the transition region between bands as a problem in matched asymptotic expansions in a thin interface limit; here the interface thickness is controlled by the "correlation length'' of the polymer solution.

This project is continuing in several directions, including the consideration of curved geometries such as the Taylor-Couette flow between concentric rotating cylinders. M. Cromer recently completed an NRC Postdoctoral Associateship in ACMD, and is currently on the faculty of the School of Mathematical Sciences at the Rochester Institute of Technology in New York.

[1] M. Cromer, M. Villet, G. Fredrickson and L.G. Leal, A Study of Shear Banding in Polymer Solutions, *Physics of Fluids* **26** (2014) 063101.

Estimation of Shear Stress in Machining

Timothy J. Burns
Bert W. Rust

After decades of study, the determination of accurate constitutive response models for the flow stress in materials for finite-element simulations of high-speed machining operations remains a difficult open problem. This limits the ability of manufacturers to predict optimal cutting conditions for a given process. A major reason for this limitation is that current materials testing facilities, such as a Kolsky bar laboratory, cannot measure the stress vs. strain response of materials like titanium and iron alloys under the extreme conditions of rapid heating that are present in typical high-speed metal machining operations. For example, in a fairly routine cutting process on a modern machining center, a heating rate on the order of one million degrees Celsius per second is not uncommon for carbon steels.

We are investigating a new approach to the problem of estimating flow stress in machining. The recent invention by Menon and Madhavan [1] of a cutting tool that is transparent in infrared frequencies makes it possible to obtain good in-situ temperature measurements along the chip-tool interface during a steady-state machining operation. This enables an estimate to be made of the shear stress distribution in the work material along the face of the tool under actual machining conditions, by means of an inverse method [2]. By solving a convection-diffusion problem that models the flux of heat into the chip and the tool during a cutting process, the temperature distribution along the tool face can be shown to satisfy the dimensionless equation

$$\Theta(X) = \frac{\nu}{\sqrt{\pi}} \int_0^X \frac{\Sigma(U)}{\sqrt{(X-U)}}\, dU \qquad (1)$$

Here, Θ is the normalized temperature, Σ is the normalized flow stress, $X \in [0,1]$ is the distance along the contact surface on the face of the tool, measured from the tooltip, and ν is a parameter that is O(1).

Viewed as an inverse problem, Eq. 1 is a Volterra integral equation of the first kind, Abel's equation, for the determination of $\Sigma(X)$ on [0, 1], given $\Theta(X)$. Under mild regularity assumptions on the function $\Theta(X)$, the solution to Eq. 1 is well known,

$$\frac{\nu}{\sqrt{\pi}}\Sigma(X) = \frac{1}{\pi}\frac{d}{dX}\int_0^X \frac{\Theta(U)}{\sqrt{X-U}}\, dU \qquad (2)$$

$$= \frac{1}{\pi}\left\{\frac{\Theta(0)}{\sqrt{X}} + \int_0^X \frac{\Theta'(U)}{\sqrt{X-U}}\, dU\right\}. \qquad (3)$$

It is clear from Eq. 3 that, for $\Sigma(X)$ to be continuous at X=0, the nondimensionalized temperature must satisfy $\Theta(0) = 0$. A major difficulty in applying this inverse method is that the temperature data are experimentally determined at a finite number of points, so that they are inexact, and the formulas (2) and (3) involve numerical differentiation of these data, which is an ill-posed problem. If the data are equally spaced with increment h and 2σ error bars bounded by δ, then using the midpoint product integration method, it can be shown that the error in the computed stress will be of order $\delta/h^{1/2}$ [3].

When δ is significant, some kind of regularization method is required in order to separate signal from noise in the temperature data. We are investigating the use of Rust's truncated singular components method (TSCM) [4] to invert the Abel equation and obtain an estimate of the stress. This method involves solving the linear system of equations which arises from the discretized Abel equation by truncating the singular vector expansion rather than the singular value distribution of the approximate linear system. The method is a variant of principal components regression which does not use the

singular values to choose the principal components. It produces residuals which are closer to uncorrelated white noise.

[1] T. Menon and V. Madhavan. High Accuracy Full-field Infrared Thermography of the Chip-tool Interface through Transparent Cutting Tools while Machining Ti-6Al-4V, in review.

[2] T. J. Burns, S. P. Mates, R. L. Rhorer, E. P. Whitenton and D. Basak, Inverse Method for Estimating Shear Stress in Machining, in review.

[3] P. Linz, *Analytical and Numerical Methods for Volterra Integral Equations*, SIAM, Philadelphia, 1985.

[4] B. W. Rust, Truncating the Singular Value Decomposition for Ill-Posed Problems, NISTIR 6131, July 1998.

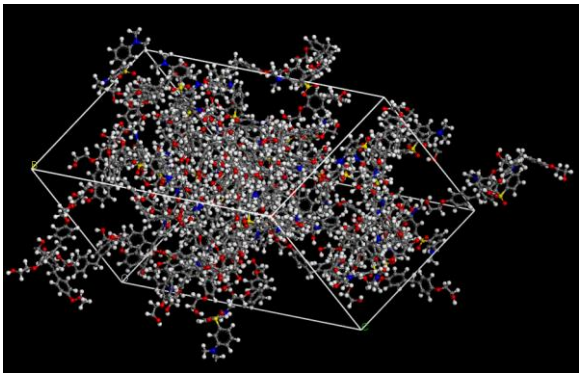

Figure 51. *Unit cell showing cross-linked polymer system containing 2000 atoms. Molecular dynamics evolves atoms by Newtonian dynamics using potential model to compute inter-atomic forces.*

Uncertainty Quantification and Molecular Dynamics Simulations of Aerospace Polymers

Andrew Dienstfrey
Paul Patrone (University of Minnesota)

With the increasing power and availability of scientific computing, the composites industry is heavily investing in molecular dynamics (MD) as a cost-effective tool for identifying next generation, high-performance materials [1, 3]. For example, in aerospace applications MD is being considered to search the combinatorially-large polymer design space for systems whose mechanical properties warrant further experimental study. While this strategy holds promise, the high-throughput demands of industry can extend simulations toward the limits of their validity. Thus, a key task is to assess confidence in such computations, rendering their predictions more informative for decision making in the materials development cycle. The growing field of uncertainty quantification (UQ) provides a useful foundation from which to develop and analyze such techniques [4].

Simulation-based prediction of the glass transition temperature T_g is an especially interesting problem against which to investigate this development. In composites T_g characterizes the boundary between elastic and fluid-like behavior of molecular constituents. Macroscopically, this transition determines the ability of a structural component, for example an airplane wing, to remain rigid at high temperatures. While T_g is both a natural and critical property characterizing polymer systems, identifying T_g from MD simulations is a challenging task. The dynamic processes associated with glass formation are inherently non-equilibrium. Moreover, the underlying molecular structure of cross-linked polymers is a realization of a large random network. Thus, in using atomistic simulations to predict T_g, it is desirable to simulate large systems over long times to sufficiently average cross-linking statistics and collective dynamics. Given that MD falls short of these scales by several orders of magnitude, the question naturally arises as to how trustworthy are estimates of T_g obtained from molecular dynamics simulations [3].

In 2014 we developed tools to address this question. We simulated a large number of epoxy-amine systems built-up of from 2000 to 16000 atoms; see Figure 51. The candidate systems were cross-reacted (*in silico*), and then cooled from 800 K to 100 K at a constant rate. Density-vs-temperature curves of glass-forming polymers exhibit asymptotic, high- and low- temperature regimes in which density, $\rho(T)$, is effectively linear. For both experimental and virtual measurement contexts, T_g is defined as the boundary temperature between these two. Ambiguity in identifying such a transition is one source of uncertainty in computational estimate of T_g; see Figure 52. To reduce this ambiguity, we propose to model curves $\rho(T)$ data as a hyperbola with parameters defined by a nonlinear optimization. We implemented two methods for propagating the uncertainty in this fitting process and showed that they result in commensurate estimates of the uncertainty of T_g for any given realization of a polymer system. However, as we have shown, this analysis reflects only part of the total uncertainty associated with MD-derived measurement of T_g. Additional sources of uncertainty arise from finite exploration of the energy landscape and limited sampling of cross-linking configurations. This year we began to account for these uncertainty sources, modeling so-called "dark-uncertainty" using a mixed-effect statistical analysis motivated by key-comparison analysis in metrology. A paper is in progress. We hope to continue and extend this work with industrial stakeholders in the coming year.

In addition to this MD-polymers application, in 2014 we also continued outreach into the broader computational material science community as part of the Materials Genome Initiative (MGI). MGI is a multi-

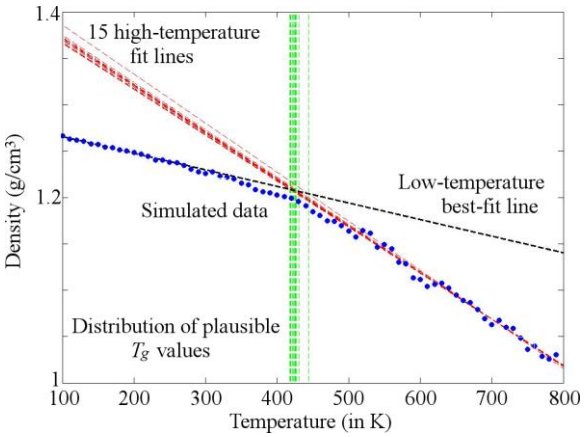

Figure 52. *Density versus temperature plot as obtained by simulation are shown as blue dots. Asymptotic linear trends can be observed at low and high temperatures. T_g is defined as the intersection of these two "best-fit" lines. Subjective determination of the high-temperature asymptotic regime results in variation of T_g .*

agency initiative launched by the White House in June 2011. The purpose of MGI is to promote creation of novel materials for use by industry with significant reductions in time and cost. Widespread availability of materials data and increased use of models and simulations are critical engines to drive this progress. In December 2013 NIST co-hosted a working conference at the Institute for Mathematics and its Applications at the University of Minnesota. The goal of that meeting was to bring together stakeholders from industry, academia, and government labs to explore the overlaps between uncertainty analysis, computation, and materials science. Results were described in a paper co-authored by a cross-cut of participants that appeared in June 2014 [2]. A key-finding emerging from workshop discussion sessions was the need to create working examples of uncertainty quantification analysis as applied to computational material science to serve as bridges between the two communities. Toward this goal we are currently organizing a follow-up working conference to be held at Purdue University, University in July of 2015. We look forward to reporting on this effort next year.

[1] B. Cowles, D. Backman and R. Dutton. Verification and Validation of ICME Methods and Models for Aerospace Applications, *Integrating Materials and Manufacturing Innovation* **1**:1 (2012).

[2] A. Dienstfrey, F. R. Phelan, S. Christensen, A. Strachan, F. Santosa and R. Boisvert, Uncertainty Quantification in Materials Modeling. *JOM* **66**:7 (July 2014), 1342-1344.

[3] C. Li and A. Strachan, Molecular Scale Simulations on Thermoset Polymers: A Review, *Journal of Polymer Science Part B: Polymer Physics* **53**:2 (2015), 103-122.

[4] J. H. Panchal, S. R. Kalindini, and D. L. McDowell, Key Computational Modeling Issues in Integrated Computational Materials Engineering, *Computer-Aided Design* **45**:1 (2013), 4-25.

Stability of a Solid-Liquid Interface during Solidification

Geoffrey McFadden
Sam Coriell (NIST MML)
Robert Sekerka (Carnegie Mellon University)

A fundamental problem in the material processing of multicomponent alloys is to determine the stability of the crystal-melt interface that separates the solid and liquid phases during growth from the melt. Instability of the interface generally leads to undesirable inhomogeneities in the solute distribution in the crystal, which can cause significant degradation of the electrical and mechanical properties of the product. The original treatment was worked out by W. W. Mullins and R. F. Sekerka in 1964 [1], and now goes under the name of *morphological stability* theory. The 1964 paper has over 2500 citations, and the work has been reviewed numerous times, including a chapter in the 1993 publication of the *Handbook of Crystal Growth* by S. Coriell and G. McFadden [2]. An updated article that includes recent work performed subsequent to that review was recently completed and has now appeared in the second edition of that handbook [3].

[1] W. W. Mullins and R. F. Sekerka, Stability of a Planar Interface during Solidification of a Dilute Binary Alloy, *Journal of Applied Physics* **35** (1964) 444-451.

[2] S. R. Coriell and G. B. McFadden, Morphological Stability, in *Handbook of Crystal Growth*, Vol. 1B, (D. T. J. Hurle, ed.), Elsevier, Amsterdam, 1993, 785-857.

[3] R. F. Sekerka, S. R. Coriell and G. B. McFadden, Morphological Stability, in *Handbook of Crystal Growth*, Vol. I, 2nd Edition, (T. Nishinaga, ed.), Elsevier, Amsterdam, 2015, 595-630.

Surface-Active Diffuse Interface Model

Sean Colbert-Kelly
Geoffrey McFadden
Frederick R. Phelan, Jr. (NIST MML)

Surfactants are chemical compounds that lower interfacial tension between two liquids or a liquid and a solid. Surfactants have important applications in detergents, droplet break-up, and reducing the risk from bubbles formed in blood due to rapid decompression [2, 3]. This research project studies the transition that occurs between two immiscible fluids with surfactant at the interface between the two fluids.

The mixing properties of the two fluids affect the interface shape dynamics. Because surfactants lower interfacial tension there are gradients in the surfactant

concentration on the drop surface under flow, giving rise to Marangoni forces that alter drop shape, breakup and coalescence dynamics, as well as flow induced migration [1]. Surfactants migrate to the fluid interface in a binary mixture due to the amphiphilic nature of these molecules [2]. The presence of the surfactant produces dramatic changes in the interfacial properties of the fluid mixture, and therefore greatly alters the stability, equilibrium properties, and the droplet dynamics of the mixture. These dynamics govern the long time stability of emulsions. Current models do not accurately model the dramatic effects of surfactants on emulsion properties and dynamics.

Discontinuities in fluid properties tend to complicate flow computations along the interface between two liquids or a liquid and a solid. Properties such as surface energy and surface viscosity also complicate such calculations. A diffuse interface model (DIM) can be useful in investigating such interfacial dynamics.

From studying previous work, this project intends to develop and analyze a description of the mixture of two immiscible fluids with surfactants where mixing can occur near the interface, while incorporating interfacial properties that many DIMs tend to ignore. Currently, it is assumed that the two liquids are considered Newtonian and incompressible, where in the interfacial region this assumption may not hold. In addition, this project will study the limiting problem of the diffuse interface model, to determine if a sharp interface model is recovered in letting the interfacial region get arbitrarily thin. It will also be of benefit to study the deformation of the droplet, and determine if the droplet will remain spherical in shape.

Represent the binary fluid by a phase field variable c, with $c \in [-1,1]$, $c = 1$ represents one fluid and $c = -1$ represents the other fluid. Represent the surfactant by the variable ψ, with $\psi \in [0,1]$, and the fluid velocity u. Then the governing equations for the binary fluid and surfactant are

$$\frac{\partial c}{\partial t} + \nabla \cdot (cu) = \nabla \cdot (D_c \nabla \mu_c)$$
$$\frac{\partial \psi}{\partial t} + \nabla \cdot (\psi u) = \nabla \cdot \left(D_\psi \nabla \mu_\psi\right).$$

D_α is the mobility constant and μ_α is the chemical potential for that particular variable. The continuity equations are coupled with the following Navier-Stokes equations

$$\nabla \cdot u = 0$$
$$\rho\left(\frac{\partial u}{\partial t} + u \cdot \nabla u\right) = -\nabla p + \nabla \cdot \eta(\nabla u + (\nabla u)^T) + \mu_c \nabla c + \mu_\psi \nabla \psi.$$

Initial analysis assumes that D_α, μ_α, *and* η are constant. Incorporating a non-constant interfacial viscosity, $\eta(x)$, is the next step to this project. Reference [4] incorporates a mixing rule in the binary case (no surfactant in the system) to incorporate the effect of interfacial viscosity describe the viscosity change in the interfacial layer due to the decreased entanglement of polymers. In the case of surfactant in the system, no method has been considered on incorporating interfacial viscosity. However, it is proposed that interfacial viscosity should be dependent on the surfactant ψ.

[1] J. T. Schwalbe, F. R. Phelan, Jr., P. M. Vlahovska, and S. D. Hudson, Interfacial Effects on Droplet Dynamics in Poiseuille Flow, *Soft Matter* **7** (2011), 7797–7804.

[2] S. Engblom, M. Do-Quang, G. Amberg, and A.-K. Tornberg, On Diffuse Interface Modeling and Simulation of Surfactants in Two-phase Fluid Flow, *Communications in Computational Physics* **14**:4 (2013), 879-915.

[3] C.-H. Teng, I.-L. Chern, and M.-C. Lai, Simulating Binary Fluid-Surfactant Dynamics By a Phase Field Model, *Discrete and Continuous Dynamical Systems Series B* **17**:4 (2012), 1289–1307.

[4] W. Yu and C. Zhou, The Effect of Interfacial Viscosity on the Droplet Dynamics under Flow Field, *Journal of Polymer Science Part B: Polymer Physics* **46**:14 (2008), 1505-1514.

Spectral-Galerkin Scheme to Study Ferroelectric Liquid Crystal Properties

Sean Colbert-Kelly
Geoffrey McFadden
Daniel Phillips (Purdue University)
Jie Shen (Purdue University)

This project considers the effect of introducing defects into a ferroelectric liquid crystal thin film. If a small foreign particle is introduced into a thin chiral smectic c (SmC*) film, a disk-like island will form around the defect several layers thicker than the surrounding thin film [1]. On the island's boundary, the director field u is tangential counterclockwise and is initially tangential in the interior of the disk, making a degree 1 vector field. However, increase in the island's size or external forces can cause distinct textural transformations in the director field. The pattern can remain unchanged or transform to what is called a simple spiral, tangential counterclockwise on the boundary and approximately radial at the smoke particle boundary [1].

The elastic energy of this system in the island can be described by

$$E_\varepsilon(u) = \frac{1}{2}\int_{B_1} k_s(\nabla \cdot u)^2 + k_b\,(\nabla \times u)^2 + \frac{1}{2\varepsilon^2}(1 - |u|^2)^2\,dx,$$

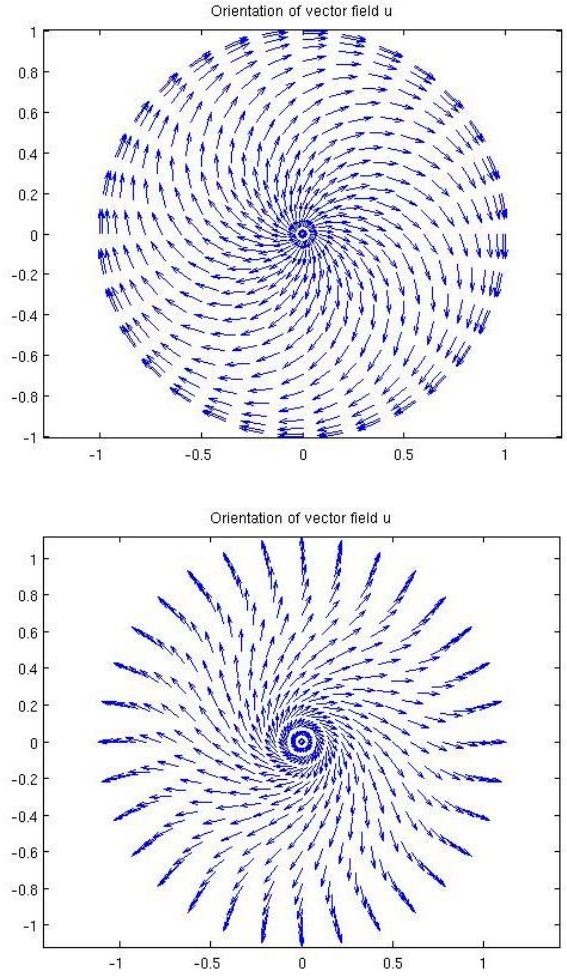

Figure 53. *Stable vector fields to the elastic energy.*

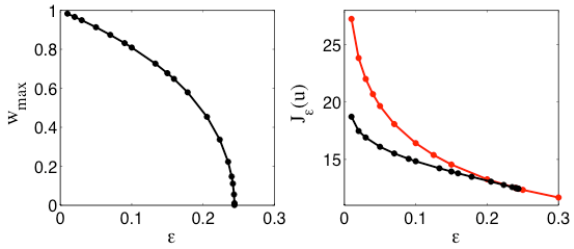

Figure 54. *Behavior of the steady-state spiral solution as a function of ε for k_s = 1.5 and k_b = 0.5.*

where k_s, k_b are the splay and bend constants for the liquid crystal, and $\varepsilon > 0$ is the radius of the defect core; in this model u is not restricted to having unit length. The director field u is given boundary conditions, i.e., $u = g$ where $|u| = 1$ and g had degree $d > 0$. For each ε, a minimizing vector field u_ε exists as $\varepsilon \longrightarrow 0, u_\varepsilon \longrightarrow u_*$. The asymptotic field u_* has degree $d = 1$ singularities and, near a singularity, a, u_* behaves locally as

$$u_* = \alpha_a \frac{x-a}{|x-a|}$$

where $\alpha_a = \pm 1$ for $k_s < k_b$ and $\alpha_a = \pm i$ for $k_s > k_b$ [2].

The purpose of this project is to develop a spectral-Galerkin numerical method for the Euler-Lagrange equations for E_ε when ε is small, so as to capture the experimental observations and analytical results described above. Thiis will enable us to view the nature of the defects computationally and observe results not currently proven analytically. Many numerical methods deal with the simpler case $k_s = k_b$, resulting in a vector version of the Allen-Cahn equation. Our method will also simulate the case $k_s \neq k_b$ [3, 4]. We develop a gradient flow stabilized scheme for the Euler-Lagrange equations and let the solutions stabilize to an equilibrium state. We discretize the Euler-Lagrange equation via a first order semi-implicit stabilized scheme. The equation is then converted into a polar geometry representation. With this representation, we can approximate the solution with a Fourier expansion in the angle variable using an FFT and then approximate the Fourier coefficients using Chebyshev polynomials in the radius variable. This scheme has been shown to be unconditionally stable with error estimates on the order of $\exp(T/\varepsilon^2)$. We tested the scheme with boundary conditions of the form $g = \exp(di\theta)$, for d any positive integer.

Figure 53 plots the minimum vector field orientation uε for the case $d = 1$. The top figure is the stable solution for the energy with values $k_s = 0.5$, $k_b = 1.5$ and $g = \exp[i(\theta - \pi/2)]$, while the bottom figure is the stable solution for the energy with values $k_s = 1.5$, $k_b = 0.5$ and $g = \exp[i\theta]$. We see that in the case $k_s < k_b$ the vector field is nearly radial near the origin. When $k_s < k_b$, the vector field is nearly tangential near the origin. This follows what was shown analytically. The plot in the case $k_s < k_b$ follows what was seen experimentally as well. In the case $k_s < k_b$ with the vector field tangential to the boundary, either clockwise or counterclockwise, the stable vector field is a simple spiral.

Lee, Konovalov, and Meyer [1] note that the size of the island also affects the transformation of the vector field: if the island radius is small the pure bend patterns rarely transform to a simple spiral. Related computational results are shown in Figure 54. The equilibrium configuration of the degree one solutions in Figure 53 can be represented in the form

$$u(r,\theta) = v(r)\hat{r}(\theta) + w(r)\hat{\theta}(\theta) = [v(r) + iw(r)]e^{i\theta}$$

where the scalar functions $v(r)$ and w(r) and represent the splay and bend components of u in the radial direction $\hat{r}(\theta)$ and angular direction $\hat{\theta}(\theta)$ respectively. The left plot is a plot of the maximum value of the bend component w as a function of ε, which describes a bifurcation from the splay solution, $w = 0$, at $\varepsilon_b \approx 0.244$. The right plot is the energy of the spiral solution (black

curve) and the splay solution (red curve) versus ε, which shows that the spiral solution is stable for $\varepsilon < \varepsilon_b$. In this study we have also performed a number of numerical simulations of both the lowest energy solution and higher energy solutions with a variety of boundary conditions of various degrees d; the higher energy solutions are generally degenerate, with several possible locations of the defects that depend on the values of k_s and k_b.

[1] J.-B. Lee, D. Konovalov and R. B. Meyer, Textural Transformations in Islands on Free Standing Smectic-C* Liquid Crystal Films, *Physical Review E* **73** (2006), 051705.

[2] S. Colbert-Kelly and D. Phillips, Analysis of a Ginzburg-Landau Type Energy Model for Smectic C* Liquid Crystals with Defects, *Annales de l'Institut Henri Poincare (C) Non Linear Analysis* **30**:6 (2013), 1009-1026.

[3] J. Shen, Efficient Spectral-Galerkin Methods III: Polar and Cylindrical Geometries, *SIAM Journal on Scientific Computing* **18**:6 (1997), 1583-1604.

[4] J. Shen and X. Yang, Numerical Approximations of Allen-Cahn and Cahn-Hilliard Equations, *Discrete and Continuous Dynamical Systems. Series A* **28**:4 (2010), 1669-1691.

High Performance Computing and Visualization

Computational capability is advancing rapidly, with the result that modeling and simulation can be done with greatly increased fidelity (e.g., higher resolution, more complex physics). However, developing the requsite large-scale parallel applications remains highly challenging, requiring expertise that scientists rarely have. In addition, the hardware landscape is changing rapidly, so new algorithmic techniques must constantly be developed. We are developing and applying such expertise for application to NIST problems. In addition, computations and laboratory experiments often produce large volumes of scientific data, which cannot be readily comprehended without some form of visual analysis. We are developing the infrastructure necessary for advanced visualization of scientific data, including the use of 3D immersive environments and applying this to NIST problems. One of our goals is to develop the 3D immersive environment into a true interactive measurement laboratory.

High Precision Calculations of Fundamental Properties of Few-Electron Atomic Systems

James Sims
Stanley Hagstrom (Indiana University)

See page 31.

Rheology of Dense Suspensions

William George
Steven Satterfield
Marc Olano
Judith Terrill
Nicos Martys (NIST EL)
Clarissa Ferraris (NIST EL)
Edward Garboczi (NIST MML)
Pascal Hébraud (CNRD/ESPCI, France)

See page 34.

Nano-structures, Nano-optics, and Control of Exciton Fine Structure with Electric and Magnetic Fields

James S. Sims
Wesley Griffin
Judith Terrill
Garnett W. Bryant (NIST PML)
Jian Chen (UMBC)

Research and development of nanotechnology, with applications ranging from smart materials to quantum computation to biolabs on a chip, is an important national priority. Semiconductor nanoparticles, also known as nanocrystals and quantum dots (QDs), are one of the most intensely studied nanoscale systems. Nanoparticles are typically 1 nm to 10 nm in size, with a thousand to a million atoms. Precise control of particle size, shape and composition allows one to tailor charge distributions and control quantum effects to tailor properties completely different from the bulk and from small clusters. As a result of enhanced quantum confinement effects, nanoparticles act as artificial, man-made atoms with discrete electronic spectra that can be exploited as light sources for novel enhanced lasers, discrete components in nanoelectronics, qubits for quantum computers, and enhanced ultrastable fluorescent labels for biosensors to detect, e.g., cancers, malaria or other pathogens, and to do cell biology.

We are working with the NIST PML to develop computationally efficient large scale simulations of such nanostructures, as well as to develop immersive visualization techniques and tools to enable analysis of highly complex computational results of this type. The electrical and optical properties of semiconductor nanocrystals and quantum dots are studied. In the most complex structures, this entails modeling structures with on the order of a million atoms. Highly parallel computational and visualization platforms are critical for obtaining the computational speeds necessary for systematic, comprehensive studies.

Parallel Computing. This year our work has focused on modulating and controlling the optical properties of self-assembled quantum dots using both electric and magnetic fields. The electric field work culminated in a paper in *Physical Review B* [1]. Calculations were carried out on NIST's 7892 processor Linux cluster.

In addition to the electric field work, we have modified the code to handle the imaginary parameters due to the magnetic field (electric field parameters are real) and there are now data input files for both electric fields and

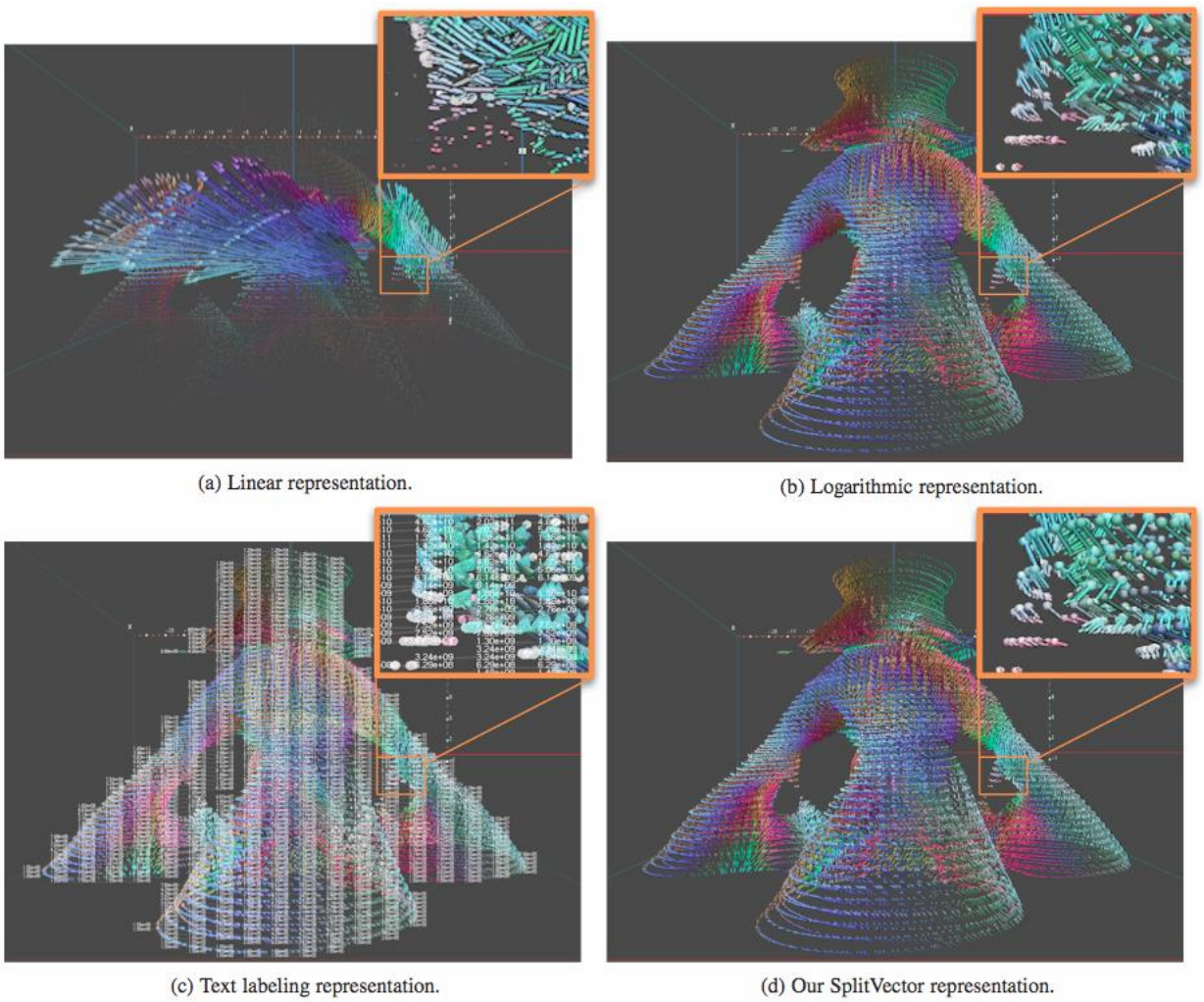

Figure 55. *Visual encodings of vector field data: (a) the linear representation fails by only showing a small range of the data; (b) a logarithmic encoding successfully shows the data, but requires more mental calculation to understand the data; (c) attaches text labels to each data point, which, while highly accurate, obscures the vector field; (d) visualizes the entire range of the data while also allowing easier fine-grain understanding of the vector data.*

magnetic fields. New computational studies incorporating the effect of magnetic fields continue to be done. In addition, code has been written which identifies the wave function states of maximum and minimum spin, which would form the qubit for quantum computing.

The addition of a magnetic field provides a probe to split excitonic states, providing a more complete spectroscopy of quantum dot optics. This allows us to isolate contributions from spin-orbit coupling, Zeeman and spatial motion. Magnetic field response depends sensitively on the QD size and shape.

We consider pyramidal and flat QDs to identify the size and shape dependence of g-factors, g-factor anisotropy and electric-field tuning, diamagnetic shifts, and spin and level mixing as a function of magnetic field magnitude and orientation.

The intrinsic spin of the electron can lead to different effects in a magnetic field depending on the QD size and shape, so it is necessary to see the effect of spin in different QD arrangements. Without visualization, it is difficult to understand what the spin distribution is and how it changes for different magnetic fields, electric fields or strain. This distribution is critical for understanding exchange interactions or electron/nucleus interactions in quantum devices. These properties are intimately connected with the performance of these structures in quantum information processing [2, 3].

In the future, the codes will be revised to incorporate deterministically placed dopants (phosphorous) in Si to simulate Si-based dopant devices that are only a few atoms wide. This will require re-evaluation of the parallelization techniques in use.

Visualization. As part of a continuing NIST grant award, Jian Chen developed a novel visual encoding method to visualize the simulation results. The new

method was necessary because the vector field data has a very large range of magnitude which causes other visual encodings to fail. In Figure 55(a), the linear representation fails by only showing a small range of the data. The small magnitude data disappears and the large magnitude data overwhelms the rest of the data. In Figure 55(b), a logarithmic encoding successfully shows the data, but requires more mental calculation to understand the data. Figure 55(c) attaches text labels to each data point, which, while highly accurate, obscures the vector field. Finally, the new encoding in Figure 55(d) visualizes the entire range of the data while also allowing easier fine-grain understanding of the vector data. The new method splits the direction and magnitude of each vector into two pieces and encodes the two pieces separately to enhance comprehension. The new encoding was developed as part of a larger visualization tool that runs on the desktop. It was created in close cooperation with Garnett Bryant in PML to ensure his requirements for data exploration were met.

The results of this work should directly benefit Bryant and his research into quantum dots and electron spin distribution. Furthermore, the novel visual encoding for vector data has larger applicability in the field of visualization. A paper describing this new visual encoding is in process. A poster describing this work is under review at IEEE VR 2015 [4]. Also, Jian Chen will be giving an oral presentation at IEEE VR 2015 about her research lab and will be discussing this work [5].

Future work will include a paper on this novel encoding approach as well as a user-study to determine its effectiveness in the CAVE. We will also work on extending the desktop visualization tool to the CAVE.

[1] G. W. Bryant, N. Malkova and J. Sims, Mechanism for Controlling the Exciton Fine Structure in Quantum Dots using Electric Fields: Manipulation of Exciton Orientation and Exchange Splitting at the Atomic Scale, *Physical Review B* **88** (2013),161301(R).

[2] G. W. Bryant and J. Sims, "g-factors, Diamagnetic Shifts and Spin Polarization in Quantum Dots: The Role of Shape, Spin Mixing and Spin Texturing," International Conference on Quantum Dots (QD2014), Pisa, Italy, May 11-16, 2014.

[3] G. W. Bryant, "Controlling Quantum Dots," Institute Seminar, University Nicholas Copernicus, Torun, Poland, October 2014. (invited)

[4] J. Chen, H. Zhao, W. Griffin, J. Terrill and G. Bryant, Validation of Split Vector Encoding and Stereoscopy for Quantitative Visualization of Quantum Physics Data in Virtual Environments (poster) IEEE Virtual Reality (VR2015), March 23-27, 2015, Arles, France.

[5] J. Chen, J. E. Terrill, H. Zhao, G. Zhang, K. Wu, A. Garbrino and Y. Zhu, Interactive Visual Computing Laboratory Research, Laboratory and Project Presentations Track, IEEE Virtual Reality (VR2015), March 23-27, 2015, Arles, France.

Modeling and Visualization of Cement Paste Hydration and Microstructure Development

John Hagedorn
Steven Satterfield
Judith Terrill
Terence Griffin
Wesley Griffin
Franz Sauer (University of California at Davis)
Earl Bellinger (SUNY Oswego)
Alicia Ouyang (River Hill High School)
Romain Desaymons (ISIMA)
Jeffrey Bullard (NIST EL)
Joshua Arnold (NIST EL)

http://www.nist.gov/itl/math/hpcvg/hydrationhpc.cfm
http://www.nist.gov/itl/math/hpcvg/hydrationvis.cfm

When cement powder is mixed with water, the hydration process that transforms the paste from a fluid suspension into a hardened solid involves complex chemical and microstructural changes. Understanding and predicting the rates of these changes is a longstanding goal. Computational modeling of the hydration of cement is challenging because it involves a large number of coupled nonlinear rate equations that must be solved in a highly irregular three-dimensional spatial domain. To address these challenges we are applying a new computational model called HydratiCA, which has several advantages over other models of cement hydration. HydratiCA uses stochastic cellular automata algorithms to simultaneously model reaction and transport phenomena in 3D. This allows us to track the detailed kinetics and equilibria that occur in a diverse range of cementious systems.

Parallelization of the model and visualization of the output data are important. With parallelization we can simulate systems that are large enough to be realistic, avoiding finite size effects, and still be able to complete the simulations in a reasonable amount of time. Over the course of the simulation time, a series of data volumes is produced at the time values of interest. Visualization of this data is valuable both for validation and for understanding of the results.

This year we requested and received from NSF a renewal of our 100,000 hour grant of computer time on the Texas Advanced Computing Center's Dell PowerEdge C8220 Cluster with Intel Xeon Phi coprocessors (Stampede). We extended our tool for analyzing the output files to study the degree of hydration over time including the duration of the drowsy period, the peak rate, and the time of the peak.

Several changes were made to the model to improve its ability to simulate the complex dissolution, nucleation and growth of cementitious solids, including:

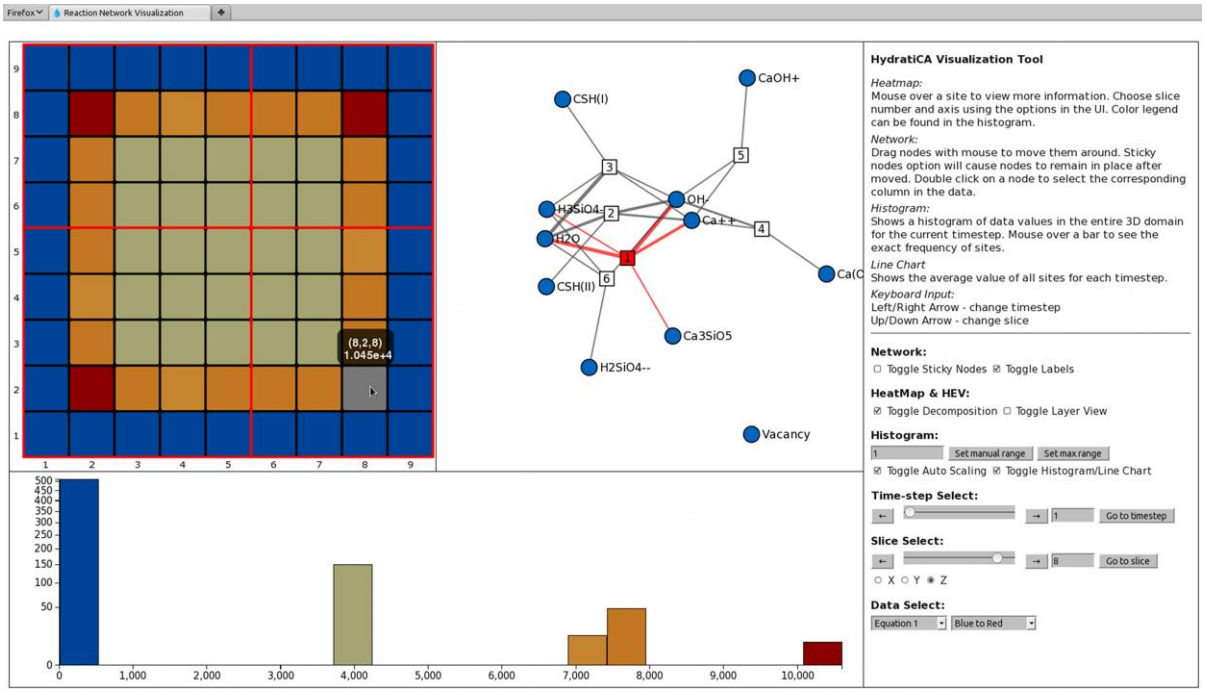

Figure 56. *2D information visualization with cross section of 3D visualization, network of chemical reactions, and activation rate histogram..*

- Development of a generalized, but empirical, rate law for dissolution that embraces a wide range of kinetic behavior, from highly nonlinear dependence on undersaturation to the standard rate law for elementary reactions. This rate law has been shown to more accurately capture the dissolution rates of C_3S, the majority mineral in unhydrated cement powders.
- Several improvements in the algorithms for heterogeneous and homogeneous nucleation and growth, so that these processes are now more closely tied to classical nucleation theory and are able to more directly accept experimental parameters that can be measured in the laboratory.

These additions to the model revealed several latent bugs in the source code, especially when implemented in a parallel computing environment, that were difficult to pinpoint. To remedy this, we developed an interactive visualization and analysis environment, which ran both in our immersive environment and on the desktop, for the model output. This environment provided a variety of visual modes that enabled precise quantitative measurements. It combined 3D scientific visualization with information visualization using D3.js running in a web browser. These two visualizations used node.js to communicate bidirectionally thereby simplifying analysis. See Figure 56 and Figure 57.

The visualization and analysis tool quickly showed what was causing the output errors and we were able to correct those bugs in the source code. In the coming year, we will be using and extending this and other tools to validate the outputs of our runs to study the rate controlling mechanism for early-age cement hydration.

[1] J. Stoian, T. Oey, J. Huang, A. Kumar, J. W. Bullard, M. Balonis, S. G. Satterfield, J. E. Terrill, N. Neithalath and G. Sant, Prehydration of Ordinary Portland Cement and its Mitigation using Limestone: New Insights from Experiments and Simulations, in review.

[2] W. Griffin, Danny Catacora, Steven Satterfield, Jeffrey Bullard and J. Terrill, Incorporating D3.js Information Visualization into Immersive Virtual Environments, poster VR2015 IEEE Virtual Reality, 23-27 March 2015, Arles, Camargue, Provence, France.

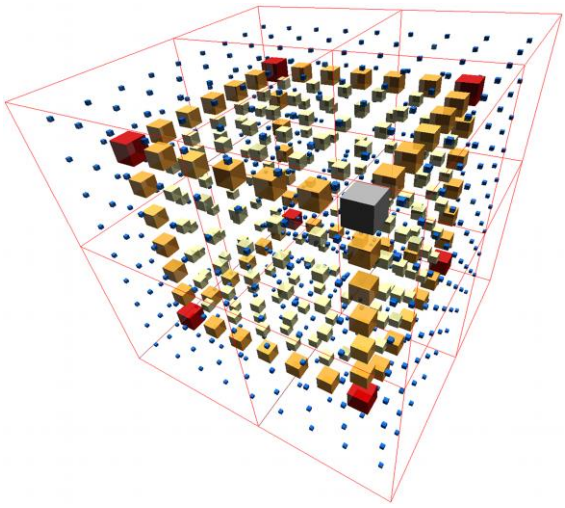

Figure 57. *3D Heat Map and Concentration Data Visualization.*

New Immersive Virtual Environment

Steve Satterfield
John Hagedorn
Wesley Griffin
Terence Griffin
Judith Terrill

The High Performance Computing and Visualization Group (HPCVG) has operated an Immersive Virtual Environment (IVE) since 2000 in support of its mission to develop the infrastructure necessary for advanced visualization of scientific data, including the use of 3D immersive environments as a true interactive measurement laboratory. HPCVG collaborates with researchers across all areas of NIST to apply the IVE and virtual measurement techniques.

During 2014, the IVE underwent a major upgrade, essentially a replacement, providing a significant improvement in visual quality. The new IVE, known as the CAVE, has a larger display area and greater graphics resolution. It is also brighter and has greater contrast. In addition it has a three way host display switch which allows one of three computers to be selected as the CAVE host at the touch of a button. This enables a primary, backup and experimental host to be available to run applications as needed. Full flexibility of video routing allows easy selection of special case configurations.

System reliability for the CAVE is very important. With the new installation a proactive approach to reliability was taken. Included with the hardware procurement, a custom software component for self-monitoring of the hardware was specified and delivered. Combined with a few existing system tests it is now possible to run automated tests nightly to confirm correct operation of many CAVE sub-systems and components. While certain tests require human observation, the automated self-test software provides a high level of confidence for on-going system availability. The self-monitoring software tests for: tracker producing head and wand data; projectors powered off when CAVE not in use; projectors shutter on/off operation; video switch operation; USB switch operation; audio switch operation; and changes in the critical /etc/X11/xorg.conf file. The self-monitoring software also includes tests run manually to check for 3D glasses synchronization or eye swap errors and a projector power cycle operation. While not specifically a test, the software includes a mechanism for powering off the projectors remotely.

Equally as important to the success of the IVE is the software used to drive the CAVE and implement the specific applications. At the lowest level, the vendor-supplied OpenGL library and Linux device driver renders and displays graphics in the graphics cards producing images output to the CAVE screens. Open SceneGraph (OSG) is the next level. It is an Open Source high performance 3D graphics toolkit and library for organizing graphics data in a hierarchical structure allowing models to be built, manipulated and rendered using OpenGL.

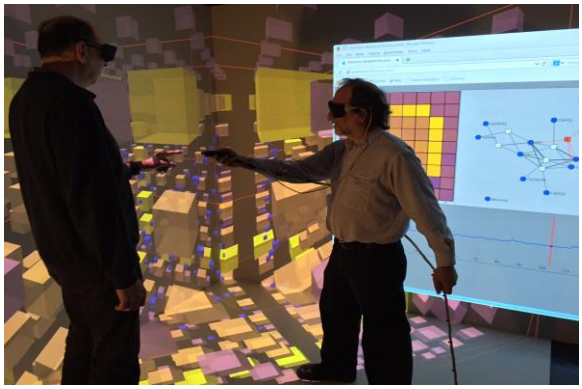

Figure 58. *A collaborative session in the HPCVG CAVE.*

IRIS (Interpreted Runtime Immersive Scenegraph) is above OSG in the stack. It is an HPCVG developed C++ software library. IRIS controls the hardware elements of the IVE, reading the tracking data to build the user view and update in real time the projected images. For a CAVE, different 3D stereo images are built for each screen such that they combine for the user into a 3D immersive view. A key feature of IRIS is that the displayed scene graph can be modified at run-time by external processes (programs and scripts) communicating via a standard Linux/UNIX facility known as a "named pipe." Another feature of IRIS and HEV is device independence. By isolating the display characteristics into specific display DSOs (distributed shared objects), the same HEV binary code can run on a full range of devices from CAVES to non-immersive desktop/laptop displays.

IDEA (IRIS Development Environment for Applications) is the level above IRIS. It is an HPCVG developed collection of commands, scripts and file formats. This collection of software tools, locally known as the "Army of Ants" follows in the tradition of the UNIX philosophy. Each of the pieces generally focuses on one simple task useful for a wide variety of applications.

Applications and demos complete the stack typically implementing an interactive visualization in a specific area of research. These applications are often built with very little programming by combining existing ants. When new tools are required, they are typically generalized as much as possible and added back into the software stack. A typical scenario combines traditional immersive visualization with 2D analysis capability and bidirectional communication between the 3D and 2D visualizations, creating an interactive virtual laboratory in the CAVE. See Figure 58 for an example of a collaborative session in HPCVG CAVE. In the coming year, besides our visualizations, we will be designing and implementing a software testing capability.

Optical Characterization of Large Immersive 3D Displays

Steve Satterfield
Judith E. Terrill
John Penczek (NIST PML)
Paul A. Boynton (NIST PML)
Timothy Scheitlin (NCAR)

Many things influence a visualization of a dataset. These include the nature of the data itself and its uncertainties, the visual representation space, the visualization algorithms, as well as algorithmic simplifications. Another factor impacting the final visualization is how accurately the images are rendered by the display system. We seek to develop a deeper understanding of each part of this process. In the current work we are studying the impact of the display on stereo visualizations.

Every display technology has its own inherent performance limitations. The non-ideality of the display introduces constraints on what information can actually be observed by the viewer. By characterizing the optical performance of the display system, we can quantitatively determine what visual information may be impaired. Operators of display facilities can use these results to evaluate how visual characteristics that are important to them are affected, understand the visual limitations of their system, and ultimately to drive improvements. The display performance data also informs scientists that create the visualization data how much of that data can actually be realized/observed. For example, the contrast ratio of an image feature can be dramatically degraded with the introduction of ambient lighting. Light contamination can be especially problematic for multi-wall CAVE systems, where the images from the adjacent screen can reduce the viewability at the region of interest. In addition, Figure 59 also illustrates how the spatial distribution of the contrast ratio on the front screen of a multi-wall CAVE system changes when the adjacent walls are turned on (right image). This report summarizes our activities in optically evaluating the viewing performance of a modern multi-wall CAVE system, and the impact of ambient lighting in general on several 3D immersive displays.

Our prior work largely focused on single-wall 3D immersive displays, see displays #1 and #2 in Table 2. The current work includes a 4-wall CAVE system that was recently installed at an offsite facility (display #3 in Table 2). The suite of tests developed for the single-wall displays were also applied to the 4-wall CAVE [1-4]. The optical characteristics measured on these systems included: luminance and color difference between left and right eye, contrast ratio between left and right eye, crosstalk between left and right eye, viewing direction dependence, head tilt dependence, luminance and color uniformity, shutter glasses characteristics, and 2D crosstalk and contrast mapping. Care was taken to separate

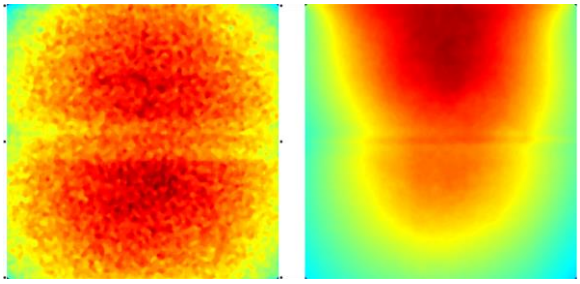

Figure 59. *Relative contrast ratio false color map of display #2 with the floor and side screens turned off (left image) and turned on (right image). Red indicates high contrast ratios.*

the contribution of light scattering from the adjacent projection walls. The front screen of the CAVE system was initially optically characterized with the adjacent walls turned off in order to evaluate the intrinsic capabilities of the display system. These measurements demonstrated that the darkroom characteristics of this new display system (display #3) had superior luminance, color, and contrast than the older single-wall systems. This demonstrated the improvements in viewing performance made by industry over time, and where further improvements can be made.

Another important aspect investigated by this study was the influence of ambient lighting. In the case of the single-wall displays, unintended light from scattering in the room or overhead lighting can add background noise to the viewing field on the screen and degrade the quality of the image. For display #1, the display is normally viewed in a dark room where the light contamination comes from scattering off the white walls in the room. However, it was determined that the scattering was sufficiently low that it had a negligible effect on the viewing performance. In contrast, display #2 is often used in a conference room format, where some overhead lights are turned on so that the audience can take notes. Although the room designers were careful to use dark materials for the reflective surfaces, some of the overhead fluorescent light was directly illuminating the presentation screen. The light contamination from the fluorescent lights produced a 63 % increase in the screen luminance (due to background noise), the contrast ratio dropped to 2.7 (from 1255), the color gamut area dropped to 3.3 % (from 36 %), and the color gamut volume was reduced to 8 % of its original value. Therefore, the ambient lighting severely impacted the viewability of the imagery. We advised the owner that this could be largely mitigated by the use of directional or local lighting at the conference table.

The influence of the concave geometry of the multi-wall CAVE system (display #3) was also evaluated for light contamination from the adjacent walls. It was determined that when the adjacent walls and floor were in the full white state (worst case scenario), the viewing

Table 2. *General characteristics of the 3-D immersive display systems measured in this study.*

Characteristic	Display System #1	Display System #2	Display System #3
Install year	2004	2009	2013
Screen size	2.67m x 2.07m	3.78m x 2.13m	4-wall CAVE (3.04m x 3.04m per wall)
Screen resolution	1280 x1024	1920 x1080	1920x1924 (2 overlapping projectors)
Projector	3-chip DLP lamp projector	3-chip DLP lamp projector	3-chip DLP lamp projector
Display type	Rear projection	Front projection	Rear projection
Nominal measurement position	1.65m high, 1.22m from front	1.46m high, 5.4m from front	1.65m high, 1.52m from front

performance of the front screen was dramatically degraded. Even when the intensity of the light from the adjacent walls and floor was reduced to more typical levels (30 % of peak white), the front screen luminance would increase by 5 %, the contrast ratio would decrease to 21 (from 1660), the color gamut area would drop to 19 % (from 28 %), and there would be a 47 % loss in the color gamut volume compared to the case with no ambient illumination. Our methods were able to quantify the impact of the light contamination, and can be applied in developing solutions to minimize its impact.

Advanced immersive display systems are currently being developed using laser sources. The polarization and narrow band properties of these light sources can have an adverse effect on the metrology tools commonly used on incoherent projection systems. Therefore a study was also conducted to evaluate the influence of laser (and LED) light sources in characterizing immersive displays. It was found that higher spectral resolution (≤ 5 nm) spectroradiometers with de-polarizing elements are generally needed for these light sources.

The experimental results of this study were analyzed and a paper was submitted for publication [5]. We will be extending our measurement of optical characteristics of displays for immersive visualization.

[1] *Information Display Measurements Standard*, V1.03, International Display Metrology Committee, Society of Information Display (2012).

[2] E. F. Kelley, K. Lang, L. D. Silverstein and M. H. Brill, Methodology for Estimating the Luminous Flux Based upon Color Primaries from Digital projection Displays, NISTIR 6657, January 2009.

[3] E. F. Kelley, K. Lang, L. D. Silverstein and M. H. Brill, Projector Flux from Primaries, *Society of Information Display Symposium Digest of Technical Papers* **40** (2009), 224-227.

[4] J. Penczek, P. A. Boynton and E. F. Kelley, Measuring 3D Crosstalk Uniformity and its Influence on Contrast Ratio, *Journal of the Society of Information Display* **21** (June 2013), 225-230.

[5] J. Penczek, S. G. Satterfield, E. F. Kelley, T. Scheitlin, J. E. Terrill and P. A. Boynton, Evaluating the Visual Performance of Stereoscopic Immersive Display Systems, in review.

Texture Compression Evaluation and Optimization

Wesley Griffin
Marc Olano

Texture compression is widely used in real-time rendering to reduce storage and bandwidth requirements. Hardware-based texture compression has not fundamentally changed since its introduction in 1999. Recently, however, interest has grown in improving texture compression. Our research has explored new techniques for reducing the bit rate for the current fixed bit rate algorithms as well as new variable bit rate algorithms that can be efficiently decoded in graphics hardware. This work benefits the rendering and visualization communities by providing a methodology for evaluating and optimizing texture compression. This work can be directly applied to existing projects to improve the quality of compressed textures.

In evaluating texture compression, the most common approach is to use some combination of the Mean Square Error (MSE), Peak Signal-to-Noise Ratio (PSNR), or visual image inspection of the compressed texture. This year we presented a paper, "Objective Image Quality Assessment of Texture Compression" at the 2014 ACM SIGGRAPH Symposium on Interactive 3D Graphics and Games [1]. This paper presents our new evaluation methodology that accounts for the two ways in which textures are used in rendering, which the MSE and PSNR measures cannot account for. We have also extended the paper to explore the relative effects between how textures are used to render objects [2]. The extended paper is currently under review in *IEEE Transactions on Visualization and Computer Graphics*. In this study, we discovered that the type of texture, combined with how it is used, has an impact on perceived quality when rendering with compressed textures.

Future work will involve implementing an optimization framework based on our evaluation methodology. By developing an optimization method, we can enable real-time rendering asset pipelines to automatically optimize texture compression rates and quality. This will further benefit the real-time rendering community by removing the highly subjective and time-consuming task of finding the right compression algorithm settings for textures.

[1] W. Griffin and M. Olano, Objective Image Quality Assessment of Texture Compression, in *Proceedings of the 2014 ACM SIGGRAPH Symposium on Interactive 3D Graphics and Games* (I3D), San Francisco, CA, March 2014, 119-126.

[2] W. Griffin and M. Olano, Evaluating Texture Compression Masking Effects using Objective Image Quality Assessment Metrics, in review.

Information Visualization for Complex Information Systems

Sandy Ressler
Kevin Mills (NIST ITL)
Chris Dabrowski (NIST ITL)
James Filliben (NIST ITL)
Mohamed Gueye (City College of New York)

http://www.nist.gov/itl/antd/emergent_behavior.cfm

This project aims to develop and evaluate a coherent set of methods to understand behavior in complex information systems, such as the Internet, computational grids and computing clouds. We are providing visualizations which help to convey the results of this project.

As an extension of work done in the previous year we produced an animation of a network based on the 2001 configuration of the Autonomous System (AS) portion of the Internet that the team uses for study. The graph consists of approximately 11,000 nodes and 47,000 edges. Using an off-the-shelf open source tool called gephi we produced a number of visualizations that have helped reveal the structure of the network. Data illustrated using gephi shown in Figure 60 was animated using alternate visualization parameters; see Figure 61. Colors correspond to data clusters using the "modularity" network metric.

We intend on using developments of the cloud computing simulation system and additional network configurations as the source for further visualizations that will impact the research process. We produced a number of visualizations using the d3.js library to visualize and compare genetic algorithms applied to cloud simulation data; see Figure 62. These were done primarily by Mohammed Gueye, a NIST SURF student during the summer of 2014. By using d3, a highly interactive toolset, we were able to give researchers choices about which simulation run to observe and to compare different sets, both topologically and via bar graph displays.

[1] K Mills, C. Dabrowski, J. Filliben and S. Ressler, "Combining Genetic Algorithms and Simulations to Search for Failure Scenarios in Systems Models," Distinguished Lecture, Mitre Cyber Security Technical Center, McLean, Virginia, October 16, 2013.

Figure 60. *Internet autonomous system graph circa 2001 in gephi tool.*

Figure 61. *Frames from animation of Internet autonomous system graph circa 2001.*

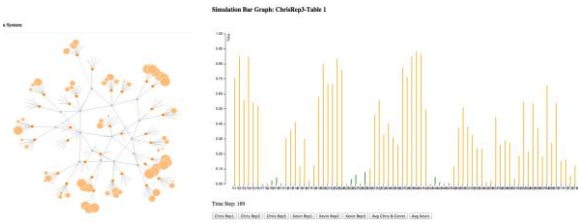

Figure 62. *Topological and bar graph visualization of simulation data.*

[2] K. Mills, C. Dabrowski, J. Filliben, S. Ressler and Y. Wan, "Predicting the Unpredictable in Complex Information Systems," Network Science Symposium, College Park, Maryland, January 24, 2014.

[3] K. Mills, C. Dabrowski, J. Filliben and S. Ressler, "Combining Genetic Algorithms and Simulation to Search for Failure Scenarios in System Models," Computer Science Interdisciplinary Seminar, George Mason University, February 19, 2014.

Visualizing the National Vulnerability Database

Sandy Ressler
Mohamed Gueye (City College of New York)

The National Vulnerability Database contains reported computer vulnerabilities in a convenient single authoritative location. We have experimented with a number of visualizations to help security researchers better identify trends and to explore the data set interactively. We have utilized the "Keshif Browser" [1]. It allows a great deal

of exploratory freedom as described on its web site: "*It presents visual summaries of your data properties, such as who, what, when and where, in its facets and timeline. You can discover relations between attributes through exploration. Filtering follows a consistent design within and across facets. After each step of exploration, the most relevant results and data properties are shown first, as they are dynamically and smoothly re-ordered.*"

With the browser users can filter across a variety of parameters, and choose among treemap, scatterplot or bullet graph visualizations. The browser follows the classic Shneiderman information seeking mantra or providing an "Overview" allowing "Zoom and Filter" with "Details on Demand".

There are three main areas for the browser. The left side allows the user to filter from among all of the properties that comprise the basis for producing a vulnerability score. After selecting one or several filters, the list of CVE vulnerabilities that match the selected filters is presented on the right. The user can then select the particular vulnerability for closer inspection. The top portion of the browser displays the selected entries on a timeline indicating when they were reported. The three rows of dots correspond to the three values the "availability-impact" parameter can occur. Finally lower right portion of the browser displays a list of the vulnerabilities that meet the filter criteria.

The illustrations in Figure 63 through Figure 65 are the three types of visualizations that can be produced by the browser: scatter plot, bullet graph, and a treemap. Each provides a different perspective on the data.

We also produced a calendar visualization displaying the quantity of vulnerabilities reported on the date. See Figure 66. One nice feature of this visualization is the ability to display the entire history of the NVD vulnerabilities on a single screen.

[1] http://www.cs.umd.edu/hcil/keshif, accessed 01/09/2014.

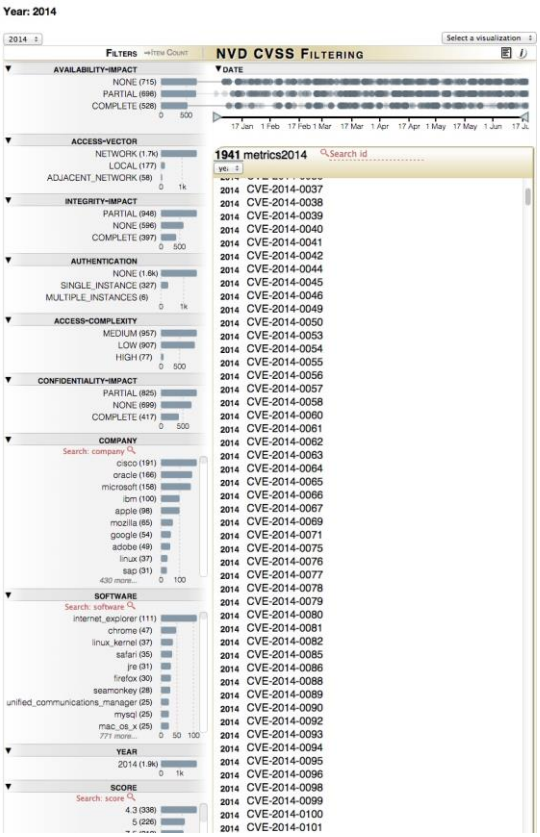

Figure 63. *NVD vulnerability data displayed in the Keshif Browser.*

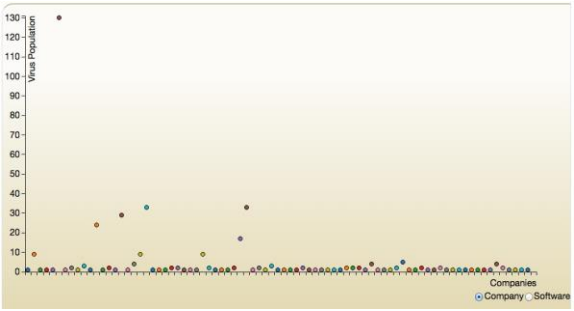

Figure 64. *NVD Data in Keshif Browser with scatterplot visualization.*

Figure 65. *NVD Data in Keshif Browser with bullet graph visualization.*

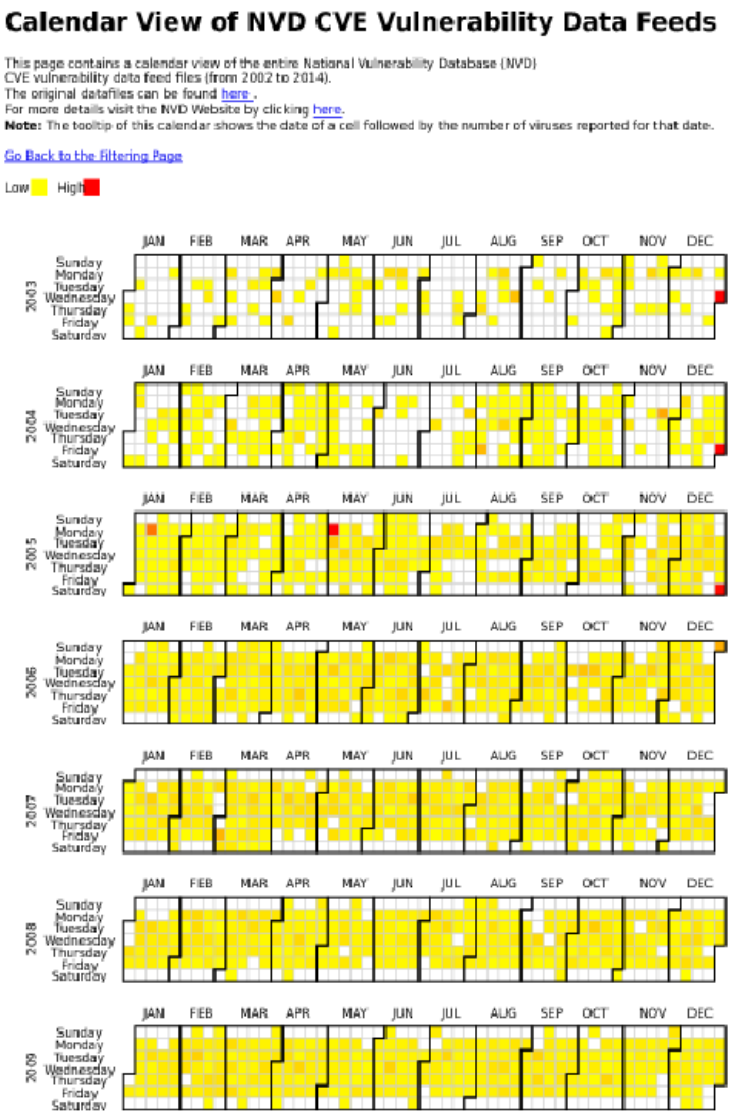

Figure 66. *Calendar view of the NVD CVE Vulnerability data set.*

WebVR Graphics

Sandy Ressler
Mohammed Gueye (City College of New York)
Tomasz Bednarz (CSIRO, Australia)

The Oculus Rift is a new virtual reality headset that is bringing about a renaissance for virtual reality (VR). The quality is relatively high and cost is low. WebVR is a new technology that enables web browsers to support VR devices "natively." We are performing this work because it has the potential to allow wide diffusion of immersive scientific visualizations with very low cost hardware. This will benefit the larger research community at NIST that already takes advantage of immersive visualization and has the potential of making that community much larger. We have managed to integrate early versions of the X3DOM standard representation of graphics with a VR headset. We plan on collaborating with partners in Australia at CSIRO to further develop these immersive capabilities as they also have common scientific visualization needs.

VR in the web browser means that, without any additional software, we can make use of the viewer's head orientation and position. The result is a display that presents the user with stereo, head-tracked images, giving the illusion of a first person point-of-view scene. We have begun to experiment with the combination of WebVR with our previous work on declarative Web3D. The results are visualizations using declarative graphics

Figure 67. *X3DOM scene functioning with Oculus Rift headset [1].*

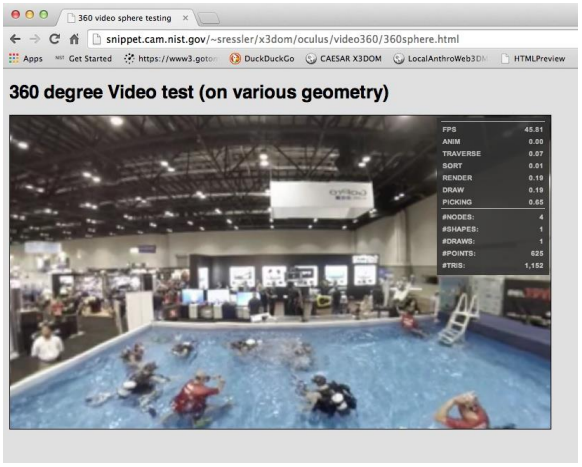

Figure 68. *360 degree video viewed from inside of sphere.*

that can function with the new generation of virtual reality headsets. See Figure 67.

In addition to geometric scenes we are experimenting with 360 degree video sources. We map the video onto both the inside and outside surfaces of a sphere; see Figure 68. Placing the viewer inside the sphere results in a video image warped to appear "correct" to the viewer. The sphere and video texture mapping are accomplished using standard X3DOM declarative constructs.

The intent is to have the ability to create 360 panoramic videos that play inside of web pages that are head-tracked. This will be extended via the use of WebRTC to the ability to have multiple collaborators sharing a single video space, which will be done in collaboration to Thomas Bednarz (CSIRO - Australia) for mining or other applications in a NIST/CSIRO collaboration.

[1] x3dom web page posting; accessed 01/08/2015

Quantum Information

An emerging discipline at the intersection of physics and computer science, quantum information science is likely to revolutionize science and technology in the same way that lasers, electronics, and computers did in the 20th century. By encoding information into quantum states of matter, one can, in theory, exploit the seemingly strange behavior of quantum systems to enable phenomenal increases in information storage and processing capability, as well as communication channels with high levels of security. Although many of the necessary physical manipulations of quantum states have been demonstrated experimentally, scaling these up to enable fully capable quantum computers remains a grand challenge. We engage in (a) theoretical studies to understand the power of quantum computing, (b) collaborative efforts with the multi-laboratory experimental quantum science program at NIST to characterize and benchmark specific physical implementations of quantum information processing, and (c) the demonstration and assessment of technologies for quantum communication.

Tamper-Resistant Cryptographic Hardware using Isolated Qubits

Yi-Kai Liu

See page 15.

Quantum Information Science

Scott Glancy
Emanuel Knill
Adam Keith (University of Colorado)
Jim van Meter (University of Colorado)
Peter Wills (University of Colorado)
Kevin Coakley (NIST ITL)
Sae Woo Nam (NIST PL)
Dietrich Leibfried (NIST PL)
David Wineland (NIST PL)
David Pappas (NIST PL)
Gerardo Ortiz (Indiana University)
Paul Kwiat (University of Illinois)

The traditional information units of classical computing are 0/1-valued bits, which may be realized as distinguishable states of physical systems. Quantum information science investigates the properties and applications of quantum bits. Formally, quantum bits have pure states defined as superpositions of two distinguishable states. Quantum bits promise to be powerful information processing units whose potential is realized when they are coupled by means of quantum gates, which generalize classical circuit elements. Applications include efficient algorithms for factoring integers and for physics simulation, protocols for secure communication, and significantly improved measurement precision. In addition, there is the potential for illuminating the foundations of physics, in particular the universality of quantum mechanics and field theory.

In the last few years, there has been tremendous experimental progress demonstrating long-lived quantum bits in diverse systems, including individually trapped atoms, superconducting circuit elements and various other solid state devices. Thus, we currently expect that quantum information processing will eventually be realized on large scales. Nevertheless, there are significant obstacles in realizing the benefits of quantum information processing. Perhaps the most challenging obstacles are to experimentally construct multi-qubit systems whose quantum states are both stable and robustly manipulable by quantum gates. One reason the two requirements are difficult to meet is that stability requires good isolation from the environment, but manipulatability involves interaction with an external controller.

Our work in quantum information science aims to characterize quantum devices in terms of their potential for information processing, determine ways of exploiting quantum control for better measurements of physical quantities such as time and space, and contribute to our understanding of the power and limitations of quantum physics as it relates to information extraction and processing. In this spirit, we investigate a broad range of subjects.

Many applications of quantum mechanics to communication and cryptography rely on experimental tests of Bell inequalities. These tests also provide the strongest evidence against local realism (LR) as a possible explanation of quantum non-determinism. While there have been many experiments demonstrating the required violation of Bell inequalities, so-far they have suffered from loopholes and problems with quantifying the evidence against LR. We have developed a powerful strategy for analyzing Bell-test data that can quantify the evidence against LR in a configuration-independent way. Two complicating features of many current Bell tests is that the required random settings choices cannot be changed fast enough and the data obtained at each setting choice consists of many time-tagged detections.

For comparison, in text-book Bell tests, exactly one detection is recorded at each setting choice. We have developed a Bell-test analysis method that can take advantage of the many detections recorded at one setting without being deceived by loopholes. We have applied this method to Bell-test data from P. Kwiat's lab at UIUC to show that it violates LR without being subject to the so-called detection loophole. A conventional analysis did not show this violation.

The statistical principles underlying our Bell-test analysis are general and have the potential for simplifying the analysis of data at high significance levels without making approximations. To investigate the regime of application of our methods, we are considering the simple problem of estimating the bias of the bits in a sequence of independent and identical random bits. We expected that a comparison of methods would require Monte-Carlo simulations, but found that analytical expressions for the performance were available even for our nominally adaptive methods. Once we have completed the comparison of methods for bit flips, we will consider the problem of estimating the mean of a bounded random variable.

In collaboration with John Bollinger's team in the NIST Ion Storage Group, we adapted a classical simulator for ions in a Penning trap with laser cooling to explore the thermodynamic temperature and non-linear behavior of axial and planar modes of a two-dimensional ion crystal. The goal is to determine experimentally difficult-to-access mode temperatures as a function of trap and laser parameters in the hope of obtaining colder and more stable crystals. This may help with planned quantum simulations and demonstrations of quantum correlations in this system.

Particles carrying quantum information are indispensable in quantum information science and emerge as fundamental excitations in most quantum condensed matter systems. In some systems these excitations are expected to take the form of non-abelian anyons, which may provide naturally protected subsystems for storing quantum information. A fundamental question is whether the different types of particle-like excitations can be described in a unified framework that captures the features of both traditional particles (bosons and fermions) as well as anyons. We have started collaboration with Gerado Ortiz of Indiana University to explore the possibility of using algebraic quantum theory for such a framework.

Measurement and information processing operates on increasingly small and fast scales where relativistic effects cannot be neglected. The emerging field of relativistic quantum information processing aims to explore these effects for precise measurement and control of information. In this spirit, we are analyzing proposed Heisenberg uncertainty relationships based on algebraic quantum field theory on curved space-time backgrounds. While they have the expected form, their application requires computing correlations of energy-momentum operators. We are planning on computing these correlations for some relevant situations such as gravitational wave detection with laser interferometry. For the algebraic approach to be generally useful, it should match the expected shot-noise limits, and we expect that it will do so.

[1] E. Cobanera, G. Ortiz and E. Knill, A Solution to the Non-Abelian Duality Problem, *Nuclear Physics B* **877** (2013), 574-597.

[2] Y. Zhang, S. Glancy and E. Knill, Efficient Quantification of Experimental Evidence Against Local Realism, *Physical Review A* **88** (2013), 052119.

[3] M. Mullan and E. Knill, Simulating and Optimizing Atomic Clock Evolution, *Physical Review A* **90** (2014), 042310.

[4] A. C. Wilson, Y. Colombe, K. R. Brown, E. Knill, D. Leibfried and D. J. Wineland, Tunable Spin-Spin Interactions and Entanglement of Ions in Separate Wells, *Nature* **512** (2014), 57-60.

[5] E. Knill, S. W. Nam, K. Coakley, S. Glancy and Y. Zhang, Bell Inequalities for Continuously Emitting Sources, in review.

Quantum Estimation Theory and Applications

Scott Glancy
Adam Keith
Emanuel Knill
Nadav Kravitz (University of Maryland)
Kevin Coakley (NIST ITL)
John Gaebler (NIST PML)
Konrad Lehnert (NIST PML)
Yiheng Lin (NIST PML)
Ting Rei Tan (NIST PML)
Yong Wan (NIST PML)
Will Kindel (University of Colorado)
Hsiang-Sheng Ku (University of Colorado)

Many emerging technologies will exploit quantum mechanical effects to enhance metrology, computation, and communication. Developing these technologies requires improved methods to measure the state of quantum systems. Quantum estimation is a statistical problem of estimating an underlying quantum state, measurement, or process by using a collection of measurements made on independently prepared copies of the state or applications of the measurement or process. Accurate quantum estimation allows experimentalists to answer the question "What is happening in my quantum experiment?" and to characterize uncertainty in that answer.

Full quantum estimation can be a demanding task, requiring a large number of different measurements to be performed on (independently prepared copies) of the

quantum system and requiring large amounts of computation to perform the estimation. One method for reducing these costs is to exploit pre-existing knowledge about the state being measured. For example, the state could be restricted to a smaller sub-set of all quantum states, such as those states that have Gaussian probability distributions for measurement results. We have developed two algorithms for estimating these Gaussian states that are orders of magnitude faster than full quantum state estimation and can be applied to data sets that are much too large to be analyzed with full quantum state estimation. One is an almost linear estimator that computes experimental means of simple functions of measurement data to estimate desired quantities. The other uses a maximum likelihood technique to compute a covariance matrix of the quantum state. The algorithms have been tested on simulated data and applied in an experiment that entangled microwave signals traveling through superconducting circuits in the JILA laboratory of Konrad Lehnert [1]. Our new algorithms will be useful to many experiments on quantum optics and nano-mechanical resonators. We are preparing a report detailing the two algorithms and comparing their performance.

NIST's Ion Storage Group has pioneered one of the world's most successful quantum computer development projects. With their recent advances in qubit preparation, logical operation, and measurement fidelities, more advanced statistical techniques are required to characterize the trapped ion quantum computers. (NIST trapped ion experiments have reported a fidelity of 99.9998 % for single qubit logic operations [2].) Working with the Ion Storage Group, we previously developed linear methods for inferring states of ions in Pauli traps from fluorescence histograms without making assumptions on the histogram shapes. Conventionally, the histograms are modeled as Poissonian distributions, but with the newer traps, this assumption fails at a significant level. The method was used to determine the fidelity of a Bell state prepared without bringing ions into the same potential well. The results from this experiment have now been published in *Nature* [3]. We are standardizing analysis protocols so that they can be used routinely for determining ion states from histograms and to integrate these protocols with the software that controls the trapped ion experiments.

During the next year we will be publicly releasing quantum estimation software that has been used in several NIST experiments. Algorithms that we have developed will be incorporated in to an open source toolbox such as the one being developed by the Quantum Toolbox in Python (QuTiP) project[20], making them available to researchers around the world.

[1] H. S. Ku, W. F. Kindel, F. Mallet, S. Glancy, K. D. Irwin, G. C. Hilton, L. R. Vale and K. W. Lehnert, Generating and Verifying Entangled Itinerant Microwave Fields with Efficient and Independent Measurements, in review.

[2] K. R. Brown, A. C. Wilson, Y. Colombe, C. Ospelkaus, A. M. Meier, E. Knill, D. Leibfried and D. J. Wineland, Single-Qubit-Gate Error Below 10^{-4} in a Trapped Ion, *Physical Review A* **84** (2011), 030303(R).

[3] A. C. Wilson, Y. Colombe, K. R. Brown, E. Knill, D. Leibfried and D. J. Wineland, Tunable Spin-Spin Interactions and Entanglement of Ions in Separate Wells, *Nature* **512** (2014), 57-60.

Phase Retrieval and Quantum State Tomography

Yi-Kai Liu
Felix Krahmer (University of Göttingen)

Phase retrieval is the task of learning an unknown vector x, given measurements of the form $|a^T x|^2$ where the vectors a are known. (That is, each measurement projects x onto the direction a, and returns the modulus, but not the phase. One wants to reconstruct these phases, in order to estimate x.) Recently, new algorithms for phase retrieval have been developed, using techniques from compressed sensing, such as random measurements and convex optimization. These algorithms have nice theoretical properties, but further work is needed to make them useful in practice.

Two major applications of phase retrieval are X-ray crystallography and quantum state tomography. In the context of quantum state tomography, phase retrieval has some advantages over other approaches, because it naturally incorporates experimental measurements that project onto the eigenbasis of each observable. However, phase retrieval also has some disadvantages over other methods: it is not as well-understood, and it seems to require complicated measurements, which are difficult to implement in an experiment.

We are studying phase retrieval using simple classes of measurements (e.g., independently sampled Bernoulli random vectors). Here it is known that phase retrieval is technically impossible, in that there exist pathological examples of vectors (e.g., the standard basis vectors) that cannot be distinguished from one another using these measurements. We identify a surprisingly large class of vectors that *can* be recovered in this setting, namely "flat" vectors x that satisfy $|x|_\infty \leq c|x|_2$, where c is some sufficiently small constant. For these "flat" vectors, we can show that phase retrieval is possible in an information-theoretic sense, and we are currently trying to give a computationally efficient method, using a convex relaxation known as PhaseLift.

A future goal of this project is to develop methods for quantum state tomography based on phase retrieval,

[20] http://qutip.org/

using measurements that are easy to implement in experiments. While random Bernoulli measurements are not suitable for this purpose, we believe that our approach can be adapted and extended to other classes of measurements, such as Fourier measurements with random phase factors, which are easier to implement.

[1] F. Krahmer and Y.-K. Liu, Phase Retrieval using Random Bernoulli Measurements, in preparation.

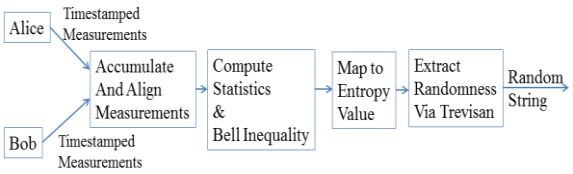

Figure 69. *Post-processing for the Bell Measurent based quantum random number generation project.*

Random Number Generation Based on Bell Inequality Violation

Scott Glancy
Stephen Jordan
Manny Knill
Paulina Kuo
Yi-Kai Liu
Alan Mink (Wagner Resources)
Xiao Tang
Lawrence Bassham (NIST ITL)
Joshua Bienfang (NIST PML)
Michaela Iorga (NIST ITL)
Alan Migdall (NIST PML)
Saewoo Nam (NIST PML)
Rene Peralta (NIST ITL)
Andrew Rukhin (NIST ITL)

Random strings of bits are a fundamental resource for cryptography whose security is notoriously difficult to test. A string of bits may pass all statistical tests of randomness and yet be useless cryptographically; it could be a uniformly random string already known by an adversary. Remarkably, it is possible to certify that certain measurement outcomes in quantum experiments could not have been known ahead of time. This can be achieved using experiments called Bell tests in which pairs of entangled photons are sent to well-separated sites and measured. The observed correlations between the measurement outcomes can be used to certify the presence of fresh randomness. The security is proven as a direct consequence of the empirically observed correlations and the assumptions that the initial random seed is secure and that signals cannot travel faster than light. The internal workings of the device needn't be trusted. This uniquely quantum-mechanical form of fundamental protection against device failure and tampering is known as device-independent security.

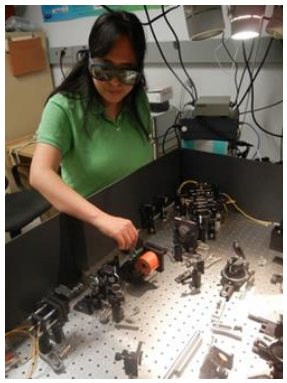

Figure 70. *Paulina Kuo is testing methods for generating entangled photons.*

The development of hardware achieving device-independent security is a challenge at the fringes of feasibility with current photonic techniques. To satisfy the conditions needed for the security proofs, it is necessary to develop and integrate fast, high-efficiency photon detectors, optical switches, and entangled-photon generators. Researchers in ACMD and several other NIST divisions are collaborating on a NIST Innovations in Measurement Science project to do this. Eventually, the resulting hardware may be put into service for cryptographic applications. In the meantime, a prototype random bit beacon at NIST is currently serving time stamped and digitally signed strings of random bits over the web[21]. The bits currently being served are generated by conventional hardware without device-independent security. A number of beacon-based cryptographic protocols for e-commerce and privacy protection have been proposed. These can now be tested in practice using the NIST beacon.

The Bell experiment needs several additional elements to form a complete cryptographic resource, some of which are illustrated in Figure 69. These include a source of random numbers to use as the initial seed, software for analyzing the outcomes of the experiment to certify the presence of fresh randomness, software to extract uniformly distributed strings of bits from the measurement outcomes, and technology to publish these strings over the internet. Division expertise has been used to develop these elements and to do theoretical and experimental work related to the Bell experiment itself.

This year, ACMD researchers developed a loophole-free method to analyze data from Bell experiments that produce entangled photons distributed randomly in time [1]. The analysis allows high confidence rejection of the hypothesis that randomness generated in the Bell experiment could have been known or predicted by a hacker. Also, ACMD researchers have in the past year tested two methods for generating entangled photons and capturing them in optical fiber with high efficiency: one based on spontaneous parametric downconversion

[21] http://www.nist.gov/itl/csd/ct/nist_beacon.cfm

[2], and one based on four-wave mixing using a micro toroid. In addition, this year saw the completion of a code-review performed within ACMD on software for distilling secure random bits from the experimental output data produced by the Bell tests.

[1] E. Knill, S. Glancy, S. W. Nam, K. Coakley and Y. Zhang, Bell Inequalities for Continuously Emitting Sources. arXiv:1409.7732 (2014)

[2] P. S. Kuo, J. S. Pelc, O. Slattery, L. Ma and X. Tang, Domain-engineered PPLN for Entangled Photon Generation and Other Quantum Information Applications, *Proceedings of the SPIE* **9136** (2014), 913403.

Computational Complexity of Quantum Field Theory

Stephen Jordan
Keith Lee (University of Toronto)
John Preskill (Caltech)
Hari Krovi (Raytheon/BBN)

Particles and fields are central objects of study in both classical and quantum physics. Classically, the instantaneous state of a point particle can be fully specified by just six numbers: its three position coordinates and its three components of momentum. In contrast, a field is in principle determined by infinitely many numbers: its values at every point in space. This makes the quantum dynamics of fields complex and difficult to analyze mathematically. This project seeks to understand these difficulties from a computational complexity perspective. In particular we ask two main questions. First, can classical computers efficiently simulate the dynamics of quantum fields? Our evidence suggests that they cannot, in general. Second, can quantum computers (once they are built) efficiently simulate the dynamics of quantum fields? Our evidence so far suggests they can.

So far, we have developed polynomial-time quantum algorithms to simulate two simple quantum field theories (massive phi-fourth theory and the massive Gross-Neveu model) within the quantum circuit model [1, 2]. These results suggest that, despite the additional mathematical complications, from a computational complexity point of view, quantum field theories are not fundamentally more powerful than the quantum dynamics of fixed numbers of particles (as described by Schrödinger's equation). Furthermore, upon successful construction of large-scale quantum computers, these algorithms can be used to obtain predictions that can then be compared with the outcomes of particle-accelerator experiments.

The fields in nature can be classified as either Fermionic or Bosonic and as either massive or massless. The quantum field theories for which we have developed quantum simulation algorithms are a massive Bosonic theory (phi-fourth) and a massive Fermionic theory (Gross-Neveu). One of our current research directions is to investigate whether quantum computers can efficiently simulate the massless case. If so, we would have the main ingredients necessary to simulate the Standard Model, which is the current most widely accepted model of fundamental physics, incorporating all known forces other than gravity into a quantum field theory framework.

Currently, we are compiling formal evidence that classical computers cannot simulate quantum field theories efficiently. Specifically, we are developing a proof that a certain formalized quantum field theory simulation problem is "BQP-hard." This means that any problem solvable in polynomial time by a quantum computer can be converted into an instance of the quantum field theory simulation problem. Thus, if one could simulate quantum field theory efficiently on a classical computer, then one could simulate quantum computers efficiently on a classical computer. It is generally believed that one cannot simulate quantum computers on classical computers. Therefore, such a BQP-hardness result can be viewed as evidence that classical computers cannot simulate the dynamics of quantum fields with polynomial runtime on the hardest instances.

[1] S. P. Jordan, K. S. M. Lee and J. Preskill. Quantum Computation of Scattering in Scalar Quantum Field Theories, *Quantum Information and Computation* **14**:11/12 (2014), 1014-1080.

[2] S. P. Jordan, K. S. M. Lee and J. Preskill. Quantum Algorithms for Fermionic Quantum Field Theories, arXiv:1404.7115 (2014).

Quantum Adiabatic Optimization

Stephen Jordan
Michael Jarret (University Maryland)

Quantum computers do not offer speedup for all computational problems. For some problems, such as factoring integers, quantum algorithms promise exponential speedup over the fastest classical algorithms. For other problems, such as computing sums modulo 2, they are known to offer no advantage over classical computation. Due to the widespread applications of optimization, the question whether quantum algorithms offer substantial speedup for optimization has long been an area of intense research interest.

In 1999, Farhi et al. proposed an intriguing framework for the design of quantum optimization algorithms called adiabatic quantum computing. Quantum adiabatic algorithms are easy to design and are guaranteed to find the optimum given sufficient runtime. The key difficulty is determining how this runtime depends on the features of the objective function of the optimization problem.

The runtime of an adiabatic quantum algorithm is determined by the gap between the lowest and second lowest eigenvalues of a matrix called the Hamiltonian. The Hamiltonian is an exponentially high dimensional matrix, so for problem sizes of practical interest it is infeasible to calculate the eigenvalue gap numerically. Due to the primitive nature of present-day quantum computational hardware it is also extremely difficult to study the eigenvalue gap experimentally. Thus there is a great need for mathematical tools to analyze eigenvalue gaps of Hamiltonians.

In this project we are investigating the effect that local minima in the objective function have on the eigenvalue gap of the resulting Hamiltonian. The strongest known upper bound on the runtime of adiabatic algorithms scales as one over the square of the eigenvalue gap. Surprisingly, it turns out that even for objective functions without local minima (whose global minima are easy to find classically by gradient descent), this eigenvalue gap can be exponentially small [1]. On the other hand, for convex optimization problems in low dimension or high symmetry, we have proven that the gap cannot be exponentially small [2]. In current work, we are importing tools from spectral graph theory to tighten and generalize these bounds.

[1] M. Jarret and S. P. Jordan, Adiabatic Optimization without Local Minima, *Quantum Information and Computation* **14**:3/4 (2015), 0181-0199.

[2] M. Jarret and S. P. Jordan. The Fundamental Gap for a class of Schrödinger Operators on Path and Hypercube graphs, *Journal of Mathematical Physics* **55**:5 (2014), 052104.

Quantum Computation and Knot Theory

Stephen Jordan
Gorjan Alagic (University of Copenhagen)
Stacey Jeffery (Caltech)
Aniruddha Bapat (Caltech)
Michael Jarret (University of Maryland)

A knot is an embedding of the circle into three-dimensional space. More generally, a link is an embedding of one or more circles into three-dimensional space. One of the central problems in low-dimensional topology is, given a pair of links, determine whether they are equivalent. That is, can one be smoothly transformed into the other without cutting strands or passing them through one another? Mathematically and computationally, this is a very difficult problem. Link invariants provide a partial solution. These are functions that take links as input and produce easy-to-distinguish objects (such as numbers or polynomials) as output. Link invariants take the same value on equivalent links. Thus, evaluating an invariant of a pair of links and obtaining different outputs is an effective means of proving that two links are topologically inequivalent.

Amazingly, it turns out that many of the known link invariants come from quantum mechanics. Specifically, matrices that satisfy the Yang-Baxter equation describe the braiding of certain quantum particles confined to two dimensions and also give rise to many of the most important link invariants. As a result, the theory of quantum information and computation can be used to help characterize both the power of link invariants for distinguishing links and the computational complexity of evaluating the link invariants.

A matrix satisfying the Yang-Baxter equation can be interpreted as a quantum logic gate. In the case that the quantum logic gate is universal for quantum computation (analogous to the universality of the NAND gate for classical computation), one can show that corresponding link invariant is BQP-complete to approximate. Thus, classical algorithms to approximate the link invariant almost certainly require exponential runtime. Building upon previous classification work of Hietarinta and Dye, we have shown that no 4x4 solution to the Yang-Baxter equation is a universal quantum gate [1]. This is bad news if one wishes to build a quantum computer using these gates, but is good news if one wishes to approximate the corresponding link invariants on classical computers. In recent work, not yet published, we have also proven that Yang-Baxter matrices can only yield nontrivial knot invariants if the corresponding quantum gates generate quantum entanglement. This may be of use in future work searching for new link invariants. In addition, we have recently proposed an approach to cryptographically obfuscating quantum and classical logic circuits using the topological equivalences of braids that the Yang-Baxter equation represents [2].

[1] G. Alagic, A. Bapat and S. Jordan. Classical Simulation of Yang-Baxter gGtes, in *Proceedings of the Ninth Conference on Theory of Quantum Computation, Communication, and Cryptography* (TQC2014), Singapore, May 21-23, 2014, 161-175.

[2] G. Alagic, S. Jeffery and S. Jordan, Partial-indistinguishability Obfuscation using Braids, in *Proceedings of the Ninth Conference on Theory of Quantum Computation, Communication, and Cryptography* (TQC2014), Singapore, May 21-23, 2014, 141-160.

Post-Quantum Cryptography

Stephen Jordan
Yi-Kai Liu
Lily Chen (NIST ITL)
Dustin Moody (NIST ITL)
Rene Peralta (NIST ITL)
Ray Perlner (NIST ITL)
Daniel Smith-Tone (NIST ITL)

Public key cryptography is a crucial tool for protecting the confidentiality and integrity of data transmitted over the Internet. Large-scale quantum computers, if they are ever built, would break many of the public key cryptosystems that are currently in use, such as RSA and elliptic curve cryptosystems. Researchers at NIST have been investigating possible replacements for these cryptosystems that would be secure against quantum attacks – so-called "post-quantum" cryptosystems. The goal of this project is to prepare for the possible development of standards in this area.

Existing proposals for post-quantum cryptosystems include lattice-based cryptosystems (such as NTRU), code-based cryptosystems (such as McEliece), multivariate cryptosystems (such as HFE and unbalanced oil-vinegar), hash-based signatures (such as Merkle trees), and key exchange protocols based on elliptic curve isogenies. However, all of these proposals face significant open questions regarding their security and practical feasibility.

In the past year we have continued to study these issues. We have obtained new results on information-set decoding of structured MDPC codes, differential properties of the HFE cryptosystem, and the security of the ABC multivariate encryption scheme. We have also updated our survey of the research literature, focusing on matrix multivariate encryption, worst-case-to-average-case reductions for the learning-with-errors problem, and various techniques for cryptanalysis.

In addition, we have engaged with the broader cryptography community. Lily Chen gave an invited talk at this year's PQCrypto conference, and Dustin Moody, Ray Perlner and Daniel Smith-Tone presented their research at that same conference. Lily Chen and Ray Perlner also contributed to a whitepaper on quantum-safe cryptography produced by the European Telecommunications Standards Institute (ETSI). Stephen Jordan taught a short course on quantum algorithms at NIST, and together with Yi-Kai Liu organized the kickoff workshop for the NIST – University of Maryland Joint Center for Quantum Information and Computer Science (QuICS). Finally, this year we hosted visits by Bo-yin Yang and Jintai Ding (on multivariate cryptography) and Vadim Lyubashevsky (on lattice-based cryptography), and we are preparing to host a workshop on post-quantum cryptography (co-located with the PKC conference) in April of 2015.

[1] T. Daniels and D. Smith-Tone, Differential Properties of the HFE Cryptosystem, in *Proceedings of PQ Crypto 2014*, Lecture Notes in Computer Science Volume **8772** (2014), 59-75.

[2] D. Moody, R. Perlner and D. Smith-Tone, An Asymptotically Optimal Structural Attack on the ABC Multivariate Encryption Scheme, in *Proceedings of PQCrypto 2014*, Lecture Notes in Computer Science **8772** (2014), 180-196.

[3] R. Perlner, Optimizing Information Set Decoding Algorithms to Attack Cyclosymmetric MDPC Codes, in *Proceedings of PQCrypto 2014*, Lecture Notes in Computer Science **772** (2014), 220-228.

High-Speed Error Correction Codes for Quantum Key Distribution

Alan Mink (Wagner Resources)
Anastase Nakassis (NIST ITL)

Quantum information science incorporates quantum mechanics into information technology. It is an emerging field thought to have the potential to cause revolutionary advances. One promising early area is quantum cryptography, specifically Quantum Key Distribution (QKD) which is a protocol that uses a pair of unsecured communication channels, a quantum channel and a classical channel, to establish a shared secret between two parties, Alice and Bob. This shared secret is then used to encrypt messages between Bob and Alice. QKD has been proven information theoretically secure, unlike classical key distribution which relies on computational complexity.

There are four stages to the QKD protocol. The first stage involves quantum mechanics; the other three involve classical processing. Stage 1 is the transmission of randomly encoded single photons over a lossy quantum channel to be measured by Bob to form the initial raw random sequence. Stage 2 is where Alice and Bob exchange information over the classical channel to "sift" their bit sequences to achieve a common sequence, but that sequence may have errors. Stage 3 is where Alice and Bob exchange information over the classical channel to reconcile and correct errors between their bit sequences without exposing the value of their bits. Stage 4 is where Alice and Bob privacy amplify their now identical bit sequences through the application of a hash function to eliminate any leaked information, yielding a smaller set of secret bits between Alice and Bob. The last two stages are referred to as post-processing.

There is a large body of information about error correction (EC) codes but QKD presents a different environment than conventional communication. For example, expected QKD error rates (1 % to 11 % vs. 0.1 % or below) are higher, error correction information is sent separately over an error free channel, the amount of information that the EC code leaks about the data must be

minimized and kept below a given limit to extract a secret and quantum data retransmission is not possible.

The research community is pursuing the next generation of QKD systems, ones that can attain higher speeds and longer distances. Our focus is on speed. Moving from the current Mb/s to the Gb/s secure key range will require highly optimized and parallel implementations of QKD post processing algorithms. The one-way EC algorithms, low density parity check (LDPC) and Polar codes tend to be coarse grained computations in that a given data set does not need to communicate until a solution is obtained. Such algorithms are amenable to parallel implementation. Each data set can be assigned to a separate computation engine, which would operate independently in parallel, but each result must be collected sequentially to maintain the required synchronization between Alice and Bob's bits. Also a single communication round trip reduces delays, a benefit as the distance between Alice and Bob increases.

For a LDPC error correction algorithm suited for QKD applications [1], we have obtained a processing rate of up to 200 Mb/s for a GPU implementation. Although in the reasonable QKD operating area the processing rate is in the 27 to 117 Mb/s range. GPU streaming did not provide any throughput increase for our implementation, possibly due to the overhead incurred from the increase in the CPU pthreads required to support GPU streaming and partly due to the overhead incurred by spawning multiple GPU kernels. Also, for streaming, the kernels' execute times are staggered and not completely in parallel. Specific GPU instructions have less performance effect for newer architectures, especially when data items are accessed only once and not reused, as is the case for LDPC, from caches dedicated to those instructions. Thus, the potential for GPUs to provide Gb/s LDPC error correction, although possible, seems less feasible, requiring up to 37 GPU boards using our LDPC implementation vs. the more palatable 10 GPU boards previously speculated.

Polar coding is the most recent scheme in the quest for an error correction code that approaches the Shannon limit, has a simple structure, and admits fast decoders. As such, it is an interesting candidate for QKD. We developed three configurations for adopting Polar codes for the QKD protocol [2]. We also experimented with a current analytical method (Z-values) to design a Polar code (generate the Frozen bit set) and found that it was not very Shannon efficient. Our approach using simulation was marginally better (~5 %) than the Shannon efficiencies cited in the literature and we developed code designs for additional QKD operating points. But such a simulation approach is not scalable, because as N grows the process of finding which bits to freeze takes longer ($N \log N$) and requires more simulation iterations. Furthermore, we found that as N grows, error correction failures increased. We speculate that this is due to floating point precision problems, since probability products have long chains and quickly approach 50 %, a value indicating no information. The difference between 50 % and the computed value can grow asymptotically small very quickly, even with extended precision.

Attached processors, such as FPGAs and GPUs, have proven to provide performance enhancements for implementations of LDPC and Polar error correction algorithms. Our experiments have so far achieved through-put rates up to 200 Mb/s, but not yet 1 Gb/s. Furthermore, our error correction efficiencies obtained for QKD operating points are more in the 40 % to 60 % range above the Shannon limit rather than the 10 % to 20 % range that is preferred. However, we are able to design codes with low failure rates, below 2 %.

[1] A. Mink and A. Nakassis, LDPC Error Correction for Gbit/s QKD, in *Proceedings of the SPIE: Defense Security & Sensing* **9123** (May 2014), 912304-1.

[2] A. Nakassis and A. Mink, Polar Codes in a QKD Environment, in *Proceedings of the SPIE: Defense Security & Sensing* **9123** (May 2014), 912305-1.

Quantum Communication

Xiao Tang
Paulina Kuo
Oliver Slattery
Lijun Ma (Theiss Research)
Weijian Chen (Washington University St. Louis)
Barry Hershman
Alan Mink (Wagner Resources)

Security is a major issue in current communication systems and networks. Quantum communication can provide unconditional security that is guaranteed by the fundamental laws of physics rather than mathematical or algorithmic computational complexity. In addition, quantum communication can transmit quantum states from one location to another, which is an important capability for any quantum information system. Our current quantum research areas include single photon creation, transmission, storage, transduction and detection. These are the fundamental building blocks for the secure quantum communications systems of the future. In such systems, one will encode information into strategically created single photons (flying qubits), transmit them and interface them with an atomic quantum memory (stationary qubits) for storage and processing. A typical example of such a system is a quantum repeater that can connect quantum computers or be used in quantum communication networks of the future.

Previous work. In previous years, the ITL quantum communication team focused on the development of single photon frequency conversion devices including up-

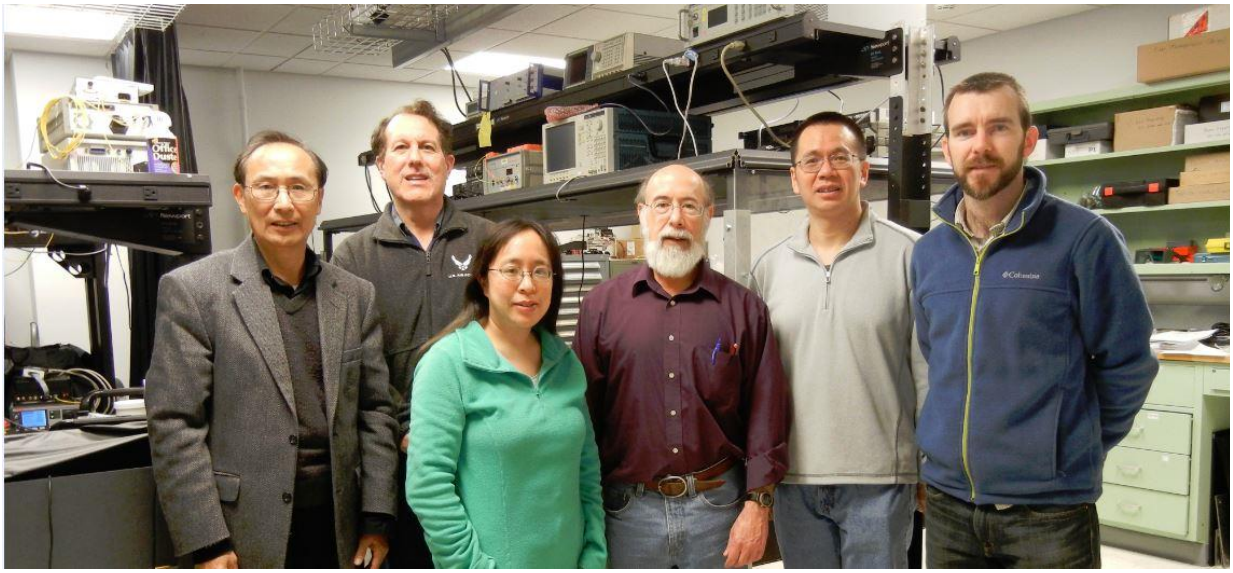

Figure 71. *Quantum communications project team (from left to right): Xiao Tang, Barry Hershman, Paulina Kuo, Alan Mink, Lijun Ma and Oliver Slattery.*

conversion devices and down-conversion single photon sources. An up-conversion device converts single photons from the telecommunication bands (lower energy) to the visible or near visible bands (higher energy) for high efficiency, low noise and high speed detection. A frequency down-conversion device is usually used to generate correlated or entangled single photon pairs. In FY 2013 we undertook work to improve the performance of the devices, and to expand their applications. Four such efforts: "Frequency correlated Bi-photon spectroscopy", "Reducing noise in single-photon-level frequency conversion", "Spectral response of an upconversion detector and spectrometer," and "Two-photon interference with continuous-wave multi-mode coherent light" [1] were completed and published. In addition, the team continuously worked to transfer their technology to US industry for commercialization through the NIST Small Business Innovative Research (SBIR) program.

Recent developments. Based on the previous work, in FY 2014, the team continued the work in the areas of photon down-conversion devices including:

- a photon pair source near 1550 nm for the NIST IMS Quantum Randomness project;
- another photon pair source at 1310 nm and 895 nm with narrow spectral linewidth; and
- a quantum interface based on frequency upconversion device.

In FY 2014, the team also expanded their research areas to include:

- quantum memory based on electromagnetically induced transparency (EIT) in a warm cesium cell;
- a photon pair source based on four-wave mixing using a micro toroid;
- study of single photon emitters in diamond thin-film substrates containing nitrogen vacancies (NV) centers, silicon vacancies (SiV) centers or nickel centers using an in-house built confocal microscope;
- support for the quantum randomness project and research in QKD protocols and standards; and
- technology transfer of a Bragg-grating enhanced single photon source.

Current developments are as follows:

1. The team jointly worked with colleagues in the NIST Physical Measurement Laboratory (PML) on the IMS 2013 project entitled "Quantum Randomness as a Secure Resource". Our responsibility is to develop an entangled photon pair source that is suitable for a loophole-free Bell test. Paulina Kuo leads the design and implementation for the photon pair source at 1535 nm and 1575 nm, which is based on Type II SPDC in a domain-engineered PPLN chip with a pump at 775 nm. The work is continued from last year and significant progress has been achieved this year. Difference frequency generation (DFG, a seeded SPDC) was demonstrated [2]. When the source is completed, it will also be a candidate for use in our future quantum repeater.
2. A non-degenerate photon pair source based on SPDC was developed in the previous years by Oliver Slattery. The source generates photon pairs at 1310 nm and 895 nm that was used to demonstrate Frequency Correlated Bi-Photon Spectroscopy in FY2013. The source can also be used to interface "flying qubits" (1310 nm for long distance transmission) and "stationary qubits" (895nm for storage and processing in

a cesium (Cs) atomic system). In this case, the bandwidth of 895-nm photons must be comparable with that of the cesium D1 line. A common way to solve the problem is to place the device in a cavity which is independently locked to an atomic transition line. The major progress this year is that the cavity is stably locked to the Cs D1 line and multi-mode narrow band SPDC photon pairs were generated. Ongoing work includes full characterization of the SPDC generated pairs and investigating alternative cavity configurations for optimal interfacing with other elements (e.g., quantum memory) of the project.

3. An upconversion device that converts single photons at 1550 nm to 852 nm using a pump at 1892 nm was constructed By Paulina Kuo. This device can be used as a detector for telecom band single photons, as well as a quantum interface to connect photons at 1550 nm (flying qubits) and the cesium atomic D2 transition line at 852 nm (stationary qubits). Currently the device implementation is completed. The conversion efficiency has reached 7 % and the noise level is reduced to an acceptable level.
4. A quantum memory is a device that can store the quantum state of a particle (e.g., a photon) and retrieve it on demand. It is a key component in many quantum information applications such as quantum repeaters. Among the variety of approaches to date, quantum memory based on electromagnetically induced transparency (EIT) stands out as the most promising and suitable approach for our current application. The team had prepared to launch this project some time ago, but were only able to start it in January 2014 when Lijun Ma re-joined the team. The experimental setup for an EIT-based quantum memory system with a warm cesium cell (≈60 ^{o}C) has been successfully completed. With this system, the slow light effect based on EIT was recently demonstrated.
5. In March 2014, the team started a joint research effort with Washington University in St. Louis (WUSTL), to study entangled photon pair generation based on four-wave mixing (FWM). Weijian Chen, a student from WUSTL performed the experiment at NIST using a micro toroid fabricated at WUSTL. The micro toroid is made of silica and forms an optical cavity with extremely high quality factor (Q) value as high as 10^8, which enables us to develop photon pair sources with very narrow bandwidth comparable to that of atomic transition lines. Furthermore, the optical coupling between the toroid and the taped fiber was demonstrated to be nearly lossless by other researchers. This unique feature allows us to develop a photon pair source with a very high so called "heralded efficiency." Thus, this source is a promising candidate for use in loophole-free Bell tests, which is a key component of the NIST IMS Quantum Randomness project. Recently, photon pair generations near 1550 nm from a micro toroid was observed at weak light power levels.
6. Confocal microscopes are commonly used for mapping nano-diamond (ND) samples and for detecting and spectrally characterizing single-photon emitters in ND. In this FY, Oliver Slattery built an in-house confocal microscope in our lab. It has been used to study Nitrogen-Vacancy (NV), Silicon-Vacancy (SiV) and Nickel color centers in ND substrates. Using the confocal microscope, we worked with Howard University and successfully helped them characterize single photon-emitters in their ND samples. We view this confocal microscope as a strong starting point to build the future of quantum information research in ITL.
7. Alan Mink developed hardware (FPGA) and software to support the NIST IMS quantum randomness project in the areas of random number generation and capturing time tagged Bell test data as well as for post-processing of quantum random number generation. He also investigated post-processing (error correction and privacy amplification) for Gb/s QKD using attached processors (e.g., FPGAs, GPUs, etc.) [3, 4] and made contribution to the international effort in the development of QKD standards.
8. During FY 2014, the Phase 1 (proof of principle) of our SBIR to generate narrow band single photon pairs using a Bragg-grating enhanced SPDC chip with a pi-phase shift was successfully completed. Funding for Phase 2 was approved and work on the Phase 2 began toward the end of FY 2014. A successful SBIR will provide a convenient and compact source of narrow-band single photon pairs that will be commercially important in future compact quantum applications. Oliver Slattery leads this effort.

Future research. In FY 2015, based on the work done in the previous year, the team will continue the efforts to improve the performance of the photon sources, the quantum interfaces and the quantum memory. In the coming years, when the performance of these devices reaches the necessary level, we will demonstrate a prototype of a quantum repeater.

[1] Y.-S. Kim, O. Slattery, P. S. Kuo and X. Tang, Two-photon Interference with Continuous-wave Multi-mode Coherent Light, *Optics Express* **22**:3 (2014), 3611-3620.

[2] P. S. Kuo, J. S. Pelc, O. Slattery, L. Ma and X. Tang, Domain-engineered PPLN for Entangled Photon Generation and Other Quantum Information Applications, in *Proceedings of the SPIE* **9136** (2014), 913403.

[3] A. Mink and A. Nakassis, LDPC Error Correction for Gbit/s QKD, in *Proceedings of the SPIE: Defense Security & Sensing* **9123** (May 2014), 912304-1.

[4] A. Nakassis and A. Mink, Polar Codes in a QKD Environment, in *Proceedings of the SPIE: Defense Security & Sensing* **9123** (May 2014), 912305-1.

Joint Center for Quantum Information and Computer Science

Dianne P. O'Leary
Ronald F. Boisvert
Jacob Taylor (NIST PML)
Carl Williams (NIST PML)
Andrew Childs (University of Maryland)

https://quics.umd.edu/

NIST and the University of Maryland (UMD), with the support and participation of the Research Directorate of the National Security Agency/Central Security Service (NSA/CSS), inaugurated a new joint venture, The Joint Center for Quantum Information and Computer Science (QuICS) on October 31, 2014. Scientists at the center will conduct basic research to understand how quantum systems can be effectively used to store, transport and process information.

The new center complements the fundamental quantum research performed at the Joint Quantum Institute (JQI), which was established in 2006 by UMD, NIST and the NSA. Focusing on one of JQI's original objectives, to fully understand quantum information, QuICS will bring together computer scientists—who have expertise in algorithm and computational complexity theory and computer architecture—with quantum information scientists and communications scientists. In particular, the center will bring together researchers from the University of Maryland Institute for Advanced Computer Studies (UMIACS); the UMD Departments of Physics and Computer Science; and the UMD Applied Mathematics and Statistics, and Scientific Computation program with NIST's Information Technology and Physical Measurement Laboratories.

Some of the topics QuICS researchers will initially examine include understanding how quantum mechanics informs computation and communication theories, determining what insights computer science can shed on quantum computing, investigating the consequences of quantum information theory for fundamental physics, and developing practical applications for theoretical advances in quantum computation and communication.

QuICS is also expected to train scientists for future industrial and academic opportunities and provide U.S. industry with cutting-edge research results. By combining the strengths of UMD and NIST, it is hoped that QuICS will become an international center for excellence in quantum computer and information science.

Dianne O'Leary, a Professor of Computer Science at UMD and a long-time faculty appointee in ACMD is a founding Director of QuICS, along with Jacob Taylor of the NIST PML. Andrew Childs, a recent hire at UMD, took over as Co-Director upon O'Leary's recent retirement. Stephen Jordan and Yi-Kai Liu, both of ACMD, have been named QuICS Fellows.

Jordan and Liu were co-organizers of a planning workshop[22] for the new center held on March 31 – April 1, 2014 in College Park. The well-attended event featured talks by Andrew Childs (University of Waterloo), Seth Lloyd (MIT), Scott Aaronson (MIT), Daniel Gottesman (Perimeter Institute), Manny Knill (NIST), and Nicolas Gisin (University of Geneva).

Figure 72. *Officials from the participating organizations gather to sign the MOU establishing QuICS. Front: Willie May, Acing Director of NIST; Mary Ann Rankin, Senior Vice President and Provost of the University of Maryland; Deborah Frinke, Director, NSA Central Security Service. Back: Carl Williams, Chief, NIST Quantum Measurements Division; Amitabh Varshney, Director, UMD Institute of Advanced Computer Studies (UMIACS); Jayanth Banavar, Dean, UMD College of Computer, Mathematical and Natural Sciences; Dianne O'Leary, UMD Dept. of Computer Science and Founding Co-Director of QuICS; Jacob Taylor, NIST Physical Measurement Lab and Founding Co-Director of QuICS; PatricknO'Shea, UMD Vice President and Chief Research Officer; Samir Khuller, Chair, UMD Dept. of Computer Science.*

[22] http://www.nist.gov/itl/math/quics-workshop.cfm

Foundations of Measurement Science for Information Systems

Modern information systems are astounding in their complexity. Software applications are built from thousands of interacting components. Computer networks interconnect millions of independently operating nodes. Large-scale networked applications provide the basis for services of national scope, such as financial transactions and power distribution. In spite of our increasing reliance on such systems, our ability to build far outpaces our ability to secure. Protocols controlling the behavior of individual nodes lead to unexpected macroscopic behavior. Local power anomalies propagate in unexpected ways leading to large-scale outages. Computer system vulnerabilities are exploited in viral attacks resulting in widespread loss of data and system availability. The actual resilience of our critical infrastructure is simply unknown. Measurement science has long provided a basis for the understanding and control of physical systems. Such deep understanding and insight is lacking for complex information systems. We seek to develop the mathematical foundations needed for a true measurement science for complex networked information systems.

Modeling of Kinetic-based Micro Energy Harvesters for Wearable and Implantable Sensors

Kamran Sayrafian
Mehdi Dadfarnia (NIST EL)
Antonio Possolo (NIST ITL)
Paul Mitcheson (Imperial College, UK)

See page 24.

An Algebraic Formulation for the Analysis and Visualization of Network Graphs

Roldan Pozo

Characterizing the topological structure of large graphs remains an important problem in network science. While it is straightforward to visualize small networks of hundreds or a few thousands of vertices and edges using conventional graph visualization packages, attempting to render large real networks is nearly impossible. This is particularly true for information networks and social networks, where the graph sizes number into the millions and billions. And with the amount of data being generated and gathered from large social media sites ever increasing, the challenge of characterizing larger and larger networks is only getting harder.

Conventional algorithms for graph visualization render such networks as a solid blot of color from which is difficult to discern meaningful information. This difficulty is strongly influenced by the presence of high-degree nodes (hubs) which entangle many parts of the graph with itself, together with the sheer volume of nodes and edges which makes rendering into a reasonable image size for viewing and printing impractical.

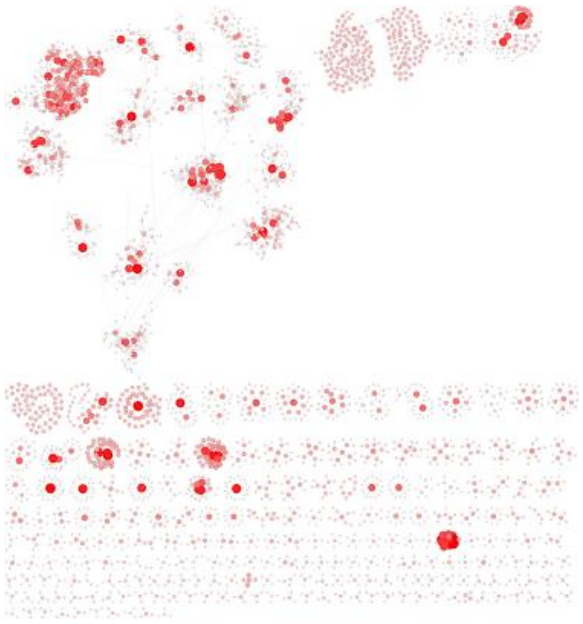

Figure 73. *Non-trivial components of math.nist.gov web graph, restricted to nodes with combined degree less than or equal to 25.(math_d4_25.png)*

An alternate approach is to visualize important network properties, rather than the actual network itself. These *network portraits* attempt to capture interesting attributes of a large graph, such as degree distribution, or its connective properties. In this research area, we focus on a particular type of information: the distribution of "fringe" communities: small connected components of a graph, in the absence of high-degree hubs. In a social science context, for example, they represent independent or rogue groups, highly connected amongst themselves, but which are often lost with the inclusion of more popular nodes.

The Q-matrix of a network, in its fundamental formation, is a connected component size distribution matrix for a series of degree-limited subgraphs of the original network (or weakly-connected component for

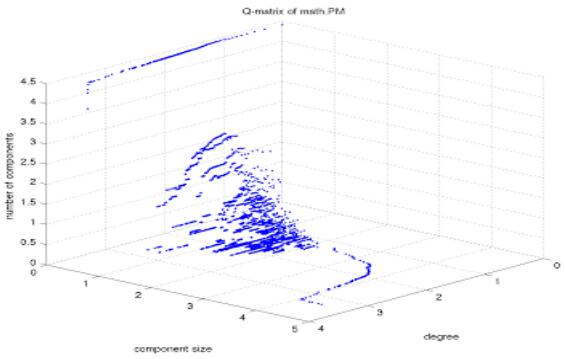

Figure 74. *Q-matrix plot of math.nist.gov webgraph (29K vertices, 62K edges) showing the component size distribution of degree-limited subgraphs.*

directed networks.) Thus, $Q(i,j)$ is the number of connected components of size j in a subgraph where the maximum degree is equal to or less than i.

Consider, for example, a Web graph, where nodes are individual pages, and edges are directed hyperlinks between two web pages. Figure 73, for example, illustrates connected components of the math.nist.gov Web graph, where nodes of degree greater than 25 have been removed.

The image reveals various structures: e.g., ladders, star, and cluster patterns representing tightly coupled webpages. These form the nucleus of fringe communities of web pages, and by varying the degree parameter we can direct the size and granularity of groups revealed. As the degree threshold is increased from 1 to the largest degree in the original graph, we can form a connected component size distribution, which can be encoded as a row of a matrix. This sparse matrix may still be too large to view directly, but can be compactly rendered by projecting its nonzero values onto the z-axis and displaying it as a three-dimensional structure, as show in Figure 74.

The Q-matrix of a graph can be considered as a generalization of its degree-distribution. However, it encodes other properties, such as the formation and growth of its giant component, its connected subparts, as well as its size parameters. In fact, common network metrics (degree distribution, number of connected components, number of vertices and edges) can be extracted from the Q-matrix using simple linear algebra operations.

Among the interesting characteristics of the Q-matrix formulation is that network graphs from similar application areas (e.g. social networks, email networks, web graphs, peer-to-peer networks, road networks, citation graphs) share similar visual characteristics, creating a potential framework for network identification and classification. Indeed, we have used the Q-matrix formulation to generate meaningful thumbnail images for network data collections. The computation of the Q-matrix is relatively efficient—graphs with millions of vertices and edges can be processed in < 60 sec.

This year we created new optimized algorithms in compiled C++ that are both efficient in space and computational time, allowing us to compute Q-matrices for networks with over 1 billion edges in less than one hour on common desktop computers. These large datasets allow us to see finer complexity patterns not present in smaller sample sets.

We are also extending research of the Q-matrix theory to generalized vertex orderings beyond that of node degree, such as PageRank, eigenvalue centrality, betweeness centrality, and k-core numbers. We are exploring alternate metrics for network communities (such as the alignment of subgraph S, which compares the sparsity of S to the number of its distinct neighbors). Furthermore, we are investigating the use of Q-matrix analysis to specific problems in the area of microbiology (genomic networks) and economics (financial market networks).

[1] R. Pozo, Q-Matrix: An Algebraic Formulation for the Analysis and Visual Characterization of Network Graphs, in review.

Measuring Networks: Monte Carlo Sampling to Approximate the Chromatic Polynomial

Yvonne Kemper
Isabel Beichl

At its heart, a network (or graph) is a collection of points (vertices) connected by lines (edges). Networks can be used to represent a variety of physical and abstract objects, and measuring characteristics of networks allows researchers to uncover and understand information encoded in the network, as well as study the systems it represents.

One example of this relates to a particular labeling of a graph G called a coloring: a proper k-coloring of the graph is an assignment of the numbers 1, 2 …, k to the vertices so that vertices connected by an edge receive different numbers. Amazingly, there exists a polynomial, the chromatic polynomial, $X_G(x)$, that evaluates to the number of k-colorings when $x=k$. The chromatic polynomial (as well as its largest integral root) has received much attention as a result of the now-resolved four-color problem, but $X_G(x)$ is also central in multiple applications, such as scheduling and assignment problems and the q-state Potts model in statistical physics. Scheduling problems occur in a variety of contexts, from algorithm design to factory procedures, and with an approximation of $X_G(x)$ it is possible to estimate the number of possible

solutions given specific parameters. For the latter, the relationship between $X_G(x)$ and the Potts model connects statistical mechanics and graph theory, allowing researchers to study phenomena such as the behavior of ferromagnets. The complex roots of $X_G(x)$ are particularly useful in this area of research.

Unfortunately, computing $X_G(x)$ for a general graph G is known to be #*P*-hard, and deciding whether or not a graph is k-colorable is NP-hard; the best known algorithm for computing $X_G(x)$ for an arbitrary graph G with n vertices has complexity $O(2^n n^{O(1)})$.

Approximation methods, however, have received little attention. The goal of these methods is to provide an evaluation close to the true answer in a fraction of the time. In the last year, we have adapted a Monte Carlo method of sequential importance sampling to be the basis of two approximation algorithms. After implementing our algorithms in both Matlab and C, we were able to compute approximations of $X_G(x)$ for graphs of much larger size than previously possible. Before, the best exact algorithms were limited to $2|E(G)| + |V(G)| < 950$ and $|V(G)| < 65$, where $|E(G)|$ is the number of edges, and $|V(G)|$ is the number of vertices. Our largest so far had 500 vertices and 62,323 edges, and larger computations are possible. We have shown our methods to have small relative error in the cases where we were able to compare to the exact polynomial. Moreover, as the expected value of our approximation is the precise value, we may further reduce error by performing further computations.

[1] Y. Kemper and I. Beichl, Monte Carlo Methods to Approximate the Chromatic Polynomial, in preparation.

An Improved Feedback Vertex Set Heuristic

James M. Shook
Isabel Beichl

To recover from deadlock it is sometimes necessary to end processes so that resources can be made available. Deadlock recovery has applications in operating systems, database systems and VLSI chip design. One would hope to end the fewest possible processes. To decide which processes to end, it is necessary to understand the relationship between processes. This can be represented by a directed graph called a dependence graph. If the dependence graph has a cycle, then deadlock has occurred and we need to end a process on that cycle. A feedback vertex set (FVS) is a set of vertices or processes that when removed from the dependence graph leave the resulting graph without cycles. Thus, the FVS gives the smallest number of processes to end to remve all deadlocks. Unfortunately, finding the smallest FVS has been shown to be NP-hard [2]. Thus, research has focused on finding an efficient heuristic for the FVS problem.

In [3] the authors presented a method that finds a FVS, F, with a running time of $O(|F| n^{2.376})$, where n is the number of nodes in the network and $|F|$ is the size of the FVS. Evidence was given that their method was superior to existing heuristics. Relating an observation made in [1], to disjoint cycle unions, we designed a method that has a running time of $O(|F| \log(n) n^2)$. For comparison we tested each algorithm on Erdös-Rényi random graphs and random k-regular graphs of various orders. Our method found smaller sets than the method in [3]. We also found that our method approximated the actual size of a minimum FVS well. A detailed analysis of our work has been submitted for publication.

[1] I. Beichl and F. Sullivan, Approximating the Permanent via Importance Sampling with Application to the Dimer Covering Problem, *Journal of Computational Physics* **149**:1 (1999), 128-147.

[2] R. Karp, Reducibility among Combinatorial Problems, in *Complexity of Computer Computations* (R. Miller and J. Thatcher, eds.), Plenum Press, 1972, 85-103.

[3] M. Lemaic and E. Speckenmeyer, Markov-Chain-Based Heuristics for the Minimum Feedback Vertex Set Problem, Computer Science Technical Report, University of Cologne, 2009.

Extremal Theorems for Degree Sequence Packing and the 2-Color Discrete Tomography Problem

James Shook
Jennifer Diemunsch (University of Colorado Denver)
Michael J. Ferrara (University of Colorado Denver)
Sogol Jahanbekam (University of Colorado Denver)

Discrete tomography is a form of image processing in which discrete objects are reconstructed using data acquired from low-dimensional projections. Discrete tomography has uses in medical imaging, electron microscopy, and materials science. In the k-color discrete tomography problem the goal is to color the entries of an $m \times n$ matrix using k colors so that each row and column receive a prescribed number of entries of each color. This problem is equivalent to packing, which we explain below, for degree sequences of k bipartite graphs with parts of sizes m and n.

We approached the problem by proving more general questions in graph packing. A sequence $\pi = (d_1, \ldots, d_n)$ is graphic if there is a simple graph G with vertex set $(v_1, \ldots, v_n)$ such that the degree v_i is d_i. We say that graphic sequences $\pi_1 = (d_1^{(1)}, \ldots, d_n^{(1)})$ and $\pi_2 = (d_1^{(2)}, \ldots, d_n^{(2)})$ *pack* if there exist edge-disjoint n-vertex graphs G_1 and G_2 such that for $j \in \{1, 2\}$, $d_{Gj}(v_i) = d_i^{(j)}$, for all $\in \{1,$

…, n}. We proved several extremal degree sequence packing theorems that parallel central results and open problems from the graph packing literature. Specifically, the main result of our work implies a degree sequence packing analogue to the widely studied Bollobás-Eldridge-Catlin graph packing conjecture found in [1] and, independently, in [2], along with a degree sequence version of the classical graph packing theorem of Sauer and Spencer found in [3]. We modified our techniques to prove several Sauer-Spencer-type theorems that have direct applications to the 2-color discrete tomography problem.

[1] B. Bollobás and S.E. Eldridge, Packings of Graphs and Applications to Computational Complexity, *Journal of Combinatorial Theory Series B* **25** (1978), 105-124.

[2] P. Catlin, Embedding Subgraphs and Coloring Graphs under Extremal Degree Conditions, Ph.D. Thesis, Ohio State University, 1976.

[3] N. Sauer and J. Spencer, Edge Disjoint Placement of Graphs, *Journal of Combinatorial Theory Series B* **25** (1978), 295-302.

Fast Sequential Creation of Random Graphs

Brian Cloteaux

Creating random degree-based graph models has become an important first step in creating a model of a network. Before about seven years ago, the only way to create a random model with a given a degree sequence would be to create an instance by the Havel-Hakimi algorithm and then do a walk on the Markov chain (MC) of edge switches in the graph. This method is fast, but little is known about bounds on the mixing time of this walk. In general, based on some conjectures made about the mixing-time time of these chains, the normal run-time is $O(m \log n)$, where n is the number of vertices and m is the number of edges. In addition, the algorithm is difficult to modify for creating graphs with given characteristics.

In 2010 Blitzstein and Diaconis [1] published a sequential importance sampling (SIS) method for creating random graphs with a given degree distribution. This algorithm allows for much more flexibility in the characteristics of the random graphs created, but unfortunately, the run-time of their method is much slower than the MC method. Former NIST NRC Postoctoral Associate Lizz Moseman [2] showed that the Blitzstein-Diaconis (BD) algorithm run time could be reduced from $O(mn^2)$ to $O(mn)$, but this still does not match the time of the MC algorithm.

We have examined ways of improving the BD algorithm by looking at the structures of edges that must be avoided at each step of the BD algorithm. For a given degree sequence d, a forced edge is an edge that must appear in every realization of d, while a forbidden edge is an edge that cannot appear in any realization of d. Using these definitions, we can informally describe the BD algorithm as randomly choosing edges that are not in the forbidden set at each step. We examined the structure of these sets of forced and forbidden edges in order to speed up checking for them during the BD algorithm, and proved several results including showing the structure of these forced and forbidden sets. In Figure 75, we show the increase in probability for finding possible graphical edge choices when we account for forbidden and forced edges.

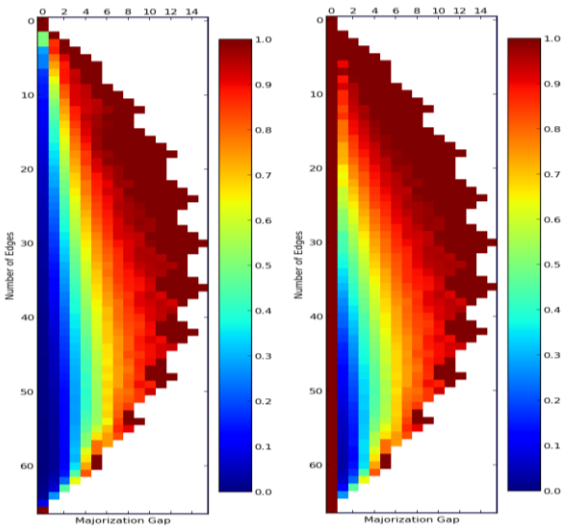

Figure 75. *The increase in probability for finding possible graphical edge choices when we account for forbidden and forced edges.*

Using these results, we have created two new versions of the BD algorithm, whose speeds approach that of the MC algorithm. We have also introduced a completely new algorithm for the sequential creation of graphs. This algorithm differs from BD algorithm because it chooses a set of edges for each step, but allows for much quicker edge acceptance times. This algorithm essentially matches the MC run-time, but still allows for the advantages of SIS approaches.

Anecdotally, we can understand the speed-up of these new algorithms from a case-study. Several years ago, we created a series of models of the autonomous system (AS) topology of the internet using a C++ implementation of the original BD code. This code took around two hours to create each model. Using the new BD algorithm, we were able to create instances from the same degree sequence in about 16 seconds. In fact, we were able to run statistical tests on the algorithm by creating over 45,000 random instances with many of these instances being larger than the AS topology degree sequence. This would have been impossible for the original BD algorithm.

[1] J. Blitzstein and P. Diaconis, A Sequential Importance Sampling Algorithm for Generating Random Graphs with Prescribed Degrees, *Internet Mathematics* **6**:4 (2010), 489.

[2] E. Moseman, Improving the Computational Efficiency of the Blitzstein Diaconis Algorithm for Generating Random Graphs of Prescribed Degree, unpublished manuscript, 2011.

Identifying Important Nodes in a Network for Rapid Communication

Fern Y. Hunt

We are studying the problem of effective communication in a network of nodes that only communicate with their neighbors. Given the pattern of communication we seek to identify a set of informed nodes of predetermined cardinality that will enable the fastest spread of information in the network. One can also seek the solution to a similar problem: find the set of informed nodes that will maximize the number of contacted nodes in some period of time. The motivation for this research is the control of large networks when the resources for direct centralized communication are limited. Thus there are potential applications, for example, to the design of sensor networks for the detection of breakdown in energy and water supply systems. There are also applications to the propagation of influence in social networks, as well as the study of gene regulatory networks.

Our mathematical approach to the fastest communication problem is to define a set function related to the time it takes for uninformed nodes to receive information from a selected set of informed nodes. The function becomes the objective function which must be minimized over the class of all subsets of nodes of maximum size *K*. This is a classic problem in combinatorial optimization and early, significant work by Nemhauser et al. [1], established important results when the objective function is a bounded submodular (or as in our case supermodular) function. Their work, and the extensive research that followed, showed that the simple intuitive approach of constructing an optimal *K* element set by first identifying the best one element set and then successively adding an element that creates the best new set containing its predecessor, results in an approximation to the optimization problem that is guaranteed to be within 1-1/*e* of optimal. Nevertheless the problem is NP-hard and the preponderance of current theoretical research shows that the ratio cannot be improved by much given the problem as stated.

In the past year we continued our reformulation of the problem so that information about the topology of the network graph and the structure of the class of optimal sets is employed in its solution. Originally the solution was required to be a subset of cardinality *K* or less (that is, an element of a matroid). In our approach sets are constrained to lie in a much smaller class of optimal and "nearly" optimal subsets (see [2] for details). This class is closed under addition of elements (as occurs in the greedy algorithm), deletion of elements (as in the backward greedy algorithm) and exchange of elements in sets of equal cardinality (as in a local search). We also stated sufficient conditions on the network graph for the existence of a greedoid containing optimal and near optimal sets—a more general set system than the original matroid and a concept better suited to the order dependence that we believe is intrinsic to the problem. Within this framework we are able to study different schemes for the stepwise construction of approximations. In addition to work on the greedoid, we also implemented an approximation method based on sets in the greedoid that are subsets of a vertex cover of the network graph. Our new method is based on greedy extensions of the smallest sized optimal and "nearly" optimal sets in a greedoid. Empirically we found the approximations to be better than the (1-1/*e*) bound of Nemhauser et al. and others, and often are an exact solution. When the greedy algorithm approximation is itself the exact solution, it is a special case of our greedy extension approach.

Pre-processing is needed to compute the optimal and "near" optimal subsets in the greedoid. If N is the number of nodes, and m is the size of the smallest optimal or near optimal set then we conjecture that the method has complexity $\mathrm{O}(N^m) \cdot poly(N)$ where $poly(N)$ is polynomial in N. The next question, of course, is why and under what conditions do these methods work? Intuitively, restricting the search space to optimal and "nearly" optimal sets excludes poorly performing sets, including bad starting points for a stepwise algorithm. The search for a deeper and more rigorous understanding is currently underway. Recent research advances by Filmus and Ward have been made using the concept of curvature for submodular and supermodular functions in the matroid case [3]. We are currently investigating curvature in our setting with a view toward obtaining bounds on the performance of our proposed method.

[1] G. Nemhauser, L. A. Wolsey and M. L. Fisher, An Analysis of Approximations for Maximizing Submodular Set Function – I, *Mathematical Programming* **14** (1978), 553-574.

[2] F. Y. Hunt, The Structure of Optimal and Near Optimal Target Sets in Consensus Models, NIST Special Publication 500-303, August 2014.

[3] Y. Filmus and J. Ward, Tight Bounds for Submodular and Supermodular Functions with Bounded Curvature, arXiv:1204.4526.

Measurement Science for Systemic Risks in Critical Infrastructures

Vladimir Marbukh

Technological advances combined with pressures of economic globalization have produced highly interconnected national and world-wide infrastructures, which have become essential for U.S. industrial competitiveness and economic security. In communication networks, cloud computing architecture, power grid, financial networks, supply chains, etc., interconnectivity makes resource sharing possible, creating load balancing capabilities at the cost of systemic risks of cascading failures/overload, virus propagation, and misuse of the additional resource access capabilities by strategic or malicious participants. We have already experienced significant strategic and economic losses due to these negative consequences. Interconnectivity, and the resulting problems, will grow with time unless serious measures are taken to mitigate the relevant risks

Paper [1] attempts to quantify systemic risk of the cloud computing infrastructure. The economic and convenience advantages of the shared cloud computing infrastructure as compared to the conventional model of owning computer resources are unquestionable. Among the economic advantages are elimination of the fixed cost and reduction of the marginal cost for users of cloud computing infrastructure due to the benefits of dynamic load balancing and the economy of scale. Results in [1] indicate that in a practically relevant parameter region, the benefits of dynamic load balancing in the "normal operating regime" come with risks of the system abruptly transitioning to a "persistently congested mode" through the process of cascading overload.

Paper [1] can be viewed as a first step in the direction of a paradigm shift in cloud design and operation: from maximizing economic benefits to identifying and managing the relevant risk/benefit tradeoffs. In particular, [1] demonstrates that economic pressures push the system to the stability boundary of the normal operating regime, making the tradeoff between "normal system performance" and the systemic risk of transitioning to a congested regime more acute. In [1] we also suggest using the Perron-Frobenius eigenvalue of the "reduced" system performance model as a measure of the systemic risk of cascading overload. Applicability of the Perron-Frobenius theory in systems with dynamic resource sharing is due to the positive feedback in the system component overload, which can spill over to the "neighboring" components.

Presentation [2] discussed a general form of systemic risk of cascading overload due to a "non-native" service being less efficient than the "native" service, e.g., as a result of an additional cost of accessing distant resources. Consistent with [1], analysis [2] indicates

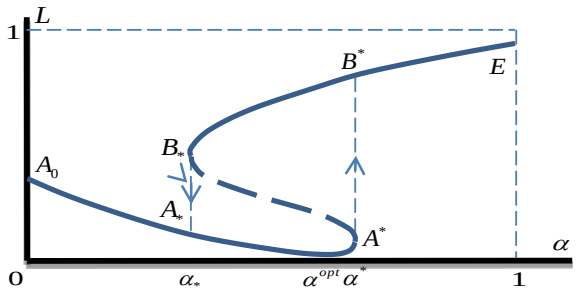

Figure 76. *Portion of lost revenue vs. level of resource sharing.*

that the systemic risk/performance tradeoff may be a result of coexistence of metastable, i.e., persistent, normal and congested system states: resource sharing is beneficial or harmful depending on the system being in the normal or congested metastable state. Moreover, peak system performance in the normal metastable state is achieved close to the stability boundary of the state.

Some of these findings are illustrated in Figure 76, which sketches a portion of system lost revenue L as a function of the level of resource sharing α.

The optimal level of resource sharing $\alpha = \alpha^{\text{opt}}$ is typically unacceptably close to the stability boundary $\alpha = \alpha^*$ of the normal metastable state represented by curve $A_0A_*A^*$. The systemic risk of a discontinuous phase transition A^*B^* to the "congested" metastable state, represented by curve B_*B^*E, can be reduced by lowering α below α^{opt} at the cost of sacrificing "normal" system performance.

Managing this systemic risk/performance tradeoff is a challenging problem due to the difficulty of real-time monitoring of the system stability margin and the tendency of strategic system components to drive the system beyond the stability boundary due to positive externalities. Since systemic risk is an inherently macroscopic phenomenon, the proposed approach is based on the reduced, i.e., macroscopic, system description in the subspace of the eigenvectors corresponding to the largest eigenvalues of the linearized system dynamic. In [3] we suggest that a similar systemic risk/performance tradeoff may be essential in software-defined networking infrastructures.

Presentations [4-5] discuss the risk of cascading failures described by the Susceptible-Infected-Susceptible (SIS) model. Presentation [4] suggests that the recently discovered phenomenon of eigenvector centrality localization may be used for characterization of the hierarchy of important infection spreaders in large-scale networks. This characterization may help with prediction and mitigation of the impact of persistent infections through regulations or incentives. In [5] we propose a tractable model describing the interplay between infection propagation on the network and the evolution of the network topology. The model assumes that infection

propagation follows a Susceptible-Infected-Susceptible (SIS) process with controlled node recovery rates and network topology evolution follows a preferential rewiring process.

[1] V. Marbukh, On Systemic Risk in the Cloud Computing Model, in *Proceedings of the 26th International Teletraffic Congress* (ITC 26), Karlskrona, Sweden, 2014.

[2] V. Marbukh, "Systemic Risk/Benefits of Interconnectivity due to Metastability," NetSci 2014, Berkeley, CA, 2014.

[3] V. Marbukh, "SDN: Systemic Risks due to Dynamic Load Balancing," Software Defined Networking Research Group, Internet Research Task Force, IETF 91, Honolulu, HI, 2014.

[4] V. Marbukh, "Eigenvector Centrality Localization and Hierarchy of Important Spreaders in Large-Scale Networks," NetSci 2014, Berkeley, CA, 2014.

[5] V. Marbukh, "Network Evolution by Preferential Rewiring with Infection Risk Mitigation: Work in Progress," Workshop on Dynamics Of and On Networks, Santa Fe Institute, Santa Fe, NM 2014.

Security of Complex, Interdependent Systems

Assane Gueye (University of Maryland)
Richard J. La (University of Maryland)

Understanding the security of large-scale, complex interconnected networks and systems has emerged as one of the key challenges information system engineers face today. Studying the system-level security of such networks or systems is hampered by the fact that security measures adopted by various agents or organizations or lack thereof produce network externalities on other organizations, resulting in so-called *interdependent security* (IDS).

In the past, there has been much research in studying how the infection of a few agents (e.g., disease outbreaks or epidemics and spread of computer viruses or malware) may spread to a large number of other agents through networks (e.g., computer networks or social networks). Most existing studies focus on scenarios where the agents are passive in that they do not take proactive measures to protect themselves based on perceived risks and threats. In many scenarios of interest, e.g., cybersecurity and disease outbreaks, however, agents can employ various measures to lower the likelihood of getting infected, often by their neighbors.

We take a first step towards correcting this current state of affairs and examine the scenarios where the nodes are strategic entities that are interested in optimizing their own objectives. We model the interdependence in security among agents, which is brought on by network externalities, using a dependency graph, in which the nodes/vertices are the organizations and an edge between two vertices indicates a dependence/relation between them. The goal of this project is to understand how the underlying network structure and properties affect the choices made by strategic agents and the resulting overall network-level security.

We focus on two different scenarios. In the first scenario [1, 2], each node has three available choices – (i) protect itself, (ii) purchase insurance for informational or financial losses, or (iii) take no protective measure. Due to the network externalities or interdependence of security, the choices made by the nodes are coupled. Using a population game model, we investigate how network properties, e.g., node degree distributions, and other system parameters, e.g., infection propagation rate, shape the choices of nodes and ensuing loss of efficiency (measured using the price of anarchy (PoA)) at Nash equilibria of population games.

In the second scenario [3], we generalize the previous model and allow nodes to choose from M (M>1) different protection levels with increasing security investment costs. In addition, they can also purchase insurance and the insurance premium depends on the protection level of the insured. Finally, the insurers may require a certain minimum level of protection before agreeing to insure organizations. We extend the key findings we obtained using the first model to these more general cases.

One of our key findings is that, as the weighted node degree distribution (where the weights are given by node degrees) becomes stochastically larger, (a) a node with a fixed degree tends to invest less in security measures, (b) somewhat surprisingly, the risk or threat seen from a neighbor diminishes, and (c) the probability that the infection of a few nodes triggers a cascade of infection, i.e., a large number of nodes become infected, climbs. These findings suggest that when the weighted node degree distribution is larger, while a node with a fixed degree may feel that the overall network-level security is better from finding (b), the network-level security measured by the probability of global cascade in fact deteriorates from finding (c). Furthermore, the PoA tends to increase with the weighted node degree distribution, indicating that the overall network-level security suffers in comparison to system optimum.

We are currently investigating how other network properties, such as network assortativity, affect the network-level security when agents are strategic [4]. Our preliminary results suggest that as the network becomes more assortative, i.e., nodes tend to be connected to other nodes with similar degrees, the overall security investments fall and the network-level security degrades. This observation reveals that it is likely more challenging to stop an epidemic in a community, whereas

preventing a wide spread of computer malwares and viruses may be easier than previously thought.

[1] R. J. La, Role of Network Topology in Cybersecurity, in *Proceedings of IEEE Conference on Decision and Control* (CDC), Los Angeles, CA, December 2014.

[2] R. J. La, Interdependent Security with Strategic Agents and Global Cascades, *IEEE/ACM Transactions on Networking*, to appear.

[3] R. J. La, Effects of Degree Distributions on Network Security—Population Game Model, in review.

[4] A. Gueye and R. J. La, "Influence of Assortativity on Network Security," Poster, NetSci Workshop, Berkeley, CA, June 2014.

This research was supported by NIST Cooperative Agreements 70NANB13H012 and 70NANB14H015.

Graph Theoretic Applications to Network Security and Security Metrics

Assane Gueye (University of Maryland)
Richard J. La (University of Maryland)
Peter Mell (NIST ITL)
Rich Harang (Army Research Laboratory)

In this project, we first studied the strength of interconnectivity between countries in the Internet, using the connectivity among autonomous domains (ASs) obtained by analysis of data available from (CAIDA) over several years [1]. Secondly, we examined how difficult it is to (i) stop the flow of information between two countries, (ii) isolate a given set of countries, or (iii) break up the Internet into a group of (disconnected) components.

To answer these questions, we created an interconnectivity map of the worldwide Internet routing infrastructure at a country level on the basis of AS-level information after filtering the CAIDA data sets. We first demonstrated that the interconnectivity among countries has increased over the years during which measurements had been taken. Then, we examined how groups of countries may use the ASs under their control/regulation to filter out the traffic of other countries (or to block entire routes). Our analysis indicates that the ability of countries to disrupt the connectivity between countries has diminished significantly from 2008 to 2013. However, we showed that the majority of the gains in robustness, i.e., increase in connectivity, goes to countries that had already displayed significant robustness to the types of attacks that we considered. The countries that had displayed higher vulnerability to such attacks did not experience a significant improvement in resilience over the same time period considered in the analysis.

In the second part of the project, we investigated the problem of creating defensive choke points within networks, and defining metrics for network resilience against attack propagation. Securely configured IPv6 networks can be made resistant to network scanning and other forms of target acquisition, forcing attackers to propagate through a network only by following existing benign communication paths. If heightened security measures are taken to protect a select group of hosts, the layer 4 network communication graph (not the physical or logical network graph) can be broken into small isolated clusters connected by a few highly protected "checkpoints'. Attackers attempting to propagate through the network will then be required to penetrate one or more checkpoints or else be limited to a small set of targets. The checkpoints increase the chance of detection and/or limit an attacker's ability to propagate through the network (depending upon the nature of the heightened security capability).

Optimal placement of checkpoints requires solving the NP-complete vertex separator problem, and so we approximated optimal solutions via a suite of heuristics. We empirically tested our approach and algorithms on data from an operational network with over 15,509 nodes and discovered that heightened security measures are only needed on 100 nodes (< 1 %) to restrict attacker propagation to no more than 15 % of the network. This enables a novel defense-in-depth layer that complements traditional security approaches. It can be enhanced with a moving defense model where the special security measures migrate between nodes following locally optimal configurations, causing uncertainty to the attackers as to where the checkpoints are deployed, and enabling defensive agility as network communication graphs change over time.

We are currently investigating how one can take into account the underlying communication graph properties in order to design more efficient algorithms for identifying effective checkpoints. In particular, we are interested in leveraging the existing literature on network science and epidemiology.

[1] P. Mell, R. Harang and A. Gueye, The Resilience of the Internet to Colluding Country Induced Connectivity Disruptions, in review.

[2] Assane Gueye, P. Mell, R. Harang and R. J. La, Moving Target Defenses with Security Checkpoints in IPv6 Networks, in preparation.

This research was supported by NIST Cooperative Agreements 70NANB13H012 and 70NANB14H015.

Uncoordinated Scheduling Strategies for Interference Mitigation across Body Area Networks

Martina Barbi (University of Bologna)
Kamran Sayrafian
Vladimir Marbukh
John Hagedorn
Judith Terrill

A Body Area Network (BAN) is a radio standard for wireless connectivity of wearable and implantable sensor nodes that are located inside or in proximity to the human body. Many applications of BANs (e.g. physiological monitoring) require reliable communication of information between the sensor nodes and their controller. As there are currently no coordinating mechanisms among multiple co-located BANs, interference caused by co-channel transmission in adjacent BANs could impact the reliability and in general quality of the service experienced by a receiver node within an individual BAN. Advanced signal processing using interference cancellation techniques has been proposed to minimize the impact of this interference. However, there are two main problems with such techniques especially when it comes to their application in BAN. First is the high complexity of the receiver which makes the implementation of interference cancellation impractical unless the number of nodes is very small. Complexity is especially a critical issue for nodes in body area networks. As they mainly rely on battery power, prolonging the lifetime of these nodes is of prime importance.

The second problem is that some interference cancellation schemes require knowledge of the channel condition (such as attenuation, phase, and delay) between each of the interferers and the receiver. Obtaining accurate estimates of the channel condition is extremely difficult for body area networks. Transmission power control has also been considered as an alternative for individual BANs to maintain reliable operation even in high interference environments. However, the complexity of the BAN channel environment and other stability issues indicate that power control alone may not be able to achieve an acceptable system performance.

Due to the possible inefficiency of power control and the stated problems with interference cancellation, interference mitigation techniques can be an attractive alternative, particularly in an environment with high interference level. These techniques can be classified into two groups: un-coordinated and coordinated mitigation. The coordinated schemes will require appropriate protocols for inter-BAN information exchange, and are envisioned to be more sophisticated. However, they might result in higher overall performance compared to uncoordinated schemes. The uncoordinated schemes require no inter-BAN communication and could result in simple implementation in the current IEEE802.15.6 international standard in BAN. Link layer adaptation is an example of an uncoordinated approach that can be used as an interference mitigation technique. Although simple to implement, the trade-off for acquiring reliable simultaneous transmission in multiple BAN scenarios is lower transmission rates.

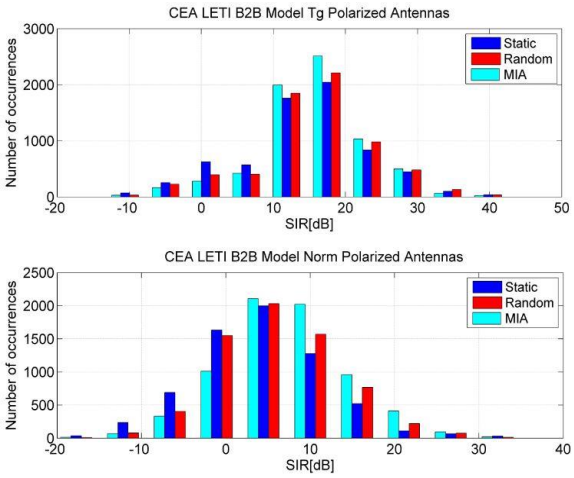

Figure 77. *Histogram of the experienced SIR for the random scenario.*

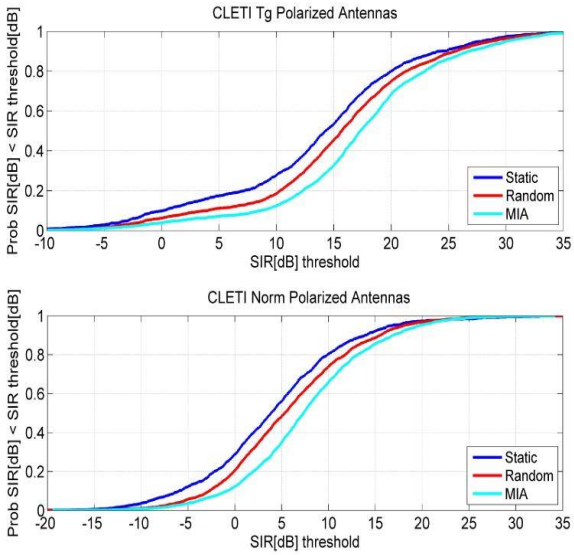

Figure 78. *CDF of the experienced SIR.*

In this project, we propose smart scheduling algorithms (i.e., slot assignment) as another alternative to mitigate inter-BAN interference. Assuming a TDMA-based MAC, the idea is to distribute simultaneous (i.e., colliding) multi-BAN transmissions across several time slots without any explicit coordination across interfering BANs. We assume that each receiver node of a BAN can measure the total interference that is being experienced at each time slot. The decision of which time slot to use

in the next transmission frame, is the key to avoid potential interference by other BANs. Taking advantage of possible correlation in the propagation channel, multiple BANs can participate in judiciously selecting appropriate slot assignment (i.e., a transmission schedule) in consecutive frames in order to avoid time-slots with high interference. This setting matches a game theory framework as multiple BANs are competing with each other to find the best transmission slot assignment that incurs the lowest interference for their target receiver.

We have proposed two simple algorithms, namely Random Assignment and Minimum Interference Allocation (MIA) to achieve the above objective. Details of these algorithms can be found in [1, 2, 3]. Figure 77 shows the resulting histogram of the Signal-to-Interference Ratios (SIR) experienced by the nodes in a system comprised of eight BANs each having three sensors. The improvement in the experienced SIRs is clearly visible under MIA or Random assignments. The platform that has been used to obtain these results has been described in [4]. Figure 77 shows results for both tangentially and normally polarized antennas used by the transmitting nodes. The eight BANs in this scenario are assumed to be moving randomly in an 8×8 m^2 room.

Figure 78 displays the cumulative distribution functions (CDF) of the experienced SIR for the above scenario. These graphs show the improvement in the system performance in a more tangible way. If the horizontal access is perceived as minimum required SIR, then the vertical access represents the link outage probability. The MIA algorithm reduces the outage probability by intelligently distributing and re-allocating simultaneous and interfering transmissions in non- or less-interfering time slots.

The results of our proposed uncoordinated slot assignment strategies show the performance improvement in mitigating cross-interference among uncoordinated BANs. Although the current version of the BAN radio interface standard (i.e., IEEE802.15.6) does not have any provision to support inter-BAN coordination, it is conceivable that any coordination might result in better performance; of course, as a trade-off with more complexity. More detailed studies and experiments are needed to determine the feasibility and effectiveness of each strategy in mitigating potential interference. We also plan to continue this study for other access protocols (e.g., CSMA) as well.

[1] V. Marbukh, K. Sayrafian and M. Alasti, Link-layer Adaptation in Body Area Networks: Balancing Reliability and Longevity, in *Proceedings the 24th Annual IEEE International Symposium on Personal Indoor and Mobile Radio Communications* (IEEE PIMRC 2013), London, UK, Sept. 2-5, 2013.

[2] V. Marbukh, K. Sayrafian, M. Barbi and M. Alasti, Inter-BAN Interference Mitigation: A Correlated Equilibrium Perspective; in *Proceedings of 11th International Conference on Wearable Micro and Nano Technologies for Personalized Health* (pHealth 2014), Vienna, Austria, June 11-13, 2014.

[3] M. Alasti, M. Barbi and K. Sayrafian, Uncoordinated Strategies for Inter-BAN Interference Mitigation; in *Proceedings of the IEEE 25th Annual International Symposium on Personal, Indoor and Mobile Radio Communications* (PIMRC 2014), Washington D.C., USA, Sept. 205, 2014

[4] K. Sayrafian, J. Hagedorn, M. Barbi, J. Terrill and M. Alasti, A Simulation Platform to Study Inter-BAN Interference"; in *Proceedings of the 4th IEEE International Conference on Cognitive Info-communications* (IEEE CogInfocom 2013), Budapest, Hungary, Dec. 2-5, 2013.

Combinatorial Testing

Raghu Kacker
D. Richard Kuhn (NIST ITL)
Yu Lei (University of Texas at Arlington)
James Lawrence
Jose Torres-Jimenez (CINVESTAV, MExico)

Combinatorial testing (CT) is an approach to detect combinatorial interaction faults, which may cause a software-system to fail when certain values of some factors occur together. Combinatorial testing is based on the insight, referred to as the *interaction rule*, that while the behavior of a software-system may be affected by a large number of factors, only a few factors are involved in a failure-inducing fault. Actual faults show that most involve one or two factors; however some may involve three, four or more factors. (A fault involving more than six factors has not been reported yet). NIST has taken leadership in advancing the technology from pair-wise to higher strength testing, making research tools and techniques favailable to US industry, and helping to promote their effective use. Many critical system failures in recent times have been traced to interaction faults in the underlying software. CT is a versatile and broadly applicable methodology that is helping to reduce testing costs in software-based systems for science, commerce, defense and security, and electronic medical systems, and is increasingly used in hardware testing as well. CT is now included in software engineering courses taught in more than twelve U.S. universities. A NIST special publication on CT [1] has been downloaded more than 28,000 times.

Test suites for CT typically involve factors with varying (mixed) numbers of test settings and often involve complex constraints among factors and their test settings. ACTS is a NIST-UTA (University of Texas at Arlington) research tool to generate high strength test suites for CT. A unique feature of ACTS is support of constraints among factor and test settings. The version 2.91 of ACTS incorporates a new algorithm which significantly improves performance of constraint handling.

We have filled over 1800 requests for ACTS.

CCM is a new research tool (developed jointly with Itzel Dominguez-Mendoza of the Center for Metrology of Mexico, CENAM) to determine combinatorial coverage of a test suite not developed from a CT viewpoint. The latest version of CCM supports constraints and has a greatly improved graphical depiction of combinatorial coverage. A parallel processing version of CCM is also available. Combinatorial deficiency of a test suite can be remedied by additional tests so CCM can help expand a test suite to satisfy stated combinatorial requirements.

ITL staff members co-organized the 3rd International Workshop on Combinatorial Testing (IWCT), which was held in conjunction with the 7th IEEE International Conference of Software Testing, Verification and Validation (ICST) in Cleveland, Ohio (March 31-April 4, 2014) to bring together researchers, developers, users, and practitioners to exchange ideas and experiences with CT methods and tools. The 2014 workshop consisted of twelve papers, one keynote address, two poster presentations, and thirty participants. The fourth IWCT is scheduled for April 13, 2015 in Graz, Austria.

With the sponsorship of NIST, a group of four students from the Carnegie Mellon University Master of Software Engineering program developed a proof-of-concept tool that integrates the power of CT with the advantages of model-driven testing and automatic test execution. The input to the tool is a graphical representation of the input domain of the artifact under test (AUT) called a Classification Tree (developed by Grimm and Grochtmann in 1993). Once created, the model is parsed and passed to *CitLab* that uses ACTS to generate the combinatorial test matrix. The test matrix may then be manually complemented with the expected result for each of the test vectors in the matrix to become a test suite. Alternatively, automated generation of expected results (through model checking or simulation) for each test vector can be used, with results integrated into the test tool through external scripts. The test suite is then fed to a *Junit* parameterized test that executes the AUT and records the pass/fail result for each test case.

Software product line (SPL) is an emerging paradigm for building a family of software systems that share similar features. The new algorithm developed by the NIST CT team for handling constraints for SPL is based on the notion of minimum invalid tuples. We compared our algorithm to an existing algorithm called ICPL, which is considered by far the best. The results are very encouraging. We show that our algorithm performed significantly better on the 15 largest feature models in a benchmark repository, both in terms of test set size and execution time. We incorporated the new algorithm into ACTS. A paper on this work was presented at the 2014 IEEE High Assurance System Engineering Conference [3].

Fault localization is one of the most difficult and time-consuming tasks during software development. We developed a spectrum-based approach that actually identifies faults inside source code by leveraging the notion of inducing combination. In particular, our approach generates a small group of tests from an inducing combination, such that the execution traces of these tests can be analyzed to quickly locate the faults. A paper was presented at ISSRE 2013 [4]. After the publication, we further refined this approach and integrated it with our earlier work on identifying inducing combinations. We conducted additional experiments to evaluate the effectiveness of the integrated approach. In particular, we made an experimental comparison with two state-of-the-art spectrum-based fault approaches. A journal paper is being prepared on the integrated approach and the new experimental results.

Test suites for CT are based on mathematical objects called covering arrays. Dr. Jose Torres-Jimenez (from the Mexican National Polytechnic Institute Center for Research and Advanced Studies, CINVESTAV) has joined the NIST CT team. He has developed an extensive library of covering arrays, called the CINVESTAV Covering Array Repository[23] (CCAR), of the smallest known number of test. This will further improve the generation test suites for combinatorial testing.

The NIST CT team has made presentations for three years at the annual NASA Independent Verification and Validation (NASA IV&V) Workshops. The title of the 2014 presentation was "Using combinatorial methods to determine test set size." NIST is working with the Johns Hopkins University Applied Physics Laboratory on a pilot project involving use of a research tool jointly developed by NIST and the U.S. Marine Corps for fault location in an area of defense and security.

[1] D. R. Kuhn, R.N. Kacker and Y. Lei, Practical Combinatorial Testing, NIST Special Publication 800-142, 2010.

[2] L. Ghandehari, J. Czerwonka, Y. Lei, S. Shafiee, R. Kacker and D. R. Kuhn, An Empirical Comparison of Combinatorial and Random Testing, in *Proceedings of 3rd International Workshop on Combinatorial Testing* (in conjunction with *7th IEEE International Conference on Software Testing, Verification and Validation*), April 2014.

[3] L. Yu, F. Duan, Y. Lei, R. N. Kacker and D. R. Kuhn, Combinatorial Test Generation for Software Product Lines using Minimum Invalid Tuples, in *Proceedings of 15th IEEE International Symposium on High Assurance System Engineering* (HASE), January 2014, 65-72.

[4] L. Ghandehari, Y. Lei, D. Kung, R. N. Kacker, D. R. Kuhn, Fault Localization Based on Failure-Inducing Combinations, in *Proceedings of 24th IEEE International Symposium on Software Reliability Engineering* (ISSRE), November 2013**,** 168-177.

[23] http://www.tamps.cinvestav.mx/~jtj/authentication.php

Mathematical Knowledge Management

We work with researchers in academia and industry to develop technologies, tools, and standards for representation, exchange, and use of mathematical data. Of particular concern are semantic-based representations which can provide the basis for interoperability of mathematical information processing systems. We apply this to the development and dissemination of reference data for applied mathematics. The centerpiece of this effort is the Digital Library of Mathematical Functions, a freely available interactive and richly linked online resource, providing essential information on the properties of the special functions of applied mathematics, the foundation of mathematical modeling in all of science and engineering.

DLMF Standard Reference Tables on Demand

Bonita Saunders
Bruce Miller
Marjorie McClain
Daniel Lozier
Andrew Dienstfrey
Chris Schanzle
Annie Cuyt (University of Antwerp)
Stefan Becuwe (University of Antwerp)
Franky Backeljauw (University of Antwerp)

See page 38.

Digital Library of Mathematical Functions

Daniel W. Lozier
Barry I. Schneider
Ronald F. Boisvert
Bruce R. Miller
Bonita V. Saunders
Marjorie A. McClain
Howard S. Cohl
Charles W. Clark (NIST PML)
Brian Antonishek (NIST ITL)
Adri B. Olde Daalhuis (University of Edinburgh)

http://dlmf.nist.gov/

Progress in science has often been catalyzed by advances in mathematics. More recently, developments in the physical sciences, such as investigations into string theory, have had influence in pure mathematics. This symbiotic relationship has been extremely beneficial to both fields. Mathematical developments have found numerous applications in practical problem-solving in all fields of science and engineering, while cutting-edge science has been a major driver of mathematical research. Often the mathematical objects at the intersection of mathematics and physical science are *mathematical functions*. Effective use of these tools requires ready access to their many properties, a need that was capably satisfied for more than 50 years by the 1964 National Bureau of Standards (NBS) *Handbook of Mathematical Functions with Formulas, Graphs, and Mathematical Tables* [1].

The 21st century successor to the NBS Handbook, the Digital Library of Mathematical Functions (DLMF) together with the accompanying book, *NIST Handbook of Mathematical Functions* [2], published by Cambridge University Press in 2010, are collectively referred to as the DLMF. The DLMF continues to remain the gold standard reference for the properties of what are termed the special functions of mathematical physics. The DLMF has considerably extended the scope of the original handbook as well as improving accessibility to the worldwide community of scientists and mathematicians. To cite a few examples, the new handbook contains more than twice as many formulas as the old one, coverage of more functions, in more detail, and an up-to-date list of references. The website covers everything in the handbook and much more: additional formulas and graphics, interactive search, live zooming and rotation of 3D graphs, internal links to symbol definitions and cross-references, and external links to online references and sources of software.

In order to help assess the impact of the DLMF project, the NIST library has undertaken a project to track citations to the DLMF, as well as to the original NBS Handbook. While the original Handbook still receives an enormous number of citations, citations to the DLMF are steadily growing. Almost 13 % of all of the citations are now to the DLMF as compared to 8 % in 2012. This is a healthy trend. See Figure 79.

Today's DLMF is the product of many years of effort by more than 50 expert contributors. Its appearance in 2010, however, was not the end of the project. Corrections to errors, clarifications, bibliographic updates, and addition of important new material all continually need to be made, and new chapters covering emerging subject areas need to be added, so as to assure the continued vitality of the DLMF deep into the 21st century. Developments currently in process at NIST include

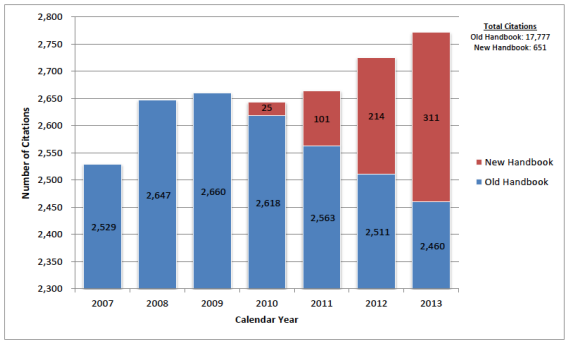

Figure 79. *Recent citation counts for the 1964 NBS handbook (blue) and the 2010 NIST Handbook (red). Citations to the classic NBS handbook still far outpace citations to the newer edition, 2460 vs. 311 in 2013, but citations to the latter are steadily growing.*

DLMF Tables [3], an on-demand table generation web service for special functions (see page 38), and the Digital Repository of Mathematical Formulae (DRMF) [4, 5], a community-based context-free compendium of mathematical formulas and associated mathematical data (see page 107).

During the period covered by this report, there have been a number of changes in the project's management structure. The Editorial Board was expanded to include Bruce R. Miller as Information Technology Editor, Bonita V. Saunders as Visualization Editor and Barry I. Schneider as Associate General Editor. These changes followed after the death of Frank W. J. Olver, the Editor in Chief of the DLMF and the retirement of Daniel W. Lozier. Lozier continues to remain active in the DLMF as General Editor on a part-time basis.

Now that the set of editors has been expanded, and in expectation of future changes in the leadership of the project, work to strengthen the rudimentary system currently in use for logging, resolving, archiving and otherwise managing feedback from users and between the editors is underway.

To summarize the year's technical accomplishments, there have been three updates of the DLMF during the period of the report. Version 1.0.7 significantly enhanced the accessibility, portability and usability of the DLMF. The default document format is now HTML5, which includes MathML, providing better accessibility and display of mathematics. All interactive 3D graphics have been recast using WebGL and X3DOM, which is now the default format. This improves portability and performance; it is now possible to interactively rotate, scale and explore function surfaces *without* downloading a special plugin. (See the next article for further details.) In Version 1.0.8, there were a number of mathematical corrections and the characters previously used for exponential e, imaginary i and differential d, were changed from special Unicode characters, not always available locally for use by browsers, to normal characters. In addition, some minor changes to page layouts were implemented. In Version 1.0.9, a few errors caught by readers were corrected, improvements in notation were made, and additional citations and clarifications were incorporated.

Future developments will continue with periodic releases correcting errors and making appropriate changes in current mathematical content. There is also likely to be a second edition of the DLMF containing some new chapters at some point in the next few years.

[1] M. Abramowitz and I. Stegun, eds., *Handbook of Mathematical Functions with Formulas, Graphs and Mathematical Tables*, Applied Mathematics Series **55**, National Bureau of Standards, Washington, DC 1964.

[2] F. Olver, D. Lozier, R. Boisvert and C. Clark, eds. *NIST Handbook of Mathematical Functions*, Cambridge University Press, 2010.

[3] D. Lozier, "Outgrowths of the Digital Library of Mathematical Functions Project, Part I: DLMF Standard Reference Tables," Challenges in 21st Century Experimental Mathematical Computation, Institute for Computational and Experimental Research in Mathematics (ICERM), Providence, RI, July, 2014.

[4] H. S. Cohl, M. A. McClain, B. V. Saunders and M. Schubotz, "Outgrowths of the Digital Library of Mathematical Functions Project, Part II: NIST Digital Repository of Mathematical Formulae," Challenges in 21st Century Experimental Mathematical Computation, Institute for Computational and Experimental Research in Mathematics, Providence, RI, July, 2014.

[5] H. S. Cohl, M. A. McClain, B. V. Saunders, M. Schubotz and J. C. Williams, Digital Repository of Mathematical Formulae, *Lecture Notes in Artificial Intelligence* **8543**, Proceedings of the Conferences on Intelligent Computer Mathematics 2014, Coimbra, Portugal, July 7-11, 2014, (S. M. Watt, J. H. Davenport, A. P. Sexton, P. Sojka and J. Urban, eds.), Springer, 419-422.

Visualization of Complex Functions Data

Bonita Saunders
Brian Antonishek (NIST ITL)
Qiming Wang
Bruce Miller
Sandy Ressler

Complex function data visualization can be a powerful tool for researchers studying mathematical or physical phenomena, but accessibility problems can severely limit its usefulness. The original 3D visualizations in the NIST Digital Library of Mathematical Functions (DLMF) were rendered using VRML and X3D, common technologies for viewing 3D web graphics that require users to download a special plugin. This was inconvenient not only for users, but also for maintainers

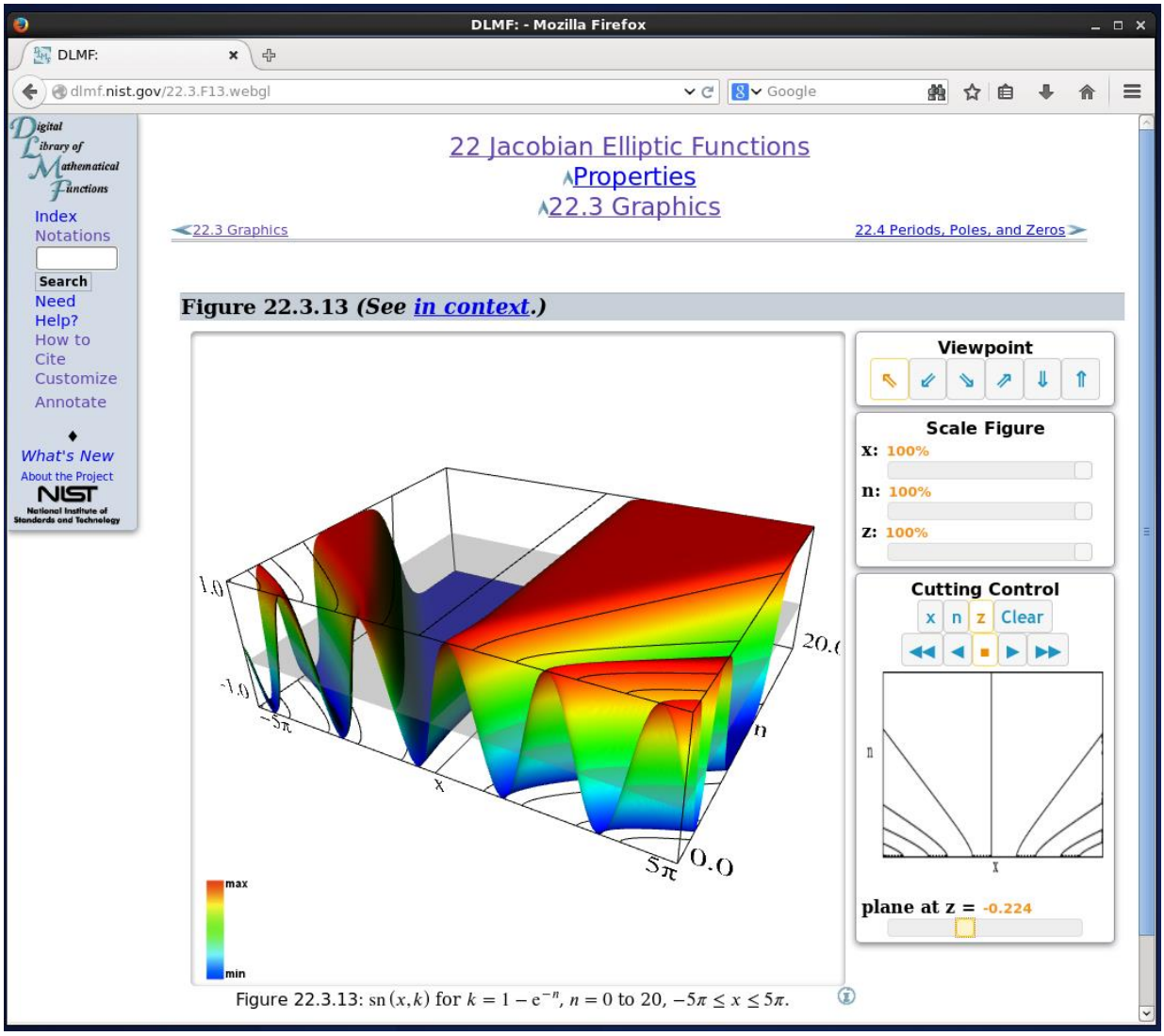

Figure 80. *DLMF webpage with embedded visualization of Jacobian elliptic function* sn*(x,k).*

since updates of the plugin, web browser, and even the operating system could affect the quality of the graphics display. To remedy this problem, we embarked on an extensive effort to convert the DLMF 3D graphics files to WebGL.

WebGL is a JavaScript API (application programming interface) for rendering 3D graphics in a web browser without a plugin. We based our WebGL code on the X3DOM framework which allowed us to build our WebGL application around X3D, an XML based graphics code. While we never found a VRML/X3D plugin that would successfully render our complex visualizations in Linux, our WebGL visualizations are visible on Windows, Mac, and Linux platforms in any WebGL enabled internet browser. Our conversion work paralleled the development of WebGL. When we began looking at the feasibility of the conversion more than two years ago, only trial versions of WebGL enabled browsers were available. Today, most common browsers, including the latest versions (11+) of Internet Explorer, can render WebGL graphics. WebGL content can even be rendered on many mobile devices. Nevertheless, since initial tests and research indicated that there were some problems with Microsoft's Internet Explorer implementation of WebGL, we decided to continue offering VRML/X3D display options to users for now. This also allows us to accommodate users who may prefer the VRML/X3D renderings.

The new WebGL visualizations were released in version 1.0.7 of the DLMF in March 2014. Figure 80 shows a graph of Jacobian elliptic function sn(*x*,*k*) imbedded in a DLMF web page. WebGL color maps are more vibrant, cutting plane curves clearer, and the interactive movement of surfaces faster and smoother. We did notice that WebGL is more particular about the quality of the underlying computational grid. A few color

map anomalies not seen in the VRML/X3D visualizations were traced to slight overlaps of grid lines. We regenerated several grids and boundary contours, greatly improving surface color maps and clipping in some WebGL visualizations.

We received very positive feedback after publicizing the new visualizations at various venues and websites, including the DLMF website, X3DOM site [4], and at several conferences and workshops [1-3]. Future work will concentrate on the reduction of graphics file sizes using adaptive grid generation, implementation of a continuous surface spin option, development of an accurate zoom, and looking at 2D visualization enhancements.

[1] B. Saunders, Q. Wang and B. Antonishek, Adaptive Composite B-Spline Grid Generation for Interactive 3D Visualizations, in *Proceedings of MASCOT/ISGG 2012*, Las Palmas de Gran Canaria, Spain, October 22-26, 2012, IMACS Series in Computational and Applied Mathematics **18** (2014), 241-250.

[2] B. Antonishek, "Look Ma—no Plug-in! (DLMF's new WebGL 3D Figures)," Web3D 2014, 19th International Conference on 3D Web Technology, Vancouver, Canada, August 10, 2014.

[3] S. Ressler and B. Antonishek, "New WebGL Graphics in the NIST DLMF," Web3D Emerging Technology Showcase, Virginia Tech Research Center, Arlington, VA, March 25, 2014.

[4] S. Ressler, NIST/DLMF uses X3DOM, http://www.X3DOM.org/?page_id=2429.

Mathematical Knowledge Management

Bruce Miller
Deyan Ginev (Jacobs University, Germany)

As web technologies continue to develop, and as the Digital Library of Mathematical Functions (DLMF) continues to be corrected and improved, so too must the Mathematical Knowledge Management (MKM) technologies we originally developed for DLMF.

This year has seen the continued development of LaTeXML, the TeX to XML to HTML converter used by the DLMF, with a major release last spring, and a minor release by the time you read this. Along with bug fixes, increased portability, general improvements to performance, fidelity and styling, the coverage of LaTeX idioms and packages has been significantly enhanced, including generation of Scalable Vector Graphics (SVG) for figures [2]. The system continues to be used as part of the infrastructure for several other projects such as: Planet Math[24]; it is used to process

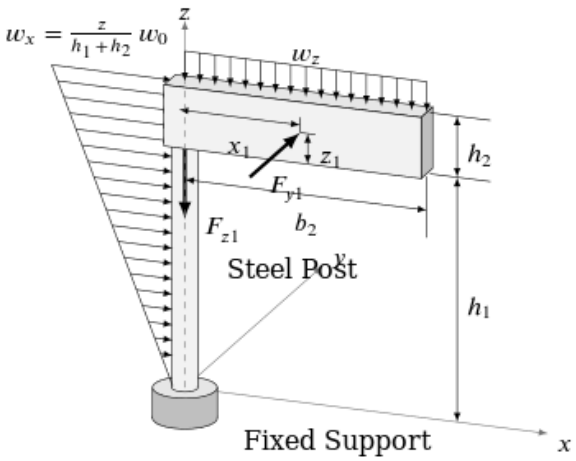

Figure 81. *Screen capture of a figure from TeXamples.org shown in a web browser. The TeX code, using the tikz package, was converted to HTML5 + SVG.*

arXiv[25] [3] manuscripts to generate test-data for research in mathematical search; and in the Digital Repository of Mathematical Formulae (DRMF; see page 107).

Most relevant to MKM are the improvements being made to representation of mathematics. Extensive use of "parallel markup" is being used whenever the semantic structure of an expression is known, or inferred from parsing. Our parallel markup separates the presentation form of the expression, its notations, from the content form, what it means. This separation allows us to more faithfully capture the finer points of mathematical typography, preserving the intended sizes and stretchiness of delimiters and display style characteristics of symbols. An upcoming release of the DLMF will benefit from these typographic improvements.

The separation also simplifies the representation of the semantic structure of the expression. Noting that this structure can often be recognized during parsing even when the exact meaning cannot; for example, it is usually clear to what expression a superscript applies, although it may not be certain that the superscript represents a power. We are exploring the concept of underspecified symbols to represent such cases.

The more closely the content form captures the exact meaning, the more useful it is for search indexing, question answering and, ultimately, for computation. At this stage of development, the result of processing a formula is, whenever possible, a correct recognition of the structure, but with some subset of the symbols being ambiguous as to their meanings. The long term goal is to resolve such meanings through a combination of semantic analysis, type checking, and where available, external declarations.

Since both presentation and content branches of the parallel markup can be tracked to the original TeX

[24] http://planetmath.org/

[25] http://arXiv.org/

markup, we are able to establish cross-referencing between the two branches. Such connections associate the meaning of a symbol with its display, or vice-versa.

In related developments, the Mathematics Markup Language (MathML) developed by the Math Working Group (BM is a member) of the World Wide Web Consortium (W3C) is on track to become an ISO standard. Also significant is the approval of HTML5 as a W3C recommendation; HTML5 includes MathML and SVG as integral components of document markup for the web.

[1] B. R. Miller, Three Years of DLMF: Web, Math and Search, *Lecture Notes in Computer Science* **7961** (2013), Springer, 288-295.

[2] B. R. Miller, D. I. Ginev and S. Oprea, E-Books and Graphics with LaTeXML, *Lecture Notes in Artificial Intelligence* **8543** (2014), Proceedings of the Conference on Intelligent Computer Mathematics, Coimbra, Portugal, July 7-11, 2014 (S. M. Watt, et al., eds.), Springer, 427-430.

[3] H. Stammerjohanns, M. Kohlhase, D. Ginev, C. David and B. Miller, Transforming Large Collections of Scientific Publications to XML, *Mathematics in Computer Science* **3**:3 (2010), 299-307.

NIST Digital Repository of Mathematical Formulae

Howard S. Cohl
Marjorie A. McClain
Bonita V. Saunders
Moritz Schubotz (Technische Universität Berlin)
Alan P. Sexton (University of Birmingham)
Jimmy Li (Richard Montgomery High School)
Shraeya Madhu (Poolesville High School)
Azeem Mohammed (Poolesville High School)
Cherry Zou (Poolesville High School)

http://gw32.iu.xsede.org/index.php/Main_page

The goal of the NIST Digital Repository of Mathematical Formulae (DRMF) project is to build a community-based online compendium of orthogonal polynomial and special function (OPSF) formulae, including related mathematical data, for a mathematically literate audience. The DRMF will (1) facilitate interaction among a community of mathematicians and scientists interested in compendia formulae data for orthogonal polynomials and special functions; (2) be expandable, allowing the input of new formulae from the literature; (3) represent the context-free full semantic information concerning individual formulas; (4) have a user friendly, consistent, and hyperlinkable viewpoint and authoring perspective; (5) contain easily searchable mathematics; and (6) take advantage of modern MathML tools for easy to read, scalably rendered content-driven mathematics. Every formula listed in the DRMF will have its own home page. Our DRMF implementation is built using MediaWiki, the wiki software used by Wikipedia. See Figure 82 for a sample DRMF formula home page. The DRMF has been described in a series of publications and talks [1-3].

A key asset in the development of DRMF context-free semantic content is the utilization of a set of LaTeX macros originally created for the NIST Digital Library of Mathematical Functions (DLMF) [26]. These macros were invented by Bruce Miller (NIST/ACMD) to achieve the encapsulation of semantic information within the NIST DLMF. These macros give us the capability to tie LaTeX commands unambiguously to mathematical functions defined in an OPSF context. There are currently 546 DLMF LaTeX macros, as well as an additional 49 which have been created specifically for the DRMF. All DLMF macros have at least one DLMF web page associated with them, and the goal is to have definition pages for all additional DRMF macros. The committed use of DLMF and DRMF macros guarantees a mathematical and structural consistency throughout the DRMF.

DRMF formula seeding is currently focused on (1) DLMF chapters 5 (Gamma Functions), 15 (Hypergeometric Function), 16 (Generalized Hypergeometric Functions and Meijer *G*-Function), 17 (*q*-Hypergeometric and Related Functions), 18 (Orthogonal Polynomials), and 25 (Zeta and Related Functions); (2) Koekoek, Lesky, and Swarttouw chapters 1 (Definitions and Miscellaneous Formulas), 9 (Hypergeometric Orthogonal Polynomials), and 14 (Basic Hypergeometric Orthogonal Polynomials) [4]; (3) Koornwinder KLS addendum LaTeX data [5]; (4) Bateman Manuscript Project (BMP) books [6]; and (5) the Wolfram Computational Knowledge of Continued Fractions Project (eCF).[27] In August, 2014, the DRMF Project obtained copyright permission and license to use BMP material as seed content for the DRMF from Adam Cochran, Associate General Counsel of Caltech. Caltech has loaned us copies of the BMP. We have forwarded these copies to Alan Sexton, Scientific Document Analysis Group, School of Computer Science, University of Birmingham, UK. (Caltech is aware of this and suggested this was the best way to get the material to Sexton.) Sexton is presently scanning the BMP and developing software to perform mathematical optical character recognition to obtain LaTeX source. With regard to seed project (1), the DLMF source already has DLMF macros inserted. However for seed projects (2-5), we are developing Python software to incorporate DLMF and DRMF macros

[26] http://dlmf.nist.gov

[27] http://blog.wolframalpha.com/2013/05/16/computational-knowledge-of-continued-fractions

into the corresponding LaTeX source. Our coding efforts have also focused on extracting formula data from LaTeX source as well as generating DRMF Wikitext. We are developing Python software for the seeding of the eCF project which involves conversion from Mathematica format to DLMF and DRMF macro incorporated LaTeX.

Current and future DRMF MediaWiki development projects include the production of formula output representations (such as semantic LaTeX, MathML, Mathematica, Maple, and Sage); incorporation of sophisticated DLMF and DRMF macro related formula search; and the development of capabilities for user community formula input.

Our current DRMF server, both public and development instances, have been deployed through the XSEDE project on the Quarry cluster at Indiana University, Bloomington, Indiana and the Wikitech server of the Wikimedia Foundation in San Francisco.

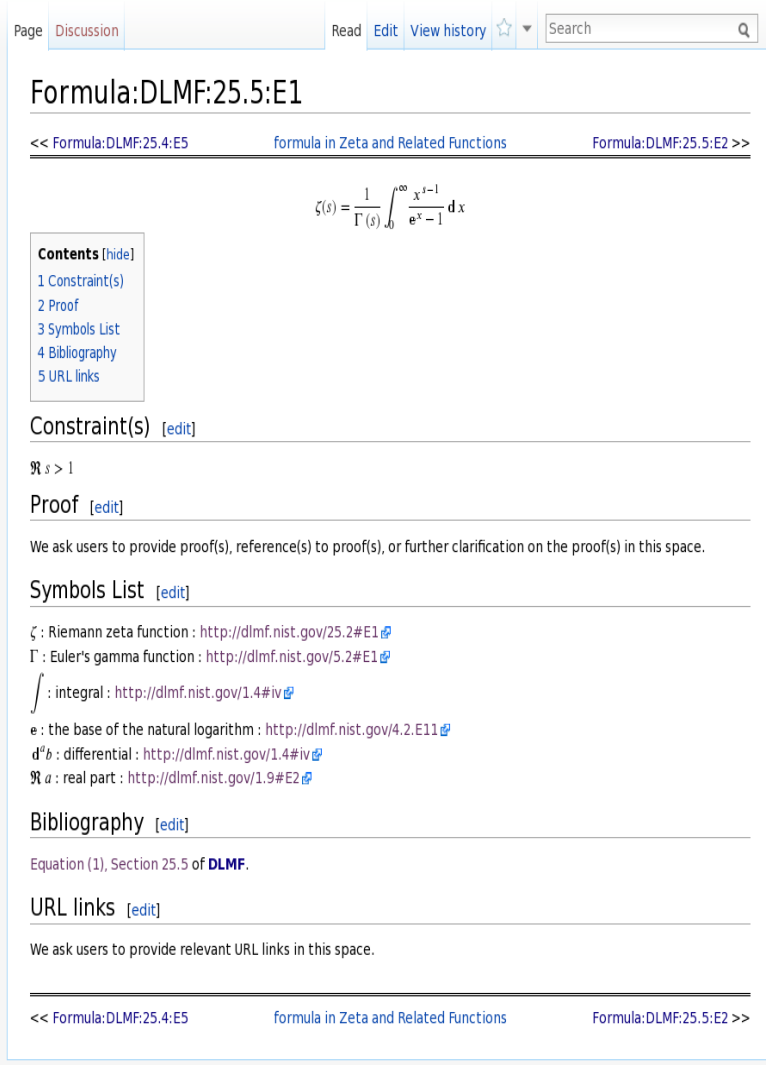

Figure 82. *Sample DRMF Formula home page.*

[1] H. S. Cohl, M. A. McClain, B. V. Saunders, M. Schubotz and J. C. Williams, Digital Repository of Mathematical Formulae, *Lecture Notes in Artificial Intelligence* **8543** (2014), Proceedings of the Conferences on Intelligent Computer Mathematics 2014, Coimbra, Portugal, July 7-11, 2014, (S. M. Watt, J. H. Davenport, A. P. Sexton, P. Sojka and J. Urban, eds.), Springer, 419-422.

[2] H. S. Cohl, M. A. McClain, B. V. Saunders and M. Schubotz, "Outgrowths of the Digital Library of Mathematical Functions Project, Part II: NIST Digital Repository of Mathematical Formulae", Workshop on Challenges in 21st Century Experimental Mathematical Computation, Institute for Computational and Experimental Research in Mathematics, Providence, Rhode Island, July, 2014.[28]

[3] H. S. Cohl, M. A. McClain, B. V. Saunders, M. Schubotz, A. Danoff, J. Li, J. Migdall, A. Liu, C. Zou, A. Mohammed and S. Madhu, "XSEDE and the NIST Digital Repository of Mathematical Formulae" XSEDE Science Gateways Community Series, August 2014.[29]

[4] R. Koekoek, P. A. Lesky and R. F. Swarttouw, Hypergeometric Orthogonal Polynomials and their *q*-Analogues, Springer Monographs in Mathematics, Springer-Verlag, Berlin, 2010.

[5] T. H. Koornwinder, Additions to the Formula Lists in "Hypergeometric Orthogonal Polynomials and their q-analogues" by Koekoek, Lesky and Swarttouw, arXiv:1401.0815, January 2014.

[6] A. Erdélyi, W. Magnus, F. Oberhettinger and F. G. Tricomi, Higher Transcendental Functions, Vols. I, II, III, Robert E. Krieger Publishing Co., Melbourne, FL, 1981.

[28] http://icerm.brown.edu/video_archive, see Programs and Workshops 2014 → Summer 2014 → Challenges in 21st Century

[29] https://www.youtube.com/watch?v=gAGqr_4AjkI&list=UU6ulv87KV32afXMLv6uWTW

Fundamental Solutions and Expansions for Special Functions and Orthogonal Polynomials

Howard S. Cohl
Roberto S. Costas-Santos (University of Alcalá)
Hans Volkmer (University of Wisconsin-Milwaukee)
Michael A. Baeder (Harvey Mudd College)
Connor MacKenzie (Westminster College)
Philbert R. Hwang (Poolesville High School)
William Xu (Montgomery Blair High School)

The concept of a function expresses the idea that one quantity (the input) completely determines another quantity (the output). Our research concerns special functions and orthogonal polynomials. A special function is a function that has appeared in the mathematical sciences so often that it has been given a name. Green's functions (named after the British mathematician George Green, who first developed the concept in the 1830s) describe the influence of natural phenomena such as electromagnetism, gravity, heat and waves. For example, in electrostatics, a Green's function describes the influence of a point charge, called the source, over all of space. The inputs for Green's functions are all of space (with the exception of a singular region), and the output is the "force" exerted from the point throughout space. Green's functions are fundamental to the study of partial differential equations and are powerful in that they provide a mechanism for obtaining their solutions.

We investigate fundamental solutions (Green's functions) of linear partial differential equations on highly symmetric Riemannian manifolds (harmonic, rank-one symmetric spaces) such as real, complex, quaternionic, and octonionic Euclidean, hyperbolic, and projective spaces. Our recent focus has been on applications of fundamental solutions for linear elliptic partial differential operators on spaces of constant curvature. For instance, we have recently submitted a paper Cohl and Palmer (2014) [1] which derives fundamental solution expansions (azimuthal Fourier and Gegenbauer) with applications to Newtonian potential theory on d-dimensional spaces of constant positive curvature, namely hyperspherical geometry. We have also recently had success in constructing closed-form expressions of a fundamental solution for the Helmholtz equation is d-dimensional spaces of constant negative curvature, namely the hyperboloid model of hyperbolic geometry, in terms of associated Legendre functions. We continue our ongoing discussion on the harmonic analysis of fundamental solutions for Laplace's equation on rank one symmetric spaces of compact and noncompact type with Gestur Olafsson (Louisiana State University).

In Cohl (2013) [2], a generalization of the generating function for Gegenbauer polynomials is derived which allows one to expand this generating function in terms of Gegenbauer polynomials with arbitrary order. This Gegenbauer polynomial expansion is useful in expanding powers of the distance between two points on d-dimensional Euclidean space in Vilenkin's polyspherical coordinates. In Cohl and Volkmer (2013) [3-4], we derived eigenfunction expansions for a fundamental solution of Laplace's equation in 3-dimensional Euclidean space in one of the most general orthogonal asymmetric confocal cyclidic coordinate systems which admit solutions through separation of variables, 5-cyclide coordinates. The harmonics in this coordinate system are given by products of solutions of second-order Fuchsian ordinary differential equations with five elementary singularities. The Dirichlet problem for the global harmonics in this coordinate system is solved using multiparameter spectral theory in the regions bounded by the asymmetric confocal cyclidic coordinate surfaces.

In the following sequence of papers, we derive specializations and generalizations of generalized and basic hypergeometric orthogonal polynomial generating functions as well as corresponding definite integrals using orthogonality.

- In Cohl, MacKenzie and Volkmer (2013) [5], generalizations of generating functions for hypergeometric orthogonal polynomials, namely Jacobi, Laguerre and Wilson polynomials are derived using connection relations with one free parameter and our series-rearrangement technique. The coefficients of these expansions are given in terms of generalized hypergeometric functions.
- Cohl and MacKenzie (2013) [6] gives an extension of the generating function for Gegenbauer polynomials to Jacobi polynomials, and re-expresses Gauss hypergeometric functions in terms of more elementary functions for certain generating functions for classical orthogonal polynomials.
- In Baeder, Cohl and Volkmer (2014) [7] we derive generalized generating functions for continuous hypergeometric orthogonal polynomials, namely Wilson, continuous Hahn, continuous dual Hahn, and Meixner-Pollaczek polynomials.
- In Cohl, Costas-Santos, and Hwang (2014) [8], our series-rearrangement technique is extended to generalizations of generating functions for basic hypergeometric orthogonal polynomials. Here we derive generalizations of generating functions for Askey-Wilson, q-ultraspherical/Rogers, q-Laguerre, and little q-Laguerre/Wall polynomials. In collaborative research with student Xu and Baeder, we are extending this work to q-hypergeometric orthogonal polynomials such as Al-Salam-Carlitz polynomials and for discrete hypergeometric orthogonal polynomials such as Meixner and Krawtchouk polynomials. As an extension of this work, in an ongoing collaborative

research project with Palmer, we are deriving dual Bessel function integrals using the method of integral transforms.

There are several connections with conferences for this project. For instance, Cohl is serving on both the Scientific Organizing and Local Organizing committees for the 13th International Symposium on Orthogonal Polynomials, Special Functions & Applications to be held on June 1-5, 2015 at NIST. In Berg (2015) [9], an open problem by Cohl is given on a very-well-poised ${}_9F_8$ generalized hypergeometric series which was presented at OPSFA12. Cohl is also serving on the Scientific and Local Organizing committees for the Orthogonal Polynomials and Special Functions Summer School 6 workshop to be held tentatively on June 17-23, 2016 at American University. This OPSF Summer School is being co-organized with Daniel Lozier, Mourad Ismail, Stephen Casey, Erik Koelink, and Willard Miller, Jr.

[1] H S. Cohl and R M. Palmer, Fourier and Gegenbauer Expansions for a Fundamental Solution of Laplace's Equation in Hyperspherical Geometry, in review.

[2] H. S. Cohl, On a Generalization of the Generating Function for Gegenbauer Polynomials, *Integral Transforms and Special Functions* **24**:10 (2013), 807-816.

[3] H. S. Cohl and H. Volkmer, Separation of Variables in an Asymmetric Cyclidic Coordinate System, *Journal of Mathematical Physics* **54**:6 (2014), 063513.

[4] H. S. Cohl and H. Volkmer, Expansions for a Fundamental Solution of Laplace's Equation on $\mathbf{R}^3$ in 5-cyclidic harmonics, *Analysis and Applications* **12**:6 (2014), 613-633. (Special Issue Dedicated to the Memory of Frank Olver)

[5] H. S. Cohl, C. MacKenzie and H. Volkmer, Generalizations of Generating Functions for Hypergeometric Orthogonal Polynomials with Definite Integrals, *Journal of Mathematical Analysis and Applications* **407**:2 (2013), 211-225.

[6] H. S. Cohl and C. MacKenzie, Generalizations and Specializations of Generating Functions for Jacobi, Gegenbauer, Chebyshev and Legendre Polynomials with Definite Integrals, *Journal of Classical Analysis* **3**:1 (2013), 17-33.

[7] M. A. Baeder, H. S. Cohl, and H. Volkmer, Generalizations of Generating Functions for Higher Continuous Hypergeometric Orthogonal Polynomials in the Askey Scheme, in review.

[8] H. S. Cohl, R. S. Costas-Santos, and P. R. Hwang, Generalizations of Generating Functions for Basic Hypergeometric Orthogonal Polynomials, in review.

Part IV

Activity Data

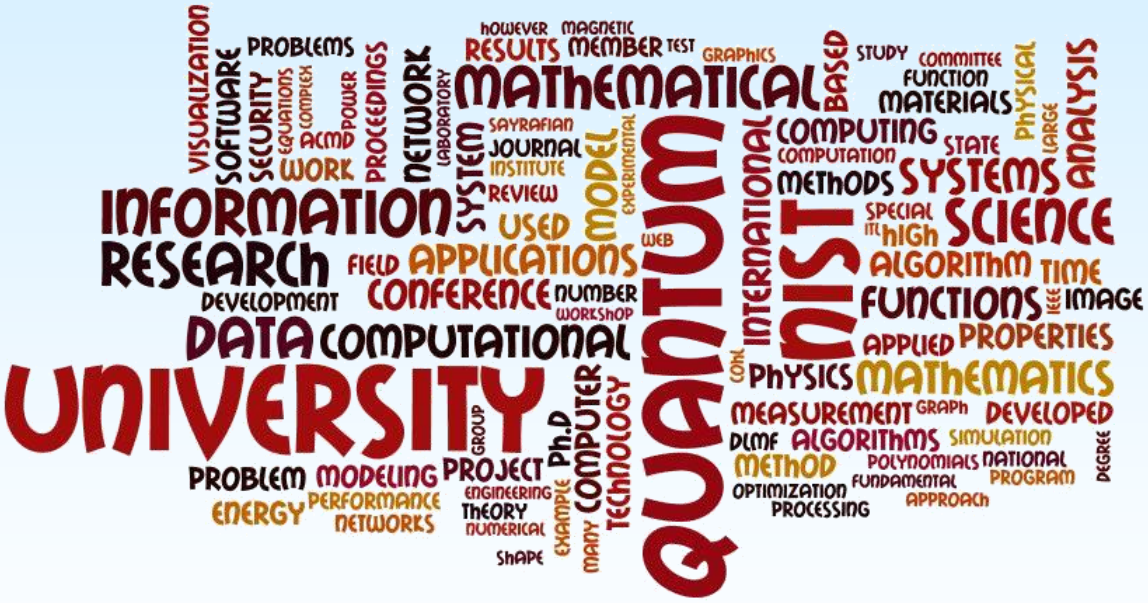

Publications

Note: Names of (co-)authors with a Division affiliation during this reporting period are underlined.

Appeared

Refereed Journals

1. D. A. Anderson, J. B. Benson and A. J. Kearsley, Foundations of Modeling in Cryobiology - I: Concentration, Gibbs Energy, and Chemical Potential Relationships, *Cryobiology* **69**:3 (2014), 349-360.
2. J. Bernal, C. Hagwood, J. Elliott, M. Halter and T. Brennan, Testing Equality of Cell Populations based on Shape and Geodesic Distance, *IEEE Transactions on Medical Imaging* **32**:12 (2013), 2230-2237.
3. I. Brezinova, A. U. J. Lode, A. I. Streltsov, L. S. Cederbaum, O. E. Alon, L. A Collins, B. I. Schneider and J. Burgdörfer, Elastic Scattering of a Bose-Einstein Condensate at a Potential Landscape, *Journal of Physics* **488** (2014), 012032.
4. J. C. Browne, R. L. DeLeon,, A. K. Patra, W. L. Barth, J. Hammond, M. D. Jones, T. R. Furlani, B. I. Schneider, S. M. Gallo, A. Ghadersohi, R. J. Gentner, J. T. Palmer, N. Simakov, M. Innus, A. E. Bruno, J. P. White, C. D. Cornelius, T. Yearke, K. Marcus, G. von Laszewski and F. Wang, Comprehensive Open-Source Resource Usage Measurement and Analysis for HPC Systems, *Concurrency and Computation: Practice and Experience* **26** (2014), 2191.
5. G. W. Bryant, N. Malkova and J. S. Sims, Mechanism for Controlling Exciton Fine Structure in Quantum Dots using Electric Fields: Manipulation of Exciton Orientation and Exchange Splitting at the Atomic Scale, *Physical Review B* **88** (2013), 161301(R).
6. A. S. Carasso, Compensating Operators and Stable Backward in Time Marching in Nonlinear Parabolic Equations, *International Journal on Geomathematics* **5** (2014), 1-16.
7. E. Cobanera, G. Ortiz and E. Knill, A Solution to the Non-Abelian Duality Problem, *Nuclear Physics B* **877** (2013), 574-597.
8. H. S. Cohl and H. Volkmer, Expansions for a Fundamental Solution of Laplace's Equation on R^3 in 5-Cyclidic Harmonics, *Analysis and Applications* **12**:6 (2014), 613-633. (Special issue decicated to the memory of Frank Olver).
9. H. S. Cohl and C. MacKenzie, Generalizations and Specializations of Generating Functions for Jacobi, Gegenbauer, Chebyshev and Legendre Polynomials with Definite Integrals, *Journal of Classical Analysis* **3**:1 (2013), 17-33.
10. H. S. Cohl, C. MacKenzie and H. Volkmer, Generalizations of Generating Functions for Hypergeometric Orthogonal Polynomials with Definite Integrals, *Journal of Mathematical Analysis and Applications* **407**:2 (2013), 211-225.
11. H. S. Cohl, On a Generalization of the Generating Function for Gegenbauer Polynomials, *Integral Transforms and Special Functions* **24**:10 (2013), 807-816.
12. A. Dienstfrey, F. R. Phelan Jr., S. Christensen, A. Strachan, F. Santosa and R. Boisvert, Uncertainty Quantification in Materials Modeling, *JOM: The Journal of the Minerals, Metals and Materials Society* **66**:7 (2014), 1342-1344.
13. A. Dienstfrey and P. Hale, Analysis for Dynamic Metrology, *Measurement Science and Technology* **25**:3 (2014), 035001.
14. A. Dienstfrey and P. Hale, Colored Noise and Regularization Parameter Selection for Waveform Metrology, *IEEE Transactions on Instrumentation and Measurement* **63:7** (2014), 1769-1778.
15. A. P. R. Eberle, N. Martys, L. Porcar, S. R. Kline, W. L. George, J. M. Kim, P. D. Butler and N. J. Wagner, Shear Viscosity and Structural Scalings in Model Adhesive Hard-Sphere Gels, *Physical Review E* **89** (2014), 050302.
16. C. F. Ferraris, N. S. Martys and W. L. George, Development of Standard Reference Materials for Cement-Based Materials, *Journal of Cement and Concrete Composites* **54** (2014), 29-33.
17. Z. Gimbutas and S. Veerapaneni, A Fast Algorithm for Spherical Grid Rotations and its Application to Singular Quadrature, *SIAM Journal on Scientific Computing* **35**:6 (2013), A2738-A2751.
18. X. Guan, K. Bartschat, B. I. Schneider and L. Koesterke, Resonance Effects in Two-Photon Double Ionization of H_2 by Femtosecond XUV Laser Pulses, *Physical Review A* **88** (2013), 043402.
19. X. Guan, K. Bartschat, B. I. Schneider and L. Koesterke, Alignment and Pulse-Duration Effects in Two-Photon Double Ionization of H_2 by Femtosecond XUV Laser Pulses, *Physical Review A* **90** (2014), 043416.
20. M. Jarret and S. P. Jordan, Adiabatic Optimization without Local Minima, *Quantum Information and Computation* **15**:3/4 (2015), 0181-0199.

21. M. Jarret and S. P. Jordan, The Fundamental Gap for a Class of Schrodinger Operators on the Path and Hypercube Graphs, *Journal of Mathematical Physics* **55**:5 (2014), 0552104.

22. S. P. Jordan, Strong Equivalence of Reversible Circuits Is CoNP-Complete, *Quantum Information and Computation* **14**:15/16 (2014), 1302-1307.

23. S. P. Jordan, K. S. M. Lee and J. Preskill, Quantum Computation of Scattering in Scalar Quantum Field Theories, *Quantum Information and Computation* **14**:11/12 (2014), 1014-1080.

24. A. J. Kearsley, Y. Gadhyan and W. E. Wallace, Stochastic Regression Modeling of Chemical Spectra, *Chemometrics and Intelligent Laboratory Systems* **139** (2014), 26-32.

25. P. S. Kuo, J. Bravo-Abad and G. S. Solomon, Second-Harmonic Generation Using $\bar{4}$-Quasi-Phasematching in a GaAs Whispering-Gallery-Mode Microcavity, *Nature Communications* **5** (2014), 3109.

26. M. Liard, N. S. Martys, W. L. George, D. Lootens and P. Hebraud, Scaling Laws For The Flow Of Generalized Newtonian Suspensions, *Journal of Rheology* **58**:6 (2014), 1993.

27. H. Mahboubi, J. Habibi, A. G. Aghdam and K. Sayrafian, Distributed Deployment Strategies for Efficient Coverage in a Network of Mobile Sensors with Prioritized Sensing Field, *IEEE Transactions on Industrial Informatics* **9**:1 (2013), 451-461.

28. H. Mahboubi, K. Moezzi, A. G. Aghdam and K. Sayrafian, Distributed Deployment Algorithms for Efficient Coverage in a Network of Mobile Sensors with Non-identical Sensing Capabilities, *IEEE Transactions on Vehicular Technology* **63**:8 (2014), 3998-4016.

29. H. Mahboubi, K. Moezzi, A. G. Aghdam, K. Sayrafian and V. Marbukh, Distributed Deployment Algorithms for Improved Coverage in a Network of Wireless Mobile Sensors, *IEEE Transactions on Industrial Informatics* **10**:1 (2014), 163-174.

30. W. F. Mitchell and M. A. McClain, A Comparison of *hp*-Adaptive Strategies for Elliptic Partial Differential Equations, *ACM Transactions on Mathematical Software* **41**:1 (2014), 2.

31. M. Mullan and E. Knill, Simulating And Optimizing Atomic Clock Evolution, *Physical Review A* **90** (2014), 042310.

32. F. A. Potra, Interior Point Methods for Sufficient Horizontal LCP in a Wide Neighborhood of the Central Path with Best Known Iteration Complexity, *SIAM Journal on Optimization* **24**:1 (2014), 1-28.

33. I. Şahin, M. A. Simaan and A. J. Kearsley, Successive Frequency Domain Minimization for Time Delay Estimation, *Signal Processing* **98** (2014), 96-101.

34. R. F. Sekerka, W. J. Boettinger and G. B. McFadden, Surface Morphologies due to Grooves at Moving Grain Boundaries Having Stress-Driven Fluxes, *Acta Materialia* **61** (2013), 7216-7226.

35. J. S. Sims and S. A. Hagstrom, Hylleraas-Configuration-Interaction Nonrelativistic Energies For The 1 S Ground States of the Beryllium Isoelectronic Sequence, *Journal of Chemical Physics* **140** (2014), 224312.

36. M. J. Stevens, S. Glancy, S. W. Nam and R. P. Mirin, Third-Order Antibunching from an Imperfect Single-Photon Source, *Optics Express* **22** (2014), 3244-3260.

37. A. Streib, N. Streib, I. Beichl and F. Sullivan, A Binomial Approximation Method for the Ising Model, *Journal of Statistical Physics* **156**:3 (2014), 593-605.

38. F. Sullivan and I. Beichl, Permanents Alpha-Permanents and Sinkhorn Balancing, *Computational Statistics*, **29**:6 (2014), 1793-1798.

39. F. Vico, L. Greengard and Z. Gimbutas, Boundary Integral Equation Analysis on the Sphere, *Numerische Mathematik* **128**:3 (2014), 463-487.

40. J. C. Wu, A. F. Martin and R. N. Kacker, Bootstrap Variability Studies In ROC Analysis On Large Datasets, *Communications in Statistics - Simulation and Computation* **43** (2014), 225-236.

41. A. C. Wilson, Y. Colombe, K. R. Brown, E. Knill, D. Leibfried and D. J. Wineland, Tunable Spin-Spin Interactions and Entanglement of Ions in Separate Wells, *Nature* **512** (2014), 57-60.

42. Y. Zhang, S. Glancy and E. Knill, Efficient Quantification of Experimental Evidence Against Local Realism, *Physical Review A* **88** (2013), 052119.

Journal of Research of NIST

1. A. S. Carasso, A Framework for Reproducible Latent Fingerprint Enhancements, *Journal of Research of the NIST* **119** (2014), 212-226.

2. B. Cloteaux, M. D. LaMar, E. Moseman and J. Shook, Threshold Digraphs, *Journal of Research of the NIST* **119** (2014), 227-234.

3. A. Pearlman, R. Datla, R. N. Kacker and C. Cao, Translating Radiometric Requirements for Satellite Sensors to Match International Standards, *Journal of Research of NIST*, **119** (2014), 272-276.

Book Chapters

1. F. Maggioni, M. Bertocchi, E. Allevi, F.A. Potra and S. W. Wallace, Stochastic Second-Order Cone Programming In Mobile Ad-Hoc Networks: Sensitivity To Input Parameters, Chapter 17 in *Stochastic Programming: Applications in Finance, Energy and Logistics* (H. I. Gassmann, S. W. Wallace and W. T. Ziemba, eds,), World Scientific, (2013), 467-486.

In Conference Proceedings

1. G. Alagic, S. Jeffery and S. Jordan, Partial-Indistinguishability Obfuscation Using Braids, in *Proceedings of the Ninth Conference on Theory of Quantum Computation, Communication, and Cryptography* (TQC2014), (S. T. Flammia and A. W. Harrow, eds.), Leibnitz International Proceedings in Informatics **27** (2014), 141-160.
2. G. Alagic, A. Bapat and S. Jordan, Classical Simulation of Yang-Baxter Gates, in *Proceedings of the Ninth Conference on Theory of Quantum Computation, Communication, and Cryptography* (TQC2014)), (S. T. Flammia and A. W. Harrow, eds.), Liebnitz International Proceedings in Informatics **27** (2014), 161-175.
3. M. Alasti, M. Barbi and K. Sayrafian, Uncoordinated Strategies for Inter-BAN Interference Mitigation, in *Proceedings of the IEEE 25th International Symposium on Personal, Indoor and Mobile Radio Communications* (PIMRC 2014), Washington, DC, September 2014.
4. R. Alléaume, T. Chapuran, C. Chunnilall, I. Degiovanni, N. Lutkenhaus, V. Martin, M. Peev, A. Mink, M. Lucamarini, A. Shields and M. Ward, Worldwide Standardization Activity for Quantum Key Distribution, in *Proceedings of IEEE Globecom 2014*, Austin, TX, December 2014.
5. S. Banik, S. Sarkar and R. N. Kacker, Security Analysis Of The RC4+ Stream Cipher, in *Progress in Cryptology – INDOCRYPT 2013*, Lecture Notes in Computer Science **8250** (2013), 297-307.
6. T. Bednarz, J. A. Taylor, W. Huang, W. Griffin, S. G. Satterfield, J. G. Hagedorn and J. Terrill, High-Performance Visualization in Science and Research, *Proceedings of IEEE Vis 2014*, Paris, France, November 9-14, 2014, (Practitioner Experiences Poster Track).
7. H. S. Cohl, M. A. McClain, B. V. Saunders, M. Schubotz and J. C. Williams, Digital Repository of Mathematical Formulae, in *Proceedings of the Conferences on Intelligent Computer Mathematics*, Coimbra, Portugal, July 7-11, 2014, (S. M. Watt, et al. Eds), Lecture Notes in Artificial Intelligence **8543** (2014), 419-422.
8. M. Dadfarnia, K. Sayrafian, P. Mitcheson and J. Baras, Maximizing Output Power of a CFPG Micro Energy-Harvester for Wearable Medical Sensors, in *Proceedings of the 4th International Conference on Wireless Mobile Communication and Healthcare (MobiHealth 2014)*, Athens, Greece, November 2-5, 2014.
9. M. A. Davies, T. L. Schmitz and T. J. Burns, The Stability Of Milling: An Impact Oscillator With Delay, in *Proceedings of the 17th U.S. National Congress on Theoretical and Applied Mechanics*, Michigan State University, East Lansing, MI, June 15-20, 2014. (Special Symposium in Celebration of Francis C. Moon's 75th Birthday)
10. C. F. Ferraris, N. S. Martys, W. L. George, Development of Standard Reference Materials for Cement-Based Materials, in *Proceedings of the 5th North American Conference on the Design and Use of Self-Consolidating Concrete*, Chicago, IL, May 12-15, 2013.
11. J. T. Fong, N. A. Heckert, J. J. Filliben, P. V. Marcal and S. W. Freiman, A New Approach to Finding a Risk-Informed Safety Factor for "Fail-Safe" Pressure Vessel and Piping Design, in *Proceedings of the 2014 International Symposium on Structural Integrity (ISSI)*, Lanzhou, China, August 20-23, 2014, 3-23.
12. J. T. Fong, N. A. Heckert, J. J. Filliben, L. Ma, K. F. Stupic, K. E. Keenan and S. E. Russek**,** A Design-of-Experiments Approach to FEM Uncertainty Analysis for Optimizing Magnetic Resonance Imaging RF Coil Design, in *Proceedings of 2014 International COMSOL Users Conference*, Boston, MA, October 8-10, 2014.
13. L. Ghandehari, J. Czerwonka, Y. Lei, S. Shafiee, R. N. Kacker and R. Kuhn, An Empirical Comparison of Combinatorial and Random Testing, in *Proceedings of 3rd International Workshop on Combinatorial Testing*, Cleveland, OH, March 31-April 4, 2014, 68-77.
14. L. Ghandehari, Y. Lei, D. Kung, R. N. Kacker, R. Kuhn, Fault Localization Based On Failure-Inducing Combinations, in *Proceedings of 24th IEEE International Symposium on Software Reliability Engineering* (ISSRE2013), Pasadena, CA, November 4-7, 2013, 168-177.

15. W. Griffin and M. Olano, Objective Image Quality Assessment of Texture Compression, in *Proceedings of the 2014 ACM SIGGRAPH Symposium on Interactive 3D Graphics and Games (I3D)*, San Franciso, CA, March 2014, 119-126.

16. X. Guan, K. Bartschat, B. I. Schneider and L. Koesterke, Effects of Autoionizing States on Two-Photon Double Ionization of the H_2 Molecule, in *Proceedings of the XXVIII International Conference on Photonic, Electronic and Atomic Collisions* (ICPEAC 2013) Journal of Physics: Conference Series **488** (2014), 012024.

17. J. Hagedorn, K. Sayrafian, K. Yazdandoost and J. Terrill, A 4D Immersive Platform to Visualize RF Propagation in BAN, in *Proceedings of the 8th European Conference on Antennas & Propagation* (EuCAP 2014), Den Hague, Netherlands, April 6-11, 2014.

18. P. S. Kuo, J. S. Pelc, O. Slattery, L. Ma and X. Tang, Domain-Engineered PPLN for Entangled Photon Generation and Other Quantum Information Applications, in *Nonlinear Optics and Its Applications VIII and Quantum Optics III* (B. J. Eggleton, et al., eds.), Proceedings of the SPIE **9136** (2014), 913403.

19. R. J. La, Role of Network Topology in Cybersecurity, in *Proceedings of IEEE Conference on Decision and Control (CDC)*, Los Angeles, CA, December 2014.

20. Y.-K. Liu, Building One-Time Memories from Isolated Qubits, in *Proceedings of the 5th Conference on Innovations in Theoretical Computer Science* (ITCS 2014), Princeton, NJ, January 12-14, 2014, 269-286.

21. Y.-K. Liu, Single-Shot Security for One-Time Memories in the Isolated Qubit Model, in *Advances in Cryptology – CRYPTO 2014*, Lecture Notes in Computer Science **8617** (2014), 19-36.

22. H. Mahboubi, A. Aghdam, K. Sayrafian, Efficient Field Coverage in Mobile Sensor Networks: A CPS Perspective, in *Proceedings of the International Workshop on Robotic Sensor Networks*, CPS Week 2014, Berlin, Germany, April 13-17, 2014.

23. V. Marbukh, On Systemic Risk in the Cloud Computing Model, in *Proceedings of the 2014 26th International Teletraffic Congress (ITC)*, Karlskrona, Sweden, September 9-11, 2014.

24. V. Marbukh, K. Sayrafian, M. Barbi, and M. Alasti, Inter-BAN Interference Mitigation: A Correlated Equilibrium Perspective, in *pHealth'14: Proceedings of 11th International Conference on Wearable Micro and Nano Technologies for Personalized Health* (2014), 111-115.

25. B. R. Miller, D. I. Ginev, S. Oprea, E-Books and Graphics with LaTeXML E-Books and Graphics with LaTeXML, in *Proceedings of Conference on ntelligent Computer Mathematics, Coimbra, Portugal, July 7--11, 2014* (S. M. Watt, et al. eds.) Lecture Notes in Artificial Intelligence **8543** (2014), 427-430.

26. K. Mills, C. Dabrowski, J. Filliben and S. Ressler, Combining Genetic Algorithms and Simulation to Search for Failure Scenarios in System Models, in *Proceedings of the 5th International Conference on Advances in Simulation* Venice, Italy (2013), 81.

27. A. Mink and A. Nakassis, LDPC Error Correction for Gbit/s QKD, in *Defense Security & Sensing*, Proceedings of the SPIE **9123**, (2014), 912304.

28. A. Nakassis and A. Mink, Polar Codes in a QKD Environment, in *Defense Security & Sensing*, Proceedings of the SPIE **9123**, (2014), 912305.

29. S. Ressler and K. Leber, Web Based 3D Visualization and Interaction for Whole Body Laser Scans, in *Proceedings of the International Conferences on 3D Body Scanning Technologies* (2013), 166-172.

30. B. Saunders, Q. Wang and B. Antonishek, Adaptive Composite B-Spline Grid Generation for Interactive 3D Visualizations, in *Proceedings of MASCOT/ISGG 2012 International IMACS/ISGG and Biannual Conference of Grid Generation*, Las Palmas de Gran Canaria, Spain, October 22-26, 2012, IMACS Series in Computational and Applied Mathematics **18** (2014), 241-250.

31. K. Sayrafian, J. Hagedorn, M. Barbi, J. Terrill and M. Alasti, A Simulation Platform to Study Inter-BAN Interference, in *Proceedings of the 4th IEEE International Conference on Cognitive Infocommunications (IEEE CogInfocom 2013)* (2013), 345-350.

32. B. I. Schneider, L. A. Collins, X. Guan, K. Bartschat and D. Feder, Time-Dependent Computational Methods for Matter Under Extreme Conditions, Advances in *Proceedings of the 240 Conference: Science's Great Challenges*, (A. Dinner, ed.), Advances in Chemical Physics **157** (2014), 195-214.

33. V. Stanford, L. Diduch, A. Fillinger, K. Sayrafian, Connecting Medical Devices through ASTM-2761-09: Schedule Conflict Detection Prototype, in *Proceedings of the 4th Conference on Wireless Health* (2013), 20.

34. N. Yarkony, K. Sayrafian and A. Possolo, Energy Harvesting from the Human Leg Motion, in *Proceedings of the 8th International Conference on Pervasive Computing Technologies for Healthcare* (Pervasive Health 2014), Oldenburg, Germany, May 20-23, 2014, 88-92.

35. L. Yu, F. Duan, Y. Lei, R. N. Kacker, D. Richard Kuhn, Using Minimum Invalid Tuples to Handle Constraints for Combinatorial Testing of Software Product Lines, in *Proceedings of 15th IEEE International Symposium on High Assurance Systems Engineering* (HASE 2014) , Miami, FL, January 9-11, 2014.

Technical Magazine Articles

1. R. Datla and R. N. Kacker, Metrological Traceability And Remote Sensing Measurements, *GSICS Global Space-based Inter-Calibration System – GSICS, Quarterly Newsletter* **7:4** (2014).

2. Y.-K. Liu, Quantum Information: Show, Don't Tell, *Nature Physics* **10**:9 (2014), 625–626.

Technical Reports

1. R. F. Boisvert (ed.), Applied and Computational Mathematics Division, Summary of Activities for Fiscal Year 2013, NISTIR 7994, March 2014.

2. H. Guan, A. Dienstfrey, M. Theofanos and B. Stanton, A Measurement Metric For Latent Fingerprint Processing, NISTIR 8017, July 2014.

3. F. Y. Hunt, The Structure of Optimal and Near Optimal Target Sets in Consensus Models, NIST Special Publication 500-303, August 6, 2014.

4. J. C. Wu, A. F. Martin, C. S. Greenberg and R. N. Kacker, Measurement Uncertainties of Three Score Distributions and Two Thresholds with Data Dependency, NISTIR 8025, September, 2014.

Accepted

1. A. Anandkumar, D. P. Foster, D. Hsu, S. M. Kakade and Y.-K. Liu, A Spectral Algorithm for Latent Dirichlet Allocation, *Algorithmica*.

2. T. J. Burns, S. P. Mates, R. L. Rhorer, E. P. Whitenton and D. Basak, Inverse Method for Estimating Shear Stress in Machining, *Journal of the Mechanics and Physics of Solids*.

3. J. Chen, J. Terill, H. Zhao, G. Zhang, K. Wu, A. Garbrino and Y. Zhu, Interactive Visual Computing Laboratory Research, IEEE Virtual Reality, Arles, Camargue, Provence, France, March 23-27, 2015.

4. J. Chen, H. Zhao, W. Griffin, J. Terrill and G. Bryant, Validation of Split Vector Encoding and Stereoscopy for Quantitative Visualization of Quantum Physics Data in Virtual Environments, VR2015 IEEE Virtual Reality, Arles, Camargue, Provence, France, March 23-27, 2015.

5. R. Datla and R. N. Kacker, Calibration Considerations for Mission Success, *NIST Handbook: Guidelines for Radiometric Calibration of Electro-Optical Instruments for Remote Sensing.*

6. G. Doğan, An Efficient Curve Evolution Algorithm for Multiphase Image Segmentation, International Conference on Energy Minimization Methods in Computer Vision and Pattern Recognition (EMMCVPR), Hong Kong, January 13-16, 2015.

7. W. Griffin, D. Catacora, S. Satterfield, J. Bullard, J. Terrill, Incorporating D3.js Information Visualization into Immersive Virtual Environments (poster), IEEE Virtual Reality, Arles, France, March 23-27, 2015.

8. J. D. Hagar, R. Kuhn, R. N. Kacker, T. L. Wissink, Introducing Combinatorial Testing to a Large System-Software Organization, *IEEE Computer.*

9. E. Knill, S. Glancy, S. W. Nam, K. Coakley and Y. Zhang, Bell Inequalities for Continuously Emitting Sources, *Physical Review A*.

10. H. S. Ku, W. F. Kindel, F. Mallet, S. Glancy, K. D. Irwin, G. C. Hilton, L. R. Vale and K. W. Lehnert, Generating and Verifying Entangled Itinerant Microwave Fields with Efficient and Independent Measurements, *Physical Review A*.

11. R. J. La, Interdependent Security with Strategic Agents and Global Cascades, *IEEE/ACM Transactions on Networking*.

12. J. F. Lawrence, R. N. Kacker and R. Kessel, Obtaining a Trapezoidal Distribution, *Communications in Statistics – Theory and Methods.*

13. H. Mahboubi, A. Aghdam, and K. Sayrafian, Self-deployment Algorithms for Coverage Improvement in Mobile Sensor Networks in Presence of Obstacles, in *Control and Systems Engineering - A Report on Decades of Contribution*.

14. R. F. Sekerka, S. R. Coriell and G. B. McFadden, Morphological Stability, in *Handbook of Crystal Growth*.

15. S. Weiss, A. Boliong and H. S. Cohl, Measurement and Analysis of the Lowest Resonant Mode of a Spherical Annular-Sector Patch Antenna, *IET Microwaves, Antennas & Propagation*.

In Review

1. D. A. Anderson, J. B. Benson and A. J. Kearsley, Foundations of Modeling in Cryobiology - II: Heat and Mass Transport in Bulk and at Cell Membrane and Ice-Liquid Interfaces.
2. M. A. Baeder, H. S. Cohl and H. Volkmer, Generalizations of Generating Functions for Higher Continuous Hypergeometric Orthogonal Polynomials in the Askey Scheme.
3. I. Beichl and Y. Kemper, Monte Carlo Methods to Approximate the Chromatic Polynomial.
4. J. Bernal, NEURBT: A Program for Computing Neural Networks for Classification using Batch Learning.
5. A. S. Carasso, Stable Explicit Time Marching In Well-Posed and Ill-Posed Nonlinear Parabolic Equations.
6. A. S. Carasso and A. E. Vladar, Recovery of Background Structures in Nanoscale Helium Ion Microscope Imagery.
7. H. S. Cohl and R. M. Palmer, Fourier and Gegenbauer Expansions for a Fundamental Solution of Laplace's Equation in Hyperspherical Geometry.
8. H. S. Cohl, R. S. Costas-Santos and P. R. Hwang, Generalizations of Generating Functions for Basic Hypergeometric Orthogonal Polynomials.
9. J. Diemunsch, M. Ferrara, S. Jahanbekam and J. Shook, Extremal Theorem for Packing a Degree Sequence with a Graph.
10. G. Doğan, J. Bernal and C. Hagwood, A Fast Algorithm for Elastic Shape Distances between Closed Planar Curves.
11. G. Doğan, J. Bernal and C. Hagwood, Fast Algorithm for Alignment of 2D Closed Curves with Application to Elastic Shape Analysis.
12. S. W. Fackler, M. J. Donahue, T. Gao, P. N. A. Nero, S.-W. Cheong, J. Cumings and I. Takeuchi, Locally Controlled Magnetic Anisotropy in Transcritical Permalloy Thin Films Using Ferroelectric $BaTiO_3$ Domains.
13. S. Fu, W. Cui, M. Hu, R. Chang, M. J. Donahue and V. Lomakin, Finite Difference Micromagnetic Solvers with Object Oriented Micromagnetic Framework on Graphics Processing Units.
14. Z. Gimbutas and L. Greengard, A Fast Multipole Method for the Evaluation of Elastostatic Fields in a Half-Space with Zero Normal Stress.
15. W. Griffin and M. Olano, Evaluating Texture Compression Masking Effects using Objective Image Quality Assessment Metrics.
16. A. Gueye, P. Mell, R. Harang and R. J. La, Moving Target Defenses with Security Checkpoints in IPv6 Networks.
17. A. Gueye and A. Lazska, Network Topology Vulnerability/Cost Tradeoff: Model, Application, and Computational Complexity.
18. A. Harvey, E. Simiu, F. A. Potra, K. Quinlan and N. Chokshi, Design-Basis Hurricane Winds and Missiles for Nuclear Power Plants.
19. S. P. Jordan, K. S. M. Lee and J. Preskill. Quantum Algorithms for Fermionic Quantum Field Theories.
20. R. N. Kacker, Probability Distributions and Coverage Probability in GUM, JCGM Documents, and Statistical Inference.
21. Y. Kemper and I. Beichl, Importance Sampling to Approximate the Coefficients of the Chromatic Polynomial.
22. R. J. La, Effects Of Degree Distributions On Network Security — Population Game Model.
23. S. A. Langer, A. C. E. Reid, F. Y. Congo, R. Lua and V. R. Coffman, Gtklogger: A Tool For Systematically Testing Graphical User Interfaces.
24. Y.-K. Liu, Privacy Amplification in the Isolated Qubits Model.
25. A. Luna, G. B. McFadden, M. I. Aladjem and K. W. Kohn, Predicted Role of NAD Utilization in the Control of Circadian Rhythms During DNA Damage Response.
26. F. Maggioni, F. A. Potra and M. Bertocchi, Stochastic Versus Robust Optimization for a Supply Transportation Problem.
27. H. Mahboubi, A. Aghdam and K. Sayrafian**,** Maximum Lifetime Strategy for Target Monitoring with Controlled Node Mobility in Sensor Networks with Obstacles.
28. H. Mahboubi, A. Aghdam and K. Sayrafian, A Joint Relocation and Sensing Range Algorithm to Improve Coverage and Lifetime in Wireless Mobile Sensor Networks.
29. H. Mahboubi, A. Aghdam and K. Sayrafian, An Energy-Efficient Target Tracking Strategy for Mobile Sensor Networks.
30. P. Mell, R. Harang, A. Gueye, The Resilience of the Internet to Colluding Country Induced Connectivity Disruptions.

31. J. L. Molaro, S. Byrne and S. A. Langer, Grain-Scale Thermoelastic Stresses and Spatiotemporal Temperature Gradients on Airless Bodies, Implications for Rock Breakdown.
32. A. Nucciotti, B. Alpert, M. Balata, D. Bennett, M. Biasotti, C. Boragno, C. Brofferio, V. Ceriale, M. De Gerone, M. Faverzani, E. Ferri, J. Fowler, F. Gatti, A. Giachero, M. Lusignoli, G. Hilton, U. Koester, M. Maino, J. Mates, S. Nisi, R. Nizzolo, G. Pessina, G. Pizzigoni, A. Puiu, S. Ragazzi, C. Reintsema, M. Ribeiro-Gomes, D. Schmidt, D. Schumann, M. Sisti, D. Swetz, F. Terranova and J. Ullom, The HOLMES Experiment.
33. A. K. Nurse, S. Colbert-Kelly, S.R. Coriell and G. B. McFadden, Equilibrium and Stability of Axisymmetric Drops on a Conical Substrate under Gravity.
34. J. Penczek, S. G. Satterfield, E. F. Kelley, D. G. Hulme, T. Scheitlin, J. Terrill and P. A. Boynton, Evaluating the Visual Performance of Stereoscopic Immersive Display Systems.
35. F. A. Potra, Sufficient Weighted Complementarity Problems.
36. S. Pourarian, J. Wen, A. J. Kearsley and A. Pertzborn, Efficient and Robust Optimization for Building Energy Simulation.
37. R. Pozo, Q-Matrix: An Algebraic Formulation for the Analysis and Visual Characterization of Network Graphs.
38. M. Schubotz, A. Youssef, V. Markl, H. S. Cohl and J. J. Li, Evaluation of Similarity-Measure Factors for Formulae based on the NTCIR-11 Math Task.
39. J. Shook and I. Beichl, Matrix Scaling: A New Heuristic for the Feedback Vertex Set Problem.
40. J. Sifuentes, Z. Gimbutas and L. Greengard, Randomized Methods for Rank-Deficient Linear Systems.
41. J. Stoian, T. Oey, J. Huang, A. Kumar, J. W. Bullard, M. Balonis, S. G. Satterfield, J. Terrill, N. Neithalath and G. Sant, Prehydration of Ordinary Portland Cement and its Mitigation using Limestone: New Insights from Experiments and Simulations.
42. A. Streib, N. Streib, I. Beichl and F. Sullivan, Stratified Sampling for the Ising Model — A Graph Theoretic Approach.
43. F. Vico, L. Greengard, M. Ferrando and Z. Gimbutas, The Decoupled Potential Integral Equation for Time-Harmonic Electromagnetic Scattering.

Invention Disclosures

1. A. S. Carasso and A. E. Vladar, Recovery Of Background Structures in Nanoscale Helium Ion Microscope Imagery, and the Use of Progressive Levy Fractional Diffusion Smoothing, NIST Office of Technology Partnerships, May 2013.

Presentations

Invited Talks

1. B. Alpert, "Efficiency-Enhanced Hybrid Gauss-Trapezoidal Quadrature Rules," Integral Equations Methods: Fast Algorithms and Applications, Banff International Research Station, December 9, 2013.
2. B. Alpert, "Mathematical Challenges in High-Throughput Microcalorimeter Spectroscopy," IMA Workshop on Math Modeling in Industry, Vancouver, B.C., August 6, 2014.
3. R. F. Boisvert, "Measurement Science for Information Systems," Bell Labs – NIST Workshop on Large Scale Networks, Alcatel-Lucent Bell Laboratories, Murray Hill, NJ, October, 25, 2013.
4. R. F. Boisvert, "Network Science at NIST," Joint University of Maryland – NIST Workshop in Network Science, College Park, MD, January 24, 2014.
5. R. F. Boisvert, "Computer Science Research in a Federal Lab," Department of Computer Science, George Washington University, March 28, 2014.
6. B. Cloteaux, "Information and Heuristics Creation," Mathematics Colloquium, George Mason University, Fairfax, VA, November 8, 2013.
7. B. Cloteaux, "Information and Heuristics Creation," Statistics Colloquium, George Mason University, Fairfax, VA, November 15, 2013.
8. H. S. Cohl, "Generalizations of Generating Functions for Orthogonal Polynomials in the Askey and q-Askey Schemes Analysis," Departamento de Matematica, Universidade de Coimbra, Portugal, July 9, 2014.
9. H. S. Cohl, M. Baeder, P. R. Hwang and H. Volkmer, "Generalizations of Orthogonal Polynomials in Askey Schemes," Department of Mathematics and Statistics Colloquium, American University, Washington, DC, April 15 2014.
10. H. S. Cohl, "Outgrowths of the Digital Library of Mathematical Functions Project: NIST Digital Repository of Mathematical Formulae," Challenges in 21st Century Experimental Mathematical Computation Conference, Institute for Computational and

Experimental Research in Mathematics, Brown University, Providence, RI, July 21, 2014.

11. H. S. Cohl, "XSEDE and the NIST Digital Repository of Mathematical Formulae," XSEDE Science Gateways Community Series, August 29, 2014.
12. S. Colbert-Kelly, "A Generalized Ginzburg-Landau model in a Planar Geometry," Department of Mathematical Sciences Colloquium, New Mexico State University, Las Cruces, NM, November 14, 2013.
13. S. Colbert-Kelly, "A Generalized Ginzburg-Landau model in a Planar Geometry," Howard University Mathematics Colloquium, Howard University, Washington, D.C., March 21, 2014.
14. S. Colbert-Kelly, "A Generalized Ginzburg-Landau model in a Planar Geometry," Applied and Computational Mathematics Seminar, George Mason University, Fairfax, VA, May 2, 2014.
15. G. Doğan, "Shape Optimization for Image Analysis," Applied and Computational Mathematics Seminar, George Mason University, Fairfax, VA, April 11, 2014.
16. J. T. Fong, "A Risk-informed and Continuous-Monitoring Approach to Fail-Safe Operation of Aging Pressure Vessels and Piping," China National Conference on Pressure Vessel Technology, Hefei, China, November 9, 2013.
17. J. T. Fong, "A Fail-Safe Design and Operation Methodology Based on Lessons Learned from the 2011 Fukushima Reactor Meltdown Incident," University of California-Irvine and National Academy of Engineering Joint Meeting on the Materials Genome, Beckman Center, Irvine, CA, February 11, 2014.
18. J. T. Fong, "Uncertainty Analysis of A Class of FEM-based Solutions Using the COMSOL Radio Frequency (RF), and MEMS Modules," Electromagnetics Division, NIST, Boulder, CO, April 3, 2014.
19. J. T. Fong, "Uncertainty Estimation and Model Validation for NDE-Based Electromagnetics Solutions Using ABAQUS and COMSOL," Department of Civil and Environmental Engineering, University of South Carolina, Columbia, SC, May 1, 2014.
20. J. T. Fong, "A New Approach to Risk-based Definition of Engineering Safety Factors Using (1) the Bootstrap Method to Estimate the Weibull Location Parameter, and (2) The Lower Tolerance Limit to Estimate a Safety Factor," Department of Statistics, University of South Carolina, Columbia, SC, May 2, 2014.
21. J. T. Fong, "Multi-Scale Modeling, Uncertainty Estimation, and Model Validation for Predicting Remaining Life of Aging Structures and Components," VTD/Mechanics Division, U.S. Army Research Laboratory, Aberdeen Proving Ground, MD, May 7, 2014.
22. J. T. Fong, "A Fail-Safe Approach to Risk-Informed Modeling of Fatigue of Aging Structures and Components," ICCES Lifetime Achievement Medal Award Lecture, International Conference on Computational and Experimental Sciences and Engineering, Changwon, South Korea, June 14, 2014.
23. J. T. Fong, "Automated Massive NDE Image Analysis, and Feature Abstracting for Fatigue Modeling of Aging Structures," 41st Quantitative Nondestructive Evaluation (QNDE) Meeting, Boise, ID, July 22, 2014.
24. J. T. Fong, "Model Selection and Experimental Design for NDE Engineers," Department of Mechanical and Power Engineering, Lanzhou University of Technology, Lanzhou, China, August 18, 2014.
25. J. T. Fong, "A New Approach to Finding a Risk-Informed Safety Factor for Fail-Safe Pressure Vessel and Piping Design," International Symposium on Structural Integrity, Lanzhou, China, August 21, 2014.
26. J. T. Fong, "Multi-Scale Modeling, Uncertainty Estimation, and Model Validation for Designing New Materials and Predicting Fatigue Life of Aging Structures," NASA Glenn Research Center, Cleveland, OH, September 10, 2014.
27. J. T. Fong, "Uncertainty Quantification in Fatigue and Risk Modeling," U.S. Army Research Laboratory, Aberdeen Proving Ground, MD, September 12, 2014.
28. S. Glancy, "Bell Inequalities for Time-tagged Detections," Quantum Theory: from Problems to Advances, Linnéuniversitetet, Växjö, Sweden, June 9, 2014.
29. A. Gueye, "Science-Based Metrics for Network Topology Resilience against Attacks," Mathematical Sciences Colloquium, College of Sciences, George Mason University, Fairfax, VA, October 18, 2013.
30. F. Hunt, "Optimal and Near Optimal Sets for the Spread of Consensus in a Network Model," Joint University of Maryland – NIST Workshop in Network Science, College Park, MD, January 24, 2014.
31. A. J. Kearsley, "Optimization and Chemical Spectroscopy at NIST," SIAM Student Chapter Meeting, University of Delaware, February 28, 2014.

32. E. Knill, "Certifying Violations of Local Realism," Southwestern Quantum Information Technology Workshop (SQUINT), February 22, 2014.
33. E. Knill, "Certifying Violations of Local Realism," Workshop on Quantum Information and Computer Science, College Park, MD, April 1, 2014.
34. P. S. Kuo, "Second-Harmonic Generation in GaAs Whispering-Gallery-Mode Microcavities," QIBEC Seminar, NIST, Gaithersburg, MD, February 18, 2014.
35. R. J. La, "Cascades in Interdependent Security with Strategic Players," Information Theory and Applications (ITA) Workshop, San Diego CA, February 2014.
36. Y.-K. Liu, "Tamper-Resistant Cryptographic Hardware in the Isolated Qubits Model," 4th International Conference on Quantum Cryptography (QCrypt 2014), Paris, France, September 1-5, 2014.
37. G. B. McFadden, "Bubble Motion and Size Variation during Thermal Migration with Phase Change," Materials Science and Technology 2013, Montreal, Canada, October 28, 2013.
38. D. G. Porter, "State of Tcl", 21st Annual Tcl/Tk Conference, Portland, OR, November 13, 2014.
39. F. A. Potra, "Weighted Complementarity Problems," AMS Spring Eastern Sectional Meeting, UMBC, Baltimore, MD, March 29-30, 2014.
40. R. Pozo, "A Network Measure for the Analysis of Large-Scale Graphs," Joint University of Maryland – NIST Workshop in Network Science, College Park, MD, January 24, 2014.
41. R. Pozo, "A Network Measure For The Analysis Of Large-Scale Graphs," Applied Dynamics Seminar, University of Maryland, College Park, MD, March 27, 2014.
42. S. Ressler, "Declarative 3D Graphics for the Web, Integrating X3DOM, jQuery, WebGL and HTML5," Gettysburg College, Gettysburg, PA, October 10, 2013.
43. S. Ressler, "What's That 3D Model Doing in my Web Browser?" NIST Model-Based Enterprise Summit 2014, Gaithersburg, MD, December 17, 2014.
44. K. Sayrafian, "A 4D Immersive Platform to Visualize RF Propagation in BAN", the 8th European Conference on Antennas & Propagation (EuCAP 2014), Den Hague, Netherlands, April 6-11, 2014.
45. K. Sayrafian, "A Simulation Platform to Study Inter-BAN Interference", IEEE International Conference on Cognitive Infocommunications, Budapest, Hungary, December 2-5, 2013.
46. J. Shook, "Threshold Digraphs," Combinatorics Seminar, George Mason University, VA, April 18, 2014.
47. J. Shook, "Matrix Scaling: A New Heuristic for the Feedback Vertex Set Problem," Mathematical Sciences Colloquium, George Mason University, VA, April 18, 2014.
48. J. Shook, "Matrix Scaling: A New Heuristic for the Feedback Vertex Set Problem," Discrete Mathematics Seminar, University of Colorado at Denver, CO, April 28, 2014
49. J. Terrill, "Science," Keynote Lecture, 25th Annual Females in Science and Technology Conference, Montgomery Blair High School, Silver Spring, MD, March 22, 2014.
50. J. Terrill, "Parallel Universes, Perpendicular Thinking, and Scientific Results," Keynote Lecture, Effective Visualization for Science and eResearch, Melbourne, Australia, March 29, 2014.

Conference Presentations

1. B. Antonishek, "Look Ma—no Plug-in! (DLMF's New WebGL 3D Figures)," Web3D 2014, 19th International Conference on 3D Web Technology, Vancouver, Canada, August 10, 2014.
2. T. Bednarz, J. A. Taylor, W. Huang, W. Griffin, L. S. G. Satterfield, J. G. Hagedorn, J. Terrill, "High-Performance Visualization in Science and Research," Practitioner Experiences Poster Track, IEEE Vis 2014, Paris France, November 9-14, 2014.
3. H. S. Cohl, "Digital Repository of Mathematical Formulae," Conferences on Intelligent Computer Mathematics, Coimbra, Portugal, July 10, 2014.
4. H. S. Cohl, M. Baeder and H. Volkmer, "Generalizations of Generating Functions for Hypergeometric and Q-Hypergeometric Orthogonal Polynomials," Spring American Mathematical Society Central Sectional Meeting, Texas Tech University, Lubbock, Texas, April 11, 2014.
5. S. Colbert-Kelly, "Analysis of Point Defects in a Ferroelectric Liquid Crystal Using a Generalized Ginzburg-Landau Model," 2013 SIAM Conference on Analysis of Partial Differential Equations, Lake Buena Vista, FL, December 8, 2013.
6. G. Doğan, "Segmentation of Microstructure Images," Material Knowledge Systems Workshop, NIST, Gaithersburg, MD, January 13, 2014.

7. G. Doğan, "A Fast Algorithm to Compute the Shape Dissimilarity of Elastic Curves," 13th Copper Mountain Conference on Iterative Methods, Copper Mountain, CO, April 9, 2014.
8. G. Doğan, "An Adaptive Shape Reconstruction Algorithm for Inverse Problems," SIAM Conference on Imaging Science, Hong Kong, May 12, 2014.
9. G. Doğan, "Minimization of Curvature Energies with Applications in Image Processing," International Conference on Advances in Applied Mathematics and Mathematical Physics (ICAAMMP), Istanbul, Turkey, August 19, 2014.
10. G. Doğan, "A Python Toolbox for Shape Optimization in Image Processing," European Conference on Python in Science (EuroScipy), Cambridge, UK, August 28, 2014.
11. M. Donahue, "A Fourth Order Demagnetization Tensor for Rectangular Prisms," 58th Annual Magnetism and Magnetic Materials Conference, Denver, CO, November 6, 2013.
12. M. Donahue, "Implementation of a Localized Fourth Order Demagnetization Tensor," 59th Annual Magnetism and Magnetic Materials Conference, Honolulu, HI, November 5, 2014.
13. Z. Gimbutas and A. Dienstfrey, "MRI simulators and their Performance," NIST Workshop on Standards for Quantitative MRI, NIST, Boulder, CO, July 16, 2014.
14. Z. Gimbutas, "Interpolation and Integration in Spaces of Singular Functions," Workshop 13w5044, Integral Equations Methods: Fast Algorithms and Applications, Banff International Research Station for Mathematical Innovation and Discovery (BIRS), Banff, Canada, December 9, 2013.
15. S. Glancy, "Practical and Fast Gaussian State Estimation," Southwest Quantum Information Technology (SQUINT) Workshop, Sante Fe, NM, February 22, 2014.
16. W. Griffin and M. Olano, "Objective Image Quality Assessment of Texture Compression," ACM SIGGRAPH Symposium on Interactive 3D Graphics and Games (I3D), San Franciso, CA, March 15, 2014.
17. X. Guan, K. Bartschat, B. I. Schneider and L. Koesterke, "Two-Photon Double-Ionization of the H_2 Molecule in Light Perpendicular to the Internuclear Axis: Effects of Pulse Duration," 45th Annual Meeting of the APS Division of Atomic, Molecular and Optical Physics, Madison, WI, June 2–6, 2014.
18. A. Gueye, A. Lazska, "Network Topology Robustness under Adversarial Environment and Budget Constraints: General Model and Computational Complexity", GameSec 2013, Fort Worth, TX, November 11-12, 2013.
19. R. N. Kacker "Coverage Probability in GUM, GUM-S1, VIM, and Statistical Inference," International Workshop on Mathematics and Statistics for Metrology (MATHMET-2014), Berlin, Germany, March 24-26, 2014.
20. P. S. Kuo, "Spectral Response and Characterization of a High-Efficiency Upconvertor for Single-Photon-Level Detection," Single Photon Workshop, Oak Ridge, TN, October 18, 2013.
21. P. S. Kuo, "Polarization-Entangled Photons from Domain-Engineered, Periodically Poled LiNbO3," CLEO Conference, San Jose, CA, June 9, 2014.
22. R. J. La, "Role of Network Topology in Cybersecurity," IEEE Conference on Decision and Control (CDC), Los Angeles, CA, December 17, 2014.
23. Y.-K. Liu, "Building One-Time Memories from Isolated Qubits," 5th Conference on Innovations in Theoretical Computer Science (ITCS 2014), Princeton, NJ, January 12-14, 2014.
24. Y.-K. Liu, "Single-Shot Security for One-Time Memories in the Isolated Qubits Model," 17th Conference on Quantum Information Processing (QIP 2014), Barcelona, Spain, February 3-7, 2014.
25. Y.-K. Liu, "Single-Shot Security for One-Time Memories in the Isolated Qubits Model," 34rd International Cryptology Conference (CRYPTO 2014), Santa Barbara, CA, August 17-21, 2014.
26. D. W. Lozier, "Outgrowths of the Digital Library of Mathematical Functions Project Part 1: DLMF Standard Reference Tables," ICERM Workshop on Challenges in 21st Century Experimental Mathematical Computation, Providence, RI, July 21, 2014.
27. V. Marbukh, "On Systemic Risk in the Cloud Computing Model," 26th International Teletraffic Congress (ITC 26), Karlskrona, Sweden, September 9-11, 2014.
28. V. Marbukh, K. Sayrafian, M. Barbi and M. Alasti, "Inter-BAN Interference Mitigation: A Correlated Equilibrium Perspective," 11th International Conference on Wearable Micro and Nano Technologies for Personalized Health (pHealth'14), Vienna, Austria, June 11-13, 2014.
29. N. S. Martys, D. Lootens, W. L. George, P. Hebraud and M. Liard, "Universal Scaling Of Microscopic

And Macroscopic Behavior In Spherical Non-Colloidal Suspensions With A Non-Newtonian Fluid Matrix," Society of Rheology 85th Annual Meeting, Montreal, Quebec, Canada, October 13-17, 2013.

30. G. B. McFadden, "A Cross-Benchmarking and Validation Initiative for Tokamak 3D Equilibrium Calculations," 56th Annual Meeting of the APS Division of Plasma Physics, New Orleans, LA, October 28, 2014.
31. B. R. Miller, D. I. Ginev, S. Oprea, E-Books and Graphics with LaTeXML, Conference on Intelligent Computer Mathematics, Coimbra, Portugal, July 10, 2014.
32. W. F. Mitchell, "Recent Advances in PHAML," SIAM Conference on Parallel Processing for Scientific Computing, Portland, OR, February 18, 2014.
33. W. F. Mitchell and M. A. McClain, "Performance of *hp*-Adaptive Strategies for Elliptic Partial Differential Equations," 12th International Conference of Numerical Analysis and Applied Mathematics, Rhodes, Greece, September 24, 2014.
34. W. F. Mitchell and M. A. McClain, "Performance of *hp*-Adaptive Strategies for Elliptic Partial Differential Equations," International Conference on Spectral and High Order Methods, Salt Lake City, UT, June 24, 2014.
35. R. Pozo, "Extending Q-Matrix Frameworks for Generalized Network Centralities," SIAM Workshop on Network Science, Chicago, IL, July 7, 2014.
36. S. Ressler, "Web Based 3D Visualization and Interaction for Whole Body Laser Scans," Hometrica 2013 3D Body Scanning Technologies Conference, Long Beach, CA, Nov 2013.
37. S. Ressler and B. Antonishek, "New WebGL graphics in the NIST DLMF," Web3D Emerging Technology Showcase, Virginia Tech Research Center, Arlington, VA, March 25, 2014.
38. S. Ressler, "Web 3D Showcase," Web3D 2014, Vancouver, Canada, August 11, 2014.
39. B. Rust and K. Mullen, "The Metrology of Supernova Lightcurves," 223rd Meeting of the American Astronomical Society, Washington, DC, January 6, 2014.
40. B. Rust and M. Leventhal, "Evidence for Accelerated Radioactive Decay (ARD) Models of Supernova Lightcurves in the Low Redshift Universe," 224th Meeting of the American Astronomical Society, Boston, MA, June 2, 2014.
41. B. Rust, "The Metrology of Type Ia Supernova Lightcurves," 225th Meeting of the American Astronomical Society, Seattle, WA, January 5, 2015.
42. B. Saunders, "Using Adaptive Composite B-Spline Grid Generation to Enhance 3D Web Visualizations," SIAM Conference on Geometric and Physical Modeling (GD/SPM13), Denver, CO, November 14, 2013.
43. B. Saunders, "WebGL: Interactive 3D Graphics on the Web without a Plugin," MAA MD-DC-VA Spring Section Meeting, James Madison University, Harrisonburg, VA, April 26, 2014.
44. B. Saunders, Q. Wang, B. Antonishek, B. Miller, "Adaptive Composite B-Spline Mesh Generation for 3D Visualization," 8th International Conference on Curves and Surfaces, Paris, France, June 17, 2014.
45. K. Sayrafian, "Efficient Field Coverage in Mobile Sensor Networks: A CPS Perspective," International Workshop on Robotic Sensor Networks, CPS Week, Berlin. Germany, April 14, 2014.
46. K. Sayrafian, "Energy Harvesting from Human Leg Motion," 8th International Conference on Pervasive Computing Technologies for Healthcare (Pervasive Health 2014), Oldenberg, Germany, May 21, 2014.
47. K. Sayrafian, "Uncoordinated Strategies for Inter-BAN Interference Mitigation," IEEE 25th Annual International Symposium on Personal, Indoor and Mobile Radio Communications (PIMRC 2014), Washington, DC, September 2, 2014.
48. K. Sayrafian, "Maximizing Output Power of a CFPG Micro Energy-Harvester for Wearable Medical Sensors," 4th International Conference on Wireless Mobile Communication and Healthcare (MobiHealth 2014), Athens, Greece, November 5, 2014.
49. B. I. Schneider, "Novel Numerical Approaches to Solving the Time-Dependent Schrödinger's Equation," Concepts of Mathematical Physics in Chemistry, Playa del Carmen, Quintana Roo, México, December 10, 2014.
50. J. Terrill, "Immersive Visualization at NIST, Birds of a Feather (BOF)," Immersive Visualization for Science and Research, 41st International Conference and Exhibition on Computer Graphics and Interactive Technologies, SIGGRAPH 2014, August 11, 2014, Vancouver, CA.

Poster Presentations

1. T. Bednarz, J. A. Taylor, W. Huang, W. Griffin, S. G. Satterfield, J. G. Hagedorn and J. Terrill, "High-Performance Visualization in Science and Research," Practitioner Experiences Poster Track, IEEE Vis 2014, Paris, France, November 9-14, 2014.
2. A. J. Kearsley, "Stochastic Regression Modeling of Noisy Spectra," PITTCON Conference and Expo, Chicago IL, March 4, 2014.
3. A. J. Kearsley, "Analysis of Chemical Spectra by Stochastic Regression, Stochastic Processes and Applications," Buenos Aires, Argentina, July 30, 2014.
4. P. S. Kuo, "Quantum Communications Research at NIST Information Technology Laboratory," Workshop on Quantum Information and Computer Science, College Park, MD, March 31, 2014.
5. A. Gueye and R. J. La, "Influence of Assortativity on Network Security," International Conference on Network Science (NetSci), Berkeley, CA, June 5, 2014.
6. V. Marbukh, "Systemic Risk/Benefits of Interconnectivity due to Metastability," International Conference on Network Science (NetSci), Berkeley, CA, June 5, 2014.
7. V. Marbukh, "Eigenvector Centrality Localization and Hierarchy of Important Spreaders in Large-Scale Networks," NetSci, Berkeley, CA, June 5, 2014.
8. P. Mell, R. Harang and A. Gueye, "The Resilience of the Internet to Colluding Country Induced Connectivity Disruptions," MPACT Week, University of Maryland, College Park, MD, October 17, 2014.

Web Services

1. Adaptive Mesh Refinement Benchmark Problems[30]: a collection of partial differential equations suitable for testing and benchmarking adaptive mesh refinement algorithms.
2. AnthroWeb3DMeasure[31]: A tool for Web3D based anthropometric visualization and measurement.
3. Digital Library of Mathematical Functions[32]: a repository of information on the special functions of applied mathematics.
4. DLMF Standard Reference Tables on Demand[33]: tables of values for special functions, with guaranteed accuracy to high precision.
5. Guide to Available Mathematical Functions[34]: a virtual repository of mathematical software components. (dormant)
6. Matrix Market[35]: a repository of matrices for testing of algorithms and software for numerical linear algebra. (dormant)
7. µMAG[36]: a collection of micromagnetic reference problems and submitted solutions.
8. SciMark[37]: a benchmark for scientific computing in Java. (dormant)

Software Released

1. ACTS[38]: Combinatorial test suite generation with support of constraints. Version 2.9 – Y. Lei, R. N. Kacker, D. R. Kuhn.
2. LaTeXML[39]: A LaTeX to XML converter. Version 0.8.0 – B. R. Miller.
3. OOF2[40]: Finite element modeling of material microstructures. Version 2.1.11 – S. Langer.
4. OOF3D[41]: Finite element modeling of material microstructures in 3D. Version 3.0.0 – S. Langer and Yannick Congo.
5. OOMMF[42]: Object Oriented MicroMagnetic Framework. Version 1.2a5bis — D. Porter and M. Donahue.
6. PHAML[43]: Solution of elliptic partial differential equations using finite elements, *hp*-adaptive refinement and multigrid methods. Version 1.14.0 – W. F. Mitchell.
7. Itcl: C++ inspired object oriented commands for Tcl. Versions 4.0.1, 4.0.2 – D. G. Porter.
8. sqlite3: Bindings to the SQLite database engine for Tcl. Versions 3.8.4.3, 3.8.5, 3.8.6, 3.8.7.1 – D. G. Porter.

[30] http://math.nist.gov/amr-benchmark
[31] http://math.nist.gov/~SRessler/x3dom/aw3dm.xhtml
[32] http://dlmf.nist.gov/
[33] http://dlmftables.uantwerpen.be/
[34] http://gams.nist.gov/
[35] http://math.nist.gov/matrixmarket/
[36] http://www.ctcms.nist.gov/mumag/mumag.org.html
[37] http://math.nist.gov/scimark/
[38] http://csrc.nist.gov/groups/SNS/acts/
[39] http://dlmf.nist.gov/LaTeXML/
[40] http://www.ctcms.nist.gov/oof/oof2/index.html
[41] http://www.ctcms.nist.gov/oof/oof3d/
[42] http://math.nist.gov/oommf/
[43] http://math.nist.gov/phaml/

9. Tcl/Tk[44]: Extensible scripting language and GUI toolkit. Versions 8.5.16, 8.5.17, 8.6.2, 8.6.3 – D. G. Porter.
10. TDBC: Database connection commands for Tcl. Versions 1.0.1, 1.0.2 - D. G. Porter.
11. Thread: Thread management commands for Tcl. Version 2.7.1 - D. G. Porter.

Conferences, Minisymposia, Lecture Series, Courses

ACMD Seminar Series

B. Cloteaux served as Chair of the ACMD Seminar Series. There were 22 talks presented during this period; all talks are listed chronologically.

1. M. Enriquez (MITRE), "*Systemizing the Solution of Simulation-Driven Optimization Problems,*" November 26, 2013.
2. H. Antil (George Mason University), "*Optimal Control of Free Boundary Problems with Surface Tension Effects,"* December 3, 2013.
3. S. Kimmel (MIT), "*Quantum Adversary Upper Bound,"* December 17, 2013.
4. G. Alagic (CalTech), "*Classical and Quantum Circuit Obfuscation,*" January 17, 2014.
5. H. Volksmer (University of Wisconsin-Milwaukee), "*Interior and Exterior Harmonics in a 5-Cyclidic Coordinate System,"* January 28, 2014.
6. J. Fish (NYU), "*Practical Multiscaling,*" February 12, 2014.
7. A. Makowski (University of Maryland), "*On the Intersection of Random Graphs with an Application to Random Key Pre-Distribution,*" February 26, 2014.
8. K. Sellers (Georgetown University), "*A Flexible Statistical Control Chart for Dispersed Count Data,*" March 4, 2014.
9. A. L. Tits (University of Maryland), "*Constraint Reduction for Linear and Convex Optimization,*" March 11, 2014.
10. R. Costas-Santos (Universidad de Alcala, Spain), "*An Overview of Classical Orthogonal Polynomials,*" March 25, 2014.
11. A. N. Vidyashankar (George Mason University), "*Dynamical Random Effects Driven Preferential Attachment Models,"* April 1, 2014.
12. M. Jarret (University of Maryland), "*Adiabatic Optimization and the Fundamental Gap Theorem,"* May 27, 2014.
13. D. Katz (Argonne National Labs), "*Parallel and Distributed Application Paradigms,*" May 30, 2014.
14. S. D. Casey (American University), "*The Analysis of Periodic Point Processes (Pi, the Primes, Periodicities, and Probability),"* June 3, 2014.
15. J. Shook (ACMD), "*Matrix Scaling: A New Heuristic for the Feedback Vertex Set Problem,"* June 10, 2014.
16. C. Monteleoni (George Washington University), "*Clustering Algorithms for Streaming and Online Settings,"* June 17, 2014.
17. M. Mascagni (Florida State University and ACMD), "*Random Number Generation Using Normal Numbers,"* June 24, 2014.
18. Y. Kemper (ACMD), "*Problems of Enumeration and Realizability on Matroids, Simplicial Complexes, and Graphs,"* August 6, 2014.
19. Y. Baryshnikov (University of Illinois), "*On the Dimension(s) of the Internet,"* August 13, 2014.
20. M. Beck (San Francisco State University), "*(Enumeration Results for) Signed Graphs,"* August 28, 2014.
21. H. Edelsbrunner (IST Austria), "*Approximation and Convergence of the First Intrinsic Volume,"* September 5, 2014.
22. R. Lehoucq (Sandia National Labs), "*A Computational Spectral Graph Theory Tutorial,"* September 17, 2014.

Conference Organization

1. H. S. Cohl, Member, Scientific Committee, 13th International Symposium on Orthogonal Polynomials, Special Functions, and Applications (OPSFA-13), Gaithersburg, MD, June 1-5, 2015.
2. H. S. Cohl, Co-Organizer, Orthogonal Polynomials and Special Functions Summer School 6, American University, Summer 2016.
3. A. Dienstfrey, Co-Chair, Program Committee, IMA Workshop on Uncertainty Quantification for Materials Modeling, (UQ4MM), West Lafayette, IN, July 2015.

[44] All releases made in role as Tcl Release Manager are available from http://sf.net/projects/tcl/files/Tcl/.

4. G. Doğan, Co-Organizer, Minisymposium on Manifolds, Shapes and Topologies in Imaging, SIAM Conference on Imaging Science, Hong Kong, May 12, 2014.
5. M. Donahue, Co-Organizer, Micromagnetics II session, Magnetism and Magnetic Materials Conference, Honolulu, HI, November 3-7, 2014.
6. W. Griffin, Publicity Chair, ACM SIGGRAPH Symposium on Interactive 3D Graphics and Games (I3D), San Francisco, CA, March 14-16, 2014.
7. W. Griffin, Publicity Chair, ACM SIGGRAPH Symposium on Interactive 3D Graphics and Games (I3D), San Francisco, CA, February 27 – March 1, 2015.
8. A. Gueye, Co-Organizer, UMD-NIST Workshop on Network Science, College Park, MD, January 24, 2014.
9. F. Hunt, Member, Organizing Committee, Infinite Possibilities Conference, Corvallis, OR, March 1-3, 2015.
10. S. Jordan and Y.-K. Liu, Co-Organizers, UMD-NIST Workshop on Quantum Information and Computer Science (QuICS), College Park, MD, March 31 – April 1, 2014.
11. R. N. Kacker, Co-Organizer, Member Program Committee, Third International Workshop on Combinatorial Testing (IWCT 2014), Cleveland Ohio March 30 - April 2, 2014.
12. P. S. Kuo, Member, Program Committee, CLEO Conference, Science & Innovations (S&I) Committee 4: Nonlinear Optical Technologies, San Jose, CA, June 8-13, 2014.
13. Y.-K. Liu, Member, Program Committee, 6th International Conference on Post-Quantum Cryptography (PQCrypto), Waterloo, Canada, October 1-3, 2014.
14. D. W. Lozier, Co-Chair, Scientific Committee, 13th International Symposium on Orthogonal Polynomials, Special Functions, and Applications (OPSFA-13), Gaithersburg, MD, June 1-5, 2015.
15. M. Mascagni, Co-Organizer, Minisymposium, "Monte Carlo Methods for Solving Partial Differential Equations," Ninth International Congress on Industrial and Applied Mathematics (ICIAM), 2015, Beijing, China.
16. M. Mascagni, Member, International Program Committee, International Conference on Computational Science (ICCS), Reykjavík, Iceland, June 1-3, 2015.
17. M. Mascagni, Member, International Program Committee for the International Conference on Computational Science (ICCS), Cairns, Australia, June 10-12, 2014.
18. M. Mascagni, Member, Technical Program Committee, SC14, New Orleans, LA, November 16-21, 2014.
19. M. Mascagni, Member, Emerging Technology Committee, SC14, New Orleans, LA, November 16-21, 2014.
20. B. R. Miller, Member, Program Committee, Conferences on Intelligent Computer Mathematics, University of Coimbra, Portugal, July 7-11, 2014.
21. B. R. Miller, Member, Program Committee, Conferences on Intelligent Computer Mathematics, Washington, DC, July 13-17, 2015.
22. B. R. Miller and A. Youssef, Co-Organizers, Conferences on Intelligent Computer Mathematics, Washington, DC, July 13-17, 2015.
23. W. F. Mitchell, Member, Scientific Committee, International Conference of Numerical Analysis and Applied Mathematics (ICNAAM), Rhodes, Greece, September 23-29, 2015.
24. Y. Parker and J. Terrill, Co-Organizers, NIST Booth, International Conference for High Performance Computing, Networking, Storage and Analysis (SC13), Denver, CO, November 18- 21, 2013.
25. Y. Parker and J. Terrill, Co-Organizers, NIST Booth, International Conference for High Performance Computing, Networking, Storage and Analysis (SC14), New Orleans, LA, November 17-20, 2014.
26. F. A. Potra, Co-Organizer, Nonlinear Programming Stream, 20th Conference of the International Federation of Operational Research Societies, Barcelona, Spain, July 13-18, 2014.
27. S. Ressler, Co-Organizer, Web3D Showcase, Web3D, Conference, Vancouver Canada, August 11, 2014.
28. K. Sayrafian, Member, Technical Program Committee, Symposium on Sensing, Propagation, and Wireless Networks for Healthcare Applications, Singapore, April 21-24, 2014.
29. K. Sayrafian, Member, Technical Program Committee, 8th International Symposium on Medical Information and Communication Technology (ISMICT 2014), Florence, Italy, April 2-4, 2014.
30. K. Sayrafian, Member, Technical Program Committee, IEEE Symposium on Computer

Applications and Industrial Electronics (ISCAIE 2014), Penang, Malaysia, April 7-8, 2014.

31. K. Sayrafian, Member, Technical Program Committee, 8th International Conference on Sensor Technologies and Applications (SENSORCOMM 2014), Lisbon, Portugal, November 16-20, 2014..
32. K. Sayrafian, Member, Technical Program Committee, 4th International Conference on the Internet of Things (IoT 2014), Cambridge, MA, October 6-8, 2014.
33. K. Sayrafian, Executive and Technical Program Committee Co-Chair, 25th IEEE Annual International Symposium on Personal, Indoor and Mobile Radio Communications (IEEE PIMRC), Washington, DC, September 2-5, 2014.
34. B. I. Schneider, Chair, Novel Hardware and Software Paradigms Track**,** XXVI IUPAP Conference on Computational Physics, Boston, MA, August, 11-14, 2014.
35. X. Tang, Program Committee, Quantum Communications and Quantum Imaging XII (OP415), SPIE Optics and Photonics Conference, San Diego, CA, August 9-13, 2015.
36. J. Terrill and T. Bednarz, Co-Organizers, Immersive Visualization for Science and Research Birds of a Feather (BOF) Session, 41st International Conference and Exhibition on Computer Graphics and Interactive Technologies (SIGGRAPH 2014), Vancouver, Canada, August 13, 2014.

Other Professional Activities

Internal

1. I. Beichl, Co-Director, ITL Summer Undergraduate Research Fellowship (SURF) Program, 2014.
2. R. F. Boisvert, Member, ITL Diversity Committee.
3. R. F. Boisvert, Member, NIST Scientific Computing Steering Group.
4. H. Cohl, Co-Director, ITL Summer Undergraduate Research Fellowship (SURF) Program, 2015.
5. A. Dienstfrey, NIST Materials Genome Initiative (MGI) Program Committee.
6. A. Dienstfrey, Member, ITL Cyber-Physical Systems Strategic Planning Committee.
7. S. Glancy, Member, NIST Boulder SURF Committee.
8. S. Glancy, Member, ITL Diversity Committee.
9. A. Kearsley, Member, ITL Awards Committee.
10. Y. Kemper, Member, NIST MML-Postdoctoral Association Leadership Committee.
11. K. Sayrafian, Member, ITL Cyber-Physical Systems Strategic Planning Committee.
12. C. Schanzle, Alternate Member, NIST Scientific Computing Steering Group.

External

Editorial

1. I. Beichl, Member, Editorial Board, *Computing in Science & Engineering.*
2. R. F. Boisvert, Associate Editor, *ACM Transactions on Mathematical Software*.
3. R. F. Boisvert, Area Moderator (Numerical Analysis, Mathematical Software, and Computational Science, Engineering and Finance), arXiv Computing Research Repository.
4. H. S. Cohl, Guest Editor, *Symmetry, Integrability and Geometry: Methods and Applications, Special Issue on Orthogonal Polynomials, Special Functions and Applications*.
5. A. Dienstfrey, Associate Editor, *International Journal of Uncertainty Quantification*.
6. Z. Gimbutas, Member, Editorial Board, *Advances in Computational Mathematics*.
7. M. Mascagni, Associate Editor, *ACM Transactions on Mathematical Software*.
8. M. Mascagni, Member, Editorial Advisory Board, *Molecular Based Mathematical Biology*.
9. M. Mascagni, Member, Editorial Board, *Mathematics and Computers in Simulation*.
10. M. Mascagni, Member, Editorial Board, *Monte Carlo Methods and Applications*.
11. M. Mascagni, Member, Editorial Board, *Advances in Computing, Theory and Practice*.
12. W. F. Mitchell, Editor, *Journal of Numerical Analysis, Industrial and Applied Mathematics*.
13. D. P. O'Leary, Editor-in-Chief, *SIAM Journal on Matrix Analysis and Applications*.
14. D. P. O'Leary, Member, Editorial Board, Education Section, *SIAM Review.*
15. D. P. O'Leary, Member, Editorial Board, *SIAM Books*.
16. D. P. O'Leary, Department Editor, "Your Homework Assignment," *Computing in Science and Engineering*.

17. F. A. Potra, Regional Editor, Americas, *Optimization Methods and Software*.
18. F. A. Potra, Associate Editor, *Journal of Optimization Theory and Applications*.
19. F. A. Potra, Associate Editor, *Numerical Functional Analysis and Optimization*.
20. F. A. Potra, Associate Editor, *Optimization and Engineering*.
21. K. Sayrafian, Associate Editor, *International Journal on Wireless Information Networks (IJWIN)*.
22. K. Sayrafian, Guest Editor, I*EEE Communication Magazine*, Special Issue on "Mobile and Wearable BAN."
23. B. I. Schneider, Member, Editorial Board, *Computing in Science & Engineering*.

Boards and Committees

1. R. F. Boisvert, Member, International Federation for Information Processing (IFIP) Working Group 2.5 (Numerical Software).
2. R. F. Boisvert, Member, Association for Computing Machinery (ACM) Publications Board.
3. R. F. Boisvert, Chair, Association for Computing Machinery (ACM) Digital Library Committee.
4. R. F. Boisvert, Member, Member, Reproducibility Interest Group[45], Research Data Alliance.
5. R.F. Boisvert, Alternate NIST Representative, Subcomittee on the Materials Genome Initiative, Committee on Technology, National Science and Technology Council.
6. R. F. Boisvert, Member, Program Review Committee, Institute for Defense Analysis (IDA) Center for Computing Science.
7. R. F. Boisvert, Member, External Review Panel, Department of Computer Sciences, George Washington University.
8. A. Dienstfrey, Member, International Federation for Information Processing (IFIP) Working Group 2.5 (Numerical Software).
9. W. L. George, Member, Argonne National Laboratory, Leadership Computing Facility User Advisory Committee.
10. M. Mascagni, Member, Board of Directors, International Association for Mathematics and Computers in Simulation (IMACS).
11. M. Mascagni, Member, Technical Committee, Monte Carlo Methods, International Association for Mathematics and Computers in Simulation (IMACS).
12. M. Mascagni, Member, Peer Review Committee, Fulbright Specialist Program, Council for International Exchange of Scholars.
13. G. B. McFadden, Member, SIAM Kleinman Prize Selection Committee.
14. G. B. McFadden, Member-at-Large, SIAM Council.
15. B. R. Miller, Member, Math Working Group, World Wide Web Consortium (W3C).
16. B. R. Miller, Member, OpenMath Society.
17. D. P. O'Leary, Founding Co-Director, Joint UMD-NIST Center for Quantum Information and Computer Science (QuICS).
18. D. P. O'Leary, Member, Oversight Committee, Gene Golub SIAM Summer Schools.
19. D. G. Porter, Member, Tcl Core Team.
20. S. Ressler, Member, Web3D Consortium.
21. S. Ressler, Member, Declarative 3D for the Web Architecture Community Group, World Wide Web Consortium.
22. B. Saunders, Member, Member, Advisory Group, NSF CoSMIC Scholars Program, Towson University.
23. B. Saunders, Member, Business, Industry, and Government (BIG) Committee, Mathematical Association of America (MAA).
24. B. Saunders, Webmaster, SIAM Activity Group on Orthogonal Polynomials and Special Functions.
25. B. Saunders, Moderator, OP-SF Talk listserv, SIAM Activity Group on Orthogonal Polynomials and Special Functions.
26. K. Sayrafian, Member, External Advisory Board, NIH/NIBIB Quantum Medical Device Interoperability (QMDI) Project.
27. K. Sayrafian, Member, Wireless Medical Technologies Working Group, National Institute of Biomedical Imaging and Bioengineering, NIH.
28. B. I. Schneider, Vice-Chair and Chair-Elect, Division of Computational Physics, American Physical Society (APS).
29. B. I. Schneider, NIST Representative, Interagency Working Group on High End Computing, Federal

[45] https://rd-alliance.org/group/reproducibility-ig.html

Networking and Information Technology R&D Program (NITRD).

30. B. I. Schneider, Program Committee Chair, Division of Computational Physics, American Physical Society.
31. J. Terrill, NIST Representative, Interagency Working Group on High End Computing, Federal Networking and Information Technology R&D Program (NITRD).

Community Outreach

1. B. Alpert, Mentor, Mathematical Modeling in Industry, IMA Workshop, University of British Columbia, Vancouver, Canada, August 6-15, 2014.
2. F. Hunt, Member, Organizing Committee, Infinite Possibilities Conference, Corvallis, OR, March 1-3, 2015.
3. D. P. O'Leary, Mentor, Mentor Network, Association for Women in Mathematics.
4. M. Mascagni, Visiting Lecturer, Society for Industrial and Applied Mathematics (SIAM).
5. S. Ressler, Distinguished Speaker, Association for Computing Machinery (ACM).
6. B. Saunders. Judge (Mathematics), Siemens Competition in Math, Science and Technology, October 11-15, 2013 in Princeton, NJ.
7. B. Saunders, Organizer, Virginia Standards of Learning Tutoring Program, Northern Virginia Chapter (NoVAC) of Delta Sigma Theta Sorority, Inc. and the Dunbar Alexandria-Olympic Branch of the Boys and Girls Clubs of Greater Washington, January-May, 2014.
8. B. Saunders, Panelist, STEM (Science, Technology, Engineering, and Mathematics) Career Panel for Middle School Girls, Cora Kelly Recreation Center, Alexandria, VA, April 12, 2014.

Thesis Direction

1. Z. Gimbutas, Member, Ph.D. Thesis Committee, Sija Hao, Applied Mathematics, University of Colorado, Boulder. Title: *Numerical Methods for Solving Linear Elliptic PDEs: Direct Solvers and High Order Accurate Discretization*. Completed 2013.
2. B. R. Miller, Member, Ph.D. Thesis Committee, Deyan Ginev, Computer Science, Jacobs University, Bremen. Title: *Designing Definition Discovery – Read, Recognize, Reflect, Repeat*.
3. B. R. Miller, Member, Ph.D. Thesis Committee, Qun Zhang, Computer Science, George Washington University, Washington DC. Title: *Math-Similarity Search (MSS).*
4. K. Sayrafian, Member, Ph.D. and M.Sc. Thesis Committee, Guanqun Bao, Worcester Polytechnic Institute. Title: *On Simultaneous Localization and Mapping inside the Human Body (Body-SLAM)*. Completed 2014.
5. K. Sayrafian, Member, Ph.D. and M.Sc. Thesis Committee, Mehdi Dadfarnia, University of Maryland. Title: *Energy Harvesting Microgenerators for Medical Body Sensor Network Systems*. Completed 2014.

Awards and Recognition

1. Ronald Boisvert, Fellow, Washington Academy of Sciences, May 8, 2014.
2. Ronald Boisvert, Mathematics and Computer Science Award, Washington Academy of Sciences, May 8, 2014.
3. Jeffrey Fong, Lifetime Achievement Award, International Conference on Computational Engineering and Science (ICCES), Changwon, Korea, June 16, 2014.
4. Raghu N. Kacker, Silver Medal (joint award), Department of Commerce, December 10, 2014.
5. Emanuel Knill, Arthur S. Flemming Award, George Washington University, June 9, 2014.
6. Bruce R. Miller, Outstanding Contribution to ITL, NIST Information Technology Laboratory, August 19, 2014.
7. B. Saunders, recognized for 12 years of service as a math tutor, Boys and Girls Clubs of Greater Washington, GEICO and the Washington Wizards, Washington Wizards Basketball game, Verizon Center, December 5, 2014.
8. Kamran Sayrafian, Embassy Science Fellow, U.S. Department of State, July 2014.
9. Christopher Schanzle, Outstanding Service Award, NIST Chapter of Sigma Xi, June 5, 2014.
10. Christopher Schanzle, Outstanding Technical Support (joint award), NIST Information Technology Laboratory, August 19, 2014.
11. Y. Zhang, Scott Glancy and Emanuel Knill, Outstanding Journal Paper, NIST Information Technology Laboratory, August 19, 2014.

Grants Awarded

ACMD awards a small amount of funding through the NIST Measurement Science Grants Program for projects that make direct contributions to its research programs. Often such grants support direct cooperation between an external awardee and ACMD. This year the following new cooperative agreements were initiated.

1. Theiss Research[46]: *Quantum Memories for Long-distance Quantum Communications*, $420,821 (3 years). PI: Dr. Lijun Ma.
2. University of Maryland, College Park, MD: *Network Science Approach to Interdependent Security*, $70,590 (3 years). PI: Prof. Richard La.

External Contacts

ACMD staff members make contact with a wide variety of organizations in the course of their work. Examples of these follow.

Industrial Labs

Automation Apps
The Boeing Company
Cadence Design Systems
Centre Suisse d'Electronique et Microtechnique – CSEM (Switzerland)
Foray Technologies
Fraunhoffer
Gener8
HRL Laboratories
IBM Research
Lockheed Martin
Mechdyne
Microsoft
Northrop-Grumman
Raytheon/BBN
Schwarz Forensic Enterprises
SIKA Technology A.G. (Switzerland)
Tata Research Development and Design Centre (India)

Government/Non-profit Organizations

Air Force Office of Scientific Research
Argonne National Laboratory
Army Research Laboratory
Army Research Office
Association for Computing Machinery – ACM
National Metrology Center – CENAM (Mexico)
Center for Integration of Medicine and Innovative Technology – CIMIT
Center for Research and Advanced Studies of the National Polytechnic Institute – CINVESTAV (Mexico)
China Special Equipment Inspection and Research Institute, Beijing (China)
The Commonwealth Scientific and Industrial Research Organisation – CSIRO (Australia)
Department of Energy
Electric Power Research Institute
European Commission Joint Research Center
Food and Drug Administration
Institute for Defense Analysis Center for Computing Sciences
Indian Statistical Institute (India)
Institute for Mathematics and its Applications
Institute of Physics and Chemistry of Materials – PCMS, National Center for Scientific Research – CNRS (France)
International Federation for Information Processing – IFIP
Johns Hopkins University Applied Physics Lab
Korea Research Institute of Standards and Science
Lawrence Livermore National Laboratory
Mathematisches Forschungsinstitut Oberwolfach (Germany)
MIT Lincoln Labs
Montgomery County Maryland
NASA Glenn Research Center
NASA Independent Verification and Validation Facility
National Center for Atmospheric Research – NCAR
National Institute of Biomedical Imaging and Bioengineering
National Institutes of Health
National Institute of Science Education and Research (India)
National Physical Laboratory (UK)
National Renewable Energy Laboratory – NREL
National Science Foundation
National Oceanographic and Atmospheric Administration
Noblis
Nuclear Regulatory Commission
Oak Ridge National Laboratory
Open Math Society
Pacific Northwest National Laboratory
Poolesville High School, Montgomery County, MD
Princeton Plasma Physics Laboratory
Sandia National Laboratories
Smithsonian Institution Digitization Program Office
Society for Industrial and Applied Mathematics – SIAM
Southwest Research Institute
Theiss Research
US Air Force, Eglin Air Force Base

[46] http://www.theissresearch.org/

World Wide Web Consortium
Web3D Consortium

Universities

American University
Beijing Institute of Technology, Beijing (China)
Bowie State University
Brown University
California Institute of Technology
Carnegie Mellon University
China University of Petroleum (China)
City University of Hong Kong (China)
City University of New York
Concordia University, Montreal, Canada
Dalian University of Technology (China)
Dartmouth College
East China University of Science and Technology (China)
Federal University of Rio Grande do Norte (Brazil)
Florida State University
George Mason University
George Washington University
Georgetown University
Harvard University
Harvey Mudd College
Hood College
Howard University
Iowa State University
Imperial College, London (UK)
Indian Institute of Technology
Indiana University
Istituto per le Applicazioni del Calcolo (Italy)
Jackson State University
Jacobs University Bremen (Germany)
Kiel University (Germany)
Kings College London (UK)
Lanzhou University of Technology (China)
Louisiana State University
Lund University (Sweden)
Macquarie University (Australia)
Millersville University of Pennsylvania
Nanyang University (Singapore)
National Institute of Technology (India)
National University of Singapore (Singapore)
Ningbo University (China)
Northwestern University
New York University
Oslo University (Norway)
Ozyegin University (Turkey)
Pierre and Marie Curie University (France)
Polytechnic University of Puerto Rico
Princeton University
Purdue University
Rice University
Rochester Institute of Technology
Shandong University (China)
Smith College
Saint Olaf College
Stanford University
State University of New York at Binghamton
Swarthmore College
Texas A&M University
The College of New Jersey
Three Gorges University (China)
Tohoko University (Japan)
Towson University
Tsinghua University (China)
Tulane University
Tufts University
Ulm University (Germany)
Uniformed Services University of the Health Sciences
University at Albany
University of Alcalá (Spain)
University of Antwerp (Belgium)
University of Arizona
University of Bordeaux (France)
University of Bergamo (Italy)
University of British Columbia (Canada)
University of California at Berkeley
University of California at Davis
University of California at Irvine
University of California at San Diego
University of California at Santa Barbara
University of Campinas (Brazil)
University of Colorado at Boulder
University of Colorado at Denver
University of Copenhagen (Denmark)
University of the District of Columbia
University of Göttingen (Germany)
University of Hong Kong (China)
University of Houston
University of Illinois at Urbana-Champaign
University of Lisbon (Portugal)
University of Maryland Baltimore County
University of Maryland College Park
University of Maryland University College
University of Miami
University of Michigan
University of Montreal (Canada)
University of Northern Texas
University of Oklahoma
University of Oulu (Finland)
University of South Carolina
University of Surrey (UK)
University of Technology Sidney (Australia)
University of Texas at Arlington
University of Texas at Dallas
University of Toronto
University of Waterloo (Canada)
University of Wisconsin Milwaukee
University of Zagreb (Croatia)
Virginia Polytechnic Institute and State University
Washington University
Waterloo University

Worcester Polytechnic University
Yale University
Yokohama National University (Japan)

Part V

Appendix

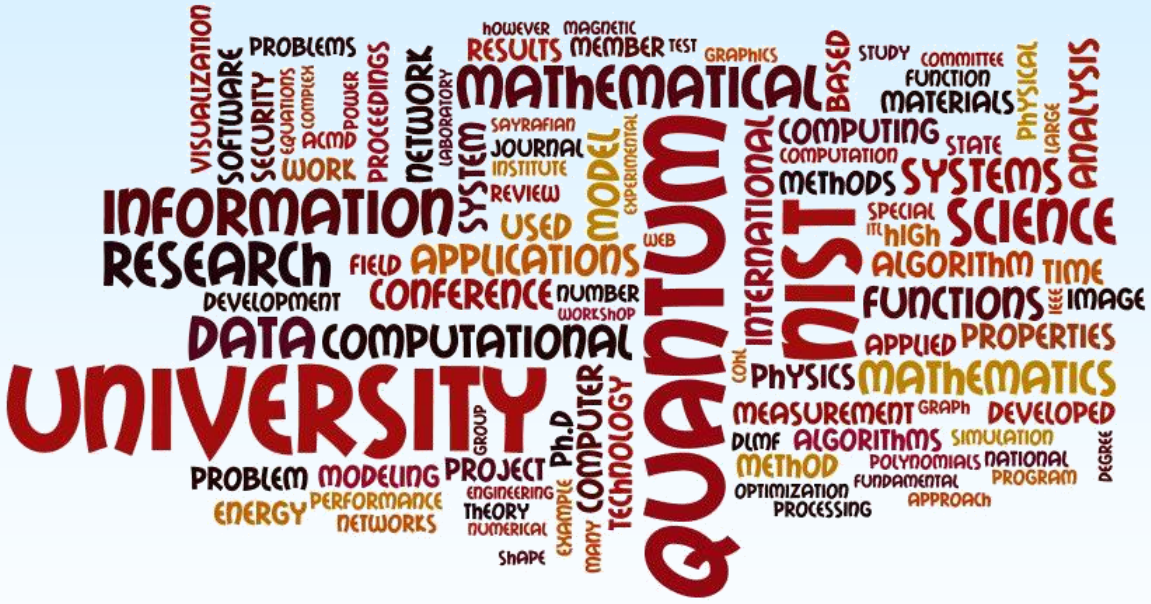

Staff

ACMD consists of full time permanent staff located at NIST laboratories in Gaithersburg, MD and Boulder, CO. This is supplemented with a variety of special appointments. The following list reflects all appointments held during any portion of the reporting period (October 2013 – December 2014). For students and interns, see Staff News on page 8. (*) Denotes staff at NIST Boulder.

Division Staff

Ronald Boisvert, *Chief*, Ph.D. (Computer Science), Purdue University, 1979
Catherine Graham, *Secretary*
Ginger White, *Administrative Assistant*, M.B.A., University of Maryland, 2014.
Robert Bohn, Ph.D. (Physical Chemistry), University of Virginia, 1991
Alfred Carasso, Ph.D. (Mathematics), University of Wisconsin, 1968
Roldan Pozo, Ph.D. (Computer Science), University of Colorado at Boulder, 1991
Kamran Sayrafian-Pour, Ph.D. (Electrical and Computer Engineering), University of Maryland, 1999
Christopher Schanzle, B.S. (Computer Science), University of Maryland Baltimore County, 1989

Mathematical Analysis and Modeling Group

Timothy Burns, *Leader*, Ph.D. (Mathematics), University of New Mexico, 1977
*Bradley Alpert, Ph.D. (Computer Science), Yale University, 1990
*Andrew Dienstfrey, Ph.D. (Mathematics), New York University, 1998
Jeffrey Fong, Ph. D. (Applied Mechanics and Mathematics), Stanford University, 1966
*Zydrunas Gimbutas, Ph.D. (Applied Mathematics), Yale University, 1999
Fern Hunt, Ph.D. (Mathematics), New York University, 1978
Raghu Kacker, Ph.D. (Statistics), Iowa State University, 1979
Anthony Kearsley, Ph.D. (Computational and Applied Mathematics), Rice University, 1996
Geoffrey McFadden, *NIST Fellow*, Ph.D. (Mathematics), New York University, 1979
Bert Rust, Ph.D. (Astronomy), University of Illinois at Urbana-Champaign, 1974

NRC Postdoctoral Associates
Sean Colbert-Kelly, Ph.D. (Mathematics), Purdue University, 2012
Michael Cromer, Ph.D. (Applied Mathematics), University of Delaware, 2011

Faculty Appointee (Name, Degree / Home Institution)
Daniel Anderson, Ph.D. / George Mason University
Dianne O'Leary, Ph.D. / University of Maryland College Park
Michael Mascagni, Ph.D. / Florida State University
Florian Potra, Ph.D. / University of Maryland Baltimore County

Guest Researchers (Name, Degree / Home Institution)
Mirit Aladjem, Ph.D. / National Institutes of Health
James Benson, Ph.D. / Northern Illinois University
David Cotrell, Ph.D. / CD-Adapco
*John Gary, Ph.D. / NIST (retired)
David Gilsinn, Ph.D. / NIST (retired)
Daniel Kaslovsky, Ph.D. / University of Colorado
Yu (Jeff) Lei, Ph.D. / University of Texas at Arlington
P. Aaron Lott, Ph.D. / Lawrence Livermore National Laboratory
Itzel Dominquez Mendoza / Centro Nacional de Metrología, Mexico
Bruce Murray, Ph.D. / SUNY Binghamton

Asha Nurse, Ph.D.
Jose Torres-Jimenez, Ph.D / CINVESTAV, Mexico
Christoph Witzgall, Ph.D. / *NIST Scientist Emeritus*

Mathematical Software Group

Michael Donahue, *Leader* Ph.D. (Mathematics), Ohio State University, 1991
Javier Bernal, Ph.D. (Mathematics), Catholic University, 1980
Howard Cohl, Ph.D. (Mathematics), University of Auckland, 2010
Stephen Langer, Ph.D. (Physics), Cornell University, 1989
Daniel Lozier, Ph.D. (Applied Mathematics), University of Maryland, 1979
Marjorie McClain, M.S. (Mathematics), University of Maryland College Park, 1984
Bruce Miller, Ph.D. (Physics), University of Texas at Austin, 1983
William Mitchell, Ph.D. (Computer Science), University of Illinois at Urbana-Champaign, 1988
Donald Porter, Ph.D. (Electrical Engineering), Washington University, 1996
Bonita Saunders, Ph.D. (Mathematics), Old Dominion University, 1985
Barry Schneider, Ph.D. (Physics), University of Chicago, 1969

Faculty Appointees (Name, Degree / Home Institution)
G.W. Stewart, Ph.D. / University of Maryland College Park
Abdou Youssef, Ph.D. / George Washington University

Contractors (Name, Degree / Home Institution)
Qiming Wang / Dakota Consulting

Guest Researchers (Name, Degree / Home Institution)
Gunay Dogan, Ph.D. / Theiss Research
Adri Olde Daalhuis, Ph.D. / University of Edinburgh
Tamara Kolda, Ph.D. / Sandia Laboratories, Livermore
Leonard Maximon, Ph.D. / George Washington University

Computing and Communications Theory Group

Ronald Boisvert, *Acting Leader*
Isabel Beichl, *Project Leader*, Ph.D. (Mathematics), Cornell University, 1981
Brian Cloteaux, Ph.D. (Computer Science), New Mexico State University, 2007
*Scott Glancy, Ph.D. (Physics), University of Notre Dame, 2003
Barry Hershman, A.A. (Electronics Engineering), Capitol College, 1979
Stephen Jordan, Ph.D. (Physics), Massachusetts Institute of Technology, 2008
*Emanuel Knill, *NIST Fellow*, Ph.D. (Mathematics), University of Colorado at Boulder, 1991
Paulina Kuo, Ph.D. (Physics), Stanford University, 2008
Yi-Kai Liu, Ph.D. (Computer Science), University of California, San Diego, 2007
Vladimir Marbukh, Ph.D. (Mathematics) Leningrad Polytechnic University, 1986
James Shook, Ph.D. (Mathematics), University of Mississippi, 2010
Oliver Slattery, M.S. (Electrical Engineering), Johns Hopkins University, 2008
Xiao Tang, *Project Leader,* Ph.D (Physics), Chinese Academy of Sciences, 1985

NRC Postdoctoral Associates
Yvonne Kemper, Ph.D. (Mathematics), University of California at Davis, 2013

Contractors (Name, Degree / Home Institution)
Alan Mink, Ph.D. / Wagner Resources

Faculty Appointees (Name, Degree / Home Institution)
James Lawrence, Ph.D. / George Mason University

Guest Researchers (Name, Degree / Home Institution)
*Bryan Eastin, PhD. / Northrup Grumman
Assane Gueye, Ph.D. / University of Maryland
Richard La, Ph.D. / University of Maryland
Lijun Ma, Ph.D. / Theiss Research
Francis Sullivan, Ph.D. / IDA Center for Computing Sciences
Amada Streib, Ph.D. / IDA Center for Computing Sciences
Noah Streib, Ph.D. / IDA Center for Computing Sciences

High Performance Computing and Visualization Group

Judith Terrill, Leader, Ph.D. (Information Technology), George Mason University, 1998
Yolanda Parker, Office Manager
William George, Ph.D. (Computer/Computational Science), Clemson University, 1995
Terence Griffin, B.S. (Mathematics), St. Mary's College of Maryland, 1987
Wesley Griffin, M.S. (Computer Science), University of Maryland Baltimore County, 2010
John Hagedorn, M.S. (Mathematics), Rutgers University, 1980
Sandy Ressler, M.F.A. (Visual Arts), Rutgers University, 1980
Steven Satterfield, M.S. (Computer Science), North Carolina State University, 1975
James Sims, Ph.D. (Chemical Physics), Indiana University, 1969

Faculty Appointees (Name, Degree / Home Institution)
Marc Olano, Ph.D. / University of Maryland Baltimore County

Guest Researchers (Name, Degree / Home Institution)
Tomasz Bednarz, Ph.D. / CSIRO, Australia
Jian Chen, Ph.D. / University of Maryland Baltimore County

Glossary of Acronyms

2D	two-dimensional
3D	three-dimensional
ACM	Association for Computing Machinery
ACMD	NIST/ITL Applied and Computational Mathematics Division
ACTS	Advanced Combinatorial Testing System
AMS	American Mathematical Society
arXiv	preprint archive housed at Cornell University (http://arxiv.org/)
AS	autonomous system
ASCE	American Society of Civil Engineers
ASTM	ASTM International, formerly known as the American Society for Testing and Materials
BAN	body area network
BD	Blitzstein-Diaconis
BMG	bulk metallic glasses
BMP	Bateman Manuscript Project
BQP	bounded-error quantum polynomial time
CAC	NIST-NTIA Center for Advanced Communications
CAIDA	Center for Applied Internet Data Analysis
Caltech	California Institute of Technology
CCS	IDA Center for Computing Sciences
CDF	cumulative distribution function
CFPG	Coulomb force parametric generator
CI	configuration interaction
CINVESTAV	Center for Research and Advanced Studies of the National Polytechnic Institute (Mexico)
CMA	University of Antwerp Computational Mathematics Research Group
CNRS	Centre National de la Recherche Scientifique (France)
CNST	NIST Center for Nanoscale Science and Technology
CPA	cryoprotective agent
CPS	cyber-physical system
CPU	central processing unit
CT	combinatorial testing
CT	computed tomography
CTL	NIST Communications Technology Laboratory
CY	calendar year
DIM	diffuse interface model
DLMF	Digital Library of Mathematical Functions
DMI	Dzyaloshinskii-Moriya interaction
DNA	deoxyribonucleic acid
DOAS	dual optical absorption spectroscopy
DOE	U.S. Department of Energy
DPD	dissipative particle dynamics
DRMF	digital repository of mathematical functions
EC	error correction
EH	energy harvesting
EIT	electromagnetically induced transparency
EL	NIST Engineering Laboratory
EBSD	electron backscatter data
ESPCI	École Supérieure de Physique et Chimie Industrielles de la Ville de Paris (France)
ETSI	European Telecommunications Standards Institute
FCU	fan coil unity
FEDVR	finite element discrete variable method
FEM	finite element method
FFT	fast Fourier transform
FPGA	field-programmable gate array
FVS	feedback vertex set

FWM	four-wave mixing
FY	fiscal year
GAMS	Guide to Available Mathematical Software
GF(2)	Galois field of two elements
GPS	Geographic Positioning System
GPU	graphics processing units
GSSM	greenhouse gas sequestration monitoring
GUI	graphical user interface
HIM	helium ion microscope
HPCVG	ACMD High Performance Computing and Visualization Group
HTML	hypertext markup language
HVAC	heating, ventilation and air conditioning
HVACSIM+	simulation testbed for HVAC systems
Hy-CI	Hylleraas-Configuration Interaction technique
ICCES	International Conference on Computational Engineering and Science
ICERM	Institute for Computational & Experimental Research in Mathematics (Brown University)
IDA	Institute for Defense Analysis
IDEA	IRIS Development Environment for Applications
IDS	interdependent security
IEEE	Institute of Electronics and Electrical Engineers
IFIP	International Federation for Information Processing
IMA	Institute for Mathematics and Its Applications
IMACS	International Association for Mathematics and Computers in Simulation
IMS	Innovations in Measurement Science
INCITE	Innovative and Novel Computational Impact on Theory and Experiment (DOE Program)
IRIS	Interpreted Runtime Immersive Scenegraph
ISGG	International Society for Grid Generation
ISIMA	Institut Supérieur d'Informatique, de Modélisation et de leurs Applications (France)
ISO	International Organization for Standardization
IT	information technology
ITL	NIST Information Technology Laboratory
ITS	NTIA Institute for Telecommunication Sciences
IVE	immersive visualization environment
IVF	in vitro fertilization
JILA	joint NIST-University of Colorado physics research institute
KLS	Koekoek, Lesky and Swarttouw
LaTeX	a math-oriented text processing system
LaTeXML	LaTeX to MathML translator
LDPC	low density parity check
LiDAR	light detection and ranging
LOCC	local operations and classical communication
LR	local realism
LTE	long-term evolution
MAA	Mathematical Association of America
MALDI-RTOF	matrix-assisted laser desorption ionization reflectron time-of-flight (mass spectrometer)
MALDI/TOF	matrix-assisted laser desorption/ionization time-of-flight (mass spectrometer)
MathML	Mathematical Markup Language (W3C standard)
MD	molecular dynamics
MDPC	moderate density parity check
MEMS	micro-electro-mechanical system
MGI	Materials Genome Initiative
MIA	minimum interference allocation
MIT	Massachusetts Institute of Technology
MKM	mathematical knowledge management
MML	NIST Material Measurement Laboratory
MPEG7	multimedia content description standard
MPI	Message Passing Interface

MRAM	magneto-resistive random access memory
MRI	magnetic resonance imaging
MSE	mean squared error
muMAG	Micromagnetic Activity Group
NASA	National Aeronautics and Space Administration
NBS	National Bureau of Standards
NCAR	National Center for Atmospheric Research
ND	nano-diamond
NDE	non-destructive evaluation
NIH	National Institutes of Health
NIST	National Institute of Standards and Technology
NISTIR	NIST Internal Report
NITRD	Networking and Information Technology Research and Development
NMR	nuclear magnetic resonance
NPSC	National Physical Science Consortium
NRC	National Research Council
NRC	US Nuclear Regulatory Commission
NSA	National Security Agency
NSF	National Science Foundation
NTIA	National Telecommunications and Information Administration
NUREG	US Nuclear Regulatory Commission
NV	nitrogen vacancy
NVD	National Vulnerability Database
NYU	New York University
OOF	Object-Oriented Finite Elements (software)
OOMMF	Object-Oriented Micromagnetic Modeling Framework (software)
OPSF	orthogonal polynomials and special functions
OSG	Open SceneGraph
PDE	partial differential equation
PHAML	Parallel Hierarchical Adaptive Multi Level (software)
PID	proportional integral derivative
PML	NIST Physical Measurement Laboratory
PPLN	periodically poled lithium niobate
PREP	Professional Research Experience Program
PSCR	NTIA Public Safety Communications Research
PSNR	peak signal-to-noise ratio
QD	quantum dot
QDPD	quarternion-based dissipative particle dynamics
QKD	quantum key distribution
QuICS	UMD-NIST Joint Center for Quantum Information and Computer Science
R&D	research and development
RF	radio frequency
SBIR	Small Business Innovative Research
SCGM	scaled conjugate gradient method
SDE	stochastic differential equation
SED	ITL Statistical Engineering Division
SEM	scanning electron microscope
SHIP	NIST Summer High School Internship Program
SIAM	Society for Industrial and Applied Mathematics
SIGACT	ACM Special Interest Group in Algorithms and Computation Theory
SIGGRAPH	ACM Special Interest Group on Graphics
SIR	signal-to-interference ratio
SIS	sequential importance sampling
SiV	silicon vacancy
SPDC	spontaneous parametric down-conversion
SPIE	International Society for Optical Engineering
SPL	software product line

SRM	standard reference material
SUNY	State University of New York
SURF	Student Undergraduate Research Fellowship
SVG	scalable vector graphics
TES	transition edge sensor
TSCM	truncated singular components method
TV	total variation
UK	United Kingdom
UMBC	University of Maryland Baltimore County
UMD	University of Maryland
UMIACS	University of Maryland Institute for Advanced Computer Studies
UQ	uncertainty quantification
USGS	US Geological Survey
VR	virtual reality
VRML	virtual reality modeling language
W3C	World Wide Web Consortium
WAS	Washington Academy of Sciences
WebGL	Web-based Graphics Library
WUSTL	Washington University St. Louis
X3D	Extensible 3D
X3DOM	an open-source framework for integrating X3D and HTML5
XSEDE	NSF eXtreme Science and Engineering Discovery Environment
XML	Extensible Markup Language